



Global Methane Budget 2000-2020

- Marielle Saunois¹, Adrien Martinez¹, Benjamin Poulter², Zhen Zhang^{3,4}, Peter A. Raymond⁵, Pierre 2
- Regnier⁶, Josep G. Canadell⁷, Robert B. Jackson⁸, Prabir K. Patra^{9,10}, Philippe Bousquet¹, Philippe 3
- Ciais¹, Edward J. Dlugokencky¹¹, Xin Lan^{11,12}, George H. Allen¹³, David Bastviken¹⁴, David J. 4
- Beerling¹⁵, Dmitry A. Belikov¹⁶, Donald R. Blake¹⁷, Simona Castaldi¹⁸, Monica Crippa^{19,20}, Bridget R. 5
- Deemer²¹, Fraser Dennison²², Giuseppe Etiope^{23,24}, Nicola Gedney²⁵, Lena Höglund-Isaksson²⁶, 6 Meredith A. Holgerson²⁷, Peter O. Hopcroft²⁸, Gustaf Hugelius²⁹, Akihiko Ito³⁰, Atul K. Jain³¹, Rajesh
- 7 8
- Janardanan³², Matthew S. Johnson³³, Thomas Kleinen³⁴, Paul B. Krummel²², Ronny Lauerwald³⁵, Tingting Li³⁶, Xiangyu Liu³⁷, Kyle C. McDonald³⁸, Joe R. Melton³⁹, Jens Mühle⁴⁰, Jurek Müller⁴¹,
- Fabiola Murguia-Flores⁴², Yosuke Niwa^{32,43}, Sergio Noce⁴⁴, Shufen Pan⁴⁵, Robert J. Parker⁴⁶, Changhui 10
- Peng^{47,48}, Michel Ramonet¹, William J. Riley⁴⁹, Gerard Rocher-Ros⁵⁰, Judith A. Rosentreter⁵¹, Motoki Sasakawa³², Arjo Segers⁵², Steven J. Smith^{53,54}, Emily H. Stanley⁵⁵, Joël Thanwerdas^{56,*}, Hanqin Tian⁵⁷, 11
- 12
- Aki Tsuruta⁵⁸, Francesco N. Tubiello⁵⁹, Thomas S. Weber⁶⁰, Guido R. van der Werf⁶¹, Douglas E. J. 13
- Worthy⁶², Yi Xi¹, Yukio Yoshida³², Wenxin Zhang⁶³, Bo Zheng^{64,65}, Qing Zhu⁴⁹, Qiuan Zhu⁶⁶, and 14
- Qianlai Zhuang³⁷ 15
- 16
- 17 ¹Laboratoire des Sciences du Climat et de l'Environnement, LSCE-IPSL (CEA-CNRS-UVSO), Université
- 18 Paris-Saclay 91191 Gif-sur-Yvette, France
- 19 ²NASA Goddard Space Flight Center, Biospheric Science Laboratory, Greenbelt, MD 20771, USA
- 20 ³National Tibetan Plateau Data Center (TPDC), State Key Laboratory of Tibetan Plateau Earth System,
- 21 Environment and Resource (TPESER), Institute of Tibetan Plateau Research, Chinese Academy of Sciences,
- 22 Beijing, 100101, China
- 23 ⁴Earth System Science Interdisciplinary Center, University of Maryland, College Park, MD 20740, USA
- 24 ⁵Yale School of the Environment, Yale University, New Haven, CT 06511, USA
- ⁶Department Geoscience, Environment & Society (BGEOSYS), Université Libre de Bruxelles, 1050 Bruxelles, 25
- 26 Belgium
- 27 ⁷Global Carbon Project, CSIRO Environment, Canberra, ACT 2601, Australia
- 28 ⁸Department of Earth System Science, Woods Institute for the Environment, and Precourt Institute for Energy,
- 29 Stanford University, Stanford, CA 94305-2210, USA
- 30 ⁹Research Institute for Global Change, JAMSTEC, 3173-25 Showa-machi, Kanazawa, Yokohama, 236-
- 31 0001, Japan
- 32 ¹⁰Research Institute for Humanity and Nature, Kyoto 6038047, Japan
- 33 ¹¹NOAA Global Monitoring Laboratory, 325 Broadway, Boulder, CO 80305, USA
- 34 ¹²Cooperative Institute for Research in Environmental Sciences, University of Colorado Boulder, CO 80303,
- 35
- ¹³Department of Geosciences, Virginia Polytechnic Institute and State University, Blacksburg, VA, USA 36
- 37 ¹⁴Department of Thematic Studies – Environmental Change, Linköping University, 581 83 Linköping, Sweden
- 38 ¹⁵School of Biosciences, University of Sheffield, UK
- 39 ¹⁶Center for Environmental Remote Sensing, Chiba University, Chiba, 263-8522, Japan
- 40 ¹⁷Department of Chemistry, University of California Irvine, 570 Rowland Hall, Irivine, CA 92697, USA
- 41 ¹⁸Dipartimento di Scienze Ambientali, Biologiche e Farmaceutiche, Università degli Studi della Campania Luigi





- 42 Vanvitelli, via Vivaldi 43, 81100 Caserta, Italy
- 43 ¹⁹European Commission, Joint Research Centre (JRC), Ispra, Italy
- 44 ²⁰Unisystems S.A., Milan, Italy
- 45 ²¹U.S. Geological Survey, Southwest Biological Science Center, Flagstaff, AZ, USA
- 46 ²²CSIRO Environment, Aspendale, Victoria 3195, Australia
- 47 ²³Istituto Nazionale di Geofisica e Vulcanologia, Sezione Roma 2, via V. Murata 605 00143 Rome, Italy
- 48 ²⁴Faculty of Environmental Science and Engineering, Babes Bolyai University, Cluj-Napoca, Romania
- 49 25 Met Office Hadley Centre, Joint Centre for Hydrometeorological Research, Maclean Building, Wallingford
- 50 OX10 8BB, UK
- 51 ²⁶Pollution Management Group (PM), International Institute for Applied Systems Analysis (IIASA), 2361
- 52 Laxenburg, Austria
- 53 ²⁷ Department of Ecology & Evolutionary Biology, Cornell University, Ithaca, NY, USA
- 54 ²⁸ School of Geography, Earth & Environmental Sciences, University of Birmingham, UK
- 55 ²⁹ Department of Physical Geography and Bolin Centre for Climate Research, Stockholm University, 106 91
- 56 Stockholm, Sweden
- 57 ³⁰ Graduate School of Agricultural and Life Sciences, The University of Tokyo, Tokyo, Japan
- 58 ³¹ Department of Atmospheric Sciences, University of Illinois, Urbana, IL 61821, USA
- 59 ³² Earth System Division, National Institute for Environmental Studies (NIES), Onogawa 16-2, Tsukuba, Ibaraki
- 60 305-8506, Japan
- 61 ³³Earth Science Division, NASA Ames Research Center, Moffett Field, CA USA.
- 62 ³⁴Max Planck Institute for Meteorology, Bundesstraße 53, 20146 Hamburg, Germany
- 63 ³⁵ Université Paris-Saclay, INRAE, AgroParisTech, UMR EcoSys, Palaiseau, France
- 64 36 LAPC, Institute of Atmospheric Physics, Chinese Academy of Sciences, Beijing, 100029, China
- 65 ³⁷Department of Earth, Atmospheric, and Planetary Sciences, Purdue University, West Lafayette, IN, USA
- 66 38Department of Earth and Atmospheric Sciences, City College of New York, City University of New York, NY,
- 67 USA
- 68 ³⁹Climate Research Division, Environment and Climate Change Canada, Victoria, BC, V8W 2Y2, Canada
- 69 ⁴⁰Scripps Institution of Oceanography, University of California San Diego, La Jolla, CA, 92037, USA
- 70 41Climate and Environmental Physics, Physics Institute and Oeschger Centre for Climate Change Research,
- 71 University of Bern, Sidlerstr. 5, 3012 Bern, Switzerland
- 72 ⁴²Instituto de Investigaciones en Ecología y Sustentabilidad, Universidad Nacional Autónoma de México,
- 73 Morelia, Mexico
- 74 43Department of Climate and Geochemistry Research, Meteorological Research Institute (MRI), Nagamine 1-1, Tsukuba,
- 75 Ibaraki 305-0052, Japan
- 76 ⁴⁴CMCC Foundation Euro-Mediterranean Center on Climate Change, Italy
- 77 ⁴⁵Department of Engineering and Environmental Studies Program, Boston College, Chestnut Hill, MA 02467,
- 78 USA
- 79 46National Centre for Earth Observation, School of Physics and Astronomy, University of Leicester, Leicester,
- 80 LE1 7RH, UK
- 81 ⁴⁷Department of Biology Sciences, Institute of Environment Science, University of Quebec at Montreal,
- 82 Montreal, OC H3C 3P8, Canada
- 83 ⁴⁸ School of Geographic Sciences, Hunan Normal University, Changsha 410081, China
- 84 ⁴⁹Climate and Ecosystem Sciences Division, Lawrence Berkeley National Lab, 1 Cyclotron Road, Berkeley, CA
- 85 94720, US
- 86 ⁵⁰Department of Forest Ecology and Management, Swedish University of Agricultural Sciences, 90183 Umeå,
- 87 Sweden
- 88 51Centre for Coastal Biogeochemistry, Faculty of Science and Engineering, Southern Cross University, Lismore,
- 89 NSW 2480, Australia
- 90 52TNO, dep. of Climate Air & Sustainability, P.O. Box 80015, NL-3508-TA, Utrecht, The Netherlands





- 91 ⁵³Joint Global Change Research Institute, Pacific Northwest National Lab, College Park, MD, USA
- 92 ⁵⁴Center for Global Sustainability, University of Maryland, College Park, MD, USA
- 93 ⁵⁵Center for Limnology, University of Wisconsin-Madison, Madison, WI, USA
- 94 ⁵⁶Empa, Swiss Federal Laboratories for Materials Science and Technology, Dübendorf, Switzerland
- 95 ⁵⁷Center for Earth System Science and Global Sustainability, Schiller Institute for Integrated Science and
- 96 Society, Department of Earth and Environmental Sciences, Boston College, Chestnut Hill, MA 02467, USA
- 97 ⁵⁸Finnish Meteorological Institute, P.O. Box 503, FI-00101, Helsinki, Finland
- 98 ⁵⁹Statistics Division, Food and Agriculture Organization of the United Nations (FAO), Viale delle
- 99 Terme di Caracalla, Rome 00153, Italy
- 100 ⁶⁰Department of Earth and Environmental Sciences, University of Rochester, Rochester, NY 14627,
- 101 USA
- ⁶¹Meteorology and Air Quality Group, Wageningen University and Research, Wageningen, the Netherlands 102
- ⁶²Environment and Climate Change Canada, 4905, Dufferin Street, Toronto, Canada 103
- 104 ⁶³Department of Physical Geography and Ecosystem Science, Lund University, Sölvegatan 12, 223 62, Lund, Sweden
- 105 ⁶⁴Institute of Environment and Ecology, Tsinghua Shenzhen International Graduate School, Tsinghua University,
- 106 Shenzhen 518055, China
- ⁶⁵State Environmental Protection Key Laboratory of Sources and Control of Air Pollution Complex, Beijing 100084, 107
- 108 China
- ⁶⁶College of Geography and Remote Sensing, Hohai University, Nanjing, 210098, China 109
- 111 *formerly at LSCE 1

110

- 113 Correspondence to: Marielle Saunois (marielle.saunois@lsce.ipsl.fr)
- 114 Abstract. Understanding and quantifying the global methane (CH₄) budget is important for assessing realistic pathways to 115 mitigate climate change. Emissions and atmospheric concentrations of CH₄ continue to increase, maintaining CH₄ as the second most important human-influenced greenhouse gas in terms of climate forcing after carbon dioxide (CO₂). The relative 116 importance of CH₄ compared to CO₂ for temperature change is related to its shorter atmospheric lifetime, stronger radiative 117 118 effect, and acceleration in atmospheric growth rate over the past decade, the causes of which are still debated. Two major 119 challenges in reducing uncertainties in the factors explaining the well-observed atmospheric growth rate arise from diverse, 120 geographically overlapping CH₄ sources and from the uncertain magnitude and temporal change in the destruction of CH₄ 121 by short-lived and highly variable hydroxyl radicals (OH). To address these challenges, we have established a consortium 122 of multi-disciplinary scientists under the umbrella of the Global Carbon Project to improve, synthesise and update the global 123 CH₄ budget regularly and to stimulate new research on the methane cycle. Following Saunois et al. (2016, 2020), we present 124 here the third version of the living review paper dedicated to the decadal CH₄ budget, integrating results of top-down CH₄ 125 emission estimates (based on in-situ and greenhouse gas observing satellite (GOSAT) atmospheric observations and an 126 ensemble of atmospheric inverse-model results) and bottom-up estimates (based on process-based models for estimating 127 land-surface emissions and atmospheric chemistry, inventories of anthropogenic emissions, and data-driven extrapolations). We present a budget for the most recent 2010-2019 calendar decade (the latest period for which full datasets are available),
- 128
- 129 for the previous decade of 2000-2009 and for the year 2020.



131

132

133

134

135

136

137

138

139

140

141142

143

144

145

146147

148

149

150

151

152

153

154

155

156

157158

159

160

161

162



The revision of the bottom-up budget in this edition benefits from important progress in estimating inland freshwater emissions, with better accounting of emissions from lakes and ponds, reservoirs, and streams and rivers. This budget also reduces double accounting across freshwater and wetland emissions and, for the first time, includes an estimate of the potential double accounting that still exists (average of 23 Tg CH₄ yr⁻¹). Bottom-up approaches show that the combined wetland and inland freshwater emissions average 248 [159-369] Tg CH₄ yr⁻¹ for the 2010-2019 decade. Natural fluxes are perturbed by human activities through climate, eutrophication, and land use. In this budget, we also estimate, for the first time, this anthropogenic component contributing to wetland and inland freshwater emissions. Newly available gridded products also allowed us to derive an almost complete latitudinal and regional budget based on bottom-up approaches. For the 2010-2019 decade, global CH₄ emissions are estimated by atmospheric inversions (top-down) to be 575 Tg CH₄ yr ¹ (range 553-586, corresponding to the minimum and maximum estimates of the model ensemble). Of this amount, 369 Tg CH₄ yr⁻¹ or ~65% are attributed to direct anthropogenic sources in the fossil, agriculture and waste and anthropogenic biomass burning (range 350-391 Tg CH₄ yr⁻¹ or 63-68%). For the 2000-2009 period, the atmospheric inversions give a slightly lower total emission than for 2010-2019, by 32 Tg CH₄ yr⁻¹ (range 9-40). Since 2012, global direct anthropogenic CH₄ emission trends have been tracking scenarios that assume no or minimal climate mitigation policies proposed by the Intergovernmental Panel on Climate Change (shared socio-economic pathways SSP5 and SSP3). Bottom-up methods suggest 16% (94 Tg CH₄ vr⁻¹) larger global emissions (669 Tg CH₄ vr⁻¹, range 512-849) than top-down inversion methods for the 2010-2019 period. The discrepancy between the bottom-up and the top-down budgets has been greatly reduced compared to the previous differences (167 and 156 Tg CH₄ yr¹ in Saunois et al. (2016, 2020), respectively), and for the first time uncertainty in bottom-up and top-down budgets overlap. The latitudinal distribution from atmospheric inversion-based emissions indicates a predominance of tropical and southern hemisphere emissions (~65% of the global budget, <30°N) compared to mid (30°N-60°N, ~30% of emissions) and high-northern latitudes (60°N-90°N, ~4% of global emissions). This latitudinal distribution is similar in the bottom-up budget though the bottom-up budget estimates slightly larger contributions for the mid and high-northern latitudes, and slightly smaller contributions from the tropics and southern hemisphere than the inversions. Although differences have been reduced between inversions and bottom-up, the most important source of uncertainty in the global CH₄ budget is still attributable to natural emissions, especially those from wetlands and inland freshwaters. We identify five major priorities for improving the CH₄ budget; i) producing a global, high-resolution map of water-saturated soils and inundated areas emitting CH₄ based on a robust classification of different types of emitting ecosystems; ii) further development of process-based models for inland-water emissions; iii) intensification of CH₄ observations at local (e.g., FLUXNET-CH₄ measurements, urban-scale monitoring, satellite imagery with pointing capabilities) to regional scales (surface networks and global remote sensing measurements from satellites) to constrain both bottom-up models and atmospheric inversions; iv) improvements of transport models and the representation of photochemical sinks in top-down inversions, and v) integration of 3D variational inversion systems using isotopic and/or co-emitted species such as ethane





- as well as information in the bottom-up inventories on anthropogenic super-emitters detected by remote sensing (mainly oil and gas sector but also coal, agriculture and landfills) to improve source partitioning.
- The data presented here can be downloaded from https://doi.org/10.18160/GKQ9-2RHT (Martinez et al., 2024).

1 Introduction

166

167

168

169

170

171

172

173174

175

176

177

178

179180

181

182

183

184

185

186

187

188

189

190

191

192 193

The average surface dry air mole fraction of atmospheric methane (CH₄) reached 1912 ppb in 2022 (Fig. 1, Lan et al., 2024), 2.6 times greater than its estimated pre-industrial value in 1750. This increase is attributable in large part to increased anthropogenic emissions arising primarily from agriculture (e.g., livestock production, rice cultivation, biomass burning), fossil fuel production and use, waste disposal, and alterations to natural CH₄ fluxes due to increased atmospheric CO₂ concentrations, land use (Woodward et al., 2010, Fluet-Chouinard et al., 2023) and climate change (Ciais et al., 2013; Canadell et al., 2021). Atmospheric CH₄ is a stronger absorber of Earth's emitted thermal infrared radiation than carbon dioxide (CO₂), as assessed by its global warming potential (GWP) relative to CO₂. For a 100-yr time horizon and without considering climate feedbacks the GWP of CH₄-fossil is 29.8 (CH₄-non fossil GWP is 27), whereas the values reach 82.5 over a 20-year horizon for CH₄-fossil and 79.7 for CH₄-non fossil (Forster et al., 2021). Although global anthropogenic emissions of CH₄ are estimated at around 359 Tg CH₄ yr⁻¹ (Saunois et al., 2020), representing around 2.5% of the global CO₂ anthropogenic emissions when converted to units of carbon mass flux for the recent decade, the emissions-based effective radiative forcing of CH₄ concentrations has contributed ~31% (1.19 W m⁻²) to the additional radiative forcing from anthropogenic emissions of greenhouse gases and their precursors (3.84 W m⁻²) over the industrial era (1750-2019) (Forster et al., 2021). Changes in other chemical compounds such as nitrogen oxides (NO_x) or carbon monoxide (CO) also influence atmospheric CH₄ through changes to its atmospheric lifetime. Emissions of CH₄ contribute to the production of ozone, stratospheric water vapour, and CO₂, and most importantly affect its own lifetime (Myhre et al., 2013; Shindell et al., 2012). CH₄ has a short lifetime in the atmosphere (about 9 years for the year 2010, Prather et al., 2012). Hence a stabilisation or reduction of CH₄ emissions leads to the stabilisation or reduction of its atmospheric concentration (assuming no change in the chemical oxidants), and therefore its radiative forcing, in only a few decades. While reducing CO₂ emissions is necessary to stabilise long-term warming, reducing CH₄ emissions is recognized as an effective option to limit climate warming in the near-term (Shindell et al., 2012; Jackson et al., 2020; Ocko et al., 2021; UNEP, 2021), because of its shorter lifetime compared to CO₂.

The momentum around the potential of CH₄ to limit near-term warming has led to the launch of the Global Methane Pledge at the November 2021 Conference of the Parties (COP 26). Signed by 150 countries, this collective effort aims at reducing global CH₄ anthropogenic emissions at least 30 percent from 2020 levels by 2030 (Global Methane Pledge, 2023). Given that global baseline CH₄ emissions are expected to grow through 2030 (by an additional 20-50 Million tons (Mt) of CH₄, UNEP 2022), the CH₄ emission reductions currently needed to reach the Global Methane Pledge objective (UNEP,



194

195

196 197

198

199

200

201

202

203

204

205206

207

208

209210

211

212

213

214215

216

217

218219

220

221

222

223

224

225

226



2022) correspond to 36% of the projected baseline emissions in 2030 (ie. if no further emission reductions were implemented). This implies that large reductions of CH₄ emissions are needed to meet the Global Methane Pledge that is consistent also with the 1.5-2°C target of the Paris Agreement (UNEP, 2022). Moreover, because CH₄ is a precursor of important air pollutants such as ozone, CH₄ emissions reductions are required by two international conventions: the United Nations Framework Convention on Climate Change (UNFCCC) and the Convention on Long Range Transport of Air Pollution (CLRTAP), making this global CH₄ budget assessment all the more critical.

Changes in the magnitude and temporal variation (annual to inter-annual) of CH₄ sources and sinks over the past decades are characterised by large uncertainties (e.g., Kirschke et al., 2013; Saunois et al., 2017; Turner et al., 2019). Also, the decadal budget suggests relative uncertainties (hereafter reported as min-max ranges) of 20-35% for inventories of anthropogenic emissions in specific sectors (e.g., agriculture, waste, fossil fuels (Tibrewal et al., 2024)), 50% for biomass burning and natural wetland emissions, and up to 100% for other natural sources (e.g., inland waters, geological sources). The uncertainty in the chemical loss of CH₄ by OH, the predominant sink of atmospheric CH₄, has been s estimated using Prather et al. (2012) and Rigby et al. (2017) estimated this uncertainty at ~10% from the uncertainty in the reaction rate between CH₄ and OH, or using methyl-chloroform measurements. Bottom-up approaches (chemistry transport models) estimate the uncertainty of the chemical loss by OH at around 15-20% (Saunois et al., 2016, 2020). This uncertainty on the OH induced loss translates, in the top-down methods, into the minimum relative uncertainty associated with global CH₄ emissions, as other CH₄ sinks (atomic oxygen and chlorine oxidations, soil uptake) are much smaller and the atmospheric growth rate is well-defined (Dlugokencky et al., 2009). Globally, the contribution of natural CH₄ emissions to total emissions can be quantified by combining lifetime estimates with reconstructed pre-industrial atmospheric CH₄ concentrations from ice cores (assuming natural emissions have not been perturbed during the anthropocene) (e.g., Ehhalt et al., 2001). Regionally or nationally, uncertainties in emissions may reach 40-60% (e.g., for South America, Africa, China, and India, see Saunois et al., 2016).

To monitor emission reductions, for example to help conduct the Paris Agreement's stocktake, sustained and long-term monitoring of anthropogenic emissions per sector is needed in particular for hotspots of emissions that may be missed in inventories (Bergamaschi et al., 2018a; Pacala, 2010; Lauvaux et al., 2022). At the same time, reducing uncertainties in all individual CH₄ sources, and thus in the overall CH₄ budget remains challenging for at least four reasons. First, CH₄ is emitted by multiple processes, including natural and anthropogenic sources, point and diffuse sources, and sources associated with at least three different production origins (i.e., microbial, thermogenic, and pyrogenic). These multiple sources and processes require the integration of data from diverse scientific communities and across multiple temporal and spatial scales. The production of accurate bottom-up estimates is complicated by the fact that anthropogenic emissions result from leakage from fossil fuel production with large differences between countries depending on technologies and practices, the fact that many large leak events are sporadic, and the location of many emissions hotspots is not well known, and from uncertain emission factors used to summarise complex microbial processes in the agriculture and waste sectors. For the



228

229

230

231

232

233

234

235

236237

238

239

240

241

242243

244

245

246

247

248249

250

251

252

253

254

255

256

257

258

259



latter, examples include difficulties in upscaling methane emissions from livestock without considering the variety of animal weight, diet and environment, and difficulties in assessing emissions from landfills depending on waste type and waste management technology. Second, atmospheric CH₄ is removed mainly by chemical reactions in the atmosphere involving OH and other radicals that have very short lifetimes (typically ~1s). Due to the short lifetime of OH, the spatial and temporal distributions of OH are highly variable. While OH can be measured locally, calculating global CH₄ loss through OH measurements requires high-resolution global OH measurements (typically half an hour to integrate cloud cover, and 1 km spatially to consider OH high reactivity and heterogeneity) which is impossible from direct OH observations. As a result, OH can only be calculated through large scale atmospheric chemistry modelling. Those simulated OH concentrations from transport-chemistry models prescribed with emissions of precursor species affecting OH still show uncertain spatio-temporal distribution from regional to global scales (Zhao et al., 2019). Third, only the net CH₄ budget (sources minus sinks) is well constrained by precise observations of atmospheric growth rates (Dlugokencky et al., 2009), leaving the sum of sources and the sum of sinks uncertain. One distinctive feature of CH₄ sources compared to CO₂ fluxes is that the oceanic contribution to the global CH₄ budget is small (~1-3%), making CH4 source estimation predominantly a terrestrial endeavour (USEPA, 2010b). Finally, we lack comprehensive observations to constrain 1) the areal extent of different types of wetlands and inland freshwater (Kleinen et al., 2012, 2020, 2021, 2023; Stocker et al., 2014; Zhang et al., 2021), 2) models of wetland and inland freshwater emission rates (Melton et al., 2013; Poulter et al., 2017; Wania et al., 2013; Bastviken et al., 2011; Wik et al., 2016a; Rosentreter et al., 2021; Bansal et al., 2023; Lauerwald et al., 2023a; Stanley et al. 2023), 3) inventories of anthropogenic emissions (Höglund-Isaksson et al., 2020; Crippa et al., 2023; USEPA, 2019), and 4) atmospheric inversions, which aim to estimate CH₄ emissions from global to regional scales (Houweling et al., 2017; Jacob et al., 2022).

The global CH₄ budget inferred from atmospheric observations by atmospheric inversions relies on regional constraints from atmospheric sampling networks, which are relatively dense for northern mid-latitudes, with various high-precision and high-accuracy surface stations, but are sparser at tropical latitudes and in the Southern Hemisphere (Dlugokencky et al., 2011). Recently, the density of atmospheric observations has increased in the tropics due to satellite-based platforms that provide column-average CH₄ mixing ratios. Despite continuous improvements in the precision and accuracy of space-based measurements (e.g., Buchwitz et al., 2016), systematic errors greater than several ppb on total column observations can still limit the usage of such data to constrain surface emissions (e.g., Jacob et al., 2022). The development of robust bias corrections on existing data can help overcome this issue (e.g., Inoue et al., 2016) and satellite data are now widely used in atmospheric inversions where they provide more global information on the distribution of fluxes and highly complement the surface networks (e.g., Lu et al., 2021).

In this context, the Global Carbon Project (GCP) seeks to develop a complete picture of the carbon cycle by establishing common, consistent scientific knowledge to support policy development and actions to mitigate greenhouse gas emissions to the atmosphere (www.globalcarbonproject.org). The objective of this paper is to analyse and synthesise the current knowledge of the global CH₄ budget, by gathering results of observations and models to better understand and





quantify the main robust features of this budget, its remaining uncertainties, and to make recommendations for improvement. We combine results from a large ensemble of bottom-up approaches (e.g., process-based models for natural wetlands, data-driven approaches for other natural sources, inventories of anthropogenic emissions and biomass burning, and atmospheric chemistry models), and top-down approaches (including CH₄ atmospheric observing networks, atmospheric inversions inferring emissions and sinks from the assimilation of atmospheric observations into models of atmospheric transport and chemistry). The focus of this work is to update the previous assessment made for the period 2000-2017 (Saunosi et al., 2020)to the more recent 2000-2020 period. More in-depth analyses of trends and year-to-year changes are left to future publications. Our current paper is a living review, published at about four-year intervals, to provide an update and new synthesis of available observational, statistical, and model data for the overall CH₄ budget and its individual components.

Kirschke et al. (2013) was the first CH₄ budget synthesis followed by Saunois et al. (2016) and Saunois et al. (2020), with companion papers by Stavert et al. (2021) on regional CH₄ budgets and Jackson et al. (2020) focusing on the last year of the budget (2017). Saunois et al. (2020) covered 2000-2017 and reported CH₄ emissions and sinks for three time periods: 1) the latest calendar decade at that time (2000-2009), 2) data for the latest available decade (2008-2017), and 3) the latest available year (2017) at the time. Here, the Global Methane Budget (GMB) covers 2000-2020 split into the 2000-2009 decade, the 2010-2019 decade (where data are available), the year 2020 affected by COVID induced changes in human activity, and briefly for 2021-2023 as per data availability (Section 6). The CH₄ budget is presented at global, latitudinal, and regional scales and data can be downloaded from https://doi.org/10.18160/GKQ9-2RHT (Martinez et al., 2024).

Six sections follow this introduction. Section 2 presents the methodology used in the budget: units, definitions of source categories, regions, data analysis; and discusses the delay between the period of study of the budget and the release date. Section 3 presents the current knowledge about CH₄ sources and sinks based on the ensemble of bottom-up approaches reported here (models, inventories, data-driven approaches). Section 4 reports atmospheric observations and top-down atmospheric inversions gathered for this paper. Section 5, based on Sections 3 and 4, provides the updated analysis of the global CH₄ budget by comparing bottom-up and top-down estimates and highlighting differences. Section 6 discusses the recent changes in atmospheric CH₄ in relation with changes in CH₄ sources and sinks. Finally, Section 7 discusses future developments, missing components, and the most critical remaining uncertainties based on our update to the global CH₄ budget.

2 Methodology

2.1 Units used

Unless specified, fluxes are expressed in teragrams of CH₄ per year (1 Tg CH₄ yr⁻¹ = 10^{12} g CH₄ yr⁻¹), while atmospheric mixing ratios are expressed as dry air mole fractions, in parts per billion (ppb), with atmospheric CH₄ annual increases, G_{ATM} , expressed in ppb yr⁻¹. In the tables, we present mean values and ranges for the two decades 2000-2009 and 2010-





2019, together with results for the most recent available year (2020). Results obtained from previous syntheses (i.e., Saunois et al., 2020 and Saunois et al., 2016) are also given for the decade 2000-2009. Following Saunois et al. (2016) and considering that the number of studies is often relatively small for many individual source and sink estimates, uncertainties are reported as minimum and maximum values of the available studies, given in brackets. In doing so, we acknowledge that we do not consider the uncertainty of the individual estimates, and we express uncertainty as the range of available mean estimates, i.e., differences across measurements/methodologies considered. These minimum and maximum values are those

presented in Section 2.5 and exclude identified outliers.

The CH₄ emission estimates are provided with up to three significant digits, for consistency across all budget flux components and to ensure the accuracy of aggregated fluxes. Nonetheless, given the values of the uncertainties in the CH₄ budget, we encourage the reader to consider not more than two digits as significant for the global total budget.

2.2 Period of the budget and availability of data

The bottom-up estimates rely on global anthropogenic emission inventories, an ensemble of process-based models for wetlands emissions, and published estimates in the literature for other natural sources. The global gridded anthropogenic inventories (see Section (3.1.1) are updated irregularly, generally every 3 to 5 years. The last reported years of available inventories were 2018 or 2019 when we started the top-down modelling activity. In order to cover the period 2000-2020, it was necessary to extrapolate the anthropogenic inventory EDGARv6 (Crippa et al., 2021) to 2020 to use it as prior information for the anthropogenic emissions in the atmospheric inversion systems as explained in the supplementary material. The land surface (wetland) models were run over the full period 2000-2020 using dynamical wetland areas, derived by remote sensing data or other models of flooded area variability (Sect. 3.2.1).

The atmospheric inversions run until mid-2021, but the last year of reported inversion results is 2020, which represents a three-year lag with the present. This is due to the long time period it takes to acquire atmospheric in-situ data and integrate models. Even though satellite observations are processed operationally and are generally available with a latency of days to weeks, by contrast surface observations can lag from months to years because of the time for flask analyses and data quality checks in (mostly) non-operational chains. In addition, the final six months of inversions must be generally ignored because the estimated fluxes are not constrained by as many observations as the previous periods. Lastly, this budget presents an extended synthesis of the most recent development regarding inland water emissions (Sect. 3.2.2) and corrections associated with double counting with wetlands.

2.3 Definition of regions

Geographically, emissions are reported globally and for three latitudinal bands (90°S-30°N, 30-60°N, 60-90°N, only for gridded products). When extrapolating emission estimates forward in time (see Sect. 3.1.1), and for the regional budget presented by Stavert et al. (2021), a set of 19 regions (oceans and 18 continental regions, see supplementary Fig. S3) were



Asia.

329

330

331

332

333

334

335

336

337

338339

340

341

342

343

344

345

346

347348

349

350

351

352

353



used. As anthropogenic emissions are often reported by country, we define these regions based on a country list (Table S1).

This approach was compatible with all top-down and bottom-up approaches considered. The number of regions was chosen to be close to the widely used TransCom inter-comparison map (Gurney et al., 2004) but with subdivisions to separate the contribution from important countries or regions for the CH₄ cycle (China, South Asia, Tropical America, Tropical Africa, United States of America, and Russia). The resulting region definition is the same as that used for the Global Carbon Project (GCP) N₂O budget (Tian et al., 2020). Compared to Saunois et al. (2020), the Oceania region has been replaced by Australasia including only Australia and New Zealand. Other territories formerly in Oceania were included in Southeast

CH₄ is emitted by different processes (i.e., biogenic, thermogenic, or pyrogenic) and can be of anthropogenic or natural

2.4 Definition of source and sink categories

origin. Biogenic CH₄ is the final product of the decomposition of organic matter by methanogenic Archaea in anaerobic environments, such as water-saturated soils, swamps, rice paddies, marine and freshwater sediments, landfills, sewage and wastewater treatment facilities, or inside animal digestive systems. Thermogenic methane is formed on geological time scales by the breakdown of buried organic matter due to heat and pressure deep in the Earth's crust. Thermogenic CH₄ reaches the atmosphere through marine and land geological gas seeps. These CH₄ emissions are increased by human activities, for instance, the exploitation and distribution of fossil fuels. Pyrogenic CH4 is produced by the incomplete combustion of biomass and other organic materials. Peat fires, biomass burning in deforested or degraded areas, wildfires, and biofuel burning are the largest sources of pyrogenic CH₄. CH₄ hydrates, ice-like cages of frozen CH₄ found in continental shelves and slopes and below sub-sea and land permafrost, can be of either biogenic or thermogenic origin. Each of these three process categories has both anthropogenic and natural components. In the following, we present the different CH₄ sources depending on their anthropogenic or natural origin, which is relevant to climate policy. Compared to the previous budgets, marginal changes have been made regarding source categories (naming and grouping), to reflect the improved estimates for inland water sources and their indirect anthropogenic component. In the previous Global Methane Budgets (Saunois et al., 2016, 2020), natural and anthropogenic emissions were split in a way that did not correspond exactly to the definition used by the UNFCCC following the IPCC guidelines (IPCC, 2006), where, for pragmatic reasons, all emissions from managed land are typically reported as anthropogenic. For instance, we considered all wetlands as natural emissions, despite some wetlands being on managed land and their emissions being partly reported as anthropogenic in UNFCCC national communications. The human induced perturbation of climate, atmospheric CO₂, and nitrogen and sulfur deposition may cause changes in wetland sources we classified as natural. Following our previous definition, emissions from wetlands, inland freshwaters, thawing permafrost, or geological leaks are accountable for "natural" emissions, even though we acknowledge that climate change and other human perturbations (e.g., eutrophication) may cause changes in those emissions. CH₄ emissions from reservoirs were also considered as natural even though reservoirs



354

355

356

357

358

359

360361

362

363

364

365

366367

368369

370

371

372

373

374

375

376

377

378

379

380

381

382

383384

385

386



are human-made. Indeed, since the 2019 refinement to the IPCC guidelines (IPCC, 2019) emissions from reservoirs and other flooded lands are considered to be anthropogenic by the UNFCCC and should be reported as such. However these estimates are not provided by inventories and not systematically reported by all countries (especially non Annex-I countries). In this budget we rename "natural sources" to "natural and indirect anthropogenic sources" to acknowledge that CH₄ emissions from reservoirs, as well as from water bodies that were perturbed by agricultural activities (drainage, eutrophication, land use change) are indirect anthropogenic emissions. As a result, here, "natural and indirect anthropogenic sources" refer to "emissions that do not directly originate from fossil, agricultural, waste, and biomass burning sources" even if they are perturbed by anthropogenic activities and climate change. Natural and indirect anthropogenic emissions are split between "Wetlands and Inland Freshwaters" and "Other natural" emissions (e.g., wild animals, termites, land geological sources, oceanic geological and biogenic sources, and terrestrial permafrost). "Anthropogenic direct sources" are caused by direct human activities since pre-industrial/pre-agricultural time (3000-2000 BC, Nakazawa et al., 1993) including agriculture, waste management, fossil fuel-related activities and biofuel and biomass burning (yet we acknowledge that a small fraction of wildfires are naturally ignited). Direct anthropogenic emissions are split between: "Agriculture and waste emissions", "Fossil fuel emissions", and "Biomass and biofuel burning emissions", assuming that all types of fires are caused by anthropogenic activities. To conclude, this budget reports "direct anthropogenic", and "natural and indirect anthropogenic" methane emissions for the five main source categories explained above for both bottom-up and top-down approaches. The sinks of methane are split into the soil uptake that can be derived from land-surface models in the bottom-up budget, and the chemical sinks. The chemical sinks are estimated by either chemistry climate or chemistry transport models in the bottom-up budget, and are further detailed in terms of vertical distribution (troposphere and stratosphere) and oxidants. Bottom-up estimates of CH₄ emissions for some processes are derived from process-oriented models (e.g., biogeochemical models for wetlands, models for termites), inventory models (agriculture and waste emissions, fossil fuel emissions, biomass and biofuel burning emissions), satellite-based models (large scale biomass burning), or observation-based upscaling models for other sources (e.g., inland water, geological sources). From these bottom-up approaches, it is possible to provide estimates for more detailed source subcategories inside each main category described above (see budget in Table 3). However, the total CH₄ emission derived from the sum of independent bottom-up estimates remains unconstrained. For atmospheric inversions (top-down approach), atmospheric methane concentration observations provide a constraint on the global methane total source if we assume the global sink is known (OH and other oxidant prescribed), or inversions are optimising also for the chemical sink. OH estimates are constrained by methyl chloroform-inversion (Montzka et al., 2011; Rigby et al., 2017; Patra et al., 2021). The inversions reported in this work solve for the total net CH₄ flux at the surface (sum of sources minus soil uptake) (e.g., Pison et al., 2013), or a limited number of source categories (e.g., Bergamaschi et al., 2013). In most of the inverse systems the atmospheric oxidant concentrations were prescribed with pre-optimized or scaled OH fields, and thus the atmospheric sink is not optimised. The assimilation of CH₄ observations alone, as reported in





this synthesis, can help to separate sources with different locations or temporal variations but cannot fully separate individual sources where they overlap in space and time in some regions. Top-down global and regional CH₄ emissions per source category were nevertheless obtained from gridded optimised fluxes, for the inversions that separated emissions into the five main GCP categories. Alternatively, for the inversion that only solved for total emissions (or for other categories other than the five described above), the prior contribution of each source category at the spatial resolution of the inversion was scaled by the ratio of the total (or embedding category) optimised flux divided by the total (or embedding category) prior flux (Kirschke et al., 2013). In other words, the prior relative mix of sources at model resolution is kept in each grid cell while total emissions are given by the atmospheric inversions. The soil uptake was provided separately to report total gross surface emissions instead of net fluxes (sources minus soil uptake).

In summary, bottom-up models and inventories emissions are presented for all relevant source processes and grouped if needed into the five main categories defined above. Top-down inversion emissions are reported globally and for the five main emission categories.

2.5 Processing of emission maps and box-plot representation of emission budgets

Common data analysis procedures have been applied to the different bottom-up models, inventories and atmospheric inversions whenever gridded products exist. Gridded emissions from atmospheric inversions, land-surface models for wetland or biomass burning were provided at the monthly scale. Emissions from anthropogenic inventories are usually available as yearly estimates. These monthly or yearly fluxes were provided on a 1°x1° grid or re-gridded to 1°x1°, then converted into units of Tg CH₄ per grid cell. Inversions with a resolution coarser than 1° were downscaled to 1° by each modelling group. Land fluxes in coastal pixels were reallocated to the neighbouring land pixel according to our 1° land-sea mask, and vice-versa for ocean fluxes. Annual and decadal means used for this study were computed from the monthly or yearly gridded 1°x1° maps.

Budgets are presented as boxplots with quartiles (25%, median, 75%), outliers, and minimum and maximum values without outliers. Outliers were determined as values below the first quartile minus three times the interquartile range, or values above the third quartile plus three times the interquartile range. Mean values reported in the tables are represented as "+" symbols in the corresponding figures.

3 Methane sources and sinks: bottom-up estimates

For each source category, a short description of the relevant processes, original data sets (measurements, models) and related methodology are given. More detailed information can be found in original publication references, in Annex A2 where the sources of data used to estimate the different sources and sinks are summarised and compared with those used in Saunois et al. (2020) and in the Supplementary Material of this study when specified in the text. The emission estimates for each source





category are compared with Saunois et al. (2020) in Table 3 and with Saunois et al. (2016) in Table S12 for the decade 2000-

The main bottom-up global inventory datasets covering direct anthropogenic emissions from all sectors (Table 1) are from

the United States Environmental Protection Agency (USEPA, 2019), the Greenhouse gas and Air pollutant Interactions and

418 2009.

419

420

421422

423424

425

426

427

428

429

430

431

432433

434

435

436

437438

439

440441

442

443

444

445

446

447

448

3.1 Anthropogenic direct sources

3.1.1 Global inventories

Synergies (GAINS) model developed by the International Institute for Applied Systems Analysis (IIASA) (Höglund-Isaksson et al., 2020) and the Emissions Database for Global Atmospheric Research (EDGARv6 and v7, Crippa et al., 2021, 2023) compiled by the European Commission Joint Research Centre (EC-JRC) and Netherlands Environmental Assessment Agency (PBL). We also used the Community Emissions Data System for historical emissions (CEDS) (Hoesly et al., 2018) developed for climate modelling and the Food and Agriculture Organization (FAO) FAOSTAT emission database (Tubiello et al., 2022), which covers emissions from agriculture and land use (including peatland fires and biomass fires). These inventories are not independent as they may use the same activity data or emission factors, as discussed below. These inventory datasets report emissions from fossil fuel production, transmission, and distribution; livestock enteric fermentation; manure management and application; rice cultivation; solid waste and wastewater. Since the level of detail provided by country and by sector varies among inventories, the data were reconciled into common categories according to Table S2. For example, agricultural waste-burning emissions treated as a separate category in EDGAR, GAINS and FAO, are included in the biofuel sector in the USEPA inventory and in the agricultural sector in CEDS. The GAINS, EDGAR and FAO estimates of agricultural waste burning were excluded from this analysis (these amounted to 1-3 Tg CH₄ vr⁻¹ in recent decades) to prevent any potential overlap with separate estimates of biomass burning emissions (e.g., GFEDv4.1s; Giglio et al. (2013); van der Werf et al (2017)). In the inventories used here, emissions for a given region/country and a given sector are usually calculated following IPCC methodology (IPCC, 2006), as the product of an activity factor and its associated emission factor. An abatement coefficient may also be used, to account for any regulations implemented to control emissions (see e.g., Höglund-Isaksson et al., 2015). These datasets differ in their assumptions and data used for the calculation; however, they are not completely independent because they often use the same activity data and some of them follow the same IPCC guidelines (IPCC, 2006). While the USEPA inventory adopts emissions reported by the countries to the UNFCCC, other inventories (FAOSTAT, EDGAR and the GAINS model) produce their own estimates using a consistent approach for all countries, typically IPCC Tier 1 methods or deriving IPCC Tier 2 emission factors from country-specific information using a consistent methodology. These other inventories compile country-specific activity data and emission factor information or, if not available, adopt IPCC default factors (Tibrewal et al., 2024; Oreggioni et al., 2021; Höglund-Isaksson et al., 2020; Tubiello, 2019). CEDS takes a different approach (Hoesly et al., 2018) and combines data from GAINS, EDGAR and FAO depending on the sector. Then their first estimates are scaled to match other individual or region-





specific inventory values when available. This process maintains the spatial information in the default emission inventories while preserving consistency with country level data. The FAOSTAT dataset (hereafter FAO-CH₄) provides estimates at the country level and is limited to agriculture (CH₄ emissions from enteric fermentation, manure management, rice cultivation, energy usage, burning of crop residues, and prescribed burning of savannahs) and land-use (peatland fires and biomass burning). FAO-CH₄ uses activity data mainly from the FAOSTAT crop and livestock production database, as reported by countries to FAO (Tubiello et al., 2013), and applies mostly the Tier 1 IPCC methodology for emissions factors (IPCC, 2006), which depends on geographic location and development status of the country. For manure, the country-scale temperature was obtained from the FAO global agro-ecological zone database (GAEZv3.0, 2012). Although country emissions are reported annually to the UNFCCC by annex I countries, and episodically by non-annex I countries, data gaps of those national inventories do not allow the inclusion of these estimates in this analysis.

In this budget, we use the following versions of these inventories that were available at the start and during the analysis (see Table 1):

- EDGARv6 which provides yearly gridded emissions by sectors from 1970 to 2018 (Crippa et al., 2021; Oreggioni et al., 2021; EDGARv6 website https://edgar.jrc.ec.europa.eu/dataset_ghg60; Monforti Ferrario et al., 2021),
- EDGARv7, which provides yearly gridded emissions by sectors from 1970 to 2020 (monthly for some sectors), but emissions from fossil fuel energy are not separated (oil and gas, and coal are lumped together see Table S2) (EDGARv7 website https://edgar.jrc.ec.europa.eu/dataset_ghg70; Crippa et al., 2023).
- GAINS model scenario version 4.0 (Höglund-Isaksson et al., 2020) which provides an annual sectorial gridded product from 1990 to 2020 both by country and gridded. USEPA (USEPA, 2019), which provides 5-year sectorial totals by country from 1990 to 2020 (estimates from 2015 onward are a projection), with no gridded distribution available. The USEPA dataset was linearly interpolated to provide yearly values from 1990-2020.
- CEDS version v_2021_04_21 which provides gridded monthly and annual country-based emissions by sectors from 1970 to 2019 (Hoesly et al., 2018; O'Rourke et al., 2021). Fossil fuel emissions for 2020 have been updated using the methodology described for CO in Zheng et al. (2023).
- FAO-CH₄ (database accessed in December 2022, FAO, 2022) containing annual country level data for the period 1961-2020, for rice, manure, and enteric fermentation; and 1990-2020 for burning savannah, crop residue and non-agricultural biomass burning.

3.1.2 Total anthropogenic direct emissions

We calculated separately the total anthropogenic emissions for each inventory by adding its values for "Agriculture and waste", "Fossil fuels" and "Biofuels" with additional large-scale biomass burning emissions data (Sect. 3.1.5). This method avoids double counting and ensures consistency within each inventory. This approach was used for the EDGARv6 and v7, CEDS and GAINS inventories, but we kept the USEPA inventory as originally reported because it includes its own estimates



481

482

483

484 485

486

487

488

489

490

491

492493

494

495

496497

498 499

500501

502

503

504

505

506

507

508

509

510511

512

513



of biomass burning emissions. FAO-CH4 was only included in the range reported for the "Agriculture and waste" category. For the latter, we calculated the range and mean value as the sum of the mean and range of the three anthropogenic subcategory estimates "Enteric fermentation and Manure", "Rice", and "Landfills and Waste". The values reported for the upper-level anthropogenic categories ("Agriculture and waste", "Fossil fuels" and "Biomass burning & biofuels") are therefore consistent with the sum of their subcategories, although there might be small percentage differences between the reported total anthropogenic emissions and the sum of the three upper-level categories. This approach provides a more accurate representation of the range of emission estimates, avoiding an artificial expansion of the uncertainty attributable to subtle differences in the definition of sub-sector categorisations between inventories. Based on the ensemble of databases detailed above, total direct anthropogenic emissions were 358 [329-387] Tg CH₄ yr⁻¹ for the decade 2010-2019 (Table 3, including biomass and biofuel burning) and 331 [305-365] Tg CH₄ yr⁻¹ for the decade 2000-2009. Our estimate for the 2000-2009 decade is within the range of Saunois et al. (2020) (334 [321-358]), Saunois et al. (2016) (338 Tg CH4 yr-1 [329-342]) and Kirschke et al. (2013) (331 Tg CH₄ yr⁻¹ [304-368]) for the same period. The slightly larger range reported herein with respect to previous estimates is due to the USEPA lower estimate for agriculture, waste and fossil emissions associated with the lowest estimate of biomass burning. Figure 2 (left) summarises or projects global CH₄ emissions of anthropogenic sources (including biomass and biofuel burning) by different datasets between 2000 and 2050. The datasets consistently estimate total anthropogenic emissions of ~300 Tg CH₄ yr⁻¹ in 2000. For the Sixth Assessment Report of the IPCC, seven main Shared Socioeconomic Pathways (SSPs) were defined for future climate projections in the Coupled Model Intercomparison Project 6 (CMIP6) (Gidden et al., 2019; O'Neill et al., 2016) ranging from 1.9 to 8.5 W m⁻² radiative forcing by the year 2100 (as shown by the number in the SSP names). For the 1970-2015 period, historical emissions used in CMIP6 (Feng et al., 2019) combine anthropogenic emissions from CEDS (Hoesly et al., 2018) and a climatological value from the GFEDv4.1s biomass burning inventory (van Marle et al., 2017). The harmonised scenarios used for CMIP6 activities start in 2015 at 388 Tg CH₄ yr⁻¹, which corresponds to the higher range of our estimates. Since CH₄ emissions continue to track scenarios that assume no or minimal climate policies (SSP5 and SSP3), it may indicate that climate policies, when present, have not yet produced sufficient results to change the emissions trajectory substantially (Nisbet et al., 2019). After 2015, the SSPs span a range of possible outcomes, but current emissions appear likely to follow the higher-emission trajectories over the next decade in terms of trend, and the peak year has not yet been reached. This illustrates the challenge of methane mitigation that lies ahead to help reach the goals of the Paris Agreement. In addition, estimates of methane atmospheric concentrations (Meinshausen et al., 2017, 2020) from the harmonised scenarios (Riahi et al., 2017) indicate that observations of global CH₄ concentrations fall well within the range of scenarios (Fig. 2 right). The CH₄ concentrations are estimated using a simple exponential decay with inferred natural emissions (Meinshausen et al., 2011), and the emergence of any trend between observations and scenarios needs to be confirmed in the following years. However, the current observed concentrations and emissions estimates lie in the upper range of the former RCPs scenarios starting in 2005 (Fig. S1). In the future, it will be important to monitor the trends from





514 2015 (the Paris Agreement) and from 2020 (Global Methane Pledge) estimated in inventories and from atmospheric 515 observations, and compare them to various scenarios.

3.1.3 Fossil fuel production and use

Most anthropogenic CH₄ emissions related to fossil fuels come from the exploitation, transportation, and usage of coal, oil, and natural gas. Additional emissions reported in this category include small industrial contributions such as the production of chemicals and metals, fossil fuel fires (e.g., underground coal mine fires and the Kuwait oil and gas fires), and transport (road and non-road transport). CH₄ emissions from the oil processing industry (e.g., refining) and production of charcoal are estimated to be a few Tg CH₄ yr⁻¹ only and are included in the transformation industry sector in the inventory. Fossil fuel fires are included in the subcategory "Oil & Gas". Emissions from industries, road and, non-road transport are reported apart from the two main subcategories "Oil & Gas" and "Coal", as in Saunois et al. (2020) and contrary to Saunois et al. (2016); each of these amounts to about 2 to 5 Tg CH₄ yr⁻¹ (Table 3). The large range (1-9 Tg CH₄ yr⁻¹) is attributable to difficulties in allocating some sectors to these sub-sectors consistently among the different inventories (See Table S2). The spatial distribution of CH₄ emissions from fossil fuels is presented in Fig. 3 based on the mean gridded maps provided by CEDS, EDGARv6, and GAINS for the 2010-2019 decade; USEPA lacks a gridded product.

Global mean emissions from fossil fuel-related activities, other industries and transport are estimated from the four global inventories (Table 1) to be of 120 [117-125] Tg CH₄ yr⁻¹ for the 2010-2019 decade (Table 3), but with large differences in the rate of change during this period across inventories. The sector accounts on average for 34% (range 31-42%) of total global anthropogenic emissions.

Coal mining.

During mining, CH₄ is emitted primarily from ventilation shafts, where large volumes of air are pumped in and out of the mine to keep the CH₄ mixing ratio below 0.5% to avoid accidental ignition, and from dewatering operations. In countries of the Organization for Economic Co-operation and Development (OECD), coalbed CH₄ is often extracted as fuel up to ten years before the coal mine starts operation, thereby reducing the CH₄ channelled through ventilation shafts during mining. In many countries, large quantities of ventilation air CH₄ are still released to the atmosphere or flared, despite efforts to extend coal mine gas recovery under the UNFCCC Clean Development Mechanisms (http://cdm.unfccc.int). CH₄ leaks also occur during post-mining handling, processing, and transportation. Some CH₄ is released from coal waste piles and abandoned mines; while emissions from these sources were believed to be low (IPCC, 2000), recent work has estimated these at 22 billion m³ (compared to 103 billion m³ from functioning coal mines) in 2010 with emissions projected to increase into the future (Kholod et al., 2020).

In 2020, more than 35% (IEA, 2023a) of the world's electricity is still produced from coal. This contribution grew in the 2000s at the rate of several percent per year, driven by Asian economic growth where large reserves exist, but global coal





consumption declined between 2014 and 2020. In 2020, the top ten largest coal producing nations accounted for ~90% of total world CH₄ emissions from coal mining; among them, the top three producers (China, United States of America, and India) produced almost two-thirds (66%) of the world's coal (IEA, 2021).

Global estimates of CH₄ emissions from coal mining show a reduced range of 37-44 Tg CH₄ yr⁻¹ for 2010-2019, compared to the previous estimate for 2008-2017 in Saunois et al. (2020) reporting a range of 29-61 Tg CH₄ yr⁻¹ for 2008-2017. This reduced range probably results from using similar activity data (mostly from IEA statistics) in the different inventories. The highest value of the range in Saunois et al. (2020) came from the CEDS inventory while the lowest came from USEPA. CEDS seems to have revised downward their estimate compared to the previous version used in Saunois et al. (2020). There were previously large discrepancies in Chinese coal emissions, with a large overestimation from EDGARv4.2 on which CEDS was based. As highlighted by Liu et al. (2021a), a county-based inventory of Chinese methane emissions also confirms the overestimation of previous EDGAR inventories and estimated total anthropogenic Chinese emissions at 38.2±5.5 Tg CH₄ yr⁻¹ for 2000-2008 (Liu et al., 2021a). Coal mining emission factors depend strongly on the type of coal extraction (underground mining emits up to 10 times more than surface mining), the geological underground structure (region-specific), history (basin uplift), and the quality of the coal (brown coal (lignite) emits more than hard coal (anthracite)). Finally, the different emission factors derived for coal mining is the main reason for the differences between inventories globally (Fig. 2).

For the 2010-2019 decade, methane emissions from coal mining represent 33% of total fossil fuel-related emissions of CH₄ (40 [37-44] Tg CH₄ yr⁻¹). An additional very small source corresponds to fossil fuel fires (mostly underground coal fires, ~0.15 Tg yr⁻¹ any year in EDGARv7).

Oil and natural gas systems.

This sub-category includes emissions from both conventional and shale oil and gas exploitation. Natural gas is composed primarily of CH₄, so both fugitive and planned emissions during the drilling of wells in gas fields, extraction, transportation, storage, gas distribution, end use, and incomplete combustion in gas flares emit CH₄ (Lamb et al., 2015; Shorter et al., 1996). Persistent fugitive emissions (e.g., due to leaky valves and compressors) should be distinguished from intermittent emissions due to maintenance (e.g., purging and draining of pipes) or incidents. During transportation, fugitive emissions can occur in oil tankers, fuel trucks and gas transmission pipelines, attributable to corrosion, manufacturing, and welding faults. According to Lelieveld et al. (2005), CH₄ fugitive emissions from gas pipelines should be relatively low, however, old distribution networks in some cities may have higher rates, especially those with cast-iron and unprotected steel pipelines (Phillips et al., 2013). Measurement campaigns in cities within the USA (e.g., McKain et al., 2015) and Europe (e.g., Defratyka et al., 2021) revealed that significant emissions occur in specific locations (e.g., storage facilities, city natural gas fueling stations, well and pipeline pressurisation/depressurisation points, sewage systems, and furnaces of buildings) along the distribution networks (e.g., Jackson et al., 2014a; McKain et al., 2015; Wunch et al., 2016). However, CH₄ emissions



579

580 581

582

583

584

585

586587

588

589

590591

592

593594

595

596

597

598 599

600

601

602

603

604 605

606

607

608

609

610



maintenance, making urban emissions difficult to scale-up from measurement campaigns, although attempts have been made (e.g., Defratyka et al., 2021). In many facilities, such as gas and oil fields, refineries, and offshore platforms, most of the associated and other waste gas generated will be flared for security reasons with almost complete conversion to CO₂, however, due to the large quantities of waste gas generated, small fractions of gas still being vented make up relatively large quantities of methane. These two processes are usually considered together in inventories of oil and gas industries. In addition, single-point failure of natural gas infrastructure can leak CH₄ at high rate for months, such as at the Aliso Canyon blowout in the Los Angeles, CA (Conley et al., 2016) or the shale gas well blowout in Ohio (Pandey et al., 2019), thus hampering emission control strategies. Production of natural gas from the exploitation of hitherto unproductive rock formations, especially shale, began in the 1970s in the US on an experimental or small-scale basis, and then, from the early 2000s, exploitation started at a large commercial scale. The shale gas contribution to total dry natural gas production in the United States reached 82% in 2023, growing rapidly from 48% in 2013 (IEA, 2023b). The possibly larger emission factors from shale gas compared to conventional gas, have been widely debated (e.g., Cathles et al., 2012; Howarth, 2019; Lewan, 2020). However, the latest studies tend to infer similar emission factors in a narrow range of 1-3% (Alvarez et al., 2018; Peischl et al., 2015; Zavala-Araiza et al., 2015), different from the widely spread rates of 3-17% from previous studies (e.g., Caulton et al., 2014; Schneising et al., 2014). CH₄ emissions from oil and natural gas systems vary greatly in different global inventories (67 to 80 Tg yr⁻¹ in 2020, Table 3). The inventories generally rely on the same sources and magnitudes for activity data, with the derived differences therefore resulting primarily from different methodologies and parameters used, including emission factors. Those factors are country- or even site-specific and the few field measurements available often combine oil and gas activities (Brandt et al., 2014), resulting in high uncertainty in emission estimates for many major oil and gas producing countries. Depending on the region, the IPCC 2006 default emission factors may vary by two orders of magnitude for oil production and one order for gas production. For instance, the GAINSv4.0 estimate of CH₄ emissions from US oil and gas systems in 2015 Tg, which is almost twice as high as EDGARv8.0 at 8.4 Tg and USEPA (UNFCCC, 2023) at 9.5 Tg. The difference can partly be explained by GAINS using a bottom-up methodology to derive country- and year-specific flows of associated petroleum gas and attributing these to recovery/reinjection, flaring or venting (Höglund-Isaksson, 2017), and partly to GAINS using a higher emission factor for unconventional gas production (Höglund-Isaksson et al., 2020). Recent quantifications using satellite observations and inversion estimate a relatively stable trend for US oil and gas systems emissions since 2010, with Lu et al. (2023) estimating 14.6 Tg for 2010, 15.9 Tg for 2014 and 15.6 Tg for 2019, Shen et al. (2022) estimating a mean of 12.6 Tg for 2018-2020, and Massakkers et al (2021) a mean of 11.1 Tg for 2010 to 2015. The stable top-down trend for the US appears not well captured in the bottom-up inventories from GAINS and EDGAR, which tend to show an increasing trend driven by increase in production volumes.

vary significantly from one city to another depending, in part, on the age of city infrastructure and the quality of its



624

625



612 and Janssens-Maenhout, 2014; Pétron et al., 2014; Zavala-Araiza et al., 2015), albeit not all (Allen et al., 2013; Cathles et 613 al., 2012; Peischl et al., 2015), suggest that the methane emissions from oil and gas industry are underestimated by 614 inventories, industries, and agencies, including the USEPA. Lauvaux et al. (2022) showed that emissions from a few high-615 emitting facilities, i.e., super-emitters (> 20 t hr⁻¹), which are usually sporadic in nature, and not accounted for in the 616 inventories, could represent 8-12% of global oil & gas emissions, or around 8 Tg CH₄ yr⁻¹. These high emitting points, located on the conventional part of the facilities, could be avoided through better operating conditions and repair of 617 malfunctions. Over the last decade, absolute CH₄ emissions almost certainly increased, since USA crude oil production 618 619 doubled and natural gas production rose by about 50% (IEA, 2023a). However, global implications of the rapidly growing 620 shale gas activity in the US remain to be determined precisely. 621 For the 2010-2019 decade, CH₄ emissions from upstream and downstream oil and natural gas sectors are estimated to represent about 56% of total fossil CH₄ emissions (67 [57-74] Tg CH₄ yr⁻¹, Table 3) based on global inventories, with a 622 623 lower uncertainty range than for coal emissions for most countries. However, it is worth noting that 8 Tg CH₄ yr⁻¹ should

Most studies (Alvarez et al., 2018; Brandt et al., 2014; Jackson et al., 2014b; Karion et al., 2013; Moore et al., 2014; Olivier

3.1.4 Agriculture and waste sector

This main category includes CH₄ emissions related to livestock production (i.e., enteric fermentation in ruminant animals and manure management), rice cultivation, landfills, and wastewater handling. Of these activities, globally and in most countries, livestock is by far the largest source of CH₄, followed by waste handling and rice cultivation. Conversely, field burning of agricultural residues is a minor source of CH₄ reported in emission inventories (a few Tg at the global scale).

be added on top of this estimate to acknowledge the ultra-emitters contribution, as done in Tibrewal et al (2024).

- The spatial distribution of CH₄ emissions from agriculture and waste handling is presented in Fig. 3 based on the mean
- gridded maps provided by CEDS, EDGARv6 and GAINS over the 2010-2019 decade.
- Global emissions from agriculture and waste for the period 2010-2019 are estimated to be 211 [195-231] Tg CH₄ yr⁻¹ (Table
- 3), representing 60% of total direct anthropogenic emissions. Agriculture emissions amount to 144 Tg CH₄ yr⁻¹, 40% of the
- direct anthropogenic emissions, with the rest coming from the fossil fuel sector (34%), waste (19%) and biomass (5%) and
- biofuel (3%) burning .
- 636 Livestock: Enteric fermentation and manure management. Domestic ruminants such as cattle, buffalo, sheep, goats, and
- camels emit CH₄ as a by-product of the anaerobic microbial activity in their digestive systems (Johnson et al., 2002). The
- 638 very stable temperatures (about 39°C) and pH (6.5-6.8) within the rumen of domestic ruminants, along with a constant plant
- 639 matter flow from grazing (cattle graze many hours per day), allow methanogenic Archaea residing within the rumen to
- produce CH₄. CH₄ is released from the rumen mainly through the mouth of multi-stomached ruminants (eructation, ~90%
- of emissions) or absorbed in the blood system. The CH₄ produced in the intestines and partially transmitted through the
- rectum is only $\sim 10\%$.





644645

646

647

648

649

650

651

652

653

654

655

656

657

658 659

660

661

662

663

664

665

666

667668

669670

671

672673

674

675

The total number of livestock continues to grow steadily. There are currently (2020) about 1.5 billion cattle globally, almost 1.3 billion sheep, and nearly as many goats (http://www.fao.org/faostat/en/#data/GE). Livestock numbers are linearly related to CH₄ emissions in inventories using the Tier 1 IPCC approach such as FAOSTAT. In practice, some non-linearity may arise due to dependencies of emissions on the total weight of the animals and their diet, which are better captured by Tier 2 and higher approaches. Cattle, due to their large population, large individual size, and particular digestive characteristics, account for the majority of enteric fermentation CH₄ emissions from livestock worldwide (Tubiello, 2019; FAO, 2022), particularly in intensive agricultural systems in wealthier and emerging economies, including the United States (USEPA, 2016). CH₄ emissions from enteric fermentation also vary from one country to another as cattle may experience diverse living conditions that vary spatially and temporally, especially in the tropics (Chang et al., 2019). Anaerobic conditions often characterise manure decomposition in a variety of manure management systems globally (e.g., liquid/slurry treated in lagoons, ponds, tanks, or pits), with the volatile solids in manure producing CH₄. In contrast, when manure is handled as a solid (e.g., in stacks or dry-lots) or deposited on pasture, range, or paddock lands, it tends to decompose aerobically and to produce little or no CH₄. However aerobic decomposition of manure tends to produce nitrous oxide (N₂O), which has a larger global warming impact than CH₄. Ambient temperature, moisture, energy contents of the feed, manure composition, and manure storage or residency time affect the amount of CH₄ produced. Despite these complexities, most global datasets used herein apply a simplified IPCC Tier 1 approach, where amounts of manure treated depend on animal numbers and simplified climatic conditions by country. Global CH₄ emissions from enteric fermentation and manure management are estimated in the range of 114-124 Tg CH₄ vr ¹, for the year 2020, in the GAINS model and CEDS, USEPA, FAO-CH₄ and EDGARv7 inventories. Using the Tier 2 method adopted from the 2019 Refinement to 2006 IPCC guidelines, a recent study (Zhang et al., 2022) estimated that global CH₄ emissions from livestock increased from 31.8 [26.5-37.1] (mean [minimum-maximum of 95% confidence interval) Tg CH₄ yr⁻¹ in 1890 to 131.7 [109.6–153.7] Tg CH₄ yr⁻¹ in 2019, a fourfold increase in the past 130 years. Chang et al. (2021) estimates enteric fermentation and manure management emissions based on mixed Tier 1&2 and Tier1 approaches and calculate livestock emissions being 120±13 and 136±15 Tg CH₄ yr⁻¹ respectively for 2018. Chang et al. (2021) and Zhang et al. (2022) estimates for 2018 or 2019 are on average a bit higher than the inventories estimates but in agreement considering the uncertainties. For the period 2010-2019, we estimated total emissions of 112 [107-118] Tg CH₄ yr⁻¹ for enteric fermentation and manure management, about one third of total global anthropogenic emissions. Rice cultivation. Most of the world's rice is grown in flooded paddy fields (Baicich, 2013). The water management systems, particularly flooding, used to cultivate rice are one of the most important factors influencing CH₄ emissions and one of the most promising approaches for CH₄ emission mitigation: periodic drainage and aeration not only cause existing soil CH₄ to oxidise, but also inhibit further CH₄ production in soils (Simpson et al., 1995; USEPA, 2016; Zhang, 2016). Upland rice

fields are not typically flooded, and therefore are not a significant source of CH₄. Other factors that influence CH₄ emissions





- 676 from flooded rice fields include fertilisation practices (i.e., the use of urea and organic fertilisers), soil temperature, soil type (texture and aggregated size), rice variety and cultivation practices (e.g., tillage, seeding, and weeding practices) (Conrad et 677 678 al., 2000; Kai et al., 2011; USEPA, 2011; Yan et al., 2009). For instance, CH₄ emissions from rice paddies increase with 679 organic amendments (Cai et al., 1997) but can be mitigated by applying other types of fertilisers (mineral, composts, biogas 680 residues) or using wet seeding (Wassmann et al., 2000). 681 The geographical distribution of rice emissions has been assessed by global (e.g., Janssens-Maenhout et al., 2019; Tubiello, 682 2019; USEPA, 2012) and regional (e.g., Castelán-Ortega et al., 2014; Chen et al., 2013; Chen and Prinn, 2006; Peng et al., 2016; Yan et al., 2009; Zhang and Chen, 2014) inventories and land surface models (Li et al., 2005; Pathak et al., 2005; Ren 683
- 2016; Yan et al., 2009; Zhang and Chen, 2014) inventories and land surface models (Li et al., 2005; Pathak et al., 2005; Ren et al., 2011; Spahni et al., 2011; Tian et al., 2010, 2011; Zhang, 2016). The emissions show a seasonal cycle, peaking in the summer months in the extra-tropics associated with monsoons and land management. Emissions from rice paddies are influenced not only by the extent of rice field area, but also by changes in the productivity of plants (Jiang et al., 2017) as these alter the CH₄ emission factor used in inventories. However, the inventories considered herein are largely based on IPCC Tier 1 methods, which mainly scale with cultivated areas and include regional specific emission factors but do not account for changes in plant productivity and detailed cultivation practices.
- The largest emissions from rice cultivation are found in Asia accounting for 30 to 50% of global emissions (Fig. 3). The decrease of CH₄ emissions from rice cultivation over recent decades is confirmed in most inventories, because of the decrease in rice cultivation area, changes in agricultural practices, and a northward shift of rice cultivation since the 1970s, as in China (e.g., Chen et al., 2013).
- Based on the global inventories considered in this study, global CH₄ emissions from rice paddies are estimated to be 32 [25-37] Tg CH₄ yr⁻¹ for the 2010-2019 decade (Table 3), or about 9% of total global anthropogenic emissions of CH₄. These estimates are consistent with the 29 Tg CH₄ yr⁻¹ estimated for the year 2000 by Carlson et al. (2017).
- Waste management. This sector includes emissions from managed and non-managed landfills (solid waste disposal on land), and wastewater handling, where all kinds of waste are deposited. CH₄ production from waste depends on the pH, moisture, and temperature of the material. The optimum pH for CH₄ emission is between 6.8 and 7.4 (Thorneloe et al., 2000). The development of carboxylic acids leads to low pH, which limits methane emissions. Food or organic waste, such as leaves and grass clippings, ferment quite easily, while wood and wood products generally ferment slowly, and cellulose and lignin even more slowly (USEPA, 2010a).
- Waste management was responsible for about 11% of total global direct anthropogenic CH₄ emissions in 2000 (Kirschke et al., 2013). A recent assessment of CH₄ emissions in the USA found landfills to account for almost 26% of total USA anthropogenic CH₄ emissions in 2014, the largest contribution of any single CH₄ source in the United States of America (USEPA, 2016). In Europe, gas control has been mandatory on all landfills since 2009, and more importantly for CH₄ emissions, the EU Landfill Directive (1999) with subsequent amendments, has diverted most biodegradable waste away





- from landfills towards source separation, recycling, composting and energy recovery, and with a legally binding target not
- to landfill more than 10% of municipal solid waste by 2035.
- 710 Wastewater from domestic and industrial sources is treated in municipal sewage treatment facilities and private effluent
- 711 treatment plants. The principal factor in determining the CH₄ generation potential of wastewater is the amount of degradable
- 712 organic material in the wastewater. Wastewater with high organic content is treated anaerobically, which leads to increased
- emissions (André et al., 2014). Excessive and rapid urban development worldwide, especially in Asia and Africa, could
- enhance methane emissions from waste unless adequate mitigation policies are designed and implemented rapidly.
- The GAINS model and CEDS and EDGAR inventories give robust emission estimates from solid waste in the range of 37-
- 716 42 Tg CH₄ yr⁻¹ for the year 2019, and more uncertain wastewater emissions in the range 20-45 Tg CH₄ yr⁻¹1.
- In our study, the global emission of CH₄ from waste management is estimated in the range of 56-80 Tg CH₄ yr⁻¹ for the
- 718 2010-2019 period with a mean value of 69 Tg CH₄ yr⁻¹, about 19% of total global anthropogenic emissions.

3.1.5 Biomass and biofuel burning

- 720 This category includes CH₄ emissions from biomass burning in forests, savannahs, grasslands, peats, agricultural residues,
- as well as, from the burning of biofuels in the residential sector (stoves, boilers, fireplaces). Biomass and biofuel burning
- 722 emit CH₄ under incomplete combustion conditions (i.e., when oxygen availability is insufficient for complete combustion),
- for example in charcoal manufacturing and smouldering fires. The amount of CH₄ emitted during the burning of biomass
- depends primarily on the amount of biomass, burning conditions, fuel moisture and the specific material burned.
- 725 In this study, we use large-scale biomass burning (forest, savannah, grassland, and peat fires) from five biomass burning
- 726 inventories (described below) and the biofuel burning contribution from anthropogenic emission inventories (EDGARv6
- and v7, CEDS, GAINS and USEPA). The spatial distribution of emissions from the burning of biomass and biofuel over
- the 2010-2019 decade is presented in Fig. 3 based on data listed in Table 1.
- At the global scale, during the period of 2010-2019, biomass and biofuel burning generated CH₄ emissions of 28 [21-39] Tg
- 730 CH₄ yr⁻¹ (Table 3), of which 30-50% is from biofuel burning.

731

719

- 732 **Biomass burning.** Fire is an important disturbance event in terrestrial ecosystems globally (van der Werf et al., 2010), and
- can be of either natural (typically ~10% of fires, ignited by lightning strikes or started accidentally) or anthropogenic origin
- 734 (~90%, human initiated fires) (USEPA, 2010b, chapter 9.1). As previously noted all fires are accounted as anthropogenic in
- 735 Table 3. Anthropogenic fires are concentrated in the tropics and subtropics, where forests, savannahs and grasslands may
- 736 be burned to clear land for agricultural purposes or to maintain pastures and rangelands. Small fires associated with
- agricultural activity, such as field burning and agricultural waste burning, are often not well detected by remote sensing
- methods and are instead estimated based on cultivated area.





- Emission rates of biomass burning vary with biomass loading (depending on the biomes) at the location of the fire, the efficiency of the fire (depending on the vegetation type), the fire type (smouldering or flaming) and emission factor (mass
- of the considered species / mass of biomass burned). Depending on the approach, these parameters can be derived using
- satellite data and/or biogeochemical model, or through simpler IPCC default approaches.
- In this study, we use five products to estimate biomass burning emissions. The Global Fire Emission Database (GFED) is
- the most widely used global biomass burning emission dataset and provides estimates from 1997 onwards. Here, we use
- 745 GFEDv4.1s (van der Werf et al., 2017), based on the Carnegie-Ames-Stanford-Approach (CASA) biogeochemical model
- (van der Werf et al., 2010) driven by satellite derived vegetation characteristics and burned area mostly from the MODerate
- 747 resolution Imaging Sensor, MODIS (Giglio et al., 2013). GFEDv4.1s (with small fires) is available at a 0.25° resolution and
- on a daily basis from 1997 to 2020. One characteristic of the GFEDv4.1s burned area is that small fires are better accounted
- for compared to GFEDv4.1 (Randerson et al., 2012), increasing carbon emissions by approximately 35% at the global scale.
- 750 The latest version GFEDv5 (Chen et al., 2023) suggest 61% higher burned area than GFEDv4.1s, in closer agreement with
- burned area products from higher resolution satellite sensors. The next budget would benefit from GFEDv5 to revisit the
- 752 estimates of biomass burning emissions (which would likely go up) based on more specific comparison studies.
- 753 The Quick Fire Emissions Dataset (QFED) is calculated using the fire radiative power (FRP) approach, in which the thermal
- energy emitted by active fires (detected by MODIS) is converted to an estimate of CH₄ flux using biome specific emissions
- 755 factors and a unique method of accounting for cloud cover. Further information related to this method and the derivation of
- 756 the biome specific emission factors can be found in Darmenov and da Silva (2015). Here we use the historical QFEDv2.5
- product available daily on a 0.1x0.1 grid for 2000 to 2020.
- The Fire INventory from the National Center for Atmospheric Research (FINNv2.5, Wiedinmyer et al., 2023) provides
- 759 daily, 1 km resolution estimates of gas and particle emissions from open burning of biomass (including wildfire, agricultural
- fires and prescribed burning) over the globe for the period 2002-2020. FINNv2.5 uses MODIS and VIIRS satellite
- observations for active fires, land cover and vegetation density.
- We use v1.3 of the Global Fire Assimilation System (GFAS, Kaiser et al., 2012), which calculates emissions of biomass
- 563 burning by assimilating Fire Radiative Power (FRP) observations from MODIS at a daily frequency and 0.5° resolution and
- 764 is available for 2000-2020.
- 765 The FAO-CH₄ yearly biomass burning emissions are based on the most recent MODIS 6 burned area products (Prosperi et
- al., 2020), coupled with a pixel level (500 m) implementation of the IPCC Tier 1 approach, and are available from 1990 to
- 767 2020 (Table 1).
- 768 The differences in emission estimates for biomass burning arise from specific geographical and meteorological conditions
- 769 and fuel composition, which strongly impact combustion completeness and emission factors. The latter vary greatly
- according to fire type, ranging from 2.2 g CH₄ kg⁻¹ dry matter burned for savannah and grassland fires up to 21 g CH₄ kg⁻¹
- dry matter burned for peat fires (van der Werf et al., 2010). Biomass burning emissions encountered large inter annual





- variability related to meteorological conditions, with generally higher emissions during El-Nino periods as in 2019 (20 [14-
- 773 28] Tg CH₄ yr⁻¹), 2015 (22 [15-28] Tg CH₄ yr⁻¹) and 2010 to a lesser extent (18 [15-29] Tg CH₄ yr⁻¹).
- In this study, based on the five aforementioned products, biomass burning emissions are estimated at 17 Tg CH₄ yr⁻¹ [12-
- 775 24] for 2010-2019, representing about 5% of total global anthropogenic CH₄ emissions.

Biofuel burning. Burning of biomass to produce energy for domestic, industrial, commercial, or transportation purposes is hereafter called biofuel burning. A largely dominant fraction of CH₄ emissions from biofuel burning comes from domestic cooking or heating in stoves, boilers, and fireplaces, mostly in open cooking fires where wood, charcoal, agricultural residues, or animal dung are burned. It is estimated that more than two billion people, mostly in developing countries, use solid biofuels to cook and heat their homes daily (André et al., 2014), and yet CH₄ emissions from biofuel combustion have received relatively little attention. Biofuel burning estimates are gathered from the CEDS, USEPA, GAINS and EDGAR inventories. Due to the sectoral breakdown of the EDGAR and CEDS inventories the biofuel component of the budget has been estimated as equivalent to the "RCO - Energy for buildings" sector as defined in Worden et al. (2017) and Hoesly et al. (2018) (Table S2). This is equivalent to the sum of the IPCC 1A4a_Commercial-institutional, 1A4b_Residential, 1A4c_Agriculture-forestry-fishing and 1A5_Other-unspecified reporting categories. This definition is consistent with that used in Saunois et al. (2016) and Kirschke et al. (2013). While this sector incorporates biofuel use, it also includes the use of other combustible materials (e.g., coal or gas) for small-scale heat and electricity generation within residential and commercial premises. Data provided by the GAINS inventory suggests that this approach may overestimate biofuels emissions by between 5 and 50%. Further study into this category would be needed to better disentangle biofuels from fossil

791 combustibles.

In our study, biofuel burning is estimated to contribute 11 [8-14] Tg CH₄ yr⁻¹ to the global CH₄ budget, about 3% of total

793 global anthropogenic CH₄ emissions for 2010-2019.

3.1.6 Other anthropogenic sources (not explicitly included in this study)

Other anthropogenic sources not included in this study are related to agriculture and land-use management. In particular, increases in agricultural areas (such as global palm oil production) have led to the clearing of natural peat forests, reducing natural peatland area and associated natural CH₄ emissions. Peatlands planted to forests (like in Northern Europe) also lead to reduced CH₄ emissions. While studies have long suggested that CH₄ emissions from peatland drainage ditches are likely to be significant (e.g., Minkkinen and Laine, 2006, Peacock et al., 2021), CH₄ emissions related to palm oil plantations have yet to be properly quantified (e.g., Manning et al, 2019). Taylor et al. (2014) have quantified global palm oil wastewater treatment fluxes to be 4 ± 32 Tg CH₄ yr⁻¹ for 2010-2013. This currently represents a small and highly uncertain source of methane but one potentially growing in the future.





3.2 Natural and indirect anthropogenic sources

As introduced in section 2.4, natural and indirect anthropogenic sources refer to pre-agricultural CH₄ emissions even if they are perturbed by anthropogenic climate change or other global change factors (e.g., eutrophication), and indirect emissions resulting from anthropogenic perturbation of the landscape (reservoirs) and the biogeochemical characteristics of soil. They include vegetated wetland emissions and inland freshwater systems (lakes, small ponds, reservoirs, and rivers), land geological sources (gas-oil seeps, mud volcanoes, microseepage, geothermal manifestations, and volcanoes), wild animals, wildfires, termites, thawing terrestrial and marine permafrost, and coastal and oceanic sources (biogenic, geological and hydrate). In water-saturated or flooded ecosystems, the decomposition of organic matter gradually depletes most of the oxygen in the soil or the sediment zone, resulting in anaerobic conditions and CH₄ production. Once produced, CH₄ can reach the atmosphere through a combination of three processes: (1) diffusive loss of dissolved CH₄ across the air-water boundary; (2) ebullition flux from sediments; and (3) flux mediated by emergent aquatic macrophytes and terrestrial plants (plant transport). On its way to the atmosphere, in the soil or water columns, CH₄ can be partly or completely oxidised by microorganisms, which use CH₄ as a source of energy and carbon (USEPA, 2010b). Concurrently, methane from the atmosphere can diffuse into the soil column and be oxidised (See Sect. 3.3.4 on soil uptake).

3.2.1 Wetlands

Wetlands are generally defined as ecosystems in which mineral or peat soils are water-saturated at some depth or where surface inundation (permanent or not) has a dominating influence on the soil biogeochemistry and determines the ecosystem species composition (USEPA, 2010b). To refine such an overly broad definition for CH₄ emissions, we define wetlands as ecosystems with inundated or saturated soils or peats where anaerobic conditions below the water table lead to CH₄ production (Matthews and Fung, 1987; USEPA, 2010b). Brackish water emissions are discussed separately in Sect. 3.2.6. Our definition of wetlands includes ombrotrophic and minerotrophic peatlands (i.e., bogs and fens), mineral soil wetlands (swamps and marshes), and seasonal or permanent floodplains. It excludes exposed water surfaces without emergent macrophytes, such as lakes, rivers, estuaries, ponds, and reservoirs (addressed in the next section), as well as rice agriculture (see Sect. 3.1.4, rice cultivation paragraph), and wastewater ponds. It also excludes coastal vegetated ecosystems (mangroves, seagrasses, salt marshes) with salinities usually >0.5 (See Sect. 3.2.6). Even with this definition, some wetlands could be considered as anthropogenic systems, being affected by human land-use changes such as impoundments, drainage, or restoration (Woodward et al., 2012). In the following, we retain the generic denomination "wetlands" for natural and human-influenced wetlands, as discussed in Sect. 2.2.

Delwiche et al., 2021; Knox et al., 2021).

The three most important factors influencing CH₄ production in wetlands are the spatial and temporal extent of anoxia

(linked to water saturation), temperature, and substrate availability (Valentine et al., 1994; Wania et al., 2010; Whalen, 2005;





834 Land surface models estimate CH₄ emissions through a series of processes, including CH₄ production, oxidation, and 835 transport. The models are then forced with inputs accounting for changing environmental factors (Melton et al., 2013; 836 Poulter et al., 2017; Tian et al., 2010; Wania et al., 2013; Xu et al., 2010). CH₄ emissions from wetlands are computed as 837 the product of an emission flux density and a CH₄ producing area or surface extent (see Supplementary Material; Bohn et al., 2015; Melton et al., 2013). The areal extent of different wetland types (having large differences in areal CH₄ emission 838 839 rates) appears to be a primary contributor to uncertainties in the absolute flux of CH₄ emissions from wetlands, with 840 meteorological response being the main source of uncertainty for seasonal and interannual variability (Poulter et al., 2017; 841 Kuhn et al., 2021; Parker et al., 2022; McNicol et al., 2023; Karlson and Bastviken 2023). 842 In this work, sixteen land surface models computing net CH₄ emissions (Table 2) were run under a common protocol with 843 a spin-up using repeated climate data from 1901-1920 to pre-industrial conditions followed by a transient simulation through 844 the end of 2020. Of the 16 models, 13 previously contributed to Saunois et al. (2020), and three models were new to this release (CH4MOD_{wetland} (Li et al., 2010), ISAM (Shu et al., 2020; Xu et al., 2021), and SDGVM (Beerling and Woodward, 845 846 2001; Hopcroft et al., 2011; Hopcroft et al., 2020)) (Table 2, see also in the Supplementary Material Table S3 for a history 847 of the contributing models). Climatic forcing uncertainties are considered in the ensemble estimate by using two climate datasets, CRU/CRU-JRA55 (Harris, 2014) and GSWP3-W5E5 (Dirmeyer et al., 2006; Kim 2017; Lange, 2019; Cucchi et 848 849 al., 2020). Atmospheric CO₂ was also prescribed in the models. For all models, two wetland area dynamic schemes were 850 applied: a diagnostic scheme using a remote sensing-based wetland area and dynamics dataset called WAD2M (Wetland 851 Area Dynamics for Methane Modeling; Zhang et al., 2021a; 2021b) available at 0.25 degree of horizontal resolution, as in 852 Saunois et al. (2020), and a prognostic scheme using internal model-specific hydrologic models. The diagnostic wetland extent product WAD2Mv1.0 (Zhang et al., 2021a) has been updated since Saunois et al. (2020) to 853 WAD2Mv2.0 (Zhang et al., 2021b) and extended to 2020. It uses the same Surface Water Microwave Product Series 854 (SWAMPSv3.2) for capturing inundation dynamics (Jenson and McDonald, 2019), which was extended to 2020. To reduce 855 856 potential double-counting with the freshwater budget, the surface areas of rivers/streams and lakes/ponds are excluded by 857 using the products Global River Widths from Landsat (GRWL) database v01.01 (Allen and Pavelsky, 2018) and HydroLakes v1.0 (Messenger et al., 2016), instead of the Global Surface Water (GSW) product (Pekel et al., 2016) used in WAD2Mv1.0. 858 859 The GRWL and Hydrolakes are also the datasets used separately in the upscaling of the freshwater budget allowing for a more consistent approach between the wetland and freshwater CH₄ budgets (Sect. 3.2.2). This update in WAD2M leads to 860 861 a downward revised annual average wetland extent by 0.5 Mkm² for the mid-high latitudes (mainly due to larger lake extent 862 in HydroLakes than in the GSW dataset) with small impacts in other regions. However, since HydroLakes includes only vectorized lakes larger than 0.1 km², smaller lakes/ponds under 0.1 km² are implicitly still included as wetlands in 863 864 WAD2Mv2.0. For the high-latitude region, the recent peatland extent product from Hugelius et al. (2020) is applied, which indicates a slightly higher peatland area by 0.2 Mkm² primarily in regions above 60°N, compared to the Northern 865 Circumpolar Soil Carbon Database (NCSCD) product (Hugelius et al., 2013) used in WAD2Mv1.0. Rice agriculture was 866



868

869

870

871

872

873

874

875

876

877878

879

880

881

882 883

884

885

886 887

888

889

890

891

892

893

894

895

896

897

898

899



removed using the Monthly Irrigated and Rainfed Crop Areas (MIRCA2000, Portmann et al. (2010)) dataset from circa 2000, as a fixed distribution. The combined remote-sensing and inventory WAD2Mv2.0 product leads to a maximum wetland area of 13.6 Mkm² during the peak season (7.9 Mkm² on annual average, with a range of 7.5 to 8.4 Mkm² from 2000-2020, about 5.2% of the global land surface). The largest wetland areas in WAD2Mv2.0 are in Amazonia, the Congo Basin, and the Western Siberian Lowlands, which in previous studies were underestimated by inventories (Bohn et al., 2015). However, the SWAMPS v3.2 dataset which serves as a proxy of temporal variations of wetland extent, has discontinuity issues over a few tropical hotspots since 2015 and hence affects the temporal variations of WAD2M. Consequently, this affects CH₄ emissions estimates for a subset of land surface models that are particularly sensitive to inundation in these hotspots. Meanwhile, prognostic estimates show moderate consistency in capturing the spatial distribution of wetland area with WAD2M, with an annual average wetland area of 8.0±2.0 Mkm² during the peak season for 2000-2020. The ensemble mean of annual wetland area anomaly by the prognostic models show reasonable agreement with satellite-based estimates in capturing the response of wetland area to climate variations (Zhang et al., in review), with higher agreement over temperate and boreal regions than in the tropics. For the wetland methane emissions estimate, we use the decadal mean from the prognostic runs and adjust these flux estimates for double counting from inland waters (described in next section) given the reliance of the prognostic models on satellite flooded area data like WAD2Mv2 to parameterize maximum wetland extent (Zhang et al., in review). The average emission from wetlands for 2010-2019 for the 16 models is plotted in Fig. 3. The zones with the largest emissions are the Amazon basin, equatorial Africa and Asia, Canada, western Siberia, eastern India, and Bangladesh. Regions where CH₄ emissions have high inter-model agreement (defined as regions where mean flux is larger than the standard deviation of the models, on a decadal mean) represent 72% of the total CH₄ flux due to natural wetlands. The different sensitivities of the models to temperature, vapour pressure, precipitation, and radiation can generate substantially different patterns, such as in India. Emission estimates over regions with lower emissions (in total) are also consistently inferred between models (e.g., Scandinavia, Continental Europe, Eastern Siberia, Central United States of America, and Southern Africa). The resulting global flux range for vegetated wetland emissions from the prognostic runs is 117-195 Tg CH₄ yr⁻¹ for the 2000-2020 period, with an average of 157 Tg CH₄ yr⁻¹ and a one-sigma standard deviation of 24 Tg CH₄ yr⁻¹. Using the prognostic set of simulations, the average ensemble emissions were 159 [119-203] Tg CH₄ yr⁻¹ for the 2010-2019 period (Table 3). The estimated average ensemble annual total from the two sets of simulations by CRU/CRU-JRA55 and GSWP3-W5E5 are 158 [126-193] and 158 [118-203] for 2010-2019, respectively. Generally, the magnitude and interannual variability agree between these two sets of simulations (Zhang et al., in review). Wetland emissions represent about 25% of the total (natural plus anthropogenic) CH₄ sources estimated by bottom-up approaches. The large range in the estimates of wetland CH₄ emissions results from difficulties in defining wetland CH₄ producing areas as well as in parameterizing terrestrial anaerobic conditions that drive sources and the oxidative conditions leading to sinks (Melton et al., 2013; Poulter





et al., 2017; Wania et al., 2013). The ensemble mean emission using the same simulation setup (i.e., diagnostic wetland extent and CRU/CRU-JRA55) in the models is 163 [117-195] Tg CH₄ yr⁻¹, higher by ~22 Tg CH₄ yr⁻¹ than the one previously reported (see Table 3, for 2000-2009 with comparison to Saunois et al., 2020). This difference is mainly due to the updated model structure and parameterizations in the wetland CH₄ models compared to the versions in the previous budget and the inclusion of three new land surface models.

For the last decade 2010-2019, we report in this budget an average ensemble estimate of 159 Tg CH₄ yr⁻¹ with a range of 119-203 (based on prognostic wetland extent runs).

3.2.2 Inland freshwater systems (lakes, ponds, reservoirs, streams, rivers)

This category includes CH₄ emissions from freshwater systems (lakes, ponds, reservoirs, streams, and rivers). Numerous advances have been made in the freshwater greenhouse gases knowledge base in the last few years (Lauerwald et al., 2023a). These advances include improvements in the underlying databases used to estimate inland water surface areas and model their dynamics, a rapidly growing number of direct measurements of methane fluxes, and improvements in our process-based understanding of methane biogeochemistry. Despite this, aspects of global freshwater methane estimates remain rather crude and continue to have large uncertainties. This includes the overall temperature dependency of methane emissions, the relative role of ebullition (i.e., bubble flux, which may represent the most important, but most difficult-to-capture emission path in many standing water bodies), fluxes from the smallest standing water bodies (sometimes referred to as ponds) having large emissions per m² but uncertain area extent, and the magnitude of anthropogenic influence on emissions, all which are discussed below.

Streams and rivers. The last global CH₄ budget used an estimate of 27 Tg CH₄ yr⁻¹ for global streams and rivers based largely on a data compilation by Stanley et al. (2016). This estimate was scaled from a simple data compilation without a spatial component or an estimate of ebullition. More recently, Rosentreter et al. (2021) performed a new data compilation of 652 flux estimates, including diffusive and ebullitive fluxes, coupled to an ice corrected surface area estimate of \sim 625,000 km² that was aggregated to 5 latitudinal bands to come up with a global estimate of 6 and 31± 17 Tg CH₄ yr⁻¹ (respectively for the median and mean \pm c.i. 95%). We believe, due to better data representation in underlying datasets, that the mean estimate of Rosentreter et al. (2021) is more representative statistically because the median does not capture hotspots and hot moments of intense ebullitive fluxes. Finally, Rocher-Ros et al. (2023) used a new Global River Methane (GRiMeDB) database (Stanley et al., 2023) with \geq 24,000 observations of CH₄ concentrations to predict \sim 28±17 Tg CH₄ yr⁻¹ (\pm c.i. 95%) river emissions globally. This approach used machine learning methods coupled to the latest spatially and temporally explicit mapping of monthly stream surface area (the smallest streams are still extrapolated) which incorporates drying and freezing effects (yearly average 672,000 km², Liu et al., 2022) and includes an ebullitive flux estimated from a correlation between measured diffusive and ebullitive emissions in the GRiMeDB database (Stanley et al., 2023). Thus, for this study we use an





estimate of 29±17 (±c.i. 95%) Tg CH₄ yr¹ for streams and rivers, which averages the mean estimate of Rosentreter et al. (2021) and Rocher-Ros et al. (2023). Currently, ebullitive fluxes remain a major unknown quantity in streams and rivers but appear to be coarsely linearly correlated in a log-space to diffusive fluxes and of similar magnitude (Rocher-Ros et al., 2023). Methodologically, the high-water velocity of many streams and rivers make measurement of ebullitive fluxes challenging (Robison et al., 2021). Effluxes are also linked to hydrology (Aho et al., 2021) although very few studies have sampled over a representative hydrograph. Plant-mediated effluxes of CH₄ in running waters also remain difficult to constrain, with a recent compilation highlighting very few measurements (Bodmer et al. 2024). Connected adjacent wetlands is a common source of CH₄ to streams and rivers (Borges et al., 2019) which may be important for the regulation of running water emissions but is currently difficult to assess at the global scale. Overall, the poor representation of sites and deficient mechanistic understanding make it difficult to model and predict methane evasion from streams and rivers using process-based models.

942943944

945

946947

948

949

950

951

952953

954

955

956

957

958959

960

961962

963964

932

933934

935

936

937

938

939

940

941

Lakes and ponds. The previous global CH₄ budget used an estimate of 71 Tg CH₄ yr⁻¹ for lakes and 18 Tg CH₄ yr⁻¹ for reservoirs. These estimates were based on an early study by Bastviken et al. (2011) coupled with a newer estimate for lakes north of 50°N (Wik et al., 2016b). There have been three new lake studies that have published their data with global estimates of 56 and 151 ± 73 (Rosentreter et al. (2021; ($\pm c.i.$ 95%); respectively for the median and mean $\pm c.i.$ 95%), 22 ± 8 (Zhuang et al., 2023; ±lake-area-weighted normalised RMSE for all parameterized lake types), process-based model), and 41±36 Tg CH₄ yr⁻¹ (Johnson et al., 2022, mean ±c.i. 95%). This large range in estimated emissions can be attributed to the differences in the datasets and methods used to calculate the surface area of small waterbodies, as well as the differences between how the flux data were analyzed and extrapolated between studies. For instance, total surface areas of all lakes and ponds of $3712-5688 \times 10^3$ km² (Rosentreter et al., 2021) and 2806×10^3 km² (Johnson et al., 2022) were used along with measurement data from 198 and 575 individual lake systems, respectively. In contrast, Zhuang et al. (2023) generated estimates using higher temporal resolution data from just 54 lakes to build a process-based model, which generated much lower flux estimates from tropical lakes than previously implemented statistical approaches, but in line with the most recent assessments by Borges et al. (2022). For this study, we explicitly excluded lakes <0.1 km² which are treated separately (see below). If we re-assess these three studies for only lakes greater than 0.1 km², we obtain global effluxes of 17 and 42.9±20.8 Tg CH₄ yr⁻¹ (Rosentreter et al. (2021); median and mean (±95% C.I.) of global flux), 21.9±8.0. (Zhuang et al., 2023, ±lakearea-weighted normalised RMSE for all parameterized lake types), and 35.3±31.0 Tg CH₄ yr⁻¹ (Johnson et al. 2022, ±95% C.I.) (with areas of 2556-3468 x10³, 2640x10³, and 2676x10³ km² respectively). Thus, for lakes >0.1 km², we propose an efflux of ~33±26 Tg CH₄ yr⁻¹ (an average of the mean from Rosentreter et al., 2021 Zhuang et al., 2023, and Johnson et al., 2022, with the average 95% C.I. from Rosentreter et al., 2021 and Johnson et al. 2022).

Small waterbody emissions, hereafter small lakes and ponds<0.1 km², remain difficult to assess. Evidence is emerging that

there is a lower limit to the power scaling laws that early studies used to extrapolate the surface area of these small systems





(Bastviken et al., 2023; Kyzivat et al., 2022). Thus, for small lakes and ponds < 0.1 km² (and >0.001 km²), we disregard the higher end surface area used in Rosentreter et al., 2021 which relied on these earlier estimates and scale their numbers to the evasion estimates to the lower end surface area of 1,002x10³ to obtain a mean flux of 33 Tg CH₄ yr⁻¹ (Rosentreter et al., 2021). Johnson et al. (2022) estimated a surface area of only 166,000 km² for this size class to obtain an efflux of 6.3 Tg CH₄ yr⁻¹, which we acknowledge as a lower limit. Averaging these two values provide a conservative estimate of ~20 [6-33] Tg CH₄ yr⁻¹, which is close to the number proposed by Holgerson and Raymond (2016) for diffusion effluxes only for this size class. The experts involved in this assessment have low confidence in this estimate. This also does not include artificial ponds, which we discuss below. As a result, CH₄ emissions from both large lakes (>0.1 km²) and small lakes and ponds (<0.1km²) are estimated at 53 [19-86] Tg CH₄ yr⁻¹, on average lower than the 71 Tg estimated in the previous budget.

Reservoirs. New mean estimates of diffusive + ebullitive CH₄ emissions from reservoirs include 15 and 24±8 (the median and mean±95% C.I. from Rosentreter et al., 2021), 10 ± 4 (Johnson et al., 2021, mean±95% C.I.), 10 (Harrison et al., 2021, low and high 95% CI 7 and 22, respectively), and 2.1 Tg CH₄ yr⁻¹ (Zhuang et al., 2023). We compile the first three estimates to a direct efflux of \sim 14 Tg CH₄ yr⁻¹ (with \pm 95% C.I. of 9 and 23). We note the fourth estimate as a lower bound, but exclude it from this budget given that it was generated via a model that only included data from six reservoir systems (Zhuang et al., 2023). We also add in an additional 12 Tg CH₄ yr⁻¹ (95% C.I, 7 and 37) that is estimated to degas in dam turbines (Harrison et al., 2021), which was not addressed in the studies by Rosentreter et al. (2021), Zhuang et al. (2023), or Johnson et al. (2021). Rocher-Ros et al. (2023) also excluded river observations below dams when executing their statistical model, and so did not capture downstream dam emissions. Thus, we use a direct reservoir emission here of \sim 13 [6-28] Tg CH₄ yr⁻¹ and estimate an additional \sim 12 [7-37] Tg CH₄ yr⁻¹ from dam turbine degassing fluxes, giving a total of 25 [13-65] Tg CH₄ yr⁻¹ from reservoirs.

Uncertainties and confidence levels. The emission estimates of lakes, reservoirs and ponds described above are limited by several uncertainties. First, a major unknown for lakes remains the size cut off and the representation of small lakes and ponds (Deemer and Holgerson, 2021), which are also more variable than larger water bodies in their CH₄ concentrations and fluxes (Rosentreter et al. 2021, Ray et al., 2023). Interestingly, there is also a lack of methane data representation from large lakes that are a large component of global lake surface area (Deemer and Holgerson, 2021; Messager et al., 2016). There is also a growing knowledge base on the importance of high CH₄ fluxes from lake littoral zones that is not yet well incorporated into global scaling efforts (e.g., Grinham et al., 2011; Natchimuthu et al., 2016), and emergent vegetation (Bastviken et al., 2023; Kyzivat et al., 2022). Ebullition is more constrained in lakes/reservoirs compared to streams/rivers but is still difficult to measure and model accurately. Finally, for all aquatic systems a greater scrutiny of the regulation (including the impact of ice-cover and seasonality) of different CH₄ emission pathways is needed.





The majority of the inland water CH₄ estimates are from a limited number of studies, some without spatial representation or reported statistical uncertainties. Furthermore, as mentioned above the knowledge base of the surface area of these ecosystems is new and rapidly expanding, but not standardised between studies leading to uncertainty (but see Lauerwald et al. 2023b), particularly for ponds. For this study, we are able to provide confidence intervals from the original studies for all fluxes except the smallest lake/pond size class.

The Surface Area of Inland Freshwaters. For all of these ecosystems, determining their surface area remains a central challenge. Since the last GMB, several methodological advances have reduced the uncertainty associated with the surface area estimates of rivers, streams, lakes, and reservoirs. Using a single geospatial dataset that includes both lakes and reservoirs (Messager et al., 2016) has decreased double counting of lakes and reservoirs (Johnson et al., 2022; Rosentreter et al., 2021). For rivers and streams, high-resolution global streamflow simulations, informed by satellite observations, enabled a much finer scale estimate of surface areas for rivers with a new temporal component (Allen and Pavelsky, 2018; Lin et al., 2019; Liu et al., 2022), although the surface for the smaller streams are still estimated indirectly, and mapping of human-created drainage ditches and canals is lacking. Seasonal ice cover and melt turnover corrections also have been newly incorporated into rivers, streams, lakes, and reservoirs (Harrison et al., 2021; Johnson et al., 2022; Lauerwald et al., 2023b; Rocher-Ros et al., 2023; Rosentreter et al., 2021; Zhuang et al., 2023). Finally, removing open water body surface areas from wetland surface areas based on geographic location has reduced double counting between these two land cover types, as described in the wetlands section of the GMB. Yet, the surface area of small lakes and ponds (<0.1 km2) is still highly uncertain, and new techniques for counting these systems and determining the overlap with wetland data bases is paramount.

Anthropogenic Contributions to Inland Freshwater Emissions. We argue that all reservoirs should be categorised as an direct anthropogenic source of emissions. Most of the surface area of reservoirs are human-made and reservoir construction leads to anoxic sediments and/or bottom waters with labile organic matter sourced from the watershed and to in-situ nutrient augmented phytoplankton production (Deemer et al., 2016; Maavara et al., 2017; Prairie et al., 2018). It is also clear that the cultural eutrophication of natural lakes is augmenting CH₄ emissions (DelSontro et al., 2018; Li et al., 2021), with shallow lakes particularly likely to experience eutrophication (Qin et al., 2020). For instance, Beaulieu et al. (2019) modelled a 15% reduction in lake CH₄ with a 25% reduction in lake phosphorus concentrations. Several recent studies have estimated that anywhere between 30 and 50% of lakes are eutrophic (Cael et al., 2022; Qin et al., 2020; Sayers et al., 2015; Wu et al., 2022). These studies estimate numerical percentages (one by depth class: Qin et al., 2020), but none have estimated the percent of lake surface area that is eutrophic nor have any determined the extent of anthropogenic vs. natural eutrophication. Still, numerous studies have noted widespread increases in eutrophication indicators across lakes due to nutrient loading and warming (Griffiths et al., 2022; Ho et al., 2019; Taranu et al., 2015), thus we estimate that ½, or 11 Tg CH₄ yr⁻¹ of CH₄ emissions from lakes >0.1 km² could be anthropogenic. Similarly, CH₄ emissions from small lakes and ponds are



1031

1032

1033

1034

1035

1036

1037 1038

1039

1040

1041 1042

1043

1044

1045

1046

1047

1048

1049

1050

1051

1052

1053

1054

1055

1056

1057

1060

1061 1062



influenced by human factors, with emissions increasing with eutrophication (Deemer and Holgerson, 2021), erosion and runoff in agricultural landscapes (Heathcote et al., 2013), and warming, the latter likely to have a disproportionately greater effect in small, shallow systems (Woolway et al., 2016). Thus, we adopt the same 1/3 number as for lakes for the proportion of anthropogenic emissions in small lakes and ponds ($<0.1 \text{ km}^2$), which amounts to 6 Tg CH₄ yr⁻¹.

There are also human-made small lakes and ponds, notably for agriculture, aquaculture, and recreation, that generally have conditions favourable for high CH₄ emissions (Downing, 2010; Holgerson and Raymond, 2016; Malerba et al., 2022; Ollivier et al., 2019; Zhao et al., 2021; Dong et al., 2023). Downing (2010) estimated that farm ponds comprise a global surface area of ~77,000 km²; using a conservative emission rate of 265 mg CH₄ m⁻² d⁻¹ and an ice correction factor of 0.6 leads to an emission of 4.5 Tg yr⁻¹ that is anthropogenically sourced from farm ponds. Here the value is rounded to 5 Tg yr⁻¹ ¹. Clearly, more work is required to assess the anthropogenic component of CH₄ emissions from lakes and ponds.

It remains difficult to parse out an anthropogenic component to stream and river CH₄ fluxes. Although some studies have noticed a temperature dependence with stream sediments (Comer-Warner et al., 2018; Zhu et al., 2020), Rocher-Ros et al. (2023) noted a small temperature dependence of CH₄ emissions in streams and rivers compared to other freshwater ecosystems, potentially due to the many other external processes affecting fluxes in these dynamic flowing ecosystems. Urbanisation can lead to elevated river CH₄ emissions, particularly in regions with elevated organic matter and nutrient loading due to limited wastewater treatment (Begum et al., 2021; Nirmal Rajkumar et al., 2008; Wang et al., 2021a). Some studies have found agricultural streams and ditches can have higher effluxes due to inputs of fine sediments (Comer-Warner et al., 2018; Crawford and Stanley, 2016), organic carbon, and nutrients (Borges et al., 2018) that lead to in-situ methane production. Furthermore, the creation of drainage ditches in organic soils tap CH₄ rich waters from water-logged horizons and heighten emissions from ex-situ sources (Peacock et al., 2021), although limitations in both the geographic scope of existing ditch emission estimates our ability to estimate global surface area of ditches precludes their inclusion in this budget. Finally, extremely high rates of CH₄ emission have been linked to ongoing permafrost thaw in Asia's Qinghai–Tibet Plateau (Zhang et al., 2020). However, the loss and disconnection of wetlands to rivers may have resulted in a decrease in the input of dissolved CH₄ from this source. A recent expert elicitation (Rosentreter, et al. submitted) reported that 35% of all inland freshwater sources were anthropogenic and given that some of the river flux is from upstream reservoirs, we assign a 30% anthropogenic contribution to the stream and river flux (9 Tg CH₄ yr⁻¹), which approximates the expert elicitation via the impact of eutrophication and urban influences.

1058 Combination (lakes, ponds, reservoirs, streams and rivers, farm ponds). Combining the aforementioned emissions from 1059

lakes $>0.1 \text{ km}^2$ ($\sim 33 \text{ [13-53] Tg CH}_4 \text{ yr}^{-1}$), small lakes and ponds $< 0.1 \text{ km}^2$ (20 [6-33] Tg CH₄ yr⁻¹), reservoirs (25 [13-65]

Tg CH₄ yr⁻¹), streams and rivers (29 [12-46] Tg CH₄ yr⁻¹) and farm ponds (5 Tg CH₄ yr⁻¹), leads to a total of ~112 Tg CH₄

yr⁻¹ from freshwater systems, with a range of [49-202] Tg CH₄ yr⁻¹. This estimate is about 50 Tg lower than in Saunois et al. (2020) and is broadly consistent with the recent regionalized estimate by Lauerwald et al. (2023b) compiled for the

32





Regional Carbon Cycle Assessment and Processes (RECCAP2, https://www.globalcarbonproject.org/reccap/; 103 Tg CH4 yr⁻¹, IQR= 82.1–134.8). The updated budget from these ecosystems and their anthropogenic components are represented on Fig 4. The gridded products for emissions from lakes and ponds by Johnson et al. (2022), from reservoirs by Johnson et al. (2021) and from streams and rivers by Rocher-Ros et al. (2023) have been combined into a single map presented in Fig. 5.

1066 1067 1068

1069

1070

1071

1072

1073

1074

1075

1076

1077

1078

1079

1080

1081

1082

1083

1084 1085

1086 1087

1088

1089

1090

1091

1092

1095

1063

1064

1065

Double-counting aquatic systems in the bottom-up estimates. To address the differences found between bottom-up and top-down CH₄ budgets, and to acknowledge advances in addressing the central issue of double counting CH₄ emissions for inland ecosystems, we introduce here a new correction term. Historically, the bottom-up estimate of global CH₄ emissions has been higher than the top-down estimate, first recognized in Kirschke et al. (2013) and confirmed in Saunois et al. (2016, 2020). The larger bottom-up emissions estimate has been partly attributed to double-counting vegetated wetland emissions with inland freshwater emissions (including lakes, ponds, rivers, streams, and reservoirs) and also the emissions of CH₄ produced in vegetated wetlands and then transported via aquatic processes and emitted from inland freshwaters (Pangala et al., 2017; Kirk and Cohen, 2023). The Saunois et al. (2020) CH₄ budget addressed the issue of double counting through the use of a revised vegetated wetland area dataset, WAD2M v1.0 (Zhang et al., 2021), that removed inland waters from the SWAMPS (Jenson and McDonald, 2019) surface-inundation dataset, allowing for independent vegetated wetlands and inland freshwater CH₄ emissions to be compiled. Yet, the Saunois et al. (2020) CH₄ budget still had a ~150 Tg CH₄ yr⁻¹ difference between bottom-up and top-down estimates. In this budget, we refined the vegetated wetland area dataset with WAD2M v2.0 (see section 3.2.1, where HydroLakes is used to remove lakes and ponds >0.1 km²). Additionally, we applied numbers from peer-reviewed publications and expert elicitation to account for lateral CH₄ flux emissions. This most recent BU budget estimates 159 [119-203] Tg CH₄ yr⁻¹ from vegetated wetlands for 2010-2019 and 112 Tg CH₄ yr⁻¹ from inland freshwaters that includes 83 Tg CH₄ yr⁻¹ from lakes, ponds, and reservoirs and 29 Tg CH₄ yr⁻¹ from rivers and streams, leading to a combined wetland and inland freshwater flux of 271 Tg CH₄ yr⁻¹. Here, we propose a correction of 20 Tg CH₄ yr⁻¹ to account for double counting of small lakes and ponds (< 0.1 km²) that are likely included in our vegetated wetlands estimate, and removing 1-3 Tg CH₄ yr⁻¹ from river emissions due to lateral transport of CH₄ originating in adjacent vegetated wetlands. The river flux correction arises from assuming that for catchments with >10% wetlands, rivers provide 5-10% of vegetated CH₄ emissions. The total double-counting correction term of 23 Tg CH₄ reduces the BU budget for combined wetlands and inland waters from 271 Tg CH₄ yr⁻¹ to 248 Tg CH₄ yr⁻¹ (see Fig. 4 and Table 3). Comparing the 2000-2009 decadal emissions from wetlands and inland freshwater ecosystems across the last three previous assessments of the budget shows a significant downward revision with 305 (183+122) Tg CH₄ yr⁻¹, 356 (147+209) Tg CH₄ yr⁻¹ and 248 (159+112-23) Tg CH₄ yr⁻¹ (respectively from Saunois et al. (2016; 2020) and this work).

1093 Finally, it is worth noting that inland freshwater ecosystems can overlap with geological seepage systems in some areas, 1094 i.e., they may occur in correspondence with geological structures that emit fossil (microbial, thermogenic, or abiotic)

CH₄ generated in the Earth's crust. Examples have been documented in the Fisherman Lake in Canada (Smith et al., 2005),



1097

1098

1099

1100

1101

1102

1103

1104

1105

1106

11071108

1109

1110

11111112

11131114

1115

1116

11171118

11191120

1121

1122

1123

1124

1125

1126

1127



in the Baikal lake (Schmid et al, 2007), and in rice paddies in Japan (Etiope et al., 2011). Thus, some gas emissions in freshwater environments, particularly as bubble plumes, can be incorrectly attributed to modern biological (ecosystem) activities if appropriate isotopic and molecular analyses are not performed.

Significant amounts of CH₄, produced within the Earth's crust, naturally migrate to the atmosphere through tectonic faults

3.2.3 Onshore and offshore geological sources

and fractured rocks. Major emissions are related to hydrocarbon formation in sedimentary basins (microbial and thermogenic methane), through continuous or episodic exhalations from onshore and shallow marine hydrocarbon seeps and through diffuse soil microseepage (Etiope, 2015). Specifically, five source categories have been considered. Four are onshore sources: gas-oil seeps, mud volcanoes, diffuse microseepage, and geothermal manifestations including volcanoes. One source is offshore: submarine seepage, which may include the same types of gas manifestations occurring on land. Etiope et al. (2019) have produced the first gridded maps of geological CH₄ emissions and their isotopic signature for these five categories, with a global total of 37.4 Tg CH₄ yr⁻¹ (reproduced in Fig. 5). However, these maps are based on incomplete data on geological sites due to missing information and difficulties in defining all current geological emitting sites. Combining the best estimates for the five categories of geological sources (from grid maps or from previous statistical and process-based models), the breakdown by category reveals that onshore microseepage dominate (24 Tg CH₄ yr⁻¹), the other categories having similar smaller contributions: as mean values, 4.7 Tg CH₄ yr⁻¹ for geothermal manifestations, about 7 Tg CH₄ yr⁻¹ for submarine seepage and 9.6 Tg CH₄ yr⁻¹ for onshore seeps and mud volcanoes. These values lead to a global bottom-up geological emission mean of 45 [27-63] Tg CH₄ yr⁻¹ (Etiope and Schwietzke, 2019). While all bottom-up and some top-down estimates, following different and independent techniques from different authors, consistently suggest a global geo-CH₄ emission in the order of 40-50 Tg yr-1, the radiocarbon (¹⁴C-CH₄) data in ice cores reported by Hmiel et al. (2020) appear to give a much lower estimate, with a minimum of about 1.6 Tg CH₄ yr⁻¹ and a maximum value of 5.4 Tg CH₄ yr⁻¹ (95 percent confidence) for the pre-industrial period. The discrepancy between Hmiel et al. (2020) and all other estimates has been discussed in Thornton et al. (2021), which demonstrated that the global near-zero geologic CH₄ emission estimate in Hmiel et al. (2020) is incompatible with the sum of multiple independent bottom-up estimates, based on a wide variety of methodologies, from individual natural geological seepage areas: for example, from the Black Sea (up to 1 Tg CH₄ yr⁻¹), the Eastern Siberian Arctic Shelf (ESAS, up to 4.6 Tg CH₄ yr⁻¹, referring mostly to thermogenic gas), onshore Alaska (up to 1.4 Tg CH₄ yr⁻¹) and a single seepage site in Indonesia (releasing 0.1 Tg CH₄ yr⁻¹ as estimated by satellite measurement) (see Thornton et al. (2021) and references therein). Jackson et al. (2020) expressed doubt about the low Hmiel et al. (2020) estimates, noting that they are difficult to reconcile with the results of many other researchers and with bottom-up approaches in general. This discrepancy highlights another main unresolved uncertainty in the methane budget. Waiting for further investigation to better understand discrepancies between radiocarbon approaches and other studies, we decided to keep the estimates from Etiope and Shwietzke (2019) for the mean values, and associate it



11291130

1131

1132

1133

1134

1135

1136

1137

1138

1139

1140

1141

11421143

1144

1145

1146

11471148

1149

1150

1151

1152

11531154

1155

1156

1157

1158

1159



to the lowest estimates reported in Etiope et al. (2019), as in Saunois et al. (2020). Thus, we report a total global geological emission of 45 [18-63] Tg CH₄ yr⁻¹, with a breakdown between offshore emissions of 7 [5-10] Tg CH₄ yr⁻¹ and onshore emissions of 38 [13-53] Tg CH₄ yr⁻¹, similar to Saunois et al. (2020). This bottom-up estimate is slightly lower than in the Saunois et al. (2016) budget mostly due to a reduction of estimated emissions of onshore and offshore seeps (see Sect. 3.2.6 for more offshore contribution explanations).

3.2.4 Termites

Termites are decomposers playing a central role in ecosystem nutrient fluxes at tropical and subtropical latitudes, in particular (Abe et al., 2000). Termites represent a natural CH4 source due to methanogenesis occurring in their hindgut during the symbiotic metabolic breakdown of lignocellulose (Sanderson, 1996; Brune, 2014). The upscaling of CH₄ emissions from termites from site to global level is characterised by high uncertainty (Sanderson, 1996; Kirschke et al., 2013; Saunois et al., 2016) due to the combination of factors that need to be considered and the scarcity of information for each of these factors for global upscaling. Needed data include termite biomass density (Sanderson, 1996), species distribution within and among ecosystems (Sugimoto et al., 1998), variation of termite CH₄ emission rates per species and dietary group (Sanderson, 1996), the role played by the termite mound structure in affecting the fraction of produced CH₄ that is effectively released into the atmosphere (Sugimoto et al., 1998; Nauer et al., 2018). In Kirschke et al. (2013) and Saunois et al. (2016) a global upscaling of termite CH₄ emissions was proposed, where CH₄ emissions, E_{CH4} (kg CH₄ ha⁻¹yr 1), were estimated as the product of three terms: termite biomass (Bioterm g fresh weight m⁻²), a scalar correction factor (LU) expressing the effect of land use/cover change on termite biomass density, a termite CH₄ emission factor (EF_{TERM}, µg CH₄ g⁻¹ Bio_{TERM} h⁻¹). The approach between the two re-analyses of CH₄ emissions varied only for the data sources of gross primary productivity (GPP) and land use which were used to attribute biomass values of termite per ecosystem surface unit, in order to cover different time spans, 1980s, 1990s and 2000s in Kirschke et al. (2013) and 2000-2007 and 2010-2016 in Saunois et al. (2016). For the present update, additional changes have been introduced compared with the previous versions. Here we summarise the key data used for the new upscaling. CH₄ fluxes were modelled between 45°S and 45°N and within 35°S and 35°N. The termite biomass density, Bioterm, for tropical ecosystems was estimated as function (Kirschke et al., 2013; Bioterm=1.21·e 0.0008·GPP) of the gross primary production (GPP, g C m⁻² yr⁻¹) using the 0.25° native resolution VODCA2GPP dataset covering the period 2001-2020 (Wild et al., 2022). Wetlands, barren areas, water bodies and artificial surfaces were excluded from this estimation and set as no data (no emissions). The scalar correction factor LU of 0.4 (60%) for agricultural areas (i.e., croplands) (Kirschke et al., 2013) was applied to the GPP value of the nearest natural areas to account for anthropic disturbance. The annual (2001-2020) land cover information was obtained from the MODIS Terra+Aqua Combined Land Cover product (MCD12C1v006; https://lpdaac.usgs.gov/products/mcd12c1v006/), using the International Geosphere-Biosphere Programme (IGP) classification with a 0.05° spatial resolution. For desert and arid lands, within 35°S and 35°N, a fixed Bioterm value of 1.56 g m⁻² was instead used (Sanderson, 1996; Heděnec et al., 2022).



11611162

1163

11641165

1166

1167

1168

11691170

1171

1172

1173

1174

1175

1176

1177

1178

1179

1180

11811182

11831184

1185

1186

11871188

1189

1190

1191



and 35°- 45° S as follows: 1.83 g m⁻² for temperate forests and grasslands (Wood and Sands, 1978; Petersen and Luxton, 1982; Sanderson, 1996; Bignell and Eggleton, 2000; King et al., 2013; conversion factor from dry to fresh biomass is 0.27 from Petersen and Luxton, 1982), 5.3 g m⁻² for scrublands and Mediterranean areas of Australia (Sanderson, 1996), 1.09 g m² for the other Mediterranean shrubland ecosystems (Heděnec et al., 2022). Other climates and land covers were set as no data. Climate zoning was defined using the Climate Zones Köppen-Geiger dataset (Beck et al., 2018), this product is representative for the 1980-2016 time period and has a 0.0083° native resolution. The EF_{TERM} was revised compared with previous estimates (Kirschke et al., 2013; Saunois et al., 2016), in order to consider the different distribution of termite families and subfamilies in the different continents and ecosystems, characterised by different feeding habits and nest typologies, as reported by Sugimoto et al. (1998), which might influence the EF. The species of each family and subfamily of the two major groups of lower and higher termites, listed by Sugimoto et al. (1998) were associated with EF values based on emissions from in-vitro experiments as reported by Sanderson (1996) and Eggleton et al. (1999), to which a correction factor (cf_{MOUND}) of 0.5 (Nauer et al., 2018) was applied in order to take into account the mound effect on the CH₄ produced by termites, once inside the nest. The average EF_{TERM} for tropical and temperate areas was hence estimated as the weighted EFTERM derived from the product of the percentage weight of each family or subfamily of termites in the "community composition" in each geographical area and ecosystem (Sugimoto et al. (1998, Table 6), the respective calculated EF of each family or subfamily, a scalar or correction factor which considers the nest type (as in Table 5 from Sugimoto et al. 1998). For desert and arid lands and temperate areas, which were not reported in Sugimoto et al. (1998), EF rates were calculated directly from data reported in literature for the most representative species which were the genus Amitermes for the former (EF from data by Sanderson 1996, Eggleton et al. 1999, Jamali et al. 2011) and the genus Reticulitermes (family Rhinotermitidea) for the latter (EF from data by Odelson and Breznak, 1983; Sanderson, 1996; Eggleton et al., 1999; Myer et al., 2021). The following EF_{TERMS} were hence obtained to scale up emissions: $3.26 \pm 1.79 \,\mu g$ CH₄ g⁻¹ termite h⁻¹ (28.56) mg CH₄ g⁻¹ termite year⁻¹) for tropical ecosystems, $1.82 \pm 1.54 \mu g$ CH₄ g⁻¹ termite h⁻¹ for temperate forests, grasslands, and Mediterranean areas, $1.24 \pm 1.22 \,\mu g \, \text{CH}_4 \, \text{g}^{-1}$ termite h⁻¹ for deserts and arid lands (warm climate). Annual CH₄ fluxes were computed for all the years from 2001 to 2020 producing 20 global maps at 0.05° resolution of yearly total emissions. A further map of the estimated error representative of the entire time period was elaborated at the same resolution as the emissions dataset. Termite CH₄ emissions over the period 2001-2020 varied between 9.7-10.8 Tg CH₄ yr⁻¹, with an average of 10.2 ± 6.2 Tg CH₄ yr⁻¹. Considering a 20-year average, tropical and subtropical moist broadleaf forests contributed to 46% of the total average flux, while tropical and subtropical grasslands, savannas, and shrublands to another 36%. In terms of regional contribution, 37.2% of fluxes were attributed to South America, 31.5% to Africa, 18.1% to Asia, 5.5% to Australia, 7.4% to North America and less than 1% to Europe. The present estimate value is within the range of previous up-scaling studies,

Similarly, fix values from the few available studies reported in literature were used to estimate Bioterm between 35°- 45° N



1195

1196

1197

11981199

12001201

1202

1203

1204

1205

1206

1207

1208

1209

1210

1211

1212

12131214

1215

1216

1217

1218

1219

1220

12211222



spanning from 2 to 22 Tg CH_4 yr⁻¹ (Ciais et al., 2013). In this study, we report a decadal value of 10 Tg CH_4 yr⁻¹ with a range of [4-16].

3.2.5 Wild animals

Wild ruminants emit CH₄ through microbial fermentation that occurs in their rumen, similarly to domesticated livestock species (USEPA, 2010b). Using a total animal population of 100-500 million, Crutzen et al. (1986) estimated the global emissions of CH₄ from wild ruminants to be in the range of 2-6 Tg CH₄ yr⁻¹. More recently, Pérez-Barbería (2017) lowered this estimate to 1.1-2.7 Tg CH₄ yr⁻¹ using a total animal population estimate of 214 million (range of 210-219), arguing that the maximum number of animals (500 million) used in Crutzen et al. (1986) was poorly justified. Moreover Pérez-Barbería (2017) also stated that the value of 15 Tg CH₄ yr⁻¹ found in the last IPCC reports is much higher than their estimate because this value comes from an extrapolation of Crutzen's work for the last glacial maximum when the population of wild animals was much larger, as originally proposed by Chappellaz et al. (1993). Recently, based on the modelling of grassland extent, Kleinen et al. (2023) also suggest that the population of wild animal during the last glacial maximum proposed by Crutzen et al. (1986) and further used by Chappellaz et al. (1993) were overestimated.

Based on these findings, the range adopted in this updated CH₄ budget is 2 [1-3] Tg CH₄ yr⁻¹ (Table 3).

3.2.6 Coastal and ocean sources

Coastal and oceanic sources comprise CH₄ release from estuaries, coastal vegetated habitats, as well as marine waters including seas and oceans. Possible sources of coastal and oceanic CH₄ include (1) in-situ biogenic production through various pathways in oxygenated sea-surface waters (Oremland, 1979; Karl et al., 2008; Lenhart et al., 2016; Repeta et al., 2016), a flux that can be enhanced in the coastal ocean because of submarine groundwater discharge (USEPA, 2010b); (2) production from shallow and marine (bare and vegetated) sediments including free gas or destabilised hydrates and thawing subsea permafrost containing modern (\(^{14}\text{C-bearing}\)) microbial gas: (3) geological marine seepage (see also Sect. 3.2.3). including hydrates, containing fossil (14C-free) microbial or thermogenic CH₄. CH₄ produced in marine sediments and seabed CH₄ seepage can be transported across the water column to the sea-surface by upwelling waters (once at the surface methane can cross the sea-air interface via diffusion) and gas bubble plumes (for instance from geological marine seeps; e.g., Judd, 2004; Etiope et al., 2019). Gas bubble plumes can generally (but not exclusively, as described below) reach the atmosphere in relatively shallow waters (<400 m) of continental shelves and coastal zones. In coastal vegetated habitats CH₄ can also be transported to the atmosphere through the aerenchyma of emergent aquatic plants (Purvaja et al., 2004). We distinguish between coastal and oceanic "geological" and "modern biogenic" CH₄ sources. Coastal and oceanic "geological" emissions refer to CH₄ seepage from the Earth's crust (mostly in hydrocarbon-rich sedimentary basins), which is typically evaluated by combining geochemical analyses (isotopic and molecular, including radiocarbon, ¹⁴C, analyses) and geological observations (degassing along faults, seeps, mud volcanoes). Geological emissions do not contain modern



1224

1225

1226

1227

1228

1229

1230

12311232

1233

1234

1235

1236

12371238

1239

1240

1241

1242

1243

1244

1245

1246

12471248

1249

1250

1251

12521253

1254

1255



biogenic gas that is fossil (14C-free). Coastal and oceanic "biogenic" CH₄ refers to CH₄ formed in situ in coastal and marine sediments and in the water column by recent or modern microbial activity (therefore with measurable amounts of radiocarbon (¹⁴C)). To avoid double-counting, we assume that all diffusive CH₄ emissions outside of geological seepage regions (identified in global grid maps; Etiope et al., 2019) are fuelled by biogenic CH₄. Finally, we briefly discuss the case of CH₄ hydrates, which can be considered either a "geological" source when they host fossil CH₄ or a "biogenic" source when they host modern CH₄. Coastal and oceanic modern biogenic methane emissions. Area-integrated diffusive modern biogenic CH4 emissions from coastal ecosystems are 1-2 magnitudes lower than from inland freshwaters but significantly higher than biogenic emissions from the open ocean (Rosentreter et al., 2021; Rosentreter et al., 2023; Weber et al., 2019). Particularly the shallow vegetated coastline fringed by mangroves, salt marshes, and seagrasses is a CH₄ hotspot in the coastal ocean, characterised by significantly higher flux densities than other coastal settings such as estuaries or the continental shelves (Rosentreter et al., 2021; Rosentreter et al., 2023). Coastal ecosystems are thus being increasingly recognized as weak global sources to the atmosphere (Weber et al., 2019; Saunois et al., 2020; Rosentreter et al., 2021). Hydrogenotrophic and acetoclastic methanogenesis are largely outcompeted by sulphate reduction in coastal/marine sediments, which is often shown by a decreasing trend of CH₄ concentrations with increasing salinity from upper tidal (low salinity) to marine (high salinity) regions. Much of the CH₄ produced below the sulfate-reduction zone is indeed re-oxidized by sedimentary anaerobic methane oxidation or re-oxidized in the water column, leading to small emissions despite much larger production (Knittel and Boetius 2009; Regnier et al., 2011). Methylated compounds such as methylamines and methyl sulphides are noncompetitive substrates that are exclusively used by methanogens, therefore methylated methanogenesis can occur in coastal regions with high sulphate concentrations, for example, in organic-rich (Maltby et al., 2018), vegetated (Schorn et al., 2022), and hypersaline coastal sediments (Xiao et al., 2018). Coastal CH₄ can be driven by the exchange of pore water or groundwater (high in CH₄) with coastal surface waters in tidal systems, referred to as tidal pumping (Ovalle et al., 1990; Call et al., 2015). Anthropogenic impacts such as wastewater pollution and land-use change can increase CH₄ fluxes in estuaries (Wells et al., 2020). A large increase of CH₄ emissions follows the conversion of natural coastal habitats to aquaculture farms (Yuan et al., 2019; Yang et al., 2022). Currently available global modern biogenic CH₄ flux data show high spatiotemporal variability within and between coastal systems, but also because of the overall global paucity of data. Therefore, global estimates have high uncertainties and show large ranges in both empirical (Rosentreter et al., 2021) and machine-learning based approaches (Weber et al., 2019). According to a recent data-driven meta-data analysis, global estuaries, including tidal systems and deltas, lagoons, and fjords, are estimated to emit median (Q1-Q3) 0.25 (0.07-0.46) Tg CH₄ yr⁻¹ (Rosentreter et al., 2023). Coastal vegetation, including mangrove forests, salt marshes, and seagrasses are estimated to emit 0.77 (0.47-1.41) Tg CH₄ yr⁻¹, which is 3 times more than global estuaries (Rosentreter et al., 2023). The combined median (Q1-Q3) emission of 1.01 (0.54-1.87) Tg

CH₄ yr⁻¹ for coastal vegetation and estuaries by Rosentreter et al. (2023) is lower than the recent observation-based global





Total shallow coastal modern biogenic CH₄ emissions based on existing data including emissions from estuaries, coastal 1257 1258 vegetation (Rosentreter et al., 2023), tidal flats, and man-made coastal aquaculture ponds (Rosentreter et al., 2021) amount 1259 to median (Q1-Q3) 1.8 (0.59-5.57) Tg CH₄ yr⁻¹. This range is about 3-4 times lower than the earlier global assessment by Borges and Abril (2011) and also lower than the value of 4-5 Tg CH₄ yr⁻¹reported in the previous CH₄ budget for inner and 1260 1261 outer estuaries including marshes and mangroves (Saunois et al., 2020), which was based on a significantly smaller dataset 1262 (n=80) and larger estuarine surface areas (Laruelle et al., 2013) than used here (Laruelle et al., 2023). 1263 The near-shore (0-50 m), inner shelf diffusive modern biogenic CH₄ flux of median (Q1-Q3) 1.33 (0.93-2.10) Tg CH₄ yr⁻¹ 1264 by Weber et al. (2019) based on machine-learning is similar to the combined shallow coastal (estuaries and coastal 1265 vegetation) median by Rosentreter et al. (2021, 2023). Adding the diffusive modern biogenic CH₄ flux for the outer shelf 1266 (50-200 m) (median (Q1-Q3) of 0.54 (0.40-0.73) Tg CH₄ yr⁻¹) and for the slope (200-2000m) (median (Q1-Q3) of 0.28 1267 (0.22-0.37) Tg CH₄ yr⁻¹) (Weber et al., 2019), and excluding geological seepage regions (Etiope et al., 2019; see below), gives a total median (Q1-Q3) of 3.95 (2.14-8.77) Tg CH₄ yr⁻¹ for combined coastal shallow, near-shore, outer shelf and 1268 1269 slope diffusive modern biogenic CH₄ emissions. The previous budget by Saunois (2020) also included poorly constrained 1270 emissions (upper bound value: 1-2 Tg CH₄ yr⁻¹) from large river plumes protruding onto the shelves. However, here we 1271 assume that emissions from large river plumes are accounted for in the near-shore and outer shelf estimates by Weber et al. 1272 (2019). Area-integrated diffusive CH₄ emissions from the open ocean and deep seas (>2000 m) are much lower than from 1273 other coastal systems but amount to median (Q1-Q3) 0.91 (0.75-1.12) Tg CH₄ yr⁻¹ because of the large surface area of the 1274 open ocean (>300 x 10⁶ km²) (Weber et al., 2019). Overall, these marine biogenic emissions are sustained by a mixture of 1275 sedimentary production and in-situ production in the sea-surface layers, as shown by, e.g., Karl et al. (2008) and Repeta et 1276 al. (2016). The total coastal and ocean diffusive modern biogenic emissions retained here amount to 5 (3-10) Tg CH₄ yr⁻¹.

synthesis including tidal flats and aquaculture ponds (median 1.49 (0.22-6.48) Tg CH₄ yr⁻¹) by Rosentreter et al. (2021).

1277 1278

1279

1280

1281

1282

1283

1284

1285

1286

1287

Coastal and oceanic geological methane emissions Submarine geological CH₄ emission is the offshore component of the general geological emissions of natural gas from the Earth's crust (Judd, 2004; Etiope, 2009; Etiope et al., 2019). The onshore components include terrestrial seeps, mud volcanoes, microseepage, and geothermal manifestations, addressed in Sect. 3.2.3. Natural gas seeping at the seabed as bubble plumes can reach the surface, generally occurs in relatively shallow waters (<400 m), but CH₄-rich bubble plumes reaching the atmosphere from depths >500 m have been observed in some cases (e.g., Solomon et al., 2009), and upwelling of bottom marine waters can, in theory, transport geological CH₄ (dissolved) to the surface from any depth. This represents, however, a small and poorly known fraction of geological CH₄ emission. Geological CH₄ can be either microbial or thermogenic, produced throughout diverse geological periods in hydrocarbon source rocks in sedimentary basins (therefore it is always fossil, ¹⁴C-free). The seepage at the seafloor is typically related to tectonic faults, sometimes forming mud diapirs and mud volcanoes (Mazzini and Etiope, 2017).





ВУ

Published estimates of geological CH₄ submarine emissions range from 3 to 20 Tg yr⁻¹, with a best guess of 7 Tg yr⁻¹ (Etiope 1288 1289 and Schwietzke, 2019; Etiope et al., 2019 and references therein). 1290 Here, the diffusive geological CH₄ emissions are estimated at 0.16 (0.11-0.24) Tg CH₄ yr⁻¹ for near-shore (0-50 m), 0.03 (0.02-0.05) Tg CH₄ yr⁻¹ for outer shelf (50-200 m), and 0.02 (0.01-0.03) Tg CH₄ yr⁻¹ for slope (200-2000 m) by calculating 1291 1292 the fraction of the Weber et al. (2019) diffusive fluxes that occur within the identified geological seepage regions from 1293 Etiope et al. (2019). No geological seepage regions were identified in the open ocean and deep seas (> 2000 m). 1294 In this study, we consider the ebullitive flux as geologically sourced CH₄. While modern biogenic CH₄ gas production 1295 appears ubiquitous in shallow sediments (Fleischer et al., 2001; Best et al., 2006), no global dataset is currently available to 1296 estimate the biogenic ebullitive CH4 flux to the atmosphere. Omission of this flux thus constitutes a significant knowledge 1297 gap in the coastal and oceanic CH₄ budget. Global geological CH₄ ebullition from continental shelf and slope, referring only 1298 to depths <200 m, were estimated at 5.06 (1.99-8.16) Tg CH₄ yr⁻¹ (Weber et al., 2019). This estimate is based on prior 1299 estimates of the geological flux from the seafloor (Hovland et al., 1993) and bubble transfer efficiency to the ocean surface 1300 (McGinnis et al., 2006). Etiope et al. (2019) estimated a partial fraction of geological emissions in the form of gas bubbles 1301 of 3.9 (1.8-6) Tg CH₄ yr⁻¹, only referring to the sum of published estimates from 15 geological seepage regions, which are 1302 also deeper than 200 m. Global extrapolation including other 16 identified seepage zones (where flux data are not available) 1303 was suggested to be at least 7 (3-10) Tg CH₄ yr⁻¹ (Etiope et al., 2019), and this value coincides with the mean emission value 1304 (best guess) derived by combining literature data, see Etiope and Schwietzke (2019) for further details. It is worth noting 1305 that the Weber et al. (2019) estimate of 5.06 (1.99-8.16) Tg CH₄ yr⁻¹, which considers only the continental shelf at depths 1306 <200 m, is compatible with the overall submarine emission of 7 (3-10) Tg CH₄ yr⁻¹ (including seeps > 200 m deep) indicated 1307 in Etiope and Schwietzke (2019) and Etiope et al. (2019). Although 300-400 m is considered a general depth limit for 1308 efficient transport (with limited oxidation and dissolution) of CH₄ bubbles to the atmosphere (e.g., Judd, 2004; Schmale et 1309 al., 2005; Etiope et al., 2019), in some cases oil coatings on bubbles inhibit gas dissolution so that CH₄-rich bubbles can 1310 reach the atmosphere from depths >500 m (e.g., Solomon et al., 2009). As mentioned above, a fraction of geological CH₄ 1311 released in deep seas (such as in the areas with gas-charged sediments inventoried in Fleischer et al., 2001) can also be 1312 transported to the surface by upwelling bottom waters. Further research is needed to better evaluate the atmospheric impact 1313 of such deep seeps. 1314 Geological submarine emissions, thus, would amount to 0.21 (0.14-0.32) Tg CH₄ yr⁻¹ in the form of a diffusive flux while 1315 the ebullitive flux would be 5.06 (3.01-7.88) Tg CH₄ yr¹, considering only < 200 m deep seepage, and 7 (3-10) Tg CH₄ yr 1316 ¹ considering all data available (Etiope and Schwietzke, 2019). Here, we select the Etiope and Schwietzke (2019) assessment 1317 in order to account for all potential seepage areas, including those located at water depths > 200m.

1318

As a result, here we report a (rounded) median of 12 Tg CH₄ yr⁻¹ with a range of 6-20 Tg CH₄ yr⁻¹ for all coastal and ocean sources.





Methane emissions from gas hydrates. Among the different origins of coastal and oceanic CH₄, hydrates have attracted a lot of attention. CH₄ hydrates (or clathrates) are ice-like crystals formed under specific temperature and pressure conditions (Milkov, 2005). Hydrates may host either modern microbial CH₄, containing ¹⁴C and formed *in situ* in shallow sediments (this type of hydrates is also called "autochthonous") or fossil, microbial or thermogenic CH₄, migrated from deeper sediments, generally from reservoirs in hydrocarbon-rich sedimentary basins (this type of hydrates is also called "allochthonous"; Milkov, 2005; Foschi et al., 2023). The total stock of marine CH₄ hydrates is large but uncertain, with global estimates ranging from hundreds to thousands of Pg CH₄ (Klauda and Sandler, 2005; Wallmann et al., 2012). Note that the highly climate-sensitive subsea permafrost reservoir beneath Arctic Ocean shelves also contributes to the hydrate inventory (Ruppel and Kassler, 2017).

Concerning more specifically atmospheric emissions from marine hydrates, Etiope (2015) points out that current estimates of CH₄ air—sea flux from hydrates (2–10 Tg CH₄ yr⁻¹ in Ciais et al., 2013, or Kirschke et al., 2013) originate from the hypothetical values of Cicerone and Oremland (1988). No experimental data or estimation procedures have been explicitly described along the chain of references since then (Denman et al., 2007; IPCC, 2001; Kirschke et al., 2013; Lelieveld et al., 1998). It was estimated that ~473 Tg CH₄ has been released into the water column over 100 years (Kretschmer et al., 2015). Those few teragrams per year become negligible once consumption within the water column has been accounted for. While events such as submarine slumps may trigger local releases of considerable amounts of CH₄ from hydrates that may reach the atmosphere (Etiope, 2015; Paull et al., 2002), on a global scale, present-day atmospheric CH₄ emissions from hydrates do not appear to be a significant source to the atmosphere, and at least formally, we should consider 0 (< 0.1) Tg CH₄ yr⁻¹ emissions.

3.2.7 Terrestrial permafrost

Permafrost is defined as frozen soil, sediment, or rock having temperatures at or below 0°C for at least two consecutive years (Harris et al., 1988). The total extent of permafrost in the Northern Hemisphere is about 14 million km² or 15% of the exposed land surface (Obu et al., 2019). As the climate warms, a rise in soil temperatures has been observed across the permafrost region, and permafrost thaw occurs when temperatures pass 0°C, often associated with melting of ice in the ground (Biskaborn et al., 2019). Permafrost thaw is most pronounced in southern and spatially isolated permafrost zones, but also occurs in northern continuous permafrost (Obu et al., 2019). Thaw occurs either as a gradual, often widespread, deepening of the active layer (surface soils that thaw every summer) or as more rapid localised thaw associated with loss of massive ground ice (thermokarst) (Turetsky et al., 2020). A total of 1000 ± 200 Pg of carbon can be found in the upper 3 meters of permafrost region soils, or 1400-2000 Pg C for all permafrost (Hugelius et al., 2014; Strauss et al., 2021).





13521353

13541355

1356

1357

1358

1359

1360

1361

1362

1363

1364

13651366

1367

1368

1369

1370

1371

1372

1373

13741375

1376

1377

1378

1379

1380

1381

1382

The thawing permafrost can generate direct and indirect CH₄ emissions. Direct CH₄ emissions are from the release of CH₄ contained within the thawing permafrost. This flux to the atmosphere is small and estimated to be a maximum of 1 Tg CH₄ yr⁻¹ at present (USEPA, 2010b). Increased seepage of geogenic CH₄ gas seeps along permafrost boundaries and lake beds may also be considered a direct flux, and this is estimated to be 2±0.4 Tg CH₄ yr⁻¹ (Walter Anthony et al., 2012). Indirect CH₄ emissions are probably more important. They are caused by 1) methanogenesis induced when the organic matter contained in thawing permafrost becomes available for microbial decomposition; 2) thaw induced soil wetting and changes in land surface hydrology possibly enhancing CH₄ production (McCalley et al., 2014; Schuur et al., 2022); and 3) the landscape topography changes driven by abrupt thaw processes and loss of ground ice, including the formation of thermokarst lakes, hill-slope thermokarst, and wetland thermokarst (Turetsky et al., 2020). Such CH₄ production is probably already significant today and is likely to become more important in the future associated with climate change and strong positive feedback from thawing permafrost (Schuur et al., 2022). However, indirect CH₄ emissions from permafrost thawing are difficult to estimate at present, with very few data to refer to, and in any case largely overlap with wetland and freshwater emissions occurring above or around thawing areas. In a recent synthesis of full permafrost region CH₄ budgets for the period 2000-2017, Hugelius et al. (2023) compared CH₄ budgets from bottom-up and top-down (atmospheric inversion models) approaches. They estimate an integrated bottom-up budget of 50 (23, 53; mean upper and lower 95% CI) Tg CH₄ yr⁻¹ while the top-down estimate is 19 (15, 24) Tg CH₄ yr⁻¹. The bottom-up estimate is based on a combination of datadriven upscaling reported by Ramage et al. (2023) and process-based model estimates for wetland CH₄ flux calculated from model ensembles used in Saunois et al. (2020). The top-down estimate is calculated from ensembles of atmospheric inversion models used in Saunois et al. (2020). Although it is difficult with direct process-attribution, fluxes of ca. 20-30 Tg CH₄ yr⁻¹ in the bottom-up budget are caused by land cover types affected by previous permafrost thaw (thermokarst lakes, wetlands, hillslope). Because pre-thaw land cover types often have near neutral CH₄ balances (Ramage et al. 2023), these fluxes can largely be seen as driven by permafrost thaw, however the thaw may have occurred decades, or even centuries, before today. Here, we choose to report only the direct emission range of 0-1 Tg CH₄ yr⁻¹, keeping in mind that current wetland, thermokarst lakes and other freshwater methane emissions already likely include a significant indirect contribution originating from thawing permafrost.

3.2.8 Vegetation

Three distinct pathways for the production and emission of CH₄ by living vegetation are considered here (see Covey and Megonigal (2019) and Bastviken et al. (2023) for extensive reviews). Firstly, plants produce CH₄ through an abiotic photochemical process induced by stress (Keppler et al., 2006). This pathway was initially questioned (e.g., Dueck et al., 2007; Nisbet et al., 2009), and although numerous studies have since confirmed aerobic emissions from plants and better resolved its physical drivers (Fraser et al., 2015), global estimates still vary by two orders of magnitude (Liu et al., 2015).

https://doi.org/10.5194/essd-2024-115 Preprint. Discussion started: 6 June 2024 © Author(s) 2024. CC BY 4.0 License.



1383

1384

1385

1386

1387

1388

1389

1390

1391

1392

1393

1394

1395

1396

13971398

1399

1400

1401

1402

1403

1404

1405

1406

14071408

1409

1410

1411

1412



This plant source has not been confirmed in-field however, and although the potential implication for the global CH₄ budget remains unclear, emissions from this source are certainly much smaller than originally estimated in Keppler et al. (2006) (Bloom et al., 2010; Fraser et al., 2015). Second, and of clearer significance, plants act as "straws", drawing up and releasing microbially produced CH₄ from anoxic soils (Cicerone and Shetter, 1981; Rice et al., 2010). For instance, in the forested wetlands of Amazonia, tree stems are the dominant ecosystem flux pathway for soil-produced CH₄, therefore, including stem emissions in ecosystem budgets can reconcile regional bottom-up and top-down estimates (Pangala et al., 2017; Gauci et al., 2021). Third, the stems of both living trees (Covey et al., 2012) and dead wood (Covey et al., 2016) provide an environment suitable for microbial methanogenesis. Static chambers demonstrate locally significant through-bark flux from both soil- (Pangala et al., 2013, 2015), and tree stem-based methanogens (Pitz and Megonigal, 2017; Wang et al., 2016). A recent synthesis indicates stem CH₄ emissions significantly increase the source strength of forested wetlands, and modestly decrease the sink strength of upland forests (Covey and Megonigal, 2019). The scientific activity covering CH₄ emissions in forested ecosystems reveals a far more complex story than previously thought, with an interplay of productive/consumptive, aerobic/anaerobic, and biotic/abiotic processes occurring between upland/wetland soils, trees, and atmosphere. Understanding the complex processes that regulate CH₄ source–sink dynamics in forests and estimating their contribution to the global CH₄ budget requires cross-disciplinary research, more observations, and new models that can overcome the classical binary classifications of wetland versus upland forest and of emitting versus uptaking soils (Barba et al., 2019; Covey and Megonigal, 2019). Although we recognize these emissions are potentially large (particularly tree transport from inundated soil), global estimates for each of these pathways remain highly uncertain and/or are currently included here within other flux category sources (e/g. inland waters, wetlands, upland soils).

3.3 Methane sinks and lifetime

CH₄ is the most abundant reactive trace gas in the troposphere and its reactivity is important to both tropospheric and stratospheric chemistry. The main atmospheric sink of CH₄ (~90% of the total sink mechanism) is oxidation by the hydroxyl radical (OH), mostly in the troposphere (Ehhalt, 1974). Other losses are by photochemistry in the stratosphere (reactions with chlorine atoms (Cl) and excited atomic oxygen (O(¹D)), oxidation in soils (Curry, 2007; Dutaur and Verchot, 2007), and by photochemistry in the marine boundary layer (reaction with Cl; Allan et al. (2007), Thornton et al. (2010)). Uncertainties in the total sink of CH₄ as estimated by atmospheric chemistry models are in the order of 20-40% (Saunois et al., 2016). It is much less (10-20%) when using atmospheric proxy methods (e.g., methyl chloroform, see below) as in atmospheric inversions (Saunois et al., 2016). In the present release of the global CH₄ budget, we estimate bottom-up CH₄ chemical sinks and lifetime mainly based on global model results from the Chemistry Climate Model Initiative (CCMI) 2022 activity (Plummer et al., 2021) and CMIP6 simulations (Collins et al., 2017).



1445



3.3.1 Tropospheric OH oxidation

1414 OH radicals are produced following the photolysis of ozone (O₃) in the presence of water vapour. OH is destroyed by 1415 reactions with carbon monoxide (CO), CH₄, and non-methane volatile organic compounds. 1416 Following the Atmospheric Chemistry and Climate Model Intercomparison Project (ACCMIP), which studied the long-term 1417 changes in atmospheric composition between 1850 and 2100 (Lamarque et al., 2013), a new series of experiments was 1418 conducted by several chemistry-climate models and chemistry-transport models participating in the Chemistry-Climate 1419 Model Initiative (CCMI) (Plummer et al., 2021). Mass-weighted OH tropospheric concentrations do not directly represent 1420 CH₄ loss, as the spatial and vertical distributions of OH affect this loss through, in particular, the temperature dependency 1421 and the distribution of CH₄ (e.g., Zhao et al., 2019). However, estimating OH concentrations and, spatial and vertical 1422 distributions is a key step in estimating methane loss through OH. Over the period 2000-2010, the global mass-weighted 1423 OH tropospheric concentration is estimated at 13.3 [11.7-18.2] x 10⁵ molecules cm⁻³ by 8 CCMI-2022 models and at 11.5 [7.9-13.5] x 10⁵ molecules cm⁻³ by 10 models contributing CMIP6 (see supplementary Table S4). The ranges calculated 1424 1425 here are larger than the ones proposed previously in Saunois et al. (2020), where the multi-model mean (11 models) global 1426 mass-weighted OH tropospheric concentration was 11.7±1.0 x 10⁵ molecules cm⁻³ (range 9.9-14.4 x 10⁵ molecules cm⁻³, 1427 Zhao et al. (2019)) consistent with the previous estimates from ACCMIP (11.7±1.0 x 10⁵ molecules cm⁻³, with a range of 1428 $10.3-13.4 \times 10^5$ molecules cm⁻³, Voulgarakis et al. (2013) for year 2000) and the estimates of Prather et al. (2012) of 11.2 ± 1.3 1429 x 10⁵ molecules cm⁻³. Nicely et al. (2017) attribute the differences in OH simulated by different chemistry transport models 1430 to, in decreasing order of importance, different chemical mechanisms, various treatments of the photolysis rate of O₃, and 1431 modelled O₃ and CO. Besides the uncertainty on global OH concentrations, there is an uncertainty in the spatial and temporal 1432 distribution of OH. Models often simulate higher OH in the northern hemisphere (NH) than in the southern hemisphere 1433 (SH), leading to a NH/SH OH ratio greater than 1 (Naik et al., 2013; Zhao et al., 2019). However, there is evidence for 1434 parity in inter-hemispheric OH concentrations (Patra et al., 2014), which needs to be confirmed by other observational and 1435 model-derived estimates. The analysis of the latest CCMI (Plummer et al., 2021) and CMIP6 (Collins et al., 2021) model 1436 outputs show that structural uncertainties in the atmospheric chemistry models remain large, probably due to inherent biases 1437 in OH precursors. Based on OH precursor observations and a chemical box model, Zhao et al. (2023) corrected the OH 3D 1438 fields simulated by two atmospheric chemistry models, resulting in tropospheric OH mean concentrations lowered by 2. 10⁵ molecules cm⁻³, leading to around 10 x 10⁵ molecules cm⁻³, and a NH/SH OH ratio closer to 1, in better agreement with 1439 1440 methyl chloroform (MCF)-based approaches. This study highlights the need for further improvement of the atmospheric 1441 chemistry model. 1442 OH concentrations and their changes can be sensitive to climate variability (Dlugokencky et al., 1996; Holmes et al., 2013; 1443 Turner et al., 2018), biomass burning (Voulgarakis et al., 2015), and anthropogenic activities. For instance, the increase of 1444 the oxidizing capacity of the troposphere in South and East Asia associated with increasing NO_x emissions (Mijling et al.,

2013) and decreasing CO emissions (Yin et al., 2015), possibly enhances CH₄ oxidation and therefore limits the atmospheric





1446 impact of increasing emissions (Dalsøren et al., 2009). Despite such large regional changes, the global mean OH 1447 concentration was suggested to have changed only slightly over the past 150 years (Naik et al., 2013). This is due to the 1448 compensating effects of the concurrent increases of positive influences on OH (water vapour, tropospheric ozone, nitrogen 1449 oxides (NO_X) emissions, and UV radiation due to decreasing stratospheric O₃), and of OH sinks (CH₄ burden, CO and non-1450 CH₄ volatile organic compound emissions and burden). CCMI models show OH inter-annual variability ranging from 0.4% 1451 to 1.8% (Zhao et al., 2019) over 2000-2010 (similar values are derived in the latest CCMI and CMIP6 activities - see 1452 supplementary Table S4), lower than the value deduced from methyl chloroform measurements (proxy, top-down approach). 1453 However, these simulations consider meteorology variability but not emission interannual variability (e.g., from biomass 1454 burning) and thus are expected to simulate lower OH inter annual variability than in reality. Using an empirical model constrained by global observations of O₃, water vapour, CH₄, and temperature as well as the simulated effects of changing 1455 NO_x emissions and tropical expansion, Nicely et al. (2017) found an inter-annual variability in OH of about 1.3-1.6% 1456 between 1980 and 2015, in agreement with methyl chloroform based estimates (Montzka et al., 2011). 1457 1458 Over 2000-2009, the tropospheric loss (tropopause height at 200 hPa) of CH₄ by OH oxidation derived from the ten and 1459 CCMI modelling activities (see supplementary Table S5) is estimated at of 546 [446-663] Tg CH₄ yr⁻¹, which is similar to the one reported previously in Saunois et al. (2020) from CCMI model (553 [476-677] Tg CH₄ yr⁻¹) and still slightly higher 1460 1461 than the one from the ACCMIP models (528 [454-617] Tg CH₄ yr⁻¹ reported in Kirschke et al. (2013) and Saunois et al. 1462 (2016).1463 For the recent 2010-2019 decade, we report a climatological value based on five models that contributed to CMIP6 runs 1464 (historic followed by SSP3-7.0 projections starting in 2015, Collins et al. (2021)) to acknowledge the impact of the rise in

3.3.2 Stratospheric loss

663] Tg CH₄ yr⁻¹

1465

1466

1467

1475

1476

In the stratosphere, CH₄ is lost through reactions with excited atomic oxygen O(¹D), atomic chlorine (Cl), atomic fluorine (F), and OH (Brasseur and Solomon, 2005; le Texier et al., 1988). Uncertainties in the chemical loss of stratospheric CH₄ are large, due to uncertain inter-annual variability in stratospheric transport as well as its chemical interactions and feedbacks with stratospheric O₃ (Portmann et al., 2012). Particularly, the fraction of stratospheric loss due to the different oxidants is still uncertain, with possibly 20-35% due to halons, about 25% due to O(¹D) mostly in the high stratosphere and the rest due to stratospheric OH (McCarthy et al., 2003).

In this study, ten chemistry climate models that contributed to CMIP6 and CCMI modelling activities (Table S5) are used

atmospheric methane on the methane chemical sink. Hence, for 2010-2019, we report the climatological value of 563 [510-

In this study, ten chemistry climate models that contributed to CMIP6 and CCMI modelling activities (Table S5) are used to provide estimates of CH₄ chemical loss, including reactions with OH, O(¹D), and Cl; CH₄ photolysis is also included but occurs only above the stratosphere. Considering a 200 hPa tropopause height, the CMIP6 and CCMI results suggest an



1482

14831484

14851486

1487

14881489

1490

1491

1492

1493

1494

1495

14961497

1498

1499

1500

1501



- estimate of 34 [10-51]Tg CH₄ yr⁻¹ for the CH₄ stratospheric sink for the 2000-2009 decade (Table S5), similar to the value
- derived from the previous CCMI activity reported in Saunois et al. (2020) (31 [12-41] Tg CH_4 yr⁻¹).
- For 2010-2019, we report here a climatological range of 11-43 Tg CH₄ yr⁻¹ associated with a mean value of 33 Tg CH₄ yr⁻¹
- based on five models that contributed to CMIP6 runs (historic followed by SSP3-7.0 projections starting in 2015; Table S5).

3.3.3 Tropospheric reaction with Cl

Halogen atoms can also contribute to the oxidation of CH₄ in the troposphere. Allan et al. (2005) measured mixing ratios of methane and δ^{13} C-CH₄ at two stations in the southern hemisphere from 1991 to 2003, and found that the apparent kinetic isotope effect (KIE) of the atmospheric CH₄ sink was significantly larger than that explained by OH alone. A seasonally varying sink due to Cl in the marine boundary layer of between 13 and 37 Tg CH₄ yr⁻¹ was proposed as the explanatory mechanism (Allan et al., 2007; Platt et al., 2004). This sink was estimated to occur mainly over coastal and marine regions, where sodium chloride (NaCl) from evaporated droplets of seawater react with NO₂ to eventually form Cl₂, which then UVdissociates to Cl. However significant production of nitryl chloride (ClNO₂) at continental sites has been recently reported (Riedel et al., 2014) and suggests the broader presence of Cl, which in turn would expand the significance of the Cl sink in the troposphere. Recently, Hossaini et al. (2016), Sherwen et al. (2016), and Wang et al. (2019b, 2021b) have made significant improvements in tropospheric chemistry modelling and they conclude to an oxidation contribution of 2.6%, 2%, 1% and 0.8%, respectively. These values correspond to a tropospheric CH₄ loss of around 12-13 Tg CH₄ yr⁻¹, 9 Tg CH₄ yr⁻¹ ¹, 5 Tg yr⁻¹, and 3 Tg CH₄ yr⁻¹respectively, much lower than the first estimates by Allan et al. (2007). The recent work of Wang et al. (2021b) is the most comprehensive modelling study and based upon Sherwen et al. (2016) and Wang et al. (2019b). Both the KIE approach and chemistry transport model simulations carry uncertainties (extrapolations based on only a few sites and use of indirect measurements, for the former and missing sources, coarse resolution, underestimation of some anthropogenic sources for the latter). However, Gromov et al. (2018) found that Cl can contribute only 0.23% the tropospheric sink of CH₄ (about 1 Tg CH₄ yr⁻¹) in order to balance the global ¹³C(CO) budget (see their Table S1). While tropospheric Cl has a marginal impact on the total CH₄ sink (few percents), it influences more significantly the atmospheric isotopic δ^{13} C-CH₄ signal and improved estimates of the tropospheric Cl amount should be used for isotopic CH₄ modelling studies (Strode et al., 2020; Thanwerdas et al., 2022b).

Each recent Cl estimate suggests a reduced contribution to the methane loss than previously reported by Allen et al. (2007).

As a result, we suggest here to use the mean, minimum and maximum of the last five estimates published since 2016, leading

to a climatological value of 6 [1-13] Tg CH₄ yr⁻¹, thus reducing both the magnitude and the uncertainty range compared to

1505 Saunois et al. (2020).

1506

1504



1508

1509

1510

1511

1512

15131514

1515

1516

1517

1518

1519

1520

1521

1522

15231524

1525

1526

15271528

1529

1530

1531

1532

1533

1534

1535

1536

1537

1538



3.3.4 Soil uptake

Unsaturated oxic soils are sinks of atmospheric CH₄ due to the presence of methanotrophic bacteria, which consume CH₄ as a source of energy. Dutaur and Verchot (2007) conducted a comprehensive meta-analysis of field measurements of CH₄ uptake spanning a variety of ecosystems. Extrapolating to the global scale, they reported a range of 36 ± 23 Tg CH₄ vr⁻¹, but also showed that stratifying the results by climatic zone, ecosystem, and soil type led to a narrower range (and lower mean estimate) of 22 ± 12 Tg CH₄ vr⁻¹. Modelling studies, employing meteorological data as external forcing, have also produced a considerable range of estimates. Using a soil depth-averaged formulation based on Fick's law with parameterizations for diffusion and biological oxidation of CH₄, Ridgwell et al. (1999) estimated the global sink strength at 38 Tg CH₄ yr⁻¹, with a range 20-51 Tg CH₄ yr⁻¹ reflecting the model structural uncertainty in the base oxidation parameter. Curry (2007) improved on the latter by employing an exact solution of the one-dimensional diffusion-reaction equation in the near-surface soil layer (i.e., exponential decrease in CH₄ concentration below the surface), a land surface hydrology model, and calibration of the oxidation rate to field measurements. This resulted in a global estimate of 28 Tg CH₄ yr⁻¹ (9-47 Tg CH₄ yr⁻¹), the result reported by Zhuang et al. (2013), Kirschke et al. (2013) and Saunois et al. (2016). Ito and Inatomi (2012) used an ensemble methodology to explore the variation in estimates produced by these parameterizations and others, which spanned the range 25-35 Tg CH₄ yr⁻¹. For the period 2000-2020, as part of the wetland emissions modelling activity, JSBACH (Kleinen et al., 2020) and VISIT (Ito and Inatomi, 2012) models compute a global CH₄ soil uptake to 18 and 35 Tg CH₄ yr⁻¹, respectively. Murguia-Flores et al. (2018) further refined the Curry (2007) model's structural and parametric representations of key drivers of soil methanotrophy, demonstrating good agreement with the observed latitudinal distribution of soil uptake (Dutaur and Verchot, 2007). Their model (MeMo) simulates a CH₄ soil sink of 37.5 Tg CH₄ yr⁻¹ for the period 2010-2019 (Fig. S4), compared to 39.5 and 31.3 Tg CH₄ yr⁻¹ using the Ridgwell et al. (1999) and Curry (2007) parameterizations, respectively, under the same meteorological forcing, run specifically for this study. For the 2000s period, the simulations estimate the soil uptake at 30.4, 36.7 and 38.3 Tg CH₄ yr⁻¹ based on the parameterization of Curry, MeMo, and Ridgwell, respectively. As part of a more comprehensive model accounting for a range of CH₄ sources and sinks, Tian et al. (2010, 2015, 2016) computed vertically-averaged CH₄ soil uptake including the additional mechanisms of aqueous diffusion and plant-mediated (aerenchyma) transport, arriving at the estimate 30±19 Tg CH₄ yr⁻¹ (Tian et al., 2016) for the 2000s. The still more comprehensive biogeochemical model of Riley et al. (2011) included vertically resolved representations of the same processes considered by Tian et al. (2016), in addition to grid cell fractional inundation and, importantly, the joint limitation of uptake by both CH4 and O2 availability in the soil column. Riley et al. (2011) estimated a global CH4 soil sink of 31 Tg CH₄ yr⁻¹ with a structural uncertainty of 15-38 Tg CH₄ yr⁻¹ (a higher upper limit resulted from an elevated gas diffusivity to mimic convective transport; as this is not usually considered, we adopt the lower upper bound associated with no limitation of uptake at low soil moisture). A model of this degree of complexity is required to explicitly simulate situations where the soil water content increases enough to inhibit the diffusion of oxygen, and the soil becomes a methane source





- (Lohila et al., 2016). This transition can be rapid, thus creating areas (for example, seasonal wetlands) that can be either a source or a sink of methane depending on the season.
- The previous Curry (2007) estimate can be revised upward slightly based on subsequent work and the increase in CH₄
- 1542 concentration since that time. Considering the latest estimates (based on VISIT, JSBACH, and Memo models, Table S6 in
- 1543 the supplementary) we report here a mean estimate of 31 [17-39] Tg CH₄ yr⁻¹ for 2000-2009 and 32 [18-40] for 2010-2019
- 1544 Tg CH₄ yr⁻¹.

3.3.5 CH₄ lifetime

The atmospheric lifetime of a given gas in steady state may be defined as the global atmospheric burden (Tg) divided by the total sink (Tg yr⁻¹) (IPCC, 2001). Global models provide an estimate of the loss of the gas due to individual sinks, which can then be used to derive lifetime due to a specific sink. For example, the tropospheric lifetime of CH₄ is determined as the global atmospheric CH₄ burden divided by the loss from OH oxidation in the troposphere, sometimes called "chemical lifetime". The total lifetime of CH₄ corresponds to the global burden divided by the total loss including tropospheric loss from OH oxidation, stratospheric chemistry and soil uptake. The CCMI (Plummer et al., 2021) and CMIP6 (Collins et al., 2021) runs estimate the tropospheric methane lifetime at about 9.2 years (average over years 2000-2009), with a range of 7.5-11 years (see Table S5). This range agrees with previous values found in ACCMIP and CCMI (9.3 [7.1-10.6] years, Voulgarakis et al. (2013), 9 [7.2-10.1] years, Saunois et al. (2020)). Adding 31 Tg to account for the soil uptake to the total chemical loss of the CMIP6 and CCMI models, we derive a total CH₄ lifetime of 8.2 years (average over 2000-2009 with a range of 6.8-9.7 years). The lifetime calculated over 2010-2019 based on CMIP6 simulations is similar (Table S5). These updated model estimates of total CH₄ lifetime agree with the previous estimates from ACCMIP (8.2 [6.4-9.2] years for year 2000, Voulgarakis et al. (2013)) and Saunois et al. (2020) based CCMI models. Reducing the large spread in CH₄ lifetime (between models, and between models and observation-based estimates) would 1) bring an improved constraint on global total methane emissions, and 2) ensure an accurate forecast of future climate.

4 Atmospheric observations and top-down inversions

4.1 Atmospheric observations

Systematic atmospheric CH₄ observations began in 1978 (Blake et al., 1982) with infrequent measurements from discrete air samples collected in the Pacific at a range of latitudes from 67°N to 53°S. Because most of these air samples were from well-mixed oceanic air masses and the measurement technique was precise and accurate, they were sufficient to establish an increasing trend and the first indication of the latitudinal gradient of methane. Spatial and temporal coverage was greatly improved soon after (Blake and Rowland, 1986) with the addition of the Earth System Research Laboratory from US National Oceanic and Atmospheric Administration (NOAA/GML) flask network (Steele et al. (1987); Lan et al. (2024), Fig.



15701571

1572

1573

1574

1575

1576

1577

1578

1579

1580

1581

1582

15831584

1585

1586

1587

1588

1589

1590

1591

1592

15931594

1595

1596

1597

1598

1599

1600



1), and the Advanced Global Atmospheric Gases Experiment (AGAGE) (Cunnold et al., 2002; Prinn et al., 2018), the Commonwealth Scientific and Industrial Research Organisation (CSIRO, Francey et al. (1999)), the University of California Irvine (UCI, Simpson et al., 2012) and in situ and flask measurements from regional networks, such as ICOS (Integrated Carbon Observation System) in Europe (https://www.icos-ri.eu/). The combined datasets provide the longest time series of globally averaged CH₄ abundances. Since the early-2000s, CH₄ column-averaged mole fractions have been retrieved through passive remote sensing from space (Buchwitz et al., 2005a, 2005b; Butz et al., 2011; Crevoisier et al., 2009; Frankenberg et al., 2005; Hu et al., 2018). Ground-based Fourier transform infrared (FTIR) measurements at fixed locations also provide time-resolved CH₄ column observations during daylight hours, and a validation dataset against which to evaluate the satellite measurements such as the Total Carbon Column Observing Network (TCCON) network (e.g., Pollard et al., 2017; Wunch et al., 2011), or Network for Detection of Atmospheric Composition Change (NDACC) (e.g., Bader et al., 2017). In this budget, in-situ observations from the different networks were used in the top-down atmospheric inversions to estimate CH₄ sources and sinks over the period 2000-2020. Satellite observations from the TANSO/FTS instrument on board the satellite GOSAT were used to estimate CH₄ sources and sinks over the period 2010-2020. Other atmospheric data (FTIR, airborne measurements, AirCore, isotopic measurements, etc.) have been used for validation by some groups, but not specifically in this study. However, further information is provided in Tables S7, S8, S9, S10, and S11 and a more comprehensive validation of the inversions is planned to use some of these data.

4.1.1 In situ CH₄ observations and atmospheric growth rate at the surface

We use globally averaged CH4 mole fractions at the Earth's surface from the four observational networks (NOAA/GML, AGAGE, CSIRO and UCI). The data are archived at the World Data Centre for Greenhouse Gases (WDCGG) of the WMO Global Atmospheric Watch (WMO-GAW) program (https://gaw.kishou.go.jp/), including measurements from other sites that are not operated as part of the four networks. The CH4 in-situ monitoring network has grown significantly over the last decade due to the emergence of laser diode spectrometers which are robust and accurate enough to allow deployments with low maintenance enabling the development of denser networks in developed countries (Stanley et al., 2018; Yver Kwok et al., 2015), and new stations in remote environments (Bian et al., 2015; Nisbet et al., 2019).

The networks differ in their sampling strategies, including the frequency of observations, spatial distribution, and methods of calculating globally averaged CH4 mole fractions. Details are given in the supplementary material of Kirschke et al. (2013). The global average values of CH4 abundances at Earth's surface presented in Fig. 1 are computed using long-term measurements from background conditions with minimal influence from immediate emissions. All measurements are calibrated against gas standards either on the current WMO reference scale or on independent scales with well-estimate differences from the WMO scale. The current WMO reference scale, maintained by NOAA/ESRL, WMO-X2004A (Dlugokencky et al., 2005) was updated in July 2015. NOAA and CSIRO global means are on this scale. AGAGE uses an independent standard scale (based on work by Tohoku University (Aoki et al., 1992) and maintained at Scripps Institution





1601 of Oceanography (SIO)), but direct comparisons of standards and indirect comparisons of atmospheric measurements show 1602 that differences are well below 5 ppb (Tans and Zwellberg, 2014; Vardag et al., 2014) and the TU-1987 scale used for 1603 AGAGE measurements is only 0.5 ppb difference from WMO-X2004A at 1900 ppb level. UCI uses another independent 1604 scale that was established in 1978 and is traceable to NIST (Flores et al., 2015; Simpson et al., 2012), but has not been 1605 included in standard exchanges with other networks so differences with the other networks cannot be quantitatively defined. 1606 Additional experimental details are presented in the supplementary material from Kirschke et al. (2013) and references 1607 therein. 1608 In Fig. 1 (a) globally averaged CH₄ and (b) its growth rate (derivative of the deseasonalized trend curve) through to 2022 1609 are plotted for the four measurement programs using a procedure of signal decomposition described in Thoning et al. (1989). 1610 We define the annual G_{ATM} as the increase in the atmospheric concentrations from Jan. 1 in one year to Jan. 1 in the next year. Agreement among the four networks is good for the global growth rate, especially since ~1990. The large differences 1611 1612 observed mainly before 1990 probably reflect the different spatial coverage of each network. The long-term behaviour of 1613 globally averaged atmospheric CH₄ shows a positive growth rate (defined as the derivative of the deseasonalized mixing 1614 ratio) that is slowing down from the early-1980s through 1998, a near-stabilisation of CH₄ concentrations from 1999 to 1615 2006, and a renewed period with positive persistent overall accelerating growth rates since 2007, slightly larger after 2014. 1616 When a constant atmospheric lifetime is assumed, the decreasing growth rate from 1983 through 2006 may imply that 1617 atmospheric CH₄ was approaching steady state, leading to no trend in emissions. The NOAA global mean CH₄ concentration 1618 was fitted with a function that describes the approach to a first-order steady state (s_S index): $[CH_4]_{ss}$ -($[CH_4]_{ss}$ -1619 $[CH_4]_0 e^{-t/\tau}$; solving for the lifetime, τ , gives 9.3 years, which is very close to current literature values (e.g., Prather et al. 1620 (2012), 9.1 ± 0.9 years). Such an approach includes uncertainties, especially due to the strong assumption of no trend in 1621 lifetime. The result of constant emissions does not agree with some study explaining the stabilisation period by decreasing 1622 emissions associated with increasing sink (e.g., Bousquet et al., 2006). However, this value seems consistent albeit higher 1623 than the chemistry climate estimates (8.2 years, see Sect. 3.3.5) 1624 From 1999 to 2006, the annual increase of atmospheric CH₄ was remarkably small at 0.6±0.1 ppb yr⁻¹. After 2006, the atmospheric growth rate has increased to a level similar to that of the mid-1990s (~5 ppb yr⁻¹), and for 2014 and 2015 even 1625 1626 to that of the 1980s (>10 ppb yr⁻¹). In the two recent years 2020 and 2021, the highest growth rates of 15 ppb yr⁻¹ and 18 1627 ppb yr¹ (see Sect. 6) were unprecedented since the 1980s. On decadal timescales, the annual increase is on average 2.2±0.3

4.1.2 Satellite data of column average CH₄

1628

1629

1630

16311632

In this budget, we use satellite data from the JAXA satellite Greenhouse Gases Observing SATellite (GOSAT) launched in January 2009 (Butz et al., 2011; Morino et al., 2011) containing the TANSO-FTS instrument, which observes in the shortwave infrared (SWIR). Different retrievals of CH₄ based on TANSO-FTS/GOSAT products are made available to the

ppb yr⁻¹ for 2000-2009, 7.6 ± 0.3 ppb yr⁻¹ for 2010-2019 and 15.2 ± 0.4 ppb yr⁻¹ for the year 2020.





community: from NIES (Yoshida et al., 2013), from SRON (Schepers et al., 2012) and from University of Leicester (Parker et al., 2020; Parker and Boesch, 2020). The three retrievals are used by the top-down systems (Table 4 and S6). Although GOSAT retrievals still show significant unexplained biases and limited sampling in cloud covered regions and in the high latitude winter, it represents an important improvement compared to the first satellite measuring CH₄ from space, SCIAMACHY (Scanning Imaging Absorption spectrometer for Atmospheric CartograpHY) both for random and systematic observation errors (see Table S2 of Buchwitz et al. (2016)).

Here, as in Saunois et al. (2020), only inversions using GOSAT retrievals are used.

4.2 Top-down inversions used in the budget

An atmospheric inversion is the optimal combination of atmospheric observations, of a model of atmospheric transport and chemistry, of a prior estimate of CH₄ sources and sinks, and of their uncertainties, to provide improved estimates of the sources and sinks, and their uncertainty. The theoretical principle of CH₄ inversions is detailed in the Supplementary Material and an overview of the different methods applied to CH₄ is presented in Houweling et al. (2017).

We consider an ensemble of inversions gathering various chemistry transport models, differing in vertical and horizontal resolutions, meteorological forcing, advection and convection schemes, and boundary layer mixing. Including these different systems is a conservative approach that allows us to cover different potential uncertainties of the inversion, among them: model transport, set-up issues, and prior dependency. General characteristics of the inversion systems are provided in Table 4. Further details can be found in the referenced papers and in the Supplementary Material. Each group was asked to provide gridded flux estimates for the period 2000-2020, using either surface or satellite data, but no additional constraints were imposed so that each group could use their preferred inversion setup. Two sets of prior emission distributions were built from the most recent inventories or model-based estimates (see Supplementary Material), but its use was not mandatory (see Table S8 to S11 for the inversion characteristics). This approach corresponds to a flux assessment, but not to a model inter-comparison as the protocol was not too stringent. Estimating posterior uncertainty is time and computer resource consuming, especially for the 4D-var approaches and Monte Carlo methods. Posterior uncertainties have not been requested for this study, but they were found to be lower than the ensemble spread in Saunois et al. (2020). Indeed, chemistry transport models differ in inter-hemispheric transport, stratospheric CH₄ profiles, and OH distribution, limitations which are not fully considered in the individual posterior uncertainty. As a result, we report the minimum-maximum range among the different top-down approaches.

Seven atmospheric inversion systems using global Eulerian transport models were used in this study; they contributed to the previous budgets that included eight atmospheric inversion systems in Saunois et al. (2016) and nine in Saunois et al. (2020). Each inversion system provided one or several simulations, including sensitivity tests varying the assimilated observations (surface or satellite), the OH inter-annual variability, or the prior fluxes ensemble. This represents a total of 24 inversion runs with different time coverage: generally, 2000-2020 for surface-based observations, and 2010-2020 for GOSAT-based





inversions (Table 4 and Table S7). In poorly observed regions, top-down surface inversions may rely on the prior estimates and bring little or no additional information to constrain (often) spatially overlapping emissions (e.g., in India, China). Also, we recall that many top-down systems solve for the total fluxes at the surface only or for some categories that may differ from the GCP categories. When multiple sensitivity tests were performed the mean of this ensemble was used not to overweight one particular inverse system. It should also be noticed that some satellite-based inversions are in fact combined satellite and surface inversions as they use surface-based inversions to correct the latitudinal bias of the satellite retrievals against the optimised atmosphere measurements to correct for errors in the transport model especially in the stratosphere (e.g., Segers et al., 2022; Maasakkers et al., 2019). Nevertheless, these inversions are still referred to as satellite-based inversions. Most of the top-down models use the OH distribution from the TRANSCOM experiment (Patra et al., 2011) either as fixed over the period or with the inter-annual variability derived by Patra et al. (2021).

Each group provided gridded monthly maps of emissions for both their prior and posterior total and for sources per category (see the categories Sect. 2.3). Results are reported in Sect. 5. Atmospheric sinks from the top-down approaches have been provided for this budget, and are compared with the values reported in Saunois et al. (2020). Not all inverse systems report their chemical sink; as a result, the global mass imbalance for the top-down budget is derived as the difference between total sources and total sinks for each model when both fluxes were reported.

5 Methane budget: top-down and bottom-up comparison

5.1 Global methane budget

5.1.1 Global total methane emissions-

Top-down estimates. At the global scale, the total annual emissions inferred by the ensemble of 24 inversions is 575 Tg CH₄ yr⁻¹ [553-586] for the 2010-2019 decade (Table 3), with the highest ensemble mean emission of 608 Tg CH₄ yr⁻¹ [581-627] for 2020. Global emissions for 2000-2009 (543 Tg CH₄ yr⁻¹) are consistent with Saunois et al. (2016, 2020) and the range for global emissions, 526-558 Tg CH₄ yr⁻¹ falls within the range in Saunois et al. (2016) (535-569) and Saunois et al. (2020) (524-560), although the ensemble of inverse systems contributing to this budget is different from Saunois et al. (2016, 2020). Changes in ensemble members contributing to the different budgets are a feature of each new GMB release and, therefore, introduce a source of variation (Table S7). The range reported gives the minimum and maximum values among studies and does not reflect the individual full uncertainties. In addition, most of the top-down models use the same OH distribution from the TRANSCOM experiment (Patra et al., 2011), which introduces less variability to the global budget than is likely justified, and so contributes to the rather low range (10%) compared to bottom-up estimates (see below).

Bottom-up estimates. The bottom-up estimates considered here differ substantially from the top-down results, with annual global emissions being about 15% larger at 669 Tg CH₄ yr⁻¹ [512-849] for 2010-2019 (Table 3). Yet, thanks to the double counting corrections in this budget, bottom-up and top-down budgets are in better agreement compared to previous GMB





releases. For the period 2000-2009, the discrepancy between bottom-up and top-down was about 30% of the top-down estimates in Saunois et al. (2016, 2020) (167 and 156 Tg CH₄ yr⁻¹, respectively), a value that has been reduced significantly in this budget (now 95 Tg CH₄ yr⁻¹ (<17%) for the same 2000-2009 period). This reduction is due to improvements from an important decrease in the estimate of emissions from natural and indirect anthropogenic emissions from bottom-up approaches, and more specifically inland freshwater emissions. From the previous budget, the estimate for inland freshwater emissions (lakes, ponds, reservoirs, rivers, and streams) has decreased from 159 Tg CH₄ yr⁻¹ to 112 Tg CH₄ yr⁻¹ (47 Tg decrease). Then, 23 Tg have been removed in the total freshwater ecosystem emissions due to double counting between vegetated wetlands and mostly small ponds and lakes (Sect. 3.2.2). As a result the combined wetland and inland freshwater emissions are estimated to be 242 Tg CH₄ yr⁻¹ for 2000-2009, compared with 306 Tg CH₄ yr⁻¹ in Saunois et al. (2020). This budget is the first that reconciles bottom-up and top-down total emissions within the uncertainty ranges. However, the uncertainty in the global budget remains high because of the large range reported for emissions from freshwater systems. Still, the upper bound of global emissions from bottom-up approaches is not consistent with top-down estimates that rely on OH burden constrained by methyl chloroform atmospheric observations and is still likely overestimated.

5.1.2 Global methane emissions per source category

The global CH₄ emissions from natural and anthropogenic sources (see Sect. 2.3) for 2010-2019 are presented in Fig. 6, Fig. 7, and Table 3. Top-down estimates attribute about 65% of total emissions to anthropogenic activities (range of 55-70%), and 35% to natural emissions. Bottom-up estimates attribute 57% of emissions to direct anthropogenic and the rest to natural plus indirect anthropogenic emissions. A current predominant role of direct anthropogenic sources of CH₄ emissions is consistent with and strongly supported by available ice core and atmospheric CH₄ records. These data indicate that atmospheric CH₄ varied around 700 ppb during the last millennium before increasing by a factor of 2.6 to ~1800 ppb since pre-industrial times. Accounting for the decrease in mean-lifetime over the industrial period, Prather et al. (2012) estimated from these data a total source of 554±56 Tg CH₄ in 2010 of which about 64% (352±45 Tg CH₄) was of direct anthropogenic origin, consistent with the range in our stop-down estimates.

Natural and indirect anthropogenic emissions. Although smaller than in previous Global Methane Budget releases, the main remaining discrepancy between top-down and bottom-up budgets is found for the natural and indirect anthropogenic emission total (105 Tg), with 311 [183-462] Tg CH₄ yr⁻¹ for bottom-up and only 206 [188-225] Tg CH₄ yr⁻¹ for top-down over the 2010-2019 decade. In the bottom-up estimates, this discrepancy comes first from the estimates in both inland freshwater sources (64 Tg) and second from other natural sources (20 Tg from geological sources, termites, oceans, and permafrost). The top-down approaches may be biased due to missing fluxes (mainly inland freshwaters) in their prior estimates.



1728

1729

1730

1731

1732

1733

1734

1735

1736

1737

1738 1739

1740

1741

1742

1743

1744 1745

1746 1747

1748

1749

1750

1751

1752

1753

1754

1755 1756

1757

1758 1759

2010-2019 at the global scale.



159 [119-203] Tg CH₄ yr⁻¹, respectively, are comparable within their range. Based on diagnostic wetland area values (see notes in Table 3), bottom-up mean wetland emissions for the 2000-2009 period are smaller in this study than those of Saunois et al. (2016) but larger than in Saunois et al. (2020). The changes in wetland emissions from bottom-up models may be related to updates on the wetland extent data set (WAD2M), the use of two different meteorological forcings for this study and a different set of models (see Sect. 3.2.1). Conversely, the current 2000-2009 mean top-down wetland estimates are lower than those of Saunois et al. (2016) and Saunois et al. (2020) (Table 3). In the bottom-up estimates, the amplitude of the range of emissions of 116-189 is roughly similar to Saunois et al. (2016) (151-222) and Saunois et al. (2020) (102-179) for 2000-2009. Here, the larger range in bottom-up estimates of wetland emissions is due to the use of GSWP3-W5E5 and greater sensibilities of some models to the climate parameters, as discussed in Sect. 3.2.1. Bottom-up and top-down estimates for wetland emissions agree better in this study (~5 Tg yr⁻¹ for 2000-2009) than in Saunois et al. (2016, 2020) (~17 Tg yr⁻¹ and ~30 Tg yr⁻¹, respectively). Natural emissions from inland freshwater systems were not included in the prior fluxes used in the top-down approaches, due to unavailable or uncertain gridded products at the start of the modelling activity. However, emissions from these inland freshwater systems may be implicitly included in the posterior estimates of the top-down models, as these two sources are close and probably overlap at the rather coarse resolution of the top-down models. This is the reason why the 'wetland emissions' in the top-down budget in fact correspond to the sum of combined wetland and inland freshwaters emissions in the bottom-up budget. The double-counting of 23 Tg CH₄ reduces the bottom-up budget for combined wetland and inland freshwaters from 271 Tg CH₄ yr⁻¹ to 248 Tg CH₄ yr⁻¹ (Sect. 3.2.2). Comparing the 2000-2009 decadal emissions from wetlands and inland freshwater ecosystems estimated by the bottom-up approaches across the last three Global Methane Budgets shows an upward and then a downward revision with 305 (183+122) Tg CH₄ yr⁻¹, 356 (147+209) Tg CH₄ yr⁻¹ and 248 (159+112-23) Tg CH₄ yr⁻¹ (respectively from Saunois et al. (2016, 2020) and this work; the sum in bracket corresponds to the sum of vegetated wetland emissions and inland water emissions estimated through the different budgets). The combined wetland and inland freshwater emissions discrepancy between bottom-up and top-down approaches amount to 105 Tg CH₄ yr⁻¹ for the 2010-2019 decade. From a top-down point of view, the sum of all the natural sources is more robust than the partitioning between wetlands, inland waters, and other natural sources. Including all known spatio-temporal distributions of natural emissions in top-down prior fluxes would be a step forward to consistently compare natural versus anthropogenic total emissions between top-down and bottom-up approaches. In the top-down budget, wetlands represent 28% on average of the total methane emissions but only 24% in the bottom-up budget (because of higher total emissions inferred). Given the large uncertainties, neither bottom-up nor top-down

For 2010-2019, the top-down and bottom-up derived estimates for wetlands emissions of 165 [145-214] Tg CH₄ yr⁻¹ and

approaches included in this study point to significant changes in wetland emissions between the two decades 2000-2009 and

For the 2010-2019 decade, top-down inversions infer "Other natural emissions" (Table 3) at 43 Tg CH₄ yr⁻¹ [40-46], whereas

the sum of the individual bottom-up emissions is 63 Tg CH₄ yr⁻¹ [24-93], contributing to a 20 Tg discrepancy between

https://doi.org/10.5194/essd-2024-115 Preprint. Discussion started: 6 June 2024 © Author(s) 2024. CC BY 4.0 License.



1760

1761

1762

1763

1764

1765

1766

1767

1768

1769

1770

1771

1772

1773

1774

1775

1776

17771778

1779

1780

1781

1782

17831784

1785

1786

1787

1788

1789

1790

1791

1792



bottom-up and top-down approaches. Atmospheric inversions infer the same amount over the decade 2000-2009 as over 2010-2019, which is almost half of the value reported in Saunois et al. (2016) (68 [21-130] Tg CH₄ yr⁻¹). This reduction in magnitude and uncertainty is due to 1) a more consistent way of considering other natural emissions in the various inverse systems (same prior estimate as in this budget) and 2) a difference in the ensemble of top-down inversions reported here compared to previous releases. It is worth noting that, most of the top-down models include about the same ocean and onshore geological emissions and termite emissions in their prior scenarios. However, none include freshwater or permafrost emissions in their prior fluxes, and thus in their posterior estimates.

Geological emissions are associated with relatively large uncertainties, and marine seepage emissions are still widely debated (Thornton et al., 2020). However, summing up all bottom-up fossil-CH₄ related sources (including anthropogenic emissions) leads to a total of 165 Tg CH₄ yr⁻¹ [135-190] in 2010-2019, which is about 29% of the top-down global CH₄ emissions, and 25% of the bottom-up total global estimate. These results agree with the value inferred from 14 C atmospheric isotopic analyses of 30% contribution of fossil-CH₄ to global emissions (Etiope et al., 2008; Lassey et al., 2007b). This total fossil fuel emissions from bottom-up approaches agrees well with the 13 C-based estimate of Schwietzke et al. (2016) of 192 ± 32 Tg CH₄ yr⁻¹. In the bottom-up budget, the larger total emissions (due to uncertainties in bottom-up estimates of natural emissions) leads to a lower fossil fuel contribution compared to Lassey et al. (2007b).

Anthropogenic direct emissions. Total anthropogenic direct emissions for the period 2010-2019 were assessed to be statistically consistent between top-down (369 Tg CH₄ yr⁻¹, range 350-391) and bottom-up approaches (358 Tg CH₄ yr⁻¹, range 329-387), albeit top-down approaches infer direct anthropogenic emissions larger by 11 Tg CH₄ yr¹ on average compared to bottom-up approaches. The partitioning of anthropogenic direct emissions between agriculture and waste, fossil fuels extraction and use, and biomass and biofuel burning, also shows good consistency between top-down and bottom-up approaches, though top-down approaches still suggest less fossil fuel and more agriculture and waste emissions than bottomup estimates (Table 3 and Fig. 6 and 7). For 2010-2019, agriculture and waste contributed an estimated 228 Tg CH₄ yr⁻¹ [213-242] in the top-down budget and 211 Tg CH₄ yr⁻¹ [195-231] in the bottom-up budget. Fossil fuel emissions contributed 115 Tg CH₄ yr⁻¹ [100-124] in the top-down budget and 120 Tg CH₄ yr⁻¹ [117-125] in the bottom-up budget. Biomass and biofuel burning contributed 27 Tg CH₄ yr⁻¹ [26-27] in the top-down budget and 28 Tg CH₄ yr⁻¹ [21-39] in the bottom-up budget. Biofuel CH₄ emissions rely on very few estimates currently (Wuebbles and Hayhoe, 2002). Although biofuel is a small source globally (~12 Tg CH₄ yr⁻¹), more estimates are needed to allow a proper uncertainty assessment. Overall for top-down inversions the global fraction of total emissions for the different source categories is 40% for agriculture and waste, 20% for fossil fuels, and 5% for biomass and biofuel burning. With the exception of biofuel emissions, the uncertainty associated with global anthropogenic emissions appears to be smaller than that of natural sources but with an asymmetric uncertainty distribution (mean significantly different than median). The relative agreement between top-down and bottomup approaches may indicate a limited capability of the inversion to separate emissions and a dependency to their prior fluxes; this agreement should therefore be treated with caution. Indeed, in poorly observed regions, top-down inversions rely on the





prior estimates and bring little or no additional information to constrain (often) spatially overlapping emissions (e.g., in India, China). Also, as many top-down systems solve for the total fluxes at the surface or for some categories that may differ from the GCP categories, their posterior partitioning relies on the prior ratio between categories that are prescribed using bottom-up inventories.

5.1.3 Global budget of total methane sinks

Top-down estimates. The annual CH₄ chemical removal from the atmosphere is estimated to be 521 Tg CH₄ yr⁻¹ averaged over the period 2010-2019, with an uncertainty of about $\pm 2\%$ (range 485-532 Tg CH₄ yr⁻¹). All the inverse models account for CH₄ oxidation by OH and O(1 D), and some include stratospheric Cl oxidation (Table S8 to S11). Most of the top-down models use the OH distribution from the TRANSCOM experiment (Patra et al., 2011) either as fixed over the period or including inter annual variability from Patra et al. (2021). This study shows no trend in OH and IAV below $\pm 4\%$, in agreement with Thompson et al. (2024) (no significant OH trend and IAV < 2%). As a result, the range of the top-down sink estimates is rather low compared to bottom-up estimates (see below). Differences between transport models affect the chemical removal of CH₄, leading to different chemical loss rates, even with the same OH distribution. However, uncertainties in the OH distribution and magnitude (around $\pm 10\%$ at the global scale, Zhao et al., 2019) are not considered in our study, while they could contribute to a significant change in the chemical sink, and then in the derived posterior emissions through the inverse process ((Zhao et al., 2020), around $\pm 17\%$ at the global scale, much larger than the model spread derived here. The chemical sink represents more than 90% of the total sink, the rest being attributable to soil uptake (35 [35-36] Tg CH₄ yr⁻¹). The rather narrow range is due to the use of the same climatological soil sink provided within the modelling protocol which is based on Murgia-Flores et al. (2018). This sink estimate used as prior in the inversions is a bit higher than the mean estimate of the soil sink calculated by bottom-up models (30 Tg CH₄ yr⁻¹, Sec. 3.3.4).

Bottom-up estimates. The total chemical loss for the 2010s reported here is 602 Tg CH₄ yr⁻¹ with an uncertainty of 21% (~125 Tg CH₄ yr⁻¹). Differences in chemistry schemes in the models (especially in the stratosphere) and in the volatile organic compound treatment probably explain most of the discrepancies among models (Zhao et al., 2019).

5.2 Latitudinal and regional methane budgets

The latitudinal and regional breakdown of the bottom-up budget is based on crude assumptions that we acknowledge here. Natural and indirect anthropogenic emissions are based on wetland gridded products from land surface models and the combination of the maps from lakes and ponds from Johnson et al. (2022), reservoirs from Johnson et al. (2022) and streams and rivers from Rocher-Ros et al. (2023), the sum of those three scaled to 89 Tg CH₄ yr⁻¹ (shown in Fig. 5) to artificially include the double counting (estimated only at the global scale) and match the global estimate. However, we acknowledge that this procedure distributes the double counting relatively to the final emission distribution and not according to the freshwater ecosystems where the double counting probably occurs. Wild animals and permafrost maps do not exist and are



1825

1826

1827

1828

1829

1830

1831

1832 1833

1834

1835 1836

1837

1838

1839

1840 1841

1842

1843

1844

1845

1846 1847

1848

1849

1850

1851

1852

1853

1854



missing from the calculation, leading to around 3 Tg CH₄ yr¹ of discrepancy. Geological and ocean sources are based on Etiope et al. (2019) and Weber et al. (2019) gridded products scaled to 50 Tg CH₄ yr⁻¹ to be consistent to the reported global values. Finally, we use the termite emission map produced for this budget and used in the global budget. The latitudinal budget does not include the estimates from FAO and USEPA for the direct anthropogenic emissions as they are only provided at country scale.

5.2.1 Latitudinal budget of total methane emissions

The latitudinal breakdown of emissions inferred from atmospheric inversions reveals a dominance of tropical emissions of 364 Tg CH₄ yr⁻¹ [337-390], representing 64% of the global total (Table 5 and 6). 32% of the emissions are from the midlatitudes (187 Tg CH₄ yr⁻¹ [160-204]) and 4% from high latitudes (above 60°N). The ranges around the mean latitudinal emissions are larger than for the global CH₄ sources. While the top-down uncertainty is less than ±5% at the global scale, it increases to $\pm 7\%$ for the tropics, to $\pm 12\%$ the northern mid-latitudes and to more than $\pm 20\%$ in the northern high-latitudes (for 2010-2019, Table 5). Both top-down and bottom-up approaches consistently show that CH₄ decadal emissions have increased by +21-27 Tg CH₄ yr⁻¹ in the tropics, and by +5-16 Tg CH₄ yr⁻¹ in the northern mid-latitudes between 2000-2009 and 2010-2019 using the mean ensemble estimate. Over 2010-2019, at the global scale, satellite-based inversions infer almost identical emissions to ground-based inversions

(difference of +1 [-3-9] Tg CH₄ yr⁻¹, with GOSAT based inversion a bit higher than surface measurements-based inversions), when comparing consistently surface versus satellite-based inversions for each system, similar to Saunois et al. (2020). This difference is much lower than the range derived between the different systems (range of 20 Tg CH₄ yr⁻¹ using surface- or satellite-based inversions). This result reflects that differences in atmospheric transport among the systems probably have more impact on the estimated global emissions than the types of observations assimilated.

As expected, considering the different coverage of observation datasets, regional distributions of inferred emissions differ depending on the nature of the observations used (satellite or surface). The largest differences (satellite-based minus surfacebased inversions) are observed over the tropical region, between -10 and +43 Tg CH₄ yr⁻¹ (90°S to 30°N), and the northern mid-latitudes (between -36 and -2 Tg CH₄ yr⁻¹). Satellite data provide stronger constraints on fluxes in tropical regions than surface data, due to a much larger spatial coverage. It is therefore not surprising that differences between these two types of observations are found in the tropical band, and consequently in the northern mid-latitudes to balance total emissions, thus affecting the north-south gradient of emissions. However, the regional patterns of these differences are not consistent through the different inverse systems. Indeed, some systems found higher emissions in the tropics when using GOSAT instead of surface observations, while others found the opposite. This difference between inversion systems may depend on whether or not a bias correction is applied to the satellite data based on surface observations, and also on the modelled horizontal and vertical transports, in the troposphere and in the stratosphere.



1878

1879



5.2.2 Latitudinal methane emissions per source category

1856 The analysis of the latitudinal CH₄ budget per source category (Fig. 8 and Table 6) can be performed both for bottom-up 1857 and top-down approaches but with limitations. Bottom-up estimates of natural and indirect anthropogenic emissions are 1858 based on assumptions as specified at the beginning of this section 5.2. For top-down estimates, as already noted, the 1859 partitioning of emissions per source category has to be considered with caution. Indeed, using only atmospheric CH₄ observations to constrain CH₄ emissions makes this partitioning largely dependent on prior emissions. However, 1860 1861 differences in spatial patterns and seasonality of emissions can be utilised to constrain emissions from different categories 1862 by atmospheric methane observations (for those inversions solving for different sources categories, see Sect. 2.3). 1863 Agriculture and waste are the largest sources of CH₄ emissions in the tropics and southern hemisphere (140 [121-150] Tg 1864 CH₄ yr⁻¹ in the bottom-up budget and 150 [135-168] Tg CH₄ yr⁻¹ in the top-down budget, about 40% of total CH₄ emissions 1865 in this region). However, combined wetland and inland freshwater emissions are nearly as large with 151 [85-234] Tg CH₄ yr⁻¹ in the bottom-up budget and 128 [112-155] Tg CH₄ yr⁻¹ in the top-down budget. Anthropogenic emissions dominate in 1866 1867 the northern mid-latitudes, with the highest contribution from agriculture and waste emissions (40% of total emissions in the top-down budget), closely followed by fossil fuel emissions (32% of total emissions, top-down budget). Boreal regions 1868 are largely dominated by inland freshwater emissions (41% and 54% of total emissions, top-down and bottom-up budget, 1869 1870 respectively). 1871 The largest discrepancies between the top-down and the bottom-up budgets are found in the mid-latitudes and boreal regions 1872 from the natural and indirect sources with bottom-up estimates twice as large as the top-down ones, especially in the inland 1873 freshwater category. 1874 The uncertainty for wetlands and inland freshwater emissions is larger in the bottom-up models than in the top-down models 1875 (mostly wetlands), while uncertainty in anthropogenic emissions is larger in the top-down models than in the bottom-up 1876 inventories. The large uncertainty in tropical inland freshwater emissions (mostly wetlands) of ±44% results from large 1877 regional differences between the bottom-up land-surface models. Although they are using the same forcings, their responses

5.2.3 Regional budget for total emissions

The regional breakdown of emissions is provided for 18 continental regions (see map in Fig. S3 and Table S1 with the

in terms of flux density show different sensitivities to temperature, water vapour pressure, precipitation, and radiation.

- 1881 country aggregation in the supplementary materials).
- At the regional scale and, for the 2010-2019 decade, total methane emissions are dominated by South East Asia with 63 [52-
- 1883 71] Tg CH₄ yr⁻¹, China with 57 [37-72] Tg CH₄ yr⁻¹, and South Asia with 52 [43-60] Tg CH₄ yr⁻¹ (top-down budget). These
- top three emitters contribute 30% of total global CH₄ emissions. The following high emitting regions are Brazil 47 [41-58]
- 1885 Tg CH₄ yr⁻¹, Equatorial Africa 47 [39-59] Tg CH₄ yr⁻¹, USA 38 [32-46] Tg CH₄ yr⁻¹, Southwest South America 38 [30-48]



1889

1890

1891

1892

1893

1894

1895

1896

1897

1898

1899 1900

1901

1902

1903

1904

1905 1906

1907

1908

1909

1910

1911

1912

1913

1914

1915

1916



- 1886 Tg CH₄ yr⁻¹, Russia 36 [27-45] Tg CH₄ yr⁻¹, Europe 31 [24-36] Tg CH₄ yr⁻¹, Middle East 31 [24-39] Tg CH₄ yr⁻¹, Northern Africa 25 [23-29] Tg CH₄ yr⁻¹, and Canada 20 [17-24] Tg CH₄ yr⁻¹. Other regions contribute less than 20 Tg CH₄ yr⁻¹.
- 1887

5.2.4 Regional budget per source category

Natural and indirect anthropogenic emissions versus direct anthropogenic emissions. In agreement with Stavert et al. (2021), natural and indirect anthropogenic emissions are dominated by Brazil, Canada, Russia, Equatorial Africa and Southeast Asia, contributing 126 Tg CH₄ yr⁻¹ in the bottom-up and 105 Tg CH₄ yr⁻¹ in the top-down budget (Table 7), i.e., 47% and 50% of the global natural and indirect anthropogenic emissions in these budgets, respectively. At regional scale also, the range of uncertainty in natural and indirect anthropogenic emissions are much larger in the bottom-up budget than in the top-down budget (Fig. S5). Except for 4 regions (Canada, Brazil, Northern South America, Southwest South America), direct anthropogenic emissions contribute more than half of the total regional emissions. Due to the large uncertainty and discrepancies in natural and indirect emissions estimates, the regional direct anthropogenic fractions may differ between the bottom-up and top-down budgets. However, in absolute values, the highest direct anthropogenic emitters are the same in the two budgets with China and South Asia being the top two by far, contributing 56 [51-66] Tg CH₄ yr⁻¹ and 45 [44-47] Tg CH₄ yr⁻¹, respectively (bottom-up values, Fig. 9 and Table 7). These two regions contribute 28% (26%) of the global direct anthropogenic emissions in the bottom-up (top-down) budget. The ranks of direct anthropogenic emitters are similar to those presented in the last budget (Stavert et al., 2021). Southeast Asia, United States of America, Middle East, Europe, Equatorial Africa, and Russia emit between 32 Tg CH₄ yr⁻¹ and 23 Tg CH₄ yr⁻¹ as direct anthropogenic emissions (bottom-up values, Fig 8). Brazil, Northern Africa, and Southwest South America emit between 10 CH₄ yr⁻¹ and 20 CH₄ yr⁻¹, while the rest of the regions emit less than 10 CH₄ yr⁻¹ direct anthropogenic emissions.

Sectoral emissions. The sectoral partitioning at the regional scale has been derived from both bottom-up and top-down approaches. However, the top-down budget has more limitations, as the sectoral partitioning is usually based on the prior fluxes fractions at the pixel scale, and assimilating only total methane observations does not allow to disentangle the different source sectors overlapping in a pixel grid. However, differences in spatial patterns and seasonality of emissions can still be constrained by atmospheric CH₄ observations for those inversions solving for different sources categories (see Sect. 2.3). Bottom-up approaches allow deeper sectorial splitting, especially in terms of direct anthropogenic emissions (Fig. 9). Table 7, Fig. 9 and Fig. 10 present the estimations of CH₄ emissions on average over 2010-2019. Fig. 10 presents the budgets for three main categories (Combined wetland and inland freshwaters, Fossil fuels and Agriculture & Waste), a more detailed figure and table including the five categories is available in the supplementary material (Fig. S6 and Table S13 to S18). Values for each individual data-set for the decades 2000-2009, 2010-2019, and the last year 2020 are made available in a spreadsheet (see Data Availability).



1945

inventory).



and generally their range is larger than in the top-down budget. In the top-down budget, this category contributes the most 1918 1919 to the regional emissions in Brazil 24 [20-33] Tg CH₄ yr⁻¹, Southeast Asia 24 [14-29] Tg CH₄ yr⁻¹ (though similar to their Agriculture and Waste emissions 24 [21-31] Tg CH₄ yr⁻¹), Equatorial Africa 22 [19-28] Tg CH₄ yr⁻¹, Southwest South 1920 America 22 [14-33] Tg CH₄ yr⁻¹, Canada 12 [9-18] Tg CH₄ yr⁻¹, Northern South America 8 [6-10] Tg CH₄ yr⁻¹, Southern 1921 1922 Africa 7 [4-9] Tg CH₄ yr⁻¹. Agriculture and Waste emissions dominates in South Asia 39 [33-43] Tg CH₄ yr⁻¹, China 30 [13-37] Tg CH₄ yr⁻¹, Europe 19 [16-23] Tg CH₄ yr⁻¹, United States of America 13 [9-16] Tg CH₄ yr⁻¹, Northern Africa 13 [12-1923 14] Tg CH₄ yr⁻¹, Central America 9 [8-10] Tg CH₄ yr⁻¹, and Korea and Japan 3 [3-4] Tg CH₄ yr⁻¹. Fossil fuel emissions 1924 1925 dominate in the Middle East 18 [11-24] Tg CH₄ yr⁻¹ and Russia 14 [8-23] Tg CH₄ yr⁻¹ (close to their combined wetland and 1926 inland freshwater emissions of 11 [8-13] Tg CH₄ yr⁻¹). 1927 The four largest contributors to the Fossil Fuel sector remain China, the Middle East, Russia, and the United States of 1928 America. Altogether they contribute 67 (64) Tg CH₄ yr⁻¹ in the bottom-up (top-down) budget, around 55% of the global fossil fuel emissions. The bottom-up and top-down approaches generally agree in terms of ensemble mean, except for China 1929 1930 for which the top-down estimates suggest lower emissions than the inventories. While Chinese fossil fuel emissions occur 1931 mainly through coal mining activity (88%), the Middle East, Russia and the USA extract mainly oil and gas (100%, 1932 80%,72%). 1933 The three largest contributors to the Agriculture and Waste sector remain South Asia, China, and Southeast Asia. Together 1934 they contribute 88 (92) Tg CH₄ yr⁻¹ in the bottom-up (top-down) budget, around 40% of the global agriculture and Waste 1935 sector. While the ensemble means tend to agree between bottom-up and top-down budgets, the uncertainty derived from the 1936 top-down approaches is larger, especially for these three regions. CH₄ emissions due to rice cultivation originate mostly 1937 from these same three regions (South East Asia, China and South Asia). Livestock management emissions occurs mainly in South Asia 20 [18-22] Tg CH₄ yr⁻¹, Brazil 12 [11-13] Tg CH₄ yr⁻¹, China 11 [8-16] Tg CH₄ yr⁻¹, and Europe 11 [10-12] Tg 1938 1939 CH₄ yr⁻¹ (bottom-up estimates). The United States of America, Equatorial Africa, Northern Africa and Southwest South America emit between 7 Tg CH₄ yr⁻¹ and 10 Tg CH₄ yr⁻¹ in this sub-sector. Other regions emit less than 4 Tg CH₄ yr⁻¹ in the 1940 1941 livestock management sector. The Waste sector emissions are dominated by three regions: China 11 [6-14] Tg CH₄ yr⁻¹, 1942 South Asia 9 [4-11] Tg CH₄ yr⁻¹, and Europe 8 [6-12] Tg CH₄ yr⁻¹ (bottom-up estimates). These three regions contribute 1943 around 40% of the global emissions of the Waste sector. It is worth noting that the uncertainty in the inventory estimates at the regional scale is around 40% (from the min-max range of the estimate, not including the uncertainty from each 1944

For most regions, "Combined wetland and inland freshwater emissions" are the most uncertain in the bottom-up budget,



1947

1948

1949

1950

1951

1952

1953

1954

19551956

1957

1958

1959

1960

1961 1962

1963

1964

1965

1966

1967

1968

1969

1970 1971

19721973

1974

19751976

1977



6 Insights on the methane cycle from 2020-2022 during which there has been unprecedented high growth rates of methane emissions

The mean emissions estimate for the last year of the budget (2020) was 608 [581-627] Tg CH₄ yr⁻¹ (Top-down), with 65% of the emissions from direct anthropogenic sources. This is 65 Tg CH₄ yr⁻¹ higher (11%) than the mean emissions of the 2000-2009 decade and 6% higher than 2010-2019. 2020 was a second highest year in terms of atmospheric CH₄ growth rate (+15.2 ppb/yr) since systematic measurements began in the late 1980s, coming in just behind the highest in 2021 at 17.97 ppb/yr. A few studies analysed the large growth rate increase between 2019 (+9.7 ppb/yr) and 2020 (+15.2 ppb/yr) of +5.4 ppb/yr (corresponding to $+14.4 \pm 2.0$ Tg CH₄ yr⁻¹) (Peng et al., 2022; Stevenson et al., 2022). Peng et al. (2022) estimated that the 2019-2020 growth rate change was almost equally due to an increase in wetland emissions $(6.9 \pm 2.1 \text{ Tg CH}_4 \text{ yr}^{-1})$ and a decrease of the OH chemical loss $(7.5 \pm 0.8 \, \mathrm{Tg} \, \mathrm{CH_4 \, yr}^{-1})$ due to reduced OH precursor emissions during the COVID lockdown (Laughner et al., 2021). The COVID19 lockdown resulted in decreased NO_x emissions and reduced fossil fuel related CH₄ emissions (Thorpe et al., 2023), leading to less OH production. At the global scale, Feng et al. (2023) calculated an emission increase of 27 Tg CH₄ yr⁻¹ between 2019 and 2020 considering constant OH, and a smaller increase of 21 Tg CH₄ yr⁻¹ when including a 1.4% decrease of OH. Increased emissions were mainly found in the northern tropics. Qu et al. (2022) also inferred a 31 Tg CH₄ yr⁻¹ increase of emissions, mostly in the tropics, half of it in Africa. Such a result is compatible with wetland driven abnormal emissions during a consecutive 3-year La Nina event spanning from 2020 to 2022 (Zhang et al., 2023; Nisbet et al., 2023). The difference in terms of methodology and approaches between these three studies make it difficult to compare them quantitatively but provide a robust understanding on the possible causes. Importantly, all the studies indicate, in various proportions, increasing CH₄ emissions in the tropics and in the boreal region, potentially driven by microbial emission from wetlands due to wetter and warmer climate, and a significant contribution of reduced OH concentrations due to COVID lockdown. Based on our ensemble of data, we find that top-down approaches infer a much larger change in CH4 emissions (median [Q1-Q3] at +23 [10-31] Tg CH₄ yr⁻¹) than bottom-up approaches (-1 [-5-3] Tg CH₄ yr⁻¹) between 2019 and 2020 (Fig. S7). Bottom-up approaches suggest a very small increase in wetland emissions (around (+1 [0-3] Tg CH₄ yr⁻¹), while top-down approaches suggest on average a larger increase for wetlands of +8 [5-11] Tg CH₄ yr⁻¹, mainly in the tropics and midlatitudes. It is worth noting that large uncertainties exist for a given year and that the inter annual variability is much lower than the ensemble spread. While bottom-up approaches suggest almost constant fossil fuel emissions and slight increase in agriculture and waste (+3 Tg CH₄ yr⁻¹), top-down approaches tend to derive higher emissions changes (+6 Tg CH₄ yr⁻¹ from the fossil fuel sector and +11 Tg CH₄ yr⁻¹ from agriculture and waste as the median over the ensemble). Biomass burning emissions decreased using both approaches by about 5 Tg CH₄ yr⁻¹ in agreement with Peng et al. (2022). Some inversions were run with IAV of OH from Patra et al. (2021) and others with constant OH. However the inferred OH IAV in 2019 and 2020 are rather low (0.3% and 0.15% on yearly average) in Patra et al. (2021), leading to a small impact in





- terms of emissions changes between 2019-2020, with +22 [9-31] (median [Q1-Q3]) based on the inversions with constant
- 1979 OH and 19 [7-28] based on the inversions with varying OH (Fig S8).
- 1980 This first analysis based on our ensemble shows how challenging it is to attribute CH₄ emissions changes to a specific sector
- or region between two years, because related uncertainties remain much larger than the targeted signal to explain. This calls
- again for further improvement of both approaches.
- NOAA estimates of 2021 and 2022 methane atmospheric growth rates 17.8.0±0.5 ppb/yr and 14.0±0.8 ppb/yr, respectively
- 1984 (Lan et al., 2024). They show a continuation of very high growth rates, challenging again our understanding of the methane
- budget. As of the time of submission of this manuscript, bottom-up estimates for anthropogenic emissions for 2021 and
- 1986 2022 are only available from the EDGARv8 data set (https://edgar.jrc.ec.europa.eu/dataset_ghg80; EDGAR, 2023). This
- research inventory suggests that anthropogenic emissions continued to increase from 2020 (374 Tg CH₄ yr⁻¹) to 2021 (379
- 1988 Tg CH₄ yr⁻¹) and 2022 (386 Tg CH₄ yr⁻¹) with around 62% of the increase due to the fossil fuel sources, 23 % from the
- 1989 Waste sector, and 14% from the agriculture sector (Table S19). The bottom-up estimate of wetland emissions for 2021-
- 1990 2023, derived from a single wetland model, indicates positive anomalies of 26 Tg CH₄ yr⁻¹ in 2020, 23 Tg CH₄ yr⁻¹ in
- 1991 2021, and 21 Tg CH₄ yr⁻¹ 2022 relative to the 2000-2006 baseline (https://earth.gov/ghgcenter/data-catalog/lpjwsl-
- 1992 wetlandch4-grid-v1; Zhang et al., 2023).

7 Future developments, missing elements, and remaining uncertainties

In this budget, robust features and uncertainties on sources and sinks estimated by bottom-up or top-down approaches have been highlighted as well as discrepancies between the two budgets. Limitations of the different approaches have also been highlighted. Four shortcomings of the CH₄ budget were already identified in Kirschke et al. (2013) and Saunois et al. (2016, 2020) and are revisited below pointing to key research areas. Although much progress has been made, they are still relevant, and actions are needed. However, these actions fall into different timescales and actors. Here, we revisit the four shortcomings of the contemporary methane budget and discuss how each weakness has been addressed since Saunois et al. (2020). Each section ends by discussing remaining research needs with a list of suggestions, from higher to lower priority.

20012002

2003

2004

2005

2006

2007

2008

1993

1. Shortcoming 1: Towards a decrease of the high uncertainty in the amount of methane emitted by wetland and inland water systems, and a weakened double counting issue.

This first shortcoming has probably received the largest interest in the last few years with significant improvements. First a community effort has been made based on more studies, documenting, or modelling more inland freshwater systems and synthesising emissions from the complex and heterogeneous ensemble of emitting areas: wetlands, ponds, lakes, reservoirs, streams, rivers, estuaries, and marine systems. The range of wetland and inland water emissions has been narrowed down with improved wetland extent and refined estimates for inland freshwater systems. Double counting between inland





- 2009 freshwater systems has been estimated for the first time and accounted for in this budget. All these improvements decreased
- 2010 the discrepancy between top-down and bottom-up estimate of combined wetland and inland freshwater emissions from
- 2011 156 Tg CH₄ yr⁻¹ in Saunois et al. (2020) down to 85 Tg CH₄ yr⁻¹ in this update for the 2000-2009 decade. Gridded maps
- for lakes, ponds, reservoirs, and streams and rivers freshwater emissions have been produced over the past years (Johnson
- et al., 2021, 2022; Rocher-Ros et al., 2023) making the spatial distribution of CH₄ sources almost complete for the first time
- and allowing better description of prior emissions in future top-down inversions.
- Next steps include on the short term from highest to lowest priority include:
- 2016 (i) integration of spatial distribution of inland waters in atmospheric inversion models to reach a full description of prior
- 2017 methane sources and sinks.
- 2018 (ii) refinement of double counting estimation and its possible reduction with more precise spatial and temporal distributions
- of the different systems contributing to inland freshwater emissions by using very high-resolution satellite data (down to
- metre resolutions) to properly separate them. The development of a dynamical global high-resolution (typically few metres)
- 2021 classification of saturated soils and inundated surfaces based on satellite data (visible and microwave), surface inventories,
- and expert knowledge.
- 2023 (iii) continuation of ongoing efforts to calibrate and evaluate land surface models for wetland emissions against in-situ
- observations such as FLUXNET-CH₄ (Knox et al., 2019; Delwiche et al., 2021) or BAWLD-CH₄ (Kuhn et al., 2021) for
- boreal regions and avoid dependence on top-down estimates. It is still critical to increase the limited number of tropical
- observations and to assimilate them in the inverse systems to help address the issue (e.g., Kallingal et al., 2023).
- 2027 (iv) continuation of ongoing efforts to develop a diversity of modelling approaches (among them process-based model or
- machine learning approaches) to estimate wetland and inland freshwater CH4 emissions, including lateral fluxes, and
- reducing upscaling issues, as done by e.g. Zhuang et al. (2023) for lakes.
- 2030 (v) continuous integration of collected flux measurements such as in the FLUXNET-CH₄ activity (Knox et al., 2019;
- Delwiche et al., 2021) or in BAWLD-CH4 data set (Kuhn et al., 2021) to provide global flux maps based on machine
- learning approaches or other approaches (Peltola et al., 2019, McNicol et al., 2023).
- 2033 Over the long run, developing measurement systems will help to improve estimates of the diversity of wetland and inland
- freshwater sources, and further reduce uncertainties:
- 2035 More systematic measurements of CH₄ fluxes and their isotopic signatures from sites reflecting the diversity of
- 2036 environment of wetlands and inland waters, complemented with environmental meta-data (e.g., soil temperature
- and moisture, vegetation types, water temperature, acidity, nutrient concentrations, NPP, soil carbon density for
- wetlands, lake morphologies) will allow us to better understand and estimate the processes of production and
- transport to the atmosphere (diffusive, ebullitive, plants mediated...) and to better constrain methane fluxes and
- their isotopic signatures in the different modelling approaches (Glagolev et al., 2011; Turetsky et al., 2014).

variations remain underconstrained.



2055

2057

2058

2059

2060

2061

2062

2063

2064

2065

2066

2067

2068

2069

2070

2071

2073

2074



- 2042 2. Shortcoming 2: Towards a better assessment of uncertainties for global methane sinks in top-down and bottom-up budgets.
- The inverse systems used here have similar caveats than those described in Saunois et al. (2016, 2020) (same OH field, same 2044 2045 kind of proxy method to optimise it) leading to quite constrained atmospheric sink and therefore total global CH₄ sources. 2046 Although we have used the latest release of CCMI-2022 (Plummer et al., 2021) and CMIP6 simulations (Collins et al., 2047 2017), the uncertainty of derived CH4 chemical loss from the chemistry climate models remains at the same (large) level 2048 compared to the previous intercomparison project ACCMIP (Lamarque et al., 2013). The causes of uncertainties on the 2049 CH₄ loss and the differences between the different OH fields derived from Chemistry Transport Models (CTM) and Climate Chemistry Models (CCM) have been widely discussed (Nicely et al., 2017; Zhao et al., 2019). These results emphasise the 2050 2051 need to first assess, and then improve, atmospheric transport and chemistry models, especially vertically, and to integrate 2052 robust representation of OH fields in atmospheric models. For the latter, Zhao et al. (2023) have proposed a new approach 2053 based on OH precursor observations and a chemical box model to improve the 3D distributions of tropospheric OH radicals 2054 obtained from atmospheric chemistry models. Finally, soil uptake estimates rely on very few studies, and interannual
- Next steps, in the short term, could include developments by the modelling community in:
 - Estimating the soil uptake with different land surface models (creating an ensemble) and discussing its variations over the past decade.
 - Assessing the impact of using updated and varying soil uptake estimates, especially considering a warmer climate in the top-down approach. Indeed, for top-down models resolving for the net flux of CH₄ at the surface integrating a larger estimate of soil uptake would allow larger emissions, and then reduce the uncertainty with the bottom-up estimates of total CH₄ sources.
 - Further studying the reactivity of the air parcels in the chemistry climate models and defining new diagnostics to assess modelled CH₄ lifetimes.
 - Applying Zhao et al. (2023) recipe to several CTM used for top-down inversions in order to increase consistency between source and sink estimates in individual approaches.
 - Developing 3D inverse methods to optimise OH using CH₄ satellite data (Zhang et al., 2018) or halogenated compounds beyond methyl chloroform (MCF), such as done in box models (Thompson et al., 2024) to derive a 3D dynamical OH field or machine learning methods using satellite data to constrain OH (Anderson et al., 2023).
 - Integrating the aforementioned different potential OH chemical fields, including also inter-annual variability, to assess the impact on the methane budget following Zhao et al. (2020).
- 2072 Over the long run, other parameters should be (better) integrated into top-down approaches, among them:
 - The magnitude of the CH₄ loss through oxidation by tropospheric Cl, a process debated in the recent literature. More modelling (e.g., Thanwerdas et al., 2022b) and instrumental studies should be devoted to reducing the





uncertainty of this potential additional sink before integrating it in top-down models. This would be especially critical if inversions using ¹³C-CH4 observations are included in GMB in the future.

3. Shortcoming 3: Towards a better partitioning of methane sources and sinks by region and process using top-down models

In this work, we report inversions assimilating satellite data from GOSAT, which bring more constraints than provided by surface stations alone, especially over tropical continents. However, we still found that satellite- and surface-based inversions, and the different inversion systems do not consistently infer the same regional flux distribution.

The estimates contributing to the Global Methane budget are further used in more specific studies focusing on the comparison of the estimates from bottom-up and top-down approaches at national (Deng et al., 2022) and regional scales, including efforts from the GCP-REgional Carbon Cycle Assessment and Processes (RECCAP2) (Petrescu et al., 2021; 2023; Tibrewal et al., 2024; Lauerwald et al., 2023b; and other RECCAP-2 publications to come, see https://www.globalcarbonproject.org/reccap/publications.htm).

Next steps, in the short term, could integrate developments to be made by the top-down community:

- Including GOSAT 2 retrievals (Noël et al., 2022; Imasu et al., 2023) for the GOSAT-based inversions and considering TROPOMI-based inversions (as done in Tsuruta et al. (2023), Shen et al. (2023), Chen et al. (2022) and Qu et al. (2021)) in the next releases once at least 8 years of data are available to provide a decadal estimate and biases are reduced for global scale use (Lorente et al., 2023; Balasu et al., 2023). Indeed, recent satellite developments have provided higher temporal and spatial resolutions of CH₄ observations in regions with poor insitu measurements (Figure S9, such as TROPOMI observations in North Africa).
- Integrating the newly available updated gridded products for the different natural sources of CH₄ in their prior fluxes (e.g. inland freshwaters) to reach a full spatial description of sources and sinks, and to be able to better compare the top-down budget with the bottom-up budget.
- Integration of the newly developed 4D variational inversion systems using isotopic species in the top-down budget (Basu et al., 2022; Thanwerdas et al., 2024; Drinkwater et al. 2023; Mannisenaho et al., 2023).
- Improving the availability of in-situ data at high temporal resolution for the scientific community, especially ones covering poorly documented regions such as China (Liu et al., 2021b; Guo et al., 2020), India (Nomura et al., 2021; Lin et al., 2015; Tiwari and Kumar, 2012) and Siberia (Sasakawa et al., 2010, 2017; Fujita et al., 2020; Winderlich et al., 2010), which are not delivered so far to international databases, or only at poor temporal resolution.
- Integrating the information from imagery satellites (e.g., TROPOMI, Carbon Mapper, Methane Sat, GHG Sat.) of high to super-emitters to improve prior fluxes of anthropogenic emissions in terms of quantity and locations for each covered sector.





- Over the long run, integrating more measurements and regional studies will help to improve the top-down systems, and further reduce the uncertainties:
 - Extending the CH₄ surface networks to poorly observed regions (e.g., Tropics, China, India, high latitudes) and to the vertical dimension: aircraft regular measurements (e.g., Filges et al., 2015; Brenninkmeijer et al., 2007; Paris et al., 2010; Sweeney et al., 2015); Aircore campaigns (e.g., Andersen et al., 2018; Membrive et al., 2017); TCCON observations (e.g., Wunch et al., 2011, 2019) remains critical to complement satellite data that do not observe well in cloudy regions and at high latitudes, and also to evaluate and eventually correct satellite biases (Buchwitz et al., 2016).
 - Extending and developing continuous isotopic measurements of CH₄ to help partitioning methane sources and to be integrated in 4D variational isotopic inversions (e.g., Yacovitch et al., 2021).
 - Integrating global data from future satellite instruments with intrinsic low-bias, such as active LIDAR techniques with MERLIN (Ehret et al., 2017), that are promising to overcome issues of systematic errors (Bousquet et al., 2018) and should provide measurements over the Arctic, contrary to the existing and planned passive missions.
 - Other co-emitted species such as radiocarbon for fossil/non-fossil emissions (Lassey et al., 2007a, 2007b; Petrenko et al., 2017), CO (e.g., Zheng et al., 2019) for biomass burning emissions, and ethane for fugitive emissions (e.g., Ramsden et al., 2022) could bring additional information for partitioning emissions.
 - 4. Shortcoming 4: Towards reducing uncertainties in the modelling of atmospheric transport in the models used in the top-down budget
 - The TRANSCOM experiment synthesised in Patra et al. (2011) showed a large sensitivity of the representation of atmospheric transport on CH₄ abundances in the atmosphere. In particular, the modelled CH₄ budget appeared to depend strongly on the troposphere-stratosphere exchange rate and thus on the model vertical grid structure and circulation in the lower stratosphere. Also, regional changes in the CH₄ budget depend on the characteristics of the atmospheric transport models used in the inversion (Bruhwiler et al., 2017; Locatelli et al., 2015). This axis of research is demanding important development from the atmospheric modelling community. Waiting for future improvements (finer horizontal and vertical resolutions, more accurate physical parameterization, increase in computing resources...), assessing atmospheric transport error and the impact on the top-down budget remain crucial and mostly rely on the use of an ensemble of models. Methodology changes that could be integrated into the next methane budget releases include:
 - Evaluating more deeply the inversions provided against independent measurements such as aircraft regular campaigns available through for example the CH4 GLOBALVIEWplus v6.0 ObsPack (Schuldt et al., 2023), the IAGOS data portal (https://iagos.aeris-data.fr/download/), the NIES portal (https://db.cger.nies.go.jp/ged/en/datasetlist/index.html) for CONTRAIL (e.g., Machida et al., 2008) and Siberian measurements (e.g., Sasakawa et al., 2017), the WDCGG data portal (https://gaw.kishou.go.jp/) for additional





flights over three other Japanese airports and Orléans, France; Aircore campaigns data set can be downloaded through the NOAA Global Monitoring Laboratory website (https://gml.noaa.gov/ccgg/arc/?id=144, Baier et al., 2021) and the French AIrCore Program for atmospheric sampling (https://aircore.aeris-data.fr, Membrive et al., 2017); TCCON observations (https://tccondata.org; e.g., Wunch et al., 2011, 2019), and use this evaluation to weight the different models used in the CH4 budget.

Next steps, in the short term, could include some development to be addressed by the top-down community to reduce atmospheric transport errors:

- Developing further methodologies to extract stratospheric partial column abundances from observations such as TCCON data (Saad et al., 2014; Wang et al., 2014), Aircore (e.g. Andersen et al., 2018; Membrive et al., 2017) or, ACE-FTS (De Mazière et al., 2018) or MIPAS (Glatthor et al., 2023) satellite data.
- Combining SWIR and TIR measurements from space to better constrain the tropospheric column, from TROPOMI and IASI for example in the MethanePlus ESA project (https://methaneplus.eu/#docs, Buchwitz etal., 2023) or GOSAT (Kuze et al., 2020).
- Porting transport models codes to run on Graphics processing Units (GPU) to achieve sub-degrees resolution global inversions (Chevallier et al., 2023).

In the long run, developments within atmospheric transport models such as the implementation of hybrid vertical coordinates (Patra et al., 2018) or of hexagonal-icosaedric grid with finer resolution (Dubos et al., 2015; Niwa et al., 2017, 2022; Lloret et al., 2023), and improvements in the simulated boundary layer dynamics are promising to reduce atmospheric transport errors.

8 Conclusions

We have built an updated global methane budget by using and synthesising a large ensemble of published methods and new results using a consistent, transparent, and traceable approach, including atmospheric observations and inversions (top-down models), process-based models for land surface emissions and atmospheric chemistry, and inventories of anthropogenic emissions (bottom-up models and inventories). For the 2010-2019 decade, global CH₄ emissions are 575 Tg CH₄ yr⁻¹ (range of 553-586 Tg CH₄ yr⁻¹), as estimated by top-down inversions. About 65% of global emissions are anthropogenic (range of 63-68%). Bottom-up models and inventories suggest larger global emissions (669 Tg CH₄ yr⁻¹ [512-849]) mostly because of larger and more uncertain natural emissions from inland freshwater systems, natural wetlands, and geological leaks, and likely some unresolved double counting of these sources. It is also likely that some of the individual bottom-up emission estimates are too high, leading to larger global emissions from the bottom-up approach than the atmospheric constraints suggest. However, the important progress in this update is that for the first time, the bottom-up and top-down budgets agree within their uncertainty ranges. This is substantial progress toward defining more accurate global methane emissions.





The latitudinal breakdown inferred from the top-down approach reveals a dominant role of tropical emissions (\sim 64%) compared to mid (\sim 32%) and high (\sim 4%) northern latitudes (above 60°N) emissions.

Our results, including an extended set of atmospheric inversions, are compared with the previous budget syntheses of Kirschke et al. (2013) and Saunois et al. (2016; 2020). They show overall good consistency when comparing the same decade (2000-2009) at the global and latitudinal scales. The magnitude and uncertainty of most natural or indirect anthropogenic sources have been revised and updated. In particular, this new budget benefits from large efforts and collaborations from the research community to provide improved estimates of the magnitude and uncertainty of the different freshwater sources and helps reduce the potential double counting at the global scale. Of note, newly available gridded datasets for lakes, ponds, reservoirs, streams, and rivers allow building latitudinal and regional estimates for all these sources for the first time in these estimates. In the next review, we hope to be able to reduce uncertainties in emissions from inland freshwater systems by better quantifying the emission factors of each contributing sub-systems (streams, rivers, lakes, ponds) and estimating double counting at regional scale or avoiding double counting by better defining the surface areas of each ecosystem. Another important priority for improvements is the uncertainty on the chemical loss of CH₄ which still needs to be better assessed in both the top-down and the bottom-up budgets. Building on the improvement of the points detailed in Sect. 7, our aim is to update this budget synthesis as a living review paper regularly (~every three or four years). Each update will produce a more recent decadal CH₄ budget, highlight changes in emissions and trends, and incorporate newly available data and model improvements.

It is still under debate why exactly there are sustained increase of atmospheric CH₄ (more than +5 ppb yr¹) since 2007 (Nisbet et al., 2019; Turner et al., 2019). Some likely explanations, already introduced by Saunois et al. (2017) and further investigated by Jackson et al. (2020) and other studies, include, by decreasing order of certainty: 1) a positive contribution from microbial and fossil sources (e.g., Nisbet et al., 2019; Schwietzke et al., 2016; Jackson et al., 2020), a negative contribution from biomass burning emissions before 2014 (Giglio et al., 2013; Worden et al., 2017); 2) a negligible role of Arctic emission changes (e.g., Nisbet et al., 2019; Saunois et al., 2017); and 3) a tropical dominance of the increasing emissions (e.g., Saunois et al., 2017; Jackson et al., 2020; Wilson et al., 2021; Drinkwater et al., 2023). Although the accelerated atmospheric methane growth rate in 2020 (15.2 ppb/yr) has found some explanation with the impact of the world Pandemia in 2020, the sustained observed growth rates in 2021 (17.8 ppb/yr) and 2022 (14 ppb/yr) still challenge our understanding of the global methane cycle. While in Jackson et al. (2020), the increase in CH₄ emissions over the last two decades is attributed entirely to direct anthropogenic emissions, the uncertainty range from the GMB ensemble is large, and the contribution from natural emissions (wetlands) is still largely uncertain. Besides the decadal change in CH₄ emissions, large inter-annual variability can occur from these natural emissions. The recent high record of CH₄ growth rate highlights the potential of large variations from natural emissions from one year to another, in particular wetland emissions (e.g., Peng et al., 2022; Feng et al., 2023). These remain the challenges to be overcome in better quantifying global methane emissions.



2209

2210

2211

2212

2213

2214

2215

2216

2217

2218 2219

2220

2221

2222

2223

2224

2225

2226



2204 The GCP will continue to support and coordinate the development of improved flux estimates for all budget components 2205 and new underlying science to support improved modelling, acquisition of observations, and data integration. At regular 2206 intervals (3-4 years), we will continue to bring all flux components together to produce an improved and updated global 2207 CH₄ budget, and provide a global benchmark for other CH₄ products and assessments.

9 Data availability

The data presented here are made available in the belief that their dissemination will lead to greater understanding and new scientific insights on the methane budget and changes to it, and help to reduce its uncertainties. The free availability of the data does not constitute permission for publication of the data. For research projects, if the data used are essential to the work to be published, or if the conclusion or results largely depend on the data, co-authorship should be considered. Full contact details and information on how to cite the data are given in the accompanying database.

The accompanying database includes a netcdf file defining the regions used, an archive with the maps of prior fluxes used in the top-down activity, an archive with data corresponding to Fig. 3 and 5, and one Excel file organised in the following spreadsheets.

The file Global Methane Budget 2000-2020 v1.0.xlsx includes (1) a summary, (2) the methane observed mixing ratio and growth rate from the four global networks (NOAA, AGAGE, CSIRO and UCI), (3) the evolution of global anthropogenic methane emissions (including biomass burning emissions) used to produce Fig. 2, (4) the global and latitudinal budgets over 2000-2009 based on bottom-up approaches, (5) the global and latitudinal budgets over 2000-2009 based on top-down approaches, (6) the global and latitudinal budgets over 2010–2019 based on bottom-up approaches, (7) the global and latitudinal budgets over 2010-2019 based on top-down approaches, (8) the global and latitudinal budgets for year 2020 based on bottom-up approaches, (9) the global and latitudinal budgets for year 2020 based on top-down approaches, and (10) the list of contributors to contact for further information on specific data.

This database is available from ICOS Carbon Portal (https://doi.org/10.18160/GKO9-2RHT, Martinez et al., 2024).

2227 Author contributions.

- 2228 MS, AM, and JT gathered the bottom-up and top-down data sets and performed the post processing and analysis.
- 2229 MS, BP, PB, PeC, and RJ coordinated the global budget. MS, BP, PB, PeC, RJ, PP and PCi contributed to the update of the
- 2230 full text and all coauthors appended comments, AM, ED, and XL produced the figures, DJB, NG, PH, AI, AJ, TK, TL, XL,
- 2231 KMcD, JMe, JMu, SP, CP, WR, HT, YY, WZ, ZZ, Qing Z, Qiuan Z and Qianlai Z performed surface land model simulations
- 2232 to compute wetland emissions. GA, DB, SC, BRD, GE, MAH, GH, MSJ, RL, SN, GRR, JAR, EHS, PRa, PRe, and TSW
- 2233 provided data sets useful for natural emission estimates and/or contributed to text on bottom-up natural emissions. LHI, SJS,
- 2234 TNF, GRvW, and MC provided anthropogenic data sets and contributed to the text for this section. AM, JT, PP, DBe, RJ,





2235 YN, AS, AT, and BZ performed atmospheric inversions to compute top-down methane emission estimates for sources and 2236 sinks. EJD, XL, DRB, PBK, JM, RJP, MR, MS, DWo, and YYo are PI of atmospheric observations used in top-down inversions and/or contributed the text describing atmospheric methane observations. FD, MS, and JT contributed to the 2237 2238 bottom-up chemical sink section by providing data sets, processing data and/or contributing to the text. FMF provided data

2239 for the soil sink.

2240 2241

Competing interests. At least one of the (co-)authors is a member of the editorial board of Earth System Science Data.

This paper is the result of a collaborative international effort under the umbrella of the Global Carbon Project, a project of

Future Earth and a research partner of the World Climate Research Programme (WCRP). We acknowledge all the people

2242 2243

2244

2245

2246

2247

2248

2249

2250

2251

2252

2253

2254

2255

2256

2257

2258

2259

2260

2261

2262

2263

2264

2265

2266 2267

Acknowledgements

and institutions who provided the data used in the global methane budget as well as the institutions funding parts of this effort (see Table A3). We are very grateful for the help provided by Alex Vermeulen in publishing the Global Methane Budget dataset on the Integrated Carbon Observation System (ICOS) website. We acknowledge the modelling groups for making their simulations available for this analysis, the joint WCRP Stratosphere-troposphere Processes And their Role in Climate/International Global Atmospheric Chemistry (SPARC/IGAC) Chemistry-Climate Model Initiative (CCMI) for organising and coordinating the model data analysis activity, and the British Atmospheric Data Centre (BADC) for collecting and archiving the CCMI model output. We acknowledge the long-term support provided by the Commonwealth Scientific and Industrial Research Organisation (CSIRO) and the National Environmental Science Program - Climate Systems Hub to coordinate and support activities of the Global Carbon Project. We are grateful to the Emissions Databse for Global Atmospheric Research (EDGAR) team (M. Crippa, D. Guizzardi, F. Pagani, M. Banja, E. Schaaf, M. Muntean, W. Becker, F. Monforti-Ferrario) for the work needed to publish the EDGAR greenhouse gas emission datasets used in this work (https://edgar.jrc.ec.europa.eu/). We are particularly indebted to the dedicated station/instrumental operators/scientists that have gathered the data and ensured their high quality. We acknowledge more specifically Katherine Jensen for her contribution to the Surface Water Microwave Product Series SWAMPS, Fortunat Joos for his contribution to simulations with the Land surface Processes and eXchanges model (LPX Bern), Ray Langenfeld for his contribution to CSIRO network, Paul Miller for his contribution to simulations with the Lund-Potsdam-Jena General Ecosystem Simulator (LPJ-GUESS), Peng Shushi for his contribution to simulations with the Organising Carbon and Hydrology In Dynamic Ecosystems (ORCHIDEE) model, Shamil Maksyutov for his contribution for simulations with the inverse model at the National Institute for Environmental Studies (NIES), Isobel Simpson for her contribution to the University of California Irvine (UCI) network, Paul Steele for his former contribution to CSIRO network, Ray Weiss for his contribution to the Advanced Global Atmospheric Gases Experiment (AGAGE) network, Christine Widenmeyer for her contribution with the Fire INventory from the National Center for Atmospheric Research





2268 (FINN) database, Xiaoming Xu for his contribution to simulations with with the The Integrated Science Assessment Model (ISAM), Yuanzhi Yao for his contribution to simulations with the Dynamicl Land Ecosystem Model (DLEM), Diego 2269 2270 Guizzardi for his contribution to EDGAR, Maria Tenkanen for her contribution with the Crabon Tracker – Europe (CTE) 2271 outputs, Giulia Conchedda for her contribution to the Food and Agriculture Organization (FAO) database. FAOSTAT data 2272 collection, analysis, and dissemination is funded through FAO regular budget funds. The contribution of relevant experts in 2273 member countries is gratefully acknowledged. We acknowledge Juha Hatakka from the Finnish Meteorological Institute 2274 (FMI) for making methane measurements at the Pallas station and sharing the data with the community. We thank Ariana 2275 Sutton-Grier and Lisamarie Windham-Myers for reviewing an earlier version of this manuscript. Any use of trade, firm, or

22772278

2276

2279 References

Abe, Y., Bignell, D. E. and Higashi, T., Eds.: Termites: Evolution, Sociality, Symbioses, Ecology, Springer Netherlands, Dordrecht., 2000.

product names is for descriptive purposes only and does not imply endorsement by the US Government.

- Aho, K.S., J.H. Fair, J.D. Hosen, E.D. Kyzivat, L.A. Logozzo, G. Rocher-Ros, L.C. Weber, B. Yoon, and P.A. Raymond:
 Distinct concentration-discharge dynamics in temperate streams and rivers: CO2 exhibits chemostasis while CH4
 exhibits source limitation due to temperature control, Limnology and Oceanography, 66(10): p. 3656-3668., 2021
- Allan, W., Lowe, D. C., Gomez, A. J., Struthers, H. and Brailsford, G. W.: Interannual variation of ¹³C in tropospheric methane: Implications for a possible atomic chlorine sink in the marine boundary layer, J. Geophys. Res.-Atmospheres, 110(D11), doi:10.1029/2004JD005650, 2005.
- Allan, W., Struthers, H. and Lowe, D. C.: Methane carbon isotope effects caused by atomic chlorine in the marine boundary layer: Global model results compared with Southern Hemisphere measurements, J. Geophys. Res.-Atmospheres, 112(D4), D04306, doi:10.1029/2006jd007369, 2007.
- Allen, D. T., Torres, V. M., Thomas, J., Sullivan, D. W., Harrison, M., Hendler, A., Herndon, S. C., Kolb, C. E., Fraser, M. P., Hill, A. D., Lamb, B. K., Miskimins, J., Sawyer, R. F. and Seinfeld, J. H.: Measurements of methane emissions at natural gas production sites in the United States, Proc Natl Acad Sci USA, 110(44), 17,768-17,773, doi:10.1073/pnas.1304880110, 2013.
- 2295 Allen, G. H., & Pavelsky, T. M.: Global extent of rivers and streams. Science, 361(6402), 585–588.
 2296 https://doi.org/10.1126/science.aat0636, 2018
- Alvarez, R. A., Zavala-Araiza, D., Lyon, D. R., Allen, D. T., Barkley, Z. R., Brandt, A. R., Davis, K. J., Herndon, S. C., Jacob, D. J., Karion, A., Kort, E. A., Lamb, B. K., Lauvaux, T., Maasakkers, J. D., Marchese, A. J., Omara, M., Pacala, S. W., Peischl, J., Robinson, A. L., Shepson, P. B., Sweeney, C., Townsend-Small, A., Wofsy, S. C. and Hamburg, S.
- 2300 P.: Assessment of methane emissions from the U.S. oil and gas supply chain, Science, 361(6398), 186–188,





- 2301 doi:10.1126/science.aar7204, 2018.
- Andersen, T., Scheeren, B., Peters, W. and Chen, H.: A UAV-based active AirCore system for measurements of greenhouse gases, Atmospheric Meas. Tech., 11(5), 2683–2699, doi:10.5194/amt-11-2683-2018, 2018.
- Anderson, D. C., Duncan, B. N., Nicely, J. M., Liu, J., Strode, S. A., and Follette-Cook, M. B.: Technical note:

 Constraining the hydroxyl (OH) radical in the tropics with satellite observations of its drivers first steps toward
- assessing the feasibility of a global observation strategy, Atmos. Chem. Phys., 23, 6319–6338,
- 2307 https://doi.org/10.5194/acp-23-6319-2023, 2023.
- André, J.-C., Boucher, O., Bousquet, P., Chanin, M.-L., Chappellaz, J. and Tardieu, B.: Le méthane: d'où vient-il et quel est son impact sur le climat?, EDP Sciences, Académie des Sciences et Technologies, Paris., 2014.
- Aoki, S., Nakazawa, T., Murayama, S. and Kawaguchi, S.: Measurements of atmospheric methane at the Japanese Antarctic Station. Syowa., Tellus, 44B(4), 273–281, doi:10.1034/j.1600-0889.1992.t01-3-00005.x., 1992.
- Arora, V. K., Melton, J. R. and Plummer, D.: An assessment of natural methane fluxes simulated by the CLASS-CTEM model, Biogeosciences, 15(15), 4683–4709, doi:10.5194/bg-15-4683-2018, 2018.
- Bader, W., Bovy, B., Conway, S., Strong, K., Smale, D., Turner, A. J., Blumenstock, T., Boone, C., Collaud Coen, M.,
- Coulon, A., Garcia, O., Griffith, D. W. T., Hase, F., Hausmann, P., Jones, N., Krummel, P., Murata, I., Morino, I.,
- Nakajima, H., O'Doherty, S., Paton-Walsh, C., Robinson, J., Sandrin, R., Schneider, M., Servais, C., Sussmann, R.
- and Mahieu, E.: The recent increase of atmospheric methane from 10 years of ground-based NDACC FTIR
- 2318 observations since 2005, Atmospheric Chem. Phys., 17(3), 2255–2277, doi:10.5194/acp-17-2255-2017, 2017.
- 2319 Baicich. P.: The Birds and Rice Connection, Bird Watch. Dig. [online] Available from: 2320 http://www.greatbirdingprojects.com/images/BWD J-A 13 BIRDS N RICE.pdf, 2013.
- Baier, B., Sweeney, C., Newberger, T., Higgs, J., Wolter, S., & NOAA Global Monitoring Laboratory : NOAA AirCore
- 2322 atmospheric sampling system profiles (Version 20230831) [Data set]. NOAA GML. https://doi.org/10.15138/6AV0-
- 2323 MY81, 2021
- Balasus, N., Jacob, D. J., Lorente, A., Maasakkers, J. D., Parker, R. J., Boesch, H., Chen, Z., Kelp, M. M., Nesser, H., and
- Varon, D. J.: A blended TROPOMI+GOSAT satellite data product for atmospheric methane using machine learning to correct retrieval biases, Atmos. Meas. Tech., 16, 3787–3807, https://doi.org/10.5194/amt-16-3787-2023, 2023.
- Bansal, S., Van Der Berg, M.P., Fern, R.R., Jones, J.W., Lo, R., McKenna, O.P., Tangen, B.A., Zhang, Z., and Gleason,
- 2328 R.A.: Large increases in methane emissions expected from North America's largest wetland complex, Sci. Adv., 9,
- 2329 eade1112, doi:10.1126/sciadv.ade1112, 2023.
- Barba, J., Bradford, M. A., Brewer, P. E., Bruhn, D., Covey, K., van Haren, J., Megonigal, J. P., Mikkelsen, T. N., Pangala,
- 2331 S. R., Pihlatie, M., Poulter, B., Rivas-Ubach, A., Schadt, C. W., Terazawa, K., Warner, D. L., Zhang, Z. and Vargas,
- 2332 R.: Methane emissions from tree stems: a new frontier in the global carbon cycle, New Phytol., 222(1), 18–28,
- 2333 doi:10.1111/nph.15582, 2019.





- Bastviken, D., Tranvik, L. J., Downing, J. A., Crill, P. M. and Enrich-Prast, A.: Freshwater Methane Emissions Offset the Continental Carbon Sink, Science, 331(6013), 50–50, doi:10.1126/science.1196808, 2011.
- Bastviken, D., C.C. Treat, S.R. Pangala, V. Gauci, A. Enrich-Prast, M. Karlson, M. Gålfalk, M.B. Romano, and H.O.
- Sawakuchi, The importance of plants for methane emission at the ecosystem scale. Aquatic Botany, 184: p. 103596, 2023.
- Basu, S., Lan, X., Dlugokencky, E., Michel, S., Schwietzke, S., Miller, J. B., Bruhwiler, L., Oh, Y., Tans, P. P., Apadula,
- F., Gatti, L. V., Jordan, A., Necki, J., Sasakawa, M., Morimoto, S., Di Iorio, T., Lee, H., Arduini, J., and Manca, G.:
- Estimating emissions of methane consistent with atmospheric measurements of methane and δ^{13} C of methane, Atmos.
- 2342 Chem. Phys., 22, 15351–15377, https://doi.org/10.5194/acp-22-15351-2022, 2022.
- Beaulieu, J.J., DelSontro, T. & Downing, J.A.: Eutrophication will increase methane emissions from lakes and
- 2344 impoundments during the 21st century. *Nat Commun* 10, 1375 , https://doi.org/10.1038/s41467-019-09100-5, 2019
- Beck, H., Zimmermann, N., McVicar, T. *et al.* Present and future Köppen-Geiger climate classification maps at 1-km resolution. *Sci Data* **5**, 180214, doi.org/10.1038/sdata.2018.214, 2018
- Beerling, D.J., Woodward, F.I., Vegetation and the Terrestrial Carbon Cycle: Modelling the First 400 Million Years.

 Cambridge University Press, Cambridge, 2001
- Begum, M.S., M.J. Bogard, D.E. Butman, E. Chea, S. Kumar, X. Lu, O.K. Nayna, L. Ran, J.E. Richey, S.M. Tareq, D.T.
- 2350 Xuan, R. Yu, and J.-H. Park, Localized Pollution Impacts on Greenhouse Gas Dynamics in Three Anthropogenically
- 2351 Modified Asian River Systems. Journal of Geophysical Research: Biogeosciences, 126(5): p. e2020JG006124, 2021
- Bergamaschi, P., Houweling, S., Segers, A., Krol, M., Frankenberg, C., Scheepmaker, R. A., Dlugokencky, E., Wofsy, S.
- 2353 C., Kort, E. A., Sweeney, C., Schuck, T., Brenninkmeijer, C., Chen, H., Beck, V. and Gerbig, C.: Atmospheric CH₄ in
- the first decade of the 21st century: Inverse modeling analysis using SCIAMACHY satellite retrievals and NOAA
- 2355 surface measurements, J. Geophys. Res. Atmospheres, 118(13), 7350–7369, doi:10.1002/jgrd.50480, 2013.
- Bergamaschi, P., DANILA, A. M., Weiss, R., Thompson, R. L., Brunner, D., Levin, I., meijer, Y., Chevallier, F., Janssens-
- Maenhout, G., Bovensmann, H., Crisp, D., Basu, S., Dlugockencky, E. J., Engelen, R., Gerbig, C., Günther, D.,
- Hammer, S., Henne, S., Houweling, S., Karstens, U., Kort, E. A., Maione, M., Manning, A. J., Miller, J., Montzka, S.,
- Pandey, S., Peters, W., Peylin, P., Pinty, B., Ramonet, M., Reimann, S., Röckmann, T., Schmidt, M., Strogies, M.,
- Sussams, J., Tarasova, O., Van Aardenne, J., Vermeulen, A. and Vogel, F.: Atmospheric monitoring and inverse
- 2361 modelling for verification of greenhouse gas inventories, EUR Scientific and Technical Research Reports,
- Publications Office of the European Union. [online] Available from: https://ec.europa.eu/jrc/en/publication/eur-
- scientific-and-technical-research-reports/atmospheric-monitoring-and-inverse-modelling-verification-greenhouse-
- 2364 gas-inventories (Accessed 17 March 2020a), 2018.
- Best, A. I., Richardson, M. D., Boudreau, B. P., Judd, A. G., Leifer, I., Lyons, A. P., et al.: Shallow Seabed Methane Gas
- 2366 Could Pose Coastal hazard. Eos Trans. AGU 87 (22), 213–217. doi:10.1029/2006EO220001, 2006





- Bian, L., Gao, Z., Sun, Y., Ding, M., Tang, J. and Schnell, R. C.: CH4 Monitoring and Background Concentration at
- 2368 Zhongshan Station, Antarctica, Atmospheric Clim. Sci., 6(1), 135–144, doi:10.4236/acs.2016.61012, 2015.
- Bignell, D.E., Eggleton, P. Termites in ecosystems. In: Abe, T., Higashi, M. and Bignell, D.E. (Eds), Termites: Evolution,
- Sociality, Symbioses, Ecology. Kluwer, Dordrecht, Netherlands, 363–387, 2000.
- Biskaborn, B.K., Smith, S.L., Noetzli, J. et al. Permafrost is warming at a global scale. Nat Commun 10, 264, https://doi-
- 2372 <u>org.insu.bib.cnrs.fr/10.1038/s41467-018-08240-4</u>, 2019
- Blake, D. R. and Rowland, F. S.: World-wide increase in tropospheric methane, 1978–1983, J. Atmospheric Chem., 4,
- 2374 43–62, 1986.
- Blake, D. R., Mayer, E. W., Tyler, S. C., Makide, Y., Montague, D. C. and Rowland, F. S.: Global Increase in Atmospheric
- 2376 Methane Concentrations between 1978 and 1980, Geophys. Res. Lett., 9(4), 477–480, 1982.
- Bloom, A. A., Lee-Taylor, J., Madronich, S., Messenger, D. J., Palmer, P. I., Reay, D. S. and McLeod, A. R.: Global
- methane emission estimates from ultraviolet irradiation of terrestrial plant foliage, New Phytol., doi:10.1111/j.1469-
- 2379 8137.2010.03259.x, 2010.
- Bohn, T. J., Melton, J. R., Ito, A., Kleinen, T., Spahni, R., Stocker, B. D., Zhang, B., Zhu, X., Schroeder, R., Glagolev, M.
- V., Maksyutov, S., Brovkin, V., Chen, G., Denisov, S. N., Eliseev, A. V., Gallego-Sala, A., McDonald, K. C., Rawlins,
- 2382 M. A., Riley, W. J., Subin, Z. M., Tian, H., Zhuang, Q. and Kaplan, J. O.: WETCHIMP-WSL: Intercomparison of
- wetland methane emissions models over West Siberia, Biogeosciences, 12(11), 3321–3349, doi:10.5194/bg-12-3321-
- 2384 2015, 2015.
- Bodmer, P., Vroom, R. J. E., Stepina, T., del Giorgio, P. A., Kosten, S.: Methane dynamics in vegetated habitats in inland
- waters: quantification, regulation, and global significance, Frontiers in Water, 5, DOI=10.3389/frwa.2023.1332968,
- 2387 2024
- 2388 Borges, A. V. and Abril, G.: Carbon Dioxide and Methane Dynamics in Estuaries, in Treatise on Estuarine and Coastal
- 2389 Science, vol. 5, pp. 119–161, Academic Press, Waltham. [online] Available from: doi:10.1016/B978-0-12-374711-
- 2390 2.00504-0, 2011.
- Borges, A., G. Abril, and S. Bouillon: Carbon dynamics and CO2 and CH₄ outgassing in the Mekong delta,
- 2392 Biogeosciences, 15: p. 1093-1114., 2018
- Borges, A.V., F. Darchambeau, T. Lambert, C. Morana, G.H. Allen, E. Tambwe, A. Toengaho Sembaito, T. Mambo, J.
- Nlandu Wabakhangazi, J.P. Descy, C.R. Teodoru, and S. Bouillon: Variations in dissolved greenhouse gases (CO2,
- 2395 CH₄, N2O) in the Congo River network overwhelmingly driven by fluvial-wetland connectivity, Biogeosciences,
- 2396 16(19): p. 3801-3834, 2019
- Borges, A. V., Deirmendjian, L., Bouillon, S., Okello, W., Lambert, T., Roland, F.A. E., Razanamahandry, V. F.,
- Voarintsoa, NR. G., Darchambeau, F., Kimirei, I. A., Descy, J-P., Allen, G. H. and Morana, C.: Greenhouse gas
- emissions from African lakes are no longer a blind spot. Sci. Adv. 8, eabi8716, DOI:10.1126/sciadv.abi8716, 2022





- Bousquet, P., Ciais, P., Miller, J. B., Dlugokencky, E. J., Hauglustaine, D. A., Prigent, C., Van der Werf, G. R., Peylin, P.,
- Brunke, E. G., Carouge, C., Langenfelds, R. L., Lathiere, J., Papa, F., Ramonet, M., Schmidt, M., Steele, L. P., Tyler,
- S. C. and White, J.: Contribution of anthropogenic and natural sources to atmospheric methane variability, Nature,
- 2403 443(7110), 439–443, 2006.
- Bousquet, P., Pierangelo, C., Bacour, C., Marshall, J., Peylin, P., Ayar, P. V., Ehret, G., Bréon, F.-M., Chevallier, F.,
- Crevoisier, C., Gibert, F., Rairoux, P., Kiemle, C., Armante, R., Bès, C., Cassé, V., Chinaud, J., Chomette, O.,
- Delahaye, T., Edouart, D., Estève, F., Fix, A., Friker, A., Klonecki, A., Wirth, M., Alpers, M. and Millet, B.: Error
- 2407 Budget of the MEthane Remote LIdar missioN and Its Impact on the Uncertainties of the Global Methane Budget, J.
- 2408 Geophys. Res. Atmospheres, 123(20), 11,766-11,785, doi:10.1029/2018JD028907, 2018.
- Brandt, A. R., Heath, G. A., Kort, E. A., O'Sullivan, F., Pétron, G., Jordaan, S. M., Tans, P., Wilcox, J., Gopstein, A. M.,
- Arent, D., Wofsy, S., Brown, N. J., Bradley, R., Stucky, G. D., Eardley, D. and Harriss, R.: Methane Leaks from North
- 2411 American Natural Gas Systems, Science, 343(6172), 733–735, doi:10.1126/science.1247045, 2014.
- 2412 Brasseur, G. P. and Solomon, S.: Aeronomy of the Middle Atmosphere: Chemistry and Physics of the Stratosphere and
- 2413 Mesosphere, 3rd ed., Springer Netherlands., 2005.
- Brenninkmeijer C. A. M., Crutzen, P., Boumard, F., Dauer, T., Dix, B., Ebinghaus, R., Filippi, D., Fischer, H., Franke, H.,
- Fries, U., Heintzenberg, J., Helleis, F., Hermann, M., Kock, H. H., Koeppel, C., Lelieveld, J., Leuenberger, M.,
- 2416 Martinsson, B. G., Miemczyk, S., Moret, H. P., Nguyen, H. N., Nyfeler, P., Oram, D., O'Sullivan, D., Penkett, S., Platt,
- 2417 U., Pupek, M., Ramonet, M., Randa, B., Reichelt, M., Rhee, T. S., Rohwer, J., Rosenfeld, K., Scharffe, D., Schlager,
- 2418 H., Schumann, U., Slemr, F., Sprung, D., Stock, P., Thaler, R., Valentino, F., van Velthoven, P., Waibel, A., Wandel,
- A., Waschitschek, K., Wiedensohler, A., Xueref-Remy, I., Zahn, A., Zech, U., and Ziereis, H.: Civil Aircraft for the
- regular investigation of the atmosphere based on an instrumented container: The new CARIBIC system, Atmos. Chem.
- 2421 Phys., 7, 4953-4976, doi:10.5194/acp-7-4953-2007, 2007.
- Bruhwiler, L. M., Basu, S., Bergamaschi, P., Bousquet, P., Dlugokencky, E., Houweling, S., Ishizawa, M., Kim, H.-S.,
- Locatelli, R., Maksyutov, S., Montzka, S., Pandey, S., Patra, P. K., Petron, G., Saunois, M., Sweeney, C., Schwietzke,
- 2424 S., Tans, P. and Weatherhead, E. C.: U.S. CH4 emissions from oil and gas production: Have recent large increases
- been detected?, J. Geophys. Res. Atmospheres, 122(7), 4070–4083, doi:10.1002/2016JD026157, 2017.
- Brune, A.: Symbiotic digestion of lignocellulose in termite guts, Nat Rev Microbiol 12, 168–180,
- 2427 doi.org/10.1038/nrmicro3182., 2014
- Buchwitz, M., de Beek, R., Burrows, J. P., Bovensmann, H., Warneke, T., Notholt, J., Meirink, J. F., Goede, A. P. H.,
- Bergamaschi, P., Korner, S., Heimann, M. and Schulz, A.: Atmospheric methane and carbon dioxide from
- SCIAMACHY satellite data: initial comparison with chemistry and transport models, Atmospheric Chem. Phys., 5,
- 2431 941–962, 2005a.
- Buchwitz, M., de Beek, R., Noel, S., Burrows, J. P., Bovensmann, H., Bremer, H., Bergamaschi, P., Korner, S. and





- Heimann, M.: Carbon monoxide, methane and carbon dioxide columns retrieved from SCIAMACHY by WFM-
- DOAS: year 2003 initial data set, Atmospheric Chem. Phys., 5, 3313–3329, 2005b.
- Buchwitz, M., Dils, B., Boesch, H., Crevoisier, C., Detmers, R., Frankenberg, C., Hasekamp, O., Hewson, W., Laeng, A.,
- Noel, S., Nothold, J., Parker, R., Reuter, M. and Schneising, O.: Product Validation and Intercomparison Report
- 2437 (PVIR) for the Essential Climate Variable (ECV) Greenhouse Gases (GHG), ESA Climate Change Initiative (CCI),
- report version 4, Feb 2016, http://www.esa-ghg-cci.org/?q=webfm_send/300., 2016.
- Buchwitz, M., Schneising, O., Vanselow, S., Houweling, S., van Peet, J., Siddans, R., Kerridge, B., Ventress, L., Knappett,
- D., Crevoisier, C., Meilhac, N., Borsdof, T., Lorente, A. and Aben, I.: Final Report of the Methane Plus ESA project,
- TN-D15/16-CH4PLUS, https://methaneplus.eu/#docs, Accessed on February 13 2024, 202
- Butz, A., Guerlet, S., Hasekamp, O., Schepers, D., Galli, A., Aben, I., Frankenberg, C., Hartmann, J. M., Tran, H., Kuze,
- A., Keppel-Aleks, G., Toon, G., Wunch, D., Wennberg, P., Deutscher, N., Griffith, D., Macatangay, R.,
- Messerschmidt, J., Notholt, J. and Warneke, T.: Toward accurate CO₂ and CH₄ observations from GOSAT, Geophys.
- 2445 Res. Lett., 38(14), L14812, doi:10.1029/2011gl047888, 2011.
- Cai, Z. C., Xing, G., Yan, X., Xu, H., Tsuruta, H., Yagi, K. and Minami, K.: Methane and nitrous oxide emissions from
- rice paddy fields as affected by nitrous fertilizers and water management, Plant Soil, 196, 7–14, 1997.
- Cael, B.B., J. Biggs, and D.A. Seekell, The size-distribution of earth's lakes and ponds: Limits to power-law behavior.
- Frontiers in Environmental Science, 10.-, 2022
- 2450 Call, M., D. T. Maher, I. R. Santos, and others.: Spatial and temporal variability of carbon dioxide and methane fluxes
- over semi-diurnal and spring—neap—spring timescales in a mangrove creek. Geochim. Cosmochim. Acta 150: 211–225.
- 2452 doi:10.1016/j.gca.2014.11.023, 2015
- 2453 Canadell, J.G., P.M.S. Monteiro, M.H. Costa, L. Cotrim da Cunha, P.M. Cox, A.V. Eliseev, S. Henson, M. Ishii, S. Jaccard,
- 2454 C. Koven, A. Lohila, P.K. Patra, S. Piao, J. Rogeli, S. Syampungani, S. Zaehle, and K. Zickfeld: Global Carbon and
- other Biogeochemical Cycles and Feedbacks. In Climate Change 2021: The Physical Science Basis. Contribution of
- 2456 Working Group I to the Sixth Assessment Report of the Intergovernmental Panel on Climate Change [Masson-
- Delmotte, V., P. Zhai, A. Pirani, S.L. Connors, C. Péan, S. Berger, N. Caud, Y. Chen, L. Goldfarb, M.I. Gomis, M.
- Huang, K. Leitzell, E. Lonnoy, J.B.R. Matthews, T.K. Maycock, T. Waterfield, O. Yelekçi, R. Yu, and B. Zhou (eds.)].
- Cambridge University Press, Cambridge, United Kingdom and New York, NY, USA, pp. 673-816, doi:
- 2460 10.1017/9781009157896.007, 2021
- Carlson, K. M., Gerber, J. S., Mueller, N. D., Herrero, M., MacDonald, G. K., Brauman, K. A., Havlik, P., O'Connell, C.
- S., Johnson, J. A., Saatchi, S. and West, P. C.: Greenhouse gas emissions intensity of global croplands, Nat. Clim.
- 2463 Change, 7(1), 63–68, doi:10.1038/nclimate3158, 2017.
- 2464 Castelán-Ortega, O. A., Carlos Ku-Vera, J. and Estrada-Flores, J. G.: Modeling methane emissions and methane
- inventories for cattle production systems in Mexico, Atmósfera, 27(2), 185–191, doi:10.1016/S0187-6236(14)71109-





- 2466 9, 2014.
- Cathles, L., Brown, L., Taam, M. and Hunter, A.: A commentary on "The greenhouse-gas footprint of natural gas in shale
- formations" by R.W. Howarth, R. Santoro, and Anthony Ingraffea, Clim. Change, 113(2), 525–535,
- 2469 doi:10.1007/s10584-011-0333-0, 2012.
- Caulton, D., Shepson, P. B., Santoro, R. L., Sparks, J. P., Howarth, R. W., Anthony R, Ingraffea, A. R., Cambaliza, M. O.
- L., Sweeney, C., Karion, A., Davis, K. J., Stirm, B. H., Montzka, S. A. and Miller, B. R.: Toward a better understanding
- and quantification of methane emissions from shale gas development, Proc. Natl. Acad. Sci. USA, 111(17), 6237–
- 2473 6242, doi:10.1073/pnas.1316546111, 2014.
- Chandra, N., P. K. Patra, J. S. H. Bisht, A. Ito, T. Umezawa, S. Morimoto, S. Aoki, G. Janssens-Maenhout, R. Fujita, M.
- Takigawa, S. Watanabe, N. Saitoh, J.G. Canadell, Emissions from the oil and gas sectors, coal mining and ruminant
- farming drive methane growth over the past three decades, J. Meteorol. Soc. Jpn., 99(2), doi:10.2151/jmsj.2021-015,
- 2477 2021.
- Chang, J., Peng, S., Ciais, P., Saunois, M., Dangal, S. R. S., Herrero, M., Havlík, P., Tian, H. and Bousquet, P.: Revisiting
- 2479 enteric methane emissions from domestic ruminants and their δ 13 C CH4 source signature, Nat. Commun., 10(1), 1–
- 2480 14, doi:10.1038/s41467-019-11066-3, 2019.
- 2481 Chang, J., Peng, S., Yin, Y., Ciais, P., Havlik, P., & Herrero, M.: The key role of production efficiency changes in
- livestock methane emission mitigation. AGU Advances, 2, e2021AV000391, https://doi.org/10.1029/2021AV000391,
- 2483 2021
- Chappellaz, J., Bluniert, T., Raynaud, D., Barnola, J. M., Schwander, J. and Stauffert, B.: Synchronous changes in
- 2485 atmospheric CH4 and Greenland climate between 40 and 8 kyr BP, Nature, 366(6454), 443-445,
- 2486 doi:10.1038/366443a0, 1993.
- Chen, H., Zhu, Q., Peng, C., Wu, N., Wang, Y., Fang, X., Jiang, H., Xiang, W., Chang, J., Deng, X. and Yu, G.: Methane
- emissions from rice paddies natural wetlands, lakes in China: Synthesis new estimate, Glob. Change Biol., 19(1), 19–
- 2489 32, doi:10.1111/gcb.12034, 2013.
- 2490 Chen, Y. H. and Prinn, R. G.: Estimation of atmospheric methane emissions between 1996 and 2001 using a three-
- dimensional global chemical transport model, J. Geophys. Res.-Atmospheres, 111(D10307),
- 2492 doi:10.1029/2005JD006058, 2006.
- Chen, Z., Jacob, D. J., Nesser, H., Sulprizio, M. P., Lorente, A., Varon, D. J., Lu, X., Shen, L., Qu, Z., Penn, E., and Yu,
- 2494 X.: Methane emissions from China: a high-resolution inversion of TROPOMI satellite observations, Atmos. Chem.
- 2495 Phys., 22, 10809–10826, https://doi.org/10.5194/acp-22-10809-2022, 2022.
- 2496 Chen, Y., Hall, J., van Wees, D., Andela, N., Hantson, S., Giglio, L., van der Werf, G. R., Morton, D. C., and Randerson,
- J. T.: Multi-decadal trends and variability in burned area from the fifth version of the Global Fire Emissions Database
- 2498 (GFED5), Earth Syst. Sci. Data, 15, 5227–5259, https://doi.org/10.5194/essd-15-5227-2023, 2023.





- 2499 Chevallier, F., Lloret, Z., Cozic, A., Takache, S., and Remaud, M.: Toward high-resolution global atmospheric inverse
- 2500 modeling using graphics accelerators. *Geophysical Research Letters*, 50(5), 1–9.
- 2501 https://doi.org/10.1029/2022GL102135, 2023
- Ciais, P., Sabine, C., Bala, G., Bopp, L., Brovkin, V., Canadell, J., Chhabra, A., DeFries, R., Galloway, J., Heimann. M,
- Jones, C., Le Quéré, C., Myneni, R. B., Piao, S. and Thornton, P.: Carbon and Other Biogeochemical Cycles, in In
- 2504 Climate Change 2013: The Physical Science Basis. Contribution of Working Group I to the Fifth Assessment Report
- of IPCC, edited by T. F. Stocker, D. Qin, G.-K. Plattner, M. Tignor, S. K. Allen, J. Boschung, A. Nauels, Y. Xia, V.
- Bex, and P. M. Midgley, Cambridge University Press, Cambridge., 2013.
- 2507 Cicerone, R. J. and Oremland, R. S.: Biogeochemical aspects of atmospheric methane, Glob. Biogeochem. Cycles, 2, 299–
- 2508 327, 1988.
- 2509 Cicerone, R. J. and Shetter, J. D.: Sources of atmospheric methane: Measurements in rice paddies and a discussion, J.
- 2510 Geophys. Res., 86, 7203–7209, 1981.
- Collins, W. J., Lamarque, J. F., Schulz, M., Boucher, O., Eyring, V, Hegglin, M. I., Maycock, A., Myhre, G., Prather, M.,
- Shindell, D. and Smith, S.J.: AerChemMIP: quantifying the effects of chemistry and aerosols in CMIP6. Geoscientific
- 2513 Model Development 10, 585–607. doi:10.5194/gmd-10-585-2017, 2017.
- Comer-Warner, S.A., P. Romeijn, D.C. Gooddy, S. Ullah, N. Kettridge, B. Marchant, D.M. Hannah, and S.
- 2515 Krause: Thermal sensitivity of CO2 and CH₄ emissions varies with streambed sediment properties. Nature
- 2516 Communications, 9(1): p. 2803, 2018
- Conley, S., Franco, G., Faloona, I., Blake, D. R., Peischl, J. and Ryerson, T. B.: Methane emissions from the 2015 Aliso
- 2518 Canyon blowout in Los Angeles, CA, Science, 351(6279), 1317–1320, doi:10.1126/science.aaf2348, 2016.
- 2519 Conrad, R., Klose, M. and Claus, P.: Phosphate Inhibits Acetotrophic Methanogenesis on Rice Roots, Appl. Environ.
- 2520 Microbiol., 66(2), 828–831, 2000.

2521 Covey, K. R. and Megonigal, J. P.: Methane production and emissions in trees and forests, New Phytol., 222(1), 35–51,

- 2522 doi:10.1111/nph.15624, 2019.
- 2523 Covey, K. R., Wood, S. A., Warren, R. J., Lee, X. and Bradford, M. A.: Elevated methane concentrations in trees of an
- 2524 upland forest, Geophys. Res. Lett., 39(15), doi:10.1029/2012gl052361, 2012.
- Covey, K. R., de Mesquita, C. P. B., Oberle, B., Maynard, D. S., Bettigole, C., Crowther, T. W., Duguid, M. C., Steven,
- B., Zanne, A. E., Lapin, M., Ashton, M. S., Oliver, C. D., Lee, X. and Bradford, M. A.: Greenhouse trace gases in
- deadwood, Biogeochemistry, 130(3), 215–226, doi:10.1007/s10533-016-0253-1, 2016.
- 2528 Crawford, J.T. and E.H. Stanley: Controls on methane concentrations and fluxes in streams draining human-dominated
- 2529 landscapes. Ecological Applications, 26(5): p. 1581-1591, 2016
- 2530 Crevoisier, C., Nobileau, D., Fiore, A. M., Armante, R., Chedin, A. and Scott, N. A.: Tropospheric methane in the tropics
- first year from IASI hyperspectral infrared observations, Atmospheric Chem. Phys., 9(17), 6337–6350, 2009.





- Crippa, M., Guizzardi, D., Solazzo, E., Muntean, M., Schaaf, E., Monforti-Ferrario, F., Banja, M., Olivier, J.G.J., Grassi,
- 2533 G., Rossi, S., Vignati, E., GHG emissions of all world countries 2021 Report, EUR 30831 EN, Publications Office of
- 2534 the European Union, Luxembourg, 2021, ISBN 978-92-76-41547-3, doi:10.2760/173513, JRC126363, 2021
- 2535 Crippa, M., Guizzardi, D., Pagani, F., Banja, M., Muntean, M., Schaaf E., Becker, W., Monforti-Ferrario, F., Quadrelli,
- 2536 R., Risquez Martin, A., Taghavi-Moharamli, P., Köykkä, J., Grassi, G., Rossi, S., Brandao De Melo, J., Oom, D.,
- Branco, A., San-Miguel, J., Vignati, E., GHG emissions of all world countries, Publications Office of the European
- 2538 Union, Luxembourg, 2023, doi:10.2760/953322, JRC134504, 2023
- 2539 Crutzen, P. J., Aselmann, I. and Seiler, W.: Methane production by domestic animals, wild ruminants, other herbivorous
- 2540 fauna, and humans, Tellus B, 38B(3–4), 271–284, doi:10.1111/j.1600-0889.1986.tb00193.x, 1986.
- Cucchi, M., Weedon, G. P., Amici, A., Bellouin, N., Lange, S., Müller Schmied, H., Hersbach, H. and Buontempo, C.:
- WFDE5: bias-adjusted ERA5 reanalysis data for impact studies. Earth System Science Data, 12, 2097–2120, 2020
- Cunnold, D. M., Steele, L. P., Fraser, P. J., Simmonds, P. G., Prinn, R. G., Weiss, R. F., Porter, L. W., O'Doherty, S.,
- Langenfelds, R. L., Krummel, P. B., Wang, H. J., Emmons, L., Tie, X. X. and Dlugokencky, E. J.: In situ measurements
- of atmospheric methane at GAGE/AGAGE sites during 1985-2000 and resulting source inferences, J. Geophys. Res.
- 2546 Atmospheres, 107(D14), doi:10.1029/2001jd001226, 2002.
- 2547 Curry, C. L.: Modeling the soil consumption of atmospheric methane at the global scale, Glob. Biogeochem. Cycles, 21(4),
- 2548 GB4012, doi:10.1029/2006gb002818, 2007.
- Dalsøren, S. B., Isaksen, I. S. A., Li, L. and Richter, A.: Effect of emission changes in Southeast Asia on global hydroxyl
- and methane lifetime, Tellus B, 61(4), 588–601, doi:10.1111/j.1600-0889.2009.00429.x, 2009.
- Darmenov, A. and da Silva, A.: The quick fire emissions dataset (QFED) Documentation of versions 2.1, 2.2 and
- 2552 2.4, Technical Report Series on Global Modeling and Data Assimilation, NASA Global Modeling and Assimilation
- 2553 Office, [online] Available from: https://gmao.gsfc.nasa.gov/pubs/docs/Darmenov796.pdf (Accessed 11 March 2020),
- 2554 2015.
- De Mazière, M., Vigouroux, C., Bernath, P. F., Baron, P., Blumenstock, T., Boone, C., Brogniez, C., Catoire, V., Coffey,
- 2556 M., Duchatelet, P., Griffith, D., Hannigan, J., Kasai, Y., Kramer, I., Jones, N., Mahieu, E., Manney, G. L., Piccolo, C.,
- 2557 Randall, C., Robert, C., Senten, C., Strong, K., Taylor, J., Tétard, C., Walker, K. A., and Wood, S.: Validation of ACE-
- 2558 FTS v2.2 methane profiles from the upper troposphere to the lower mesosphere, Atmos. Chem. Phys., 8, 2421–2435,
- 2559 https://doi.org/10.5194/acp-8-2421-2008, 2008.
- Deemer, B. R., Harrison, J. A., Li, S., Beaulieu, J. J., DelSontro, T., Barros, N., Bezerra-Neto, J. F., Powers, S. M., dos
- 2561 Santos, M. A. and Vonk, J. A.: Greenhouse Gas Emissions from Reservoir Water Surfaces: A New Global Synthesis,
- 2562 BioScience, 66(11), 949–964, doi:10.1093/biosci/biw117, 2016.
- 2563 Deemer, B.R. and M.A. Holgerson, Drivers of Methane Flux Differ Between Lakes and Reservoirs, Complicating Global
- Upscaling Efforts. Journal of Geophysical Research: Biogeosciences 126(4): p. e2019JG005600., 2021.





- Defratyka, S. M., Paris, J.-D., Yver-Kwok, C., Fernandez, J. M., Korben, P., and Bousquet, P.: Mapping Urban Methane Sources in Paris, France, Environmental Science & Technology, 55, 8583-8591, 10.1021/acs.est.1c00859, 2021.
- DelSontro, T., Beaulieu, J. J. and Downing, J. A.: Greenhouse gas emissions from lakes and impoundments: Upscaling in the face of global change, Limnol. Oceanogr. Lett., 3(3), 64–75, doi:10.1002/lol2.10073, 2018.
- Delwiche, K. B., Knox, S. H., Malhotra, A., Fluet-Chouinard, E., McNicol, G., Feron, S., Ouyang, Z., Papale, D., Trotta,
- 2570 C., Canfora, E., Cheah, Y.-W., Christianson, D., Alberto, Ma. C. R., Alekseychik, P., Aurela, M., Baldocchi, D.,
- Bansal, S., Billesbach, D. P., Bohrer, G., Bracho, R., Buchmann, N., Campbell, D. I., Celis, G., Chen, J., Chen, W.,
- 2572 Chu, H., Dalmagro, H. J., Dengel, S., Desai, A. R., Detto, M., Dolman, H., Eichelmann, E., Euskirchen, E., Famulari,
- D., Fuchs, K., Goeckede, M., Gogo, S., Gondwe, M. J., Goodrich, J. P., Gottschalk, P., Graham, S. L., Heimann, M.,
- Helbig, M., Helfter, C., Hemes, K. S., Hirano, T., Hollinger, D., Hörtnagl, L., Iwata, H., Jacotot, A., Jurasinski, G.,
- Kang, M., Kasak, K., King, J., Klatt, J., Koebsch, F., Krauss, K. W., Lai, D. Y. F., Lohila, A., Mammarella, I., Belelli
- Marchesini, L., Manca, G., Matthes, J. H., Maximov, T., Merbold, L., Mitra, B., Morin, T. H., Nemitz, E., Nilsson, M.
- B., Niu, S., Oechel, W. C., Oikawa, P. Y., Ono, K., Peichl, M., Peltola, O., Reba, M. L., Richardson, A. D., Riley, W.,
- Runkle, B. R. K., Ryu, Y., Sachs, T., Sakabe, A., Sanchez, C. R., Schuur, E. A., Schäfer, K. V. R., Sonnentag, O.,
- Sparks, J. P., Stuart-Haëntjens, E., Sturtevant, C., Sullivan, R. C., Szutu, D. J., Thom, J. E., Torn, M. S., Tuittila, E.-
- 2580 S., Turner, J., Ueyama, M., Valach, A. C., Vargas, R., Varlagin, A., Vazquez-Lule, A., Verfaillie, J. G., Vesala, T.,
- Vourlitis, G. L., Ward, E. J., Wille, C., Wohlfahrt, G., Wong, G. X., Zhang, Z., Zona, D., Windham-Myers, L., Poulter,
- B., and Jackson, R. B.: FLUXNET-CH4: a global, multi-ecosystem dataset and analysis of methane seasonality from
- 2583 freshwater wetlands, Earth Syst. Sci. Data, 13, 3607–3689, https://doi.org/10.5194/essd-13-3607-2021, 2021.
- Deng, Z., Ciais, P., Tzompa-Sosa, Z. A., Saunois, M., Qiu, C., Tan, C., Sun, T., Ke, P., Cui, Y., Tanaka, K., Lin, X.,
- Thompson, R. L., Tian, H., Yao, Y., Huang, Y., Lauerwald, R., Jain, A. K., Xu, X., Bastos, A., Sitch, S., Palmer, P. I.,
- Lauvaux, T., d'Aspremont, A., Giron, C., Benoit, A., Poulter, B., Chang, J., Petrescu, A. M. R., Davis, S. J., Liu, Z.,
- Grassi, G., Albergel, C., Tubiello, F. N., Perugini, L., Peters, W., and Chevallier, F.: Comparing national greenhouse
- gas budgets reported in UNFCCC inventories against atmospheric inversions, Earth Syst. Sci. Data, 14, 1639–1675,
- 2589 https://doi.org/10.5194/essd-14-1639-2022, 2022.
- Denman, K. L., G. Brasseur, A. Chidthaisong, P. Ciais, P. M. Cox, R. E. Dickinson, D. Hauglustaine, C. Heinze, E.
- Holland, D. Jacob, U. Lohmann, S Ramachandran, P. L. da Silva Dias, S. C. Wofsy and X. Zhang: Couplings Between
- 2592 Changes in the Climate System and Biogeochemistry, Cambridge University Press, Cambridge, United Kingdom and
- 2593 New York, NY, USA., 2007.
- Dirmeyer, P. A., Gao, X., Zhao, M., Guo, Z., Oki, T., and Hanasaki, N. GSWP-2: Multimodel analysis and implications
- for our perception of the land surface. Bulletin of the American Meteorological Society, 87(10):1381–1398, 2006.
- Dlugokencky, E. J., Dutton, E. G., Novelli, P. C., Tans, P. P., Masarie, K. A., Lantz, K. O. and Madronich, S.: Changes in
- 2597 CH₄ and CO growth rates after the eruption of Mt Pinatubo and their link with changes in tropical tropospheric UV





- 2598 flux, Geophys. Res. Lett., 23(20), 2761–2764, 1996.
- Dlugokencky, E. J., Myers, R. C., Lang, P. M., Masarie, K. A., Crotwell, A. M., Thoning, K. W., Hall, B. D., Elkins, J.
- W. and Steele, L. P.: Conversion of NOAA atmospheric dry air CH4 mole fractions to a gravimetrically prepared
- 2601 standard scale, J Geophys Res, 110(D18306), doi:10.1029/2005JD006035., 2005.
- Dlugokencky, E. J., Bruhwiler, L., White, J. W. C., Emmons, L. K., Novelli, P. C., Montzka, S. A., Masarie, K. A., Lang,
- P. M., Crotwell, A. M., Miller, J. B. and Gatti, L. V.: Observational constraints on recent increases in the atmospheric
- 2604 CH4 burden, Geophys. Res. Lett., 36, 5 PP., doi:200910.1029/2009GL039780, 2009.
- Dlugokencky, E. J., Nisbet, E. G., Fisher, R. and Lowry, D.: Global atmospheric methane: budget, changes and dangers,
- 2606 Philos. Trans. R. Soc. Math. Phys. Eng. Sci., 369(1943), 2058–2072, 2011.
- Dong, B., Xi, Y., Cui, Y., and Peng, S.: Quantifying Methane Emissions from Aquaculture Ponds in China, Environ. Sci.
- 2608 Technol., 57, 1576–1583, https://doi.org/10.1021/acs.est.2c05218, 2023.
- Downing, J.: Emerging global role of small lakes and ponds: Little things mean a lot. Limnetica, 29: p. 9-24, 2010
- Drinkwater, A., Palmer, P. I., Feng, L., Arnold, T., Lan, X., Michel, S. E., Parker, R., and Boesch, H.: Atmospheric data
- support a multi-decadal shift in the global methane budget towards natural tropical emissions, Atmos. Chem. Phys.,
- 2612 23, 8429–8452, https://doi.org/10.5194/acp-23-8429-2023, 2023.
- Dubos, T., Dubey, S., Tort, M., Mittal, R., Meurdesoif, Y. and Hourdin, F.: DYNAMICO-1.0, an icosahedral hydrostatic
- dynamical core designed for consistency and versatility, Geosci. Model Dev., 8(10), 3131–3150, doi:10.5194/gmd-8-
- 2615 3131-2015, 2015.
- Dueck, T. A., de Visser, R., Poorter, H., Persijn, S., A. Gorissen, A., W. de Visser, W., Schapendonk, A., Verhagen, J.,
- Snel, J., Harren, F. J. M., Ngai, A. K. Y., Verstappen, F., Bouwmeester, H., Voesenek, L. A. C. J. and van der Werf,
- A.: No evidence for substantial aerobic methane emission by terrestrial plants: a ¹³C-labelling approach, New Phytol.,
- 2619 doi:10.1111/j.1469-8137.2007.02103.x, 2007.

Dutaur, L. and Verchot, L. V.: A global inventory of the soil CH₄ sink, Glob. Biogeochem Cycles, 21, GB4012,

- 2621 doi:10.1029/2006GB002734, 2007.
- 2622 EDGAR (Emissions Database for Global Atmospheric Research) Community GHG Database, a collaboration between the
- European Commission, Joint Research Centre (JRC), the International Energy Agency (IEA), and comprising IEA-
- EDGAR CO2, EDGAR CH4, EDGAR N2O, EDGAR F-GASES version 8.0, European Commission, JRC (Datasets),
- 2625 available at https://edgar.jrc.ec.europa.eu/dataset_ghg80, 2023
- Eggleton, P., Homathevi, R., Jones, D., MacDonald, J., Jeeva, D., Bignell, D., Davies, R., and Maryati, M.: Termite
- assemblages, forest disturbance and greenhouse gas fluxes in Sabah, East Malaysia, Philos. T. Roy. Soc. B, 354, 1791–
- 2628 1802, doi: 10.1098/rstb.1999.0521, 1999
- Ehhalt, D., Prather, M., Dentener, F., Derwent, R., Dlugokencky, E., Holland, E., Isaksen, I., Katima, J., Kirchhoff, V.,
- 2630 Matson, P., Midgley, P. and Wang, M.: Atmospheric chemistry and greenhouse gases. In: Climate Change 2001: The





- 2631 Scientific Basis. Contribution of Working Group I to the Third Assessment Report of the Intergovernmental Panel on
- 2632 Climate Change. [Houghton, J.T., et al. (eds.)]. Cambridge University Press, Cambridge, United Kingdom and New
- 2633 York, NY, USA, pp. 239-287, 2001.
- 2634 Ehhalt, D. H.: The atmospheric cycle of methane, Tellus, 26(1–2), 58–70, doi:10.1111/j.2153-3490.1974.tb01952.x, 1974.
- Ehret, G., Bousquet, P., Pierangelo, C., Alpers, M., Millet, B., Abshire, J. B., Bovensmann, H., Burrows, J. P., Chevallier,
- 2636 F., Ciais, P., Crevoisier, C., Fix, A., Flamant, P., Frankenberg, C., Gibert, F., Heim, B., Heimann, M., Houweling, S.,
- Hubberten, H. W., Jockel, P., Law, K., Low, A., Marshall, J., Agusti-Panareda, A., Payan, S., Prigent, C., Rairoux, P.,
- Sachs, T., Scholze, M. and Wirth, M.: MERLIN: A French-German Space Lidar Mission Dedicated to Atmospheric
- 2639 Methane, Remote Sens., 9(10), 2017.
- 2640 Etiope, G.: Natural Gas Seepage. The Earth's Hydrocarbon Degassing, Springer International Publishing., 2015.
- Etiope G.: Natural emissions of methane from geological seepage in Europe. Atmosph. Environment, 43, 1430-1443,
- 2642 doi:10.1016/j.atmosenv.2008.03.014., 2009
- Etiope, G. and Schwietzke, S.: Global geological methane emissions: an update of top-down and bottom-up estimates,
- 2644 Elem Sci Anth, 7(1), 47, doi:10.1525/elementa.383, 2019.
- Etiope, G., Lassey, K. R., Klusman, R. W. and Boschi, E.: Reappraisal of the fossil methane budget and related emission
- from geologic sources, Geophys. Res. Lett., 35(9), L09307, doi:10.1029/2008gl033623, 2008.
- 2647 Etiope, G., Nakada, R., Tanaka, K. and Yoshida, N.: Gas seepage from Tokamachi mud volcanoes, onshore Niigata
- Basin (Japan): origin, post-genetic alterations and CH₄-CO₂ fluxes. App. Geochem., 26, 348-359, 2011.
- Etiope, G., Ciotoli, G., Schwietzke, S. and Schoell, M.: Gridded maps of geological methane emissions and their isotopic
- 2650 signature, Earth Syst Sci Data, 11(1), 1–22, doi:10.5194/essd-11-1-2019, 2019.
- EU-Landfill-Directive: https://eur-lex.europa.eu/legal-content/EN/TXT/?uri=CELEX:31999L0031, 1999.
- 2652 FAO: FAOSTAT Emissions Land Use database. Food and Agriculture Organization of the United Nations. Statistical
- Division., [online] Available from: http://www.fao.org/faostat/en/#data/GL (Accessed December 2022), 2022.
- Federici, S., Tubiello, F. N., Salvatore, M., Jacobs, H. and Schmidhuber, J.: New estimates of CO2 forest emissions and
- 2655 removals: 1990–2015, For. Ecol. Manag., 352, 89–98, doi:10.1016/j.foreco.2015.04.022, 2015.
- Feng, L., Braun, C., Arnold, S. R. and Gidden, M.: iiasa/emissions_downscaling: Supplemental Data,
- 2657 doi:10.5281/zenodo.2538194, 2019.
- Feng, L., Palmer, P. I., Parker, R. J., Lunt, M. F., and Bösch, H.: Methane emissions are predominantly responsible for
- record-breaking atmospheric methane growth rates in 2020 and 2021, Atmos. Chem. Phys., 23, 4863–4880,
- 2660 https://doi.org/10.5194/acp-23-4863-2023, 2023.
- Filges, A., Gerbig, C., Chen, H., Franke, H., Klaus, C., and Jordan, A.: The IAGOS-core greenhouse gas package: a
- measurement system for continuous airborne observations of CO2, CH4, H2O and CO, Tellus B, 68, 27989,
- 2663 https://doi.org/10.3402/tellusb.v67.27989, 2015.





- Fleischer, P., Orsi, T. H., Richardson, M. D., and Anderson, A. L. (2001). Distribution of free gas in marine sediments: a global overview. Geo-Marine Lett., 21, 103–122, 2001.
- Flores, E., Rhoderick, G. C., Viallon, J., Moussay, P., Choteau, T., Gameson, L., Guenther, F. R. and Wielgosz, R. I.:
 Methane standards made in whole and synthetic air compared by cavity ring down spectroscopy and gas
 chromatography with flame ionization detection for atmospheric monitoring applications, Anal. Chem., 87(6), 3272–
- 2669 3279, doi:10.1021/ac5043076, 2015.
- Fluet-Chouinard, E, Stocker, BD, Zhang, Z, Malhotra, A, Melton, JR, Poulter, B, Kaplan, JO, Goldewijk, KK, Siebert, S,
- 2671 Minayeva, T, Hugelius, G, Joosten, H, Barthelmes, A, Prigent, C, Aires, F, Hoyt, AM, Davidson, N, Finlayson, CM,
- Lehner, B, Jackson, RB, McIntyre, PB: Extensive global wetland loss over the past three centuries, Nature, 614(7947)
- 2673 281-286, doi:10.1038/s41586-022-05572-6, 2023
- Forster, P., T. Storelvmo, K. Armour, W. Collins, J.-L. Dufresne, D. Frame, D.J. Lunt, T. Mauritsen, M.D. Palmer, M.
- Watanabe, M. Wild, and H. Zhang: The Earth's Energy Budget, Climate Feedbacks, and Climate Sensitivity. In
- 2676 Climate Change 2021: The Physical Science Basis. Contribution of Working Group I to the Sixth Assessment Report
- of the Intergovernmental Panel on Climate Change [Masson-Delmotte, V., P. Zhai, A. Pirani, S.L. Connors, C. Péan,
- S. Berger, N. Caud, Y. Chen, L. Goldfarb, M.I. Gomis, M. Huang, K. Leitzell, E. Lonnoy, J.B.R. Matthews, T.K.
- Maycock, T. Waterfield, O. Yelekçi, R. Yu, and B. Zhou (eds.)]. Cambridge University Press, Cambridge, United
- 2680 Kingdom and New York, NY, USA, pp. 923–1054, doi: 10.1017/9781009157896.009, 2021
- Foschi M., Etiope G., Cartwright J.A.: Seismic evidence of extensive microbial gas migration and trapping in submarine
- 2682 marine hydrates (Rakhine Basin, Bay of Bengal). Mar. Petrol. Geol., 149, 106100,
- 2683 <u>https://doi.org/10.1016/j.marpetgeo.2023.106100.</u>, 2023
- Francey, R. J., Steele, L. P., Langenfelds, R. L. and Pak, B. C.: High precision long-term monitoring of radiatively active
- and related trace gases at surface sites and from aircraft in the southern hemisphere atmosphere, J. Atmospheric Sci.,
- 2686 56(2), 279–285, 1999.
- Frankenberg, C., Meirink, J. F., van Weele, M., Platt, U. and Wagner, T.: Assessing methane emissions from global space-
- 2688 borne observations, Science, 308(5724), 1010–1014, 2005.
- Fraser, P. J., Rasmussen, R. A., Creffield, J. W., French, J. R. and Khalil, M. A. K.: Termites and global methane Another
- 2690 assessment, J. Atmospheric Chem., 4, 295–310, 1986.
- Fraser, W. T., Blei, E., Fry, S. C., Newman, M. F., Reay, D. S., Smith, K. A. and McLeod, A. R.: Emission of methane,
- 2692 carbon monoxide, carbon dioxide and short-chain hydrocarbons from vegetation foliage under ultraviolet irradiation,
- 2693 Plant Cell Environ., 38(5), 980–989, doi:10.1111/pce.12489, 2015.
- 2694 Fujita, R., Morimoto, S., Maksyutov, S., Kim, H.-S., Arshinov, M., Brailsford, G., Aoki, S. and Nakazawa, T.: Global and
- Regional CH4 Emissions for 1995–2013 Derived From Atmospheric CH4, δ13C-CH4, and δD-CH4 Observations and
- 2696 a 715 Chemical Transport Model. J. Geophys. Res. Atmos., 125: e2020JD032903.





- 2697 https://doi.org/10.1029/2020JD032903, 2020
- Gauci, V., Figueiredo, V., Gedney, N., Pangala, S. R., Stauffer, T., Weedon, G., P. and Enrich-Prast A. Non-flooded riparian Amazon trees are a regionally significant methane source. *Phil. Trans. R. Soc. A*.3802020044620200446
- 2700 http://doi.org/10.1098/rsta.2020.0446, 2021.
- Gedney, N., Huntinford, C., Comyn Platt, E. and Wiltshire, A. Significant feedbacks of wetland methane release on climate change and the causes of their uncertainty. Env. Res. Letts. 14, 084027 doi:10.1088/1748-9326/ab2726, 2019.
- Gidden, M. J., Riahi, K., Smith, S. J., Fujimori, S., Luderer, G., Kriegler, E., Vuuren, D. P. van, Berg, M. van den, Feng, L., Klein, D., Calvin, K., Doelman, J. C., Frank, S., Fricko, O., Harmsen, M., Hasegawa, T., Havlik, P., Hilaire, J.,
- Hoesly, R., Horing, J., Popp, A., Stehfest, E. and Takahashi, K.: Global emissions pathways under different
- socioeconomic scenarios for use in CMIP6: a dataset of harmonized emissions trajectories through the end of the century, Geosci. Model Dev., 12(4), 1443–1475, doi:10.5194/gmd-12-1443-2019, 2019.
- Giglio, L., Randerson, J. T. and van der Werf, G. R.: Analysis of daily, monthly, and annual burned area using the fourth-
- generation global fire emissions database (GFED4), J. Geophys. Res. Biogeosciences, 118(1), 317–328, doi:10.1002/jgrg.20042, 2013.
- Glagolev, M., Kleptsova, I., Filippov, I., Maksyutov, S. and Machida, T.: Regional methane emission from West Siberia mire landscapes, Environ. Res. Lett., 6(4), 045214, doi:doi:10.1088/1748-9326/6/4/045214, 2011.
- Glatthor, N., von Clarmann, T., Funke, B., Garcia-Comas, M., Grabowski, U., Höpfner, M., Kellmann, S., Kiefer, M., Laeng, A., Linden, A., Lopez-Puertas, M., and Stiller, G. P.: IMK/IAA MIPAS retrievals version 8: CH4 and N2O,
- 2715 EGUsphere [preprint], https://doi.org/10.5194/egusphere-2023-919, 2023.
- Global Methane Pledge, Global Methane Pledge website: Pledges, 1 September. https://www. globalmethanepledge.org/#pledges. Accessed 28 September 2023, 2023.
- Griffiths, K., A. Jeziorski, D. Antoniades, M. Beaulieu, J.P. Smol, and I. Gregory-Eaves, Pervasive changes in algal indicators since pre-industrial times: A paleolimnological study of changes in primary production and diatom assemblages from ~200 Canadian lakes. Science of The Total Environment, 838: p. 155938., 2022.
- Grinham, A., M. Dunbabin, D. Gale, and J. Udy, Quantification of ebullitive and diffusive methane release to atmosphere from a water storage. Atmospheric Environment, 45(39): p. 7166-7173., 2011.
- Gromov, S., Brenninkmeijer, C. A. M. and Jöckel, P.: A very limited role of tropospheric chlorine as a sink of the greenhouse gas methane, Atmospheric Chem. Phys., 18(13), 9831–9843, doi:10.5194/acp-18-9831-2018, 2018.
- Guo, M., Fang, S., Liu, S., Liang, M., Wu, H., Yang, L., Li, Z., Liu, P., Zhang, F: Comparison of atmospheric CO2, CH4, and CO at two stations in the Tibetan Plateau of China, *Earth Space Sci.* 7, e2019EA001051, 2020
- Gurney, K. R., Law, R. M., Denning, A. S., Rayner, P. J., Pak, B. C., Baker, D., Bousquet, P., Bruhwiler, L., Chen, Y. H.,
- Ciais, P., Fung, I. Y., Heimann, M., John, J., Maki, T., Maksyutov, S., Peylin, P., Prather, M. and Taguchi, S.: Transcom
- 3 inversion intercomparison: Model mean results for the estimation of seasonal carbon sources and sinks, Glob.





- 2730 Biogeochem. Cycles, 18(1), GB2010, doi:10.1029/2003gb002111, 2004.
- Harris, S. A., French, H. M., Heginbottom, J. A., Johnston, G. H., Ladanyi, B., Sego, D. C. and van Everdingen, R. O.:
- 2732 Glossary of permafrost and related ground-ice terms, National Research Council of Canada. Associate Committee on
- Geotechnical Research. Permafrost Subcommittee., 1988.
- Harris, I., Jones, P.D., Osborn, T.J. and Lister, D.H.: Updated high-resolution grids of monthly climatic observations the
- 2735 CRU TS3.10 Dataset, Int. J. Climatol., 34: 623-642. https://doi.org/10.1002/joc.3711, 2014
- Harrison, J.A., Y.T. Prairie, S. Mercier-Blais, and C. Soued: Year-2020 Global Distribution and Pathways of Reservoir
- 2737 Methane and Carbon Dioxide Emissions According to the Greenhouse Gas From Reservoirs (G-res) Model. Global
- 2738 Biogeochemical Cycles 35(6): p. e2020GB006888, 2021.
- Heathcote, A. J., C. T. Filstrup, and J. A. Downing (2013): Watershed sediment losses to lakes accelerating despite
- agricultural soil conservation efforts, *PLoS One*, 8(1), e53554, doi:10.1371/journal.pone.0053554, 2013
- Heděnec, P., Jiménez, J.J., Moradi, J. et al.: Global distribution of soil fauna functional groups and their estimated litter
- 2742 consumption across biomes. Sci Rep 12, 17362, https://doi.org/10.1038/s41598-022-21563-z, 2022
- Hmiel, B., Petrenko, V. V., Dyonisius, M. N., Buizert, C., Smith, A. M., Place, P. F., Harth, C., Beaudette, R., Hua, Q.,
- Yang, B., Vimont, I., Michel, S. E., Severinghaus, J. P., Etheridge, D., Bromley, T., Schmitt, J., Faïn, X., Weiss, R. F.
- and Dlugokencky, E.: Preindustrial 14 CH 4 indicates greater anthropogenic fossil CH 4 emissions, Nature, 578(7795),
- 2746 409–412, doi:10.1038/s41586-020-1991-8, 2020.
- Ho, J.C., A.M. Michalak, and N. Pahlevan: Widespread global increase in intense lake phytoplankton blooms since the
- 2748 1980s. Nature, 574(7780): p. 667-670, 2019
- Hoesly, R. M., Smith, S. J., Feng, L., Klimont, Z., Janssens-Maenhout, G., Pitkanen, T., Seibert, J. J., Vu, L., Andres, R.
- 2750 J., Bolt, R. M., Bond, T. C., Dawidowski, L., Kholod, N., Kurokawa, J. I., Li, M., Liu, L., Lu, Z., Moura, M. C. P.,
- 2751 O'Rourke, P. R. and Zhang, Q.: Historical (1750–2014) anthropogenic emissions of reactive gases and aerosols from
- the Community Emissions Data System (CEDS), Geosci Model Dev, 11(1), 369–408, doi:10.5194/gmd-11-369-2018,
- 2753 2018.
- Höglund-Isaksson, L.: Bottom-up simulations of methane and ethane emissions from global oil and gas systems 1980 to
- 2755 2012, Environ. Res. Lett., 12(2), 024007, doi:10.1088/1748-9326/aa583e, 2017.
- Höglund-Isaksson, L., Thomson, A., Kupiainen, K., Rao, S. and Janssens-Maenhout, G.: Anthropogenic methane sources,
- emissions and future projections, Chapter 5 in AMAP Assessment 2015: Methane as an Arctic Climate Forcer, p. 39-
- 2758 59, available at http://www.amap.no/documents/doc/AMAP-Assessment-2015-Methane-as-an-Arctic-climate-
- 2759 forcer/1285., 2015.
- Höglund-Isaksson, L., Gómez-Sanabria, A., Klimont, Z., Rafaj, P., Schöpp, W.,: Technical potentials and costs for
- 2761 reducing global anthropogenic methane emissions in the 2050 timeframe -results from the GAINS model, Environ.
- 2762 Res. Comm. 2(2), https://iopscience.iop.org/article/10.1088/2515-7620/ab7457, 2020





- Holgerson, M. A. and Raymond, P. A.: Large contribution to inland water CO 2 and CH 4 emissions from very small
- 2764 ponds, Nat. Geosci., 9(3), 222–226, doi:10.1038/ngeo2654, 2016.
- Holmes, C. D., Prather, M. J., Søvde, O. A. and Myhre, G.: Future methane, hydroxyl, and their uncertainties: key climate
- and emission parameters for future predictions, Atmospheric Chem. Phys., 13(1), 285–302, doi:10.5194/acp-13-285-
- 2767 2013, 2013.
- Hopcroft, P.O., P.J. Valdes & D.J. Beerling, (2011). Simulating idealised Dansgaard-Oeschger events and their potential
- influence on the global methane cycle, Quaternary Science Reviews, 30, 3258-3268,
- 2770 doi: 10.1016/j.quascirev.2011.08.01., 2011
- Hossaini, R., Chipperfield, M. P., Saiz-Lopez, A., Fernandez, R., Monks, S., Feng, W., Brauer, P. and Glasow, R. von: A
- 2772 global model of tropospheric chlorine chemistry: Organic versus inorganic sources and impact on methane oxidation,
- 2773 J. Geophys. Res. Atmospheres, 121(23), 14,271-14,297, doi:10.1002/2016JD025756, 2016.
- Houweling, S., Bergamaschi, P., Chevallier, F., Heimann, M., Kaminski, T., Krol, M., Michalak, A. M. and Patra, P.:
- Global inverse modeling of CH₄ sources and sinks: an overview of methods, Atmospheric Chem. Phys., 17(1), 235–
- 2776 256, doi:10.5194/acp-17-235-2017, 2017.
- 2777 M. Hovland, A.G. Judd, R.A. Burke: The global flux of methane from shallow submarine sediments, Chemosphere,
- 2778 Volume 26, Issues 1–4, Pages 559-578, doi:10.1016/0045-6535(93)90442-8., 1993
- Howarth, R. W.: Ideas and perspectives: is shale gas a major driver of recent increase in global atmospheric methane?,
- 2780 Biogeosciences, 16(15), 3033–3046, doi:10.5194/bg-16-3033-2019, 2019.
- Hu, H., Landgraf, J., Detmers, R., Borsdorff, T., Brugh, J. A. de, Aben, I., Butz, A. and Hasekamp, O.: Toward Global
- Mapping of Methane With TROPOMI: First Results and Intersatellite Comparison to GOSAT, Geophys. Res. Lett.,
- 2783 45(8), 3682–3689, doi:10.1002/2018GL077259, 2018.
- Hugelius, G., Tarnocai, C., Broll, G., Canadell, J. G., Kuhry, P., & Swanson, D. K.. The Northern Circumpolar Soil Carbon
- Database: spatially distributed datasets of soil coverage and soil carbon storage in the northern permafrost regions.
- 2786 Earth System Science Data, 5(1), 3–13. https://doi.org/10.5194/essd-5-3-2013, 2013
- Hugelius, G., Strauss, J., Zubrzycki, S., Harden, J. W., Schuur, E. A. G., Ping, C. L., Schirrmeister, L., Grosse, G.,
- Michaelson, G. J., Koven, C. D., O'Donnell, J. A., Elberling, B., Mishra, U., Camill, P., Yu, Z., Palmtag, J. and Kuhry,
- 2789 P.: Estimated stocks of circumpolar permafrost carbon with quantified uncertainty ranges and identified data gaps,
- 2790 Biogeosciences, 11(23), 6573–6593, doi:10.5194/bg-11-6573-2014, 2014.
- Hugelius, Gustaf, Loisel, J., Chadburn, S., Jackson, R. B., Jones, M., MacDonald, G., et al.: Large stocks of peatland
- carbon and nitrogen are vulnerable to permafrost thaw. Proceedings of the National Academy of Sciences, 117(34),
- 2793 20438–20446. https://doi.org/10.1073/pnas.1916387117, 2020
- Hugelius, G., Ramage, J.L., Burke, E.J., Chatterjee, A., Smallman, T.L., Aalto, T., Bastos, A., Biasi, C., Canadell, J.G.,
- 2795 Chandra, N. and Chevallier, F., et al. Two decades of permafrost region CO2, CH4, and N2O budgets suggest a small





- net greenhouse gas source to the atmosphere. Preprint in ESS Open Archive. September 11, 2023. DOI:
- 2797 10.22541/essoar.169444320.01914726/v1, 2023
- 2798 IEA, Coal Information: Overview, IEA, Paris https://www.iea.org/reports/coal-information-overview, License: CC BY
- 2799 4.0, Accessed 17 January 2024, 2021
- 2800 IEA (2023), Energy Statistics Data Browser, IEA, Paris https://www.iea.org/data-and-statistics/data-tools/energy-
- 2801 <u>statistics-data-browser</u>, Accessed 17 January 2024, 2023a
- 2802 IEA, US natural gas production by source, 2013-2023, IEA, Paris https://www.iea.org/data-and-statistics/charts/us-
- 2803 natural-gas-production-by-source-2013-2023, IEA. Licence: CC BY 4.0, Accessed 17 January 2024, 2023b
- Imasu, R.; Matsunaga, T.; Nakajima, M.; Yoshida, Y.; Shiomi, K.; Morino, I.; Saitoh, N.; Niwa, Y.; Someya, Y.; Oishi,
- 2805 Y.; et al. Greenhouse Gases Observing SATellite 2 (GOSAT-2): Mission Overview. Prog. Earth Planet. Sci., 10, 33.,
- 2806 2023,
- Inoue, M., Morino, I., Uchino, O., Nakatsuru, T., Yoshida, Y., Yokota, T., Wunch, D., Wennberg, P. O., Roehl, C. M.,
- 2808 Griffith, D. W. T., Velazco, V. A., Deutscher, N. M., Warneke, T., Notholt, J., Robinson, J., Sherlock, V., Hase, F.,
- Blumenstock, T., Rettinger, M., Sussmann, R., Kyrö, E., Kivi, R., Shiomi, K., Kawakami, S., Mazière, M. D., Arnold,
- S. G., Feist, D. G., Barrow, E. A., Barney, J., Dubey, M., Schneider, M., Iraci, L. T., Podolske, J. R., Hillyard, P. W.,
- Machida, T., Sawa, Y., Tsuboi, K., Matsueda, H., Sweeney, C., Tans, P. P., Andrews, A. E., Biraud, S. C., Fukuyama,
- 2812 Y., Pittman, J. V., Kort, E. A. and Tanaka, T.: Bias corrections of GOSAT SWIR XCO2 and XCH4 with TCCON data
- and their evaluation using aircraft measurement data, Atmospheric Meas. Tech., 9(8), 3491–3512, doi:10.5194/amt-9-
- 2814 3491-2016, 2016.
- 2815 IPCC: Good Practice Guidance and Uncertainty Management in National Greenhouse Gas Inventories. Intergovernmental
- 2816 Panel on Climate Change, National Greenhouse Gas Inventories Programme. Montreal, IPCC-
- 2817 XVI/Doc.10(1.IV.2000), May 2000., 2000.
- 2818 IPCC: Climate change 2001: The scientific basis. Contribution of working group I to the third assessment report of the
- 2819 Intergovernmental Panel on Climate Change, Cambridge University Press, Cambridge, United Kingdom and New
- 2820 York, NY, USA., 2001.
- 2821 IPCC: IPCC Guidelines for National Greenhouse Gas Inventories. The National Greenhouse Gas Inventories Programme,
- Eggleston H.S., Buendia L., Miwa K., Ngara T. and Tanabe K. (eds). The Intergovernmental Panel on Climate Change,
- 2823 IPCC TSU NGGIP, IGES. Institute for Global Environmental Strategy, Hayama, Kanagawa, Japan. Available online
- at: http://www.ipcc-nggip.iges.or.jp/support/Primer 2006GLs.pdf., 2006.
- 2825 IPCC: 2019 Refinement to the 2006 IPCC Guidelines for National Greenhouse Gas Inventories IPCC. [online]
- Available from: https://www.ipcc.ch/report/2019-refinement-to-the-2006-ipcc-guidelines-for-national-greenhouse-
- 2827 gas-inventories/ (Accessed 17 March 2020), 2019.
- 2828 Ito, A. and Inatomi, M.: Use of a process-based model for assessing the methane budgets of global terrestrial ecosystems





- and evaluation of uncertainty, Biogeosciences, 9(2), 759–773, doi:10.5194/bg-9-759-2012, 2012.
- Jacob, D. J., Varon, D. J., Cusworth, D. H., Dennison, P. E., Frankenberg, C., Gautam, R., Guanter, L., Kelley, J.,
- McKeever, J., Ott, L. E., Poulter, B., Qu, Z., Thorpe, A. K., Worden, J. R., and Duren, R. M.: Quantifying methane
- emissions from the global scale down to point sources using satellite observations of atmospheric methane, Atmos.
- 2833 Chem. Phys., 22, 9617–9646, https://doi.org/10.5194/acp-22-9617-2022, 2022.
- Jackson, R. B., Down, A., Phillips, N. G., Ackley, R. C., Cook, C. W., Plata, D. L. and Zhao, K.: Natural gas pipeline
- leaks across Washington, D.C, Environ. Sci. Technol., 48(3), 2051–2058, doi:10.1021/es404474x, 2014a.
- Jackson, R. B., Vengosh, A., Carey, J. W., Davies, R. J., Darrah, T. H., O'Sullivan, F. and Pétron, G.: The Environmental
- Costs and Benefits of Fracking, Annu. Rev. Environ. Resour., 39, 327–362, doi:10.1146/annurev-environ-031113-
- 2838 144051, 2014b.
- Jackson, R. B., Saunois, M., Bousquet, P., Canadell, J. G., Poulter, B., Stavert, A. R., Poulter, B., Bergamaschi, P., Niwa,
- Y., Segers, A., Tsuruta, A.: Increasing anthropogenic methane emissions arise equally from agricultural and fossil fuel
- 2841 sources, Environmental Research Letters, 15, 7, https://doi.org/10.1088/1748-9326/ab9ed2, 2020
- Jamali, H., Livesley, S.J., Dawes, T.Z. et al. Termite mound emissions of CH₄ and CO₂ are primarily determined by
- seasonal changes in termite biomass and behaviour. *Oecologia* 167, 525–534, doi.org/10.1007/s00442-011-1991-3,
- 2844 2011
- Janssens-Maenhout, G., Crippa, M., Guizzardi, D., Muntean, M., Schaaf, E., Dentener, F., Bergamaschi, P., Pagliari, V.,
- Olivier, J., Peters, J., van Aardenne, J., Monni, S., Doering, U., Petrescu, R., Solazzo, E. and Oreggioni, G.: EDGAR
- v4.3.2 Global Atlas of the three major Greenhouse Gas Emissions for the period 1970-2012, Earth Syst Sci Data
- 2848 Discuss, 2019, 1–52, doi:10.5194/essd-2018-164, 2019.
- JAXA: GOSAT-2: Greenhouse gases Observing SATellite-2@ibuki2_JAXA"IBUKI-2", [online] Available from:
- https://global.jaxa.jp/projects/sat/gosat2/index.html (Accessed 25 March 2020), 2019.
- 2851 Jensen, K. and Mcdonald, K.: Surface Water Microwave Product Series Version 3: A Near-Real Time and 25-Year
- 2852 Historical Global Inundated Area Fraction Time Series From Active and Passive Microwave Remote Sensing, IEEE
- 2853 Geosci. Remote Sens. Lett., 16(9), 1402–1406, doi:10.1109/LGRS.2019.2898779, 2019.
- Jiang, Y., Groenigen, K. J. van, Huang, S., Hungate, B. A., Kessel, C. van, Hu, S., Zhang, J., Wu, L., Yan, X., Wang, L.,
- 2855 Chen, J., Hang, X., Zhang, Y., Horwath, W. R., Ye, R., Linquist, B. A., Song, Z., Zheng, C., Deng, A. and Zhang, W.:
- Higher yields and lower methane emissions with new rice cultivars, Glob. Change Biol., 23(11), 4728–4738,
- 2857 doi:10.1111/gcb.13737, 2017.
- Johnson, D. E., Phetteplace, H. W. and Seidl, A. F.: Methane, nitrous oxide and carbon dioxide emissions from ruminant
- livestock production systems, edited by J. Takahashi and B. A. Young, pp. 77-85, Elsevier, Amsterdam, The
- Netherlands., 2002.
- Johnson, M.S., E. Matthews, J. Du, V. Genovese, and D. Bastviken, Methane Emission From Global Lakes: New





- Spatiotemporal Data and Observation-Driven Modeling of Methane Dynamics Indicates Lower Emissions, Journal of Geophysical Research: Biogeosciences, 127(7): p. e2022JG006793, 2022
- Johnson, M. S., E. Matthews, D. Bastviken, B. Deemer, J. Du, and V. Genovese, Spatiotemporal methane emission from
- global reservoirs, Journal of Geophysical Research: Biogeosciences, 126, e2021JG006305, https://doi.org/10.1029/2021JG006305, 2021
- 2800 <u>Int.ps.//doi.org/10.1029/20213/0000303</u>, 2021
- Judd, A.G. (2004). Natural seabed seeps as sources of atmospheric methane, Environ. Geol., 46, 988–996, 2004.
- Jung, M., Reichstein, M., Margolis, H. A., Cescatti, A., Richardson, A. D., Arain, M. A., Arneth, A., Bernhofer, C., Bonal,
- D., Chen, J., Gianelle, D., Gobron, N., Kiely, G., Kutsch, W., Lasslop, G., Law, B. E., Lindroth, A., Merbold, L.,
- Montagnani, L., Moors, E. J., Papale, D., Sottocornola, M., Vaccari, F., and Williams, C.: Global patterns of land-
- atmosphere fluxes of carbon dioxide, latent heat, and sensible heat derived from eddy covariance, satellite, and
- 2872 meteorological observations, J. Geophys. Res., 116, G00J07,https://doi.org/10.1029/2010jg001566, 2011.
- Kai, F. M., Tyler, S. C., Randerson, J. T. and Blake, D. R.: Reduced methane growth rate explained by decreased Northern
- 2874 Hemisphere microbial sources, Nature, 476(7359), 194–197, 2011.
- Kaiser, J. W., Heil, A., Andreae, M. O., Benedetti, A., Chubarova, N., Jones, L., Morcrette, J. J., Razinger, M., Schultz,
- 2876 M. G., Suttie, M. and van der Werf, G. R.: Biomass burning emissions estimated with a global fire assimilation system
- based on observed fire radiative power, Biogeosciences, 9(1), 527–554, doi:10.5194/bg-9-527-2012, 2012.
- Kallingal, J. T., Lindström, J., Miller, P. A., Rinne, J., Raivonen, M., and Scholze, M.: Optimising CH₄ simulations from
- the LPJ-GUESS model v4.1 using an adaptive MCMC algorithm, Geosci. Model Dev. Discuss. [preprint],
- 2880 https://doi.org/10.5194/gmd-2022-302, in review, 2023.
- Karion, A., Sweeney, C., Pétron, G., Frost, G., Michael Hardesty, R., Kofler, J., Miller, B. R., Newberger, T., Wolter, S.,
- Banta, R., Brewer, A., Dlugokencky, E., Lang, P., Montzka, S. A., Schnell, R., Tans, P., Trainer, M., Zamora, R. and
- 2883 Conley, S.: Methane emissions estimate from airborne measurements over a western United States natural gas field,
- 2884 Geophys. Res. Lett., 40(16), 4393–4397, doi:10.1002/grl.50811, 2013.
- Karl, D., Beversdorf, L., Björkman, K. et al. Aerobic production of methane in the sea. Nature Geosci 1, 473-478,
- 2886 <u>https://doi.org/10.1038/ngeo234</u>), 2008
- 2887 Karlson, M., and Bastviken, D.: Multi-Source Mapping of Peatland Types Using Sentinel-1, Sentinel-2, and Terrain
- Derivatives—A Comparison Between Five High-Latitude Landscapes. Journal of Geophysical Research:
- 2889 Biogeosciences 128, e2022JG007195. https://doi.org/10.1029/2022JG007195, 2023
- Keppler, F., Hamilton, J. T. G., Brass, M. and Rockmann, T.: Methane emissions from terrestrial plants under aerobic
- 2891 conditions, Nature, 439, 187–191, doi:10.1038/nature04420, 2006.
- 2892 Kholod, N., Evans, M., Pilcher, R. C., Roshchanka, V., Ruiz, F., Coté, M. and Collings, R.: Global methane emissions
- from coal mining to continue growing even with declining coal production, J. Clean. Prod., 256, 120489,
- 2894 doi:10.1016/j.jclepro.2020.120489, 2020.





- Kim H., Global Soil Wetness Project Phase 3 Atmospheric Boundary Conditions (Experiment 1) [Data set]. Data Integration and Analysis System (DIAS)., https://doi.org/10.20783/DIAS.501, 2017
- King, J.R., Warren, R.J., Bradford, M.A. Correction: Social Insects Dominate Eastern US Temperate Hardwood Forest Macroinvertebrate Communities in Warmer Regions. PLOS ONE 8(10): 10.1371/annotation/87285c86-f1df-4f8bbc08-d64643d351f4, 2013.
- 2900 Kirk, L, and MJ Cohen: River Corridor Sources Dominate CO₂ Emissions From a Lowland River Network. Journal of 2901 Geophysical Research, Biogeosciences, 128(1), e2022JG006954, 2023.
- Kirschke, S., Bousquet, P., Ciais, P., Saunois, M., Canadell, J. G., Dlugokencky, E. J., Bergamaschi, P., Bergmann, D.,
- Blake, D. R., Bruhwiler, L., Cameron-Smith, P., Castaldi, S., Chevallier, F., Feng, L., Fraser, A., Heimann, M.,
- Hodson, E. L., Houweling, S., Josse, B., Fraser, P. J., Krummel, P. B., Lamarque, J. F., Langenfelds, R. L., Le Quere,
- 2905 C., Naik, V., O'Doherty, S., Palmer, P. I., Pison, I., Plummer, D., Poulter, B., Prinn, R. G., Rigby, M., Ringeval, B.,
- Santini, M., Schmidt, M., Shindell, D. T., Simpson, I. J., Spahni, R., Steele, L. P., Strode, S. A., Sudo, K., Szopa, S.,
- van der Werf, G. R., Voulgarakis, A., van Weele, M., Weiss, R. F., Williams, J. E. and Zeng, G.: Three decades of
- 2908 global methane sources and sinks, Nat. Geosci., 6(10), 813–823, doi:10.1038/ngeo1955, 2013.
- Klauda, J. B. and Sandler, S. I.: Global distribution of methane hydrate in ocean sediment, Energy Fuels, 19(2), 459–470, 2010 2005.
- Kleinen, T., Brovkin, V. and Schuldt, R. J.: A dynamic model of wetland extent and peat accumulation: results for the Holocene, Biogeosciences, 9(1), 235–248, doi:10.5194/bg-9-235-2012, 2012.
- Kleinen, T., Mikolajewicz, U., and Brovkin, V.: Terrestrial methane emissions from the Last Glacial Maximum to the preindustrial period, Clim. Past, 16, 575–595, doi:10.5194/cp-16-575-2020, 2020.
- Kleinen, T., Gromov, S., Steil, B., and Brovkin, V.: Atmospheric methane underestimated in future climate projections, Environ. Res. Lett., 16, 094006, doi:10.1088/1748-9326/ac1814, 2021.
- Kleinen, T., Gromov, S., Steil, B., and Brovkin, V.: Atmospheric methane since the last glacial maximum was driven by wetland sources, Clim. Past, 19, 1081–1099, doi:10.5194/cp-19-1081-2023, 2023
- Knittel K and Boetius A: Anaerobic oxidation of methane: progress with an unknown process methane. Annu Rev
 Microbiol 63:311–334, 2009
- Knox, S. H., Jackson, R. B., Poulter, B., McNicol, G., Fluet-Chouinard, E., Zhang, Z., Hugelius, G., Bousquet, P.,
- 2922 Canadell, J. G., Saunois, M., Papale, D., Chu, H., Keenan, T. F., Baldocchi, D., Torn, M. S., Mammarella, I., Trotta,
- 2923 C., Aurela, M., Bohrer, G., Campbell, D. I., Cescatti, A., Chamberlain, S., Chen, J., Chen, W., Dengel, S., Desai, A.
- 2924 R., Euskirchen, E., Friborg, T., Gasbarra, D., Goded, I., Goeckede, M., Heimann, M., Helbig, M., Hirano, T., Hollinger,
- D. Y., Iwata, H., Kang, M., Klatt, J., Krauss, K. W., Kutzbach, L., Lohila, A., Mitra, B., Morin, T. H., Nilsson, M. B.,
- Niu, S., Noormets, A., Oechel, W. C., Peichl, M., Peltola, O., Reba, M. L., Richardson, A. D., Runkle, B. R. K., Ryu,
- 2927 Y., Sachs, T., Schäfer, K. V. R., Schmid, H. P., Shurpali, N., Sonnentag, O., Tang, A. C. I., Ueyama, M., Vargas, R.,





- Vesala, T., Ward, E. J., Windham-Myers, L., Wohlfahrt, G. and Zona, D.: FLUXNET-CH4 Synthesis Activity:
- Objectives, Observations, and Future Directions, Bull. Am. Meteorol. Soc., 100(12), 2607–2632, doi:10.1175/BAMS-
- 2930 D-18-0268.1, 2019.
- Knox, S. H., Bansal, S., McNicol, G., Schafer, K., Sturtevant, C., Ueyama, M., et al.:. Identifying dominant environmental
- 2932 predictors of freshwater wetland methane fluxes across diurnal to seasonal time scales. Global Change Biology,
- 2933 27(15), 3582–3604. https://doi.org/10.1111/gcb.15661, 2021
- Kretschmer, K., Biastoch, A., Rüpke, L. and Burwicz, E.: Modeling the fate of methane hydrates under global warming,
- 2935 Glob. Biogeochem Cycles, 29(5), 610–625, doi:1002/2014GB005011, 2015.
- Kuhn, M.A., Varner, R.K., Bastviken, D., Crill, P., MacIntyre, S., Turetsky, M., Walter Anthony, K., McGuire, A.D., and
- Olefeldt, D. (2021). BAWLD-CH4: a comprehensive dataset of methane fluxes from boreal and arctic ecosystems.
- 2938 Earth Syst. Sci. Data 13, 5151-5189. 10.5194/essd-13-5151-2021.
- 2939 Kuze A, Kikuchi N, Kataoka F, Suto H, Shiomi K, Kondo Y. Detection of Methane Emission from a Local Source Using
- 2940 GOSAT Target Observations. *Remote Sensing*, 12(2):267. https://doi.org/10.3390/rs12020267, 2020
- Kyzivat, E.D., L.C. Smith, F. Garcia-Tigreros, C. Huang, C. Wang, T. Langhorst, J.V. Fayne, M.E. Harlan, Y. Ishitsuka,
- D. Feng, W. Dolan, L.H. Pitcher, K.P. Wickland, M.M. Dornblaser, R.G. Striegl, T.M. Pavelsky, D.E. Butman, and
- 2943 C.J. Gleason, The Importance of Lake Emergent Aquatic Vegetation for Estimating Arctic-Boreal Methane Emissions.
- Journal of Geophysical Research: Biogeosciences 127(6): p. e2021JG006635, 2022.
- Lamarque, J. F., Shindell, D. T., Josse, B., Young, P. J., Cionni, I., Eyring, V., Bergmann, D., Cameron-Smith, P., Collins,
- W. J., Doherty, R., Dalsoren, S., Faluvegi, G., Folberth, G., Ghan, S. J., Horowitz, L. W., Lee, Y. H., MacKenzie, I.
- A., Nagashima, T., Naik, V., Plummer, D., Righi, M., Rumbold, S. T., Schulz, M., Skeie, R. B., Stevenson, D. S.,
- 2948 Strode, S., Sudo, K., Szopa, S., Voulgarakis, A. and Zeng, G.: The Atmospheric Chemistry and Climate Model
- 2949 Intercomparison Project (ACCMIP): overview and description of models, simulations and climate diagnostics, Geosci.
- 2950 Model Dev., 6(1), 179–206, doi:10.5194/gmd-6-179-2013, 2013.
- Lamb, B. K., Edburg, S. L., Ferrara, T. W., Howard, T., Harrison, M. R., Kolb, C. E., Townsend-Small, A., Dyck, W.,
- 2952 Possolo, A. and Whetstone, J. R.: Direct Measurements Show Decreasing Methane Emissions from Natural Gas Local
- 2953 Distribution Systems in the United States, Environ. Sci. Technol., 49(8), 5161–5169, doi:10.1021/es505116p, 2015.
- 2954 Lan, X., K.W. Thoning, and E.J. Dlugokencky: Trends in globally-averaged CH4, N2O, and SF6 determined from NOAA
- 2955 Global Monitoring Laboratory measurements. Version 2024-02, https://doi.org/10.15138/P8XG-AA10, 2024
- 2956 Lange S., WFDE5 over land merged with ERA5 over the ocean (W5E5). V. 1.0. 2019. doi:10.5880/pik.2019.023, 2019
- 2957 Laruelle, G. G., Dürr, H. H., Lauerwald, R., Hartmann, J., Slomp, C. P., Goossens, N. and Regnier, P. A. G.: Global multi-
- scale segmentation of continental and coastal waters from the watersheds to the continental margins, Hydrol. Earth
- 2959 Syst. Sci., 17(5), 2029–2051, doi:10.5194/hess-17-2029-2013, 2013.





- Laruelle, G. G., Rosentreter, J. A. & Regnier P.: Extrapolation based regionalized re-evaluation of the global estuarine
- surface area. Preprint at Earth ArXiv https://doi.org/10.31223/X5X664, 2023.
- Lassey, K. R., Etheridge, D. M., Lowe, D. C., Smith, A. M. and Ferretti, D. F.: Centennial evolution of the atmospheric methane budget: what do the carbon isotopes tell us?, Atmospheric Chem. Phys., 7(8), 2119–2139, 2007a.
- Lassey, K. R., Lowe, D. C. and Smith, A. M.: The atmospheric cycling of radiomethane and the "fossil fraction" of the methane source, Atmospheric Chem. Phys., 7(8), 2141–2149, 2007b.
- Lauerwald, R., Allen, G.H., Deemer, B.R., Liu, S., Maavara, T., Raymond, P., Alcott, L., Bastviken, D., Hastie, A.,
- Holgerson, M.A., Johnson, M.S., Lehner, B., Lin, P., Marzadri, A., Ran, L., Tian, H., Yang, X., Yao, Y. and Regnier,
- P. Inland water greenhouse gas budgets for RECCAP2: 1. State-of- the-art of global scale assessments. *Global*
- 2969 Biogeochemical Cycles, 37, e2022GB007657. https://doi. org/10.1029/2022GB007657, 2023a.
- Lauerwald, R., Allen, G.H., Deemer, B.R., Liu, S., Maavara, T., Raymond, P., Alcott, L., Bastviken, D., Hastie, A.,
- Holgerson, M.A., Johnson, M.S., Lehner, B., Lin, P., Marzadri, A., Ran, L., Tian, H., Yang, X., Yao, Y. and Regnier,
- 2972 P. Inland water greenhouse gas budgets for RECCAP2: 2 Regionalization and homogenization of estimates following
- the RECCAP2 framework, Global Biogeochemical Cycles, 37, e2022GB007658. https://doi.
- 2974 org/10.1029/2022GB007658, 2023b.
- Laughner, J. L., Neu, J. L., Schimel, D., Wennberg, P. O., Barsanti, K., Bowman, K. W., Chatterjee, A., Croes, B. E.,
- Fitzmaurice, H. L., Henze, D. K., Kim, J., Kort, E. A., Liu, Z., Miyazaki, K., Turner, A. J., Anenberg, S., Avise, J.,
- 2977 Cao, H., Crisp, D., de Gouw, J., Eldering, A., Fyfe, J. C., Goldberg, D. L., Gurney, K. R., Hasheminassab, S., Hopkins,
- F., Ivey, C. E., Jones, D. B. A., Liu, J., Lovenduski, N. S., Martin, R. V., McKinley, G. A., Ott, L., Poulter, B., Ru, M.,
- Sander, S. P., Swart, N., Yung, Y. L., and Zeng, Z.-C.: Societal shifts due to COVID-19 reveal large-scale complexities
- and feedbacks between atmospheric chemistry and climate change, P. Natl. Acad. Sci. USA, 118, e2109481118,
- 2981 https://doi.org/10.1073/pnas.2109481118, 2021.
- Lauvaux, T., Giron, C., Mazzolini, M., d'Aspremont, A., Duren, R., Cusworth, D., Shindell, D., and Ciais, P.: Global
- assessment of oil and gas methane ultra-emitters, Science, 375, 557–561, https://doi.org/10.1126/science.abj4351,
- 2984 2022.
- 2985 Lelieveld, J., Crutzen, P. J. and Dentener, F. J.: Changing concentration, lifetime and climate forcing of atmospheric
- 2986 methane, Tellus Ser. B-Chem. Phys. Meteorol., 50(2), 128–150, doi:10.1034/j.1600-0889. 1998. t01-1-00002.x, 1998.
- Lelieveld, J., Lechtenbohmer, S., Assonov, S. S., Brenninkmeijer, C. A. M., Dienst, C., Fischedick, M. and Hanke, T.:
- 2988 Greenhouse gases: Low methane leakage from gas pipelines, Nature, 434(7035), 841–842, doi:10.1038/434841a, 2005.
- Lenhart, K., Klintzsch, T., Langer, G., Nehrke, G., Bunge, M., Schnell, S. and Keppler, F.: Evidence for methane
- 2990 production by the marine algae *Emiliania huxlevi*, Biogeosciences, 13(10), 3163–3174, doi:10.5194/bg-13-3163-2016,
- 2991 2016.
- Lewan, M. D.: Comment on Ideas and perspectives: is shale gas a major driver of recent increase in global atmospheric





- 2993 methane? by Robert W. Howarth (2019), Biogeosciences Discuss., 1–10, doi:10.5194/bg-2019-419, 2020.
- Li, C., Frolking, S., Xiao, X., Moore, B., Boles, S., Qiu, J., Huang, Y., Salas, W. and Sass, R.: Modeling impacts of farming
- 2995 management alternatives on CO₂, CH₄, and N₂O emissions: A case study for water management of rice agriculture of
- 2996 China, Glob. Biogeochem. Cycles, 19(3), doi:10.1029/2004gb002341, 2005.
- 2997 Li T, Huang Y, Zhang W, Song C: CH4MODwetland: A biogeophysical model for simulating methane emissions from
- 2998 natural wetlands. Ecological Modelling 221: 666–680, 2010.
- Li, Y., J. Shang, C. Zhang, W. Zhang, L. Niu, L. Wang, and H. Zhang, The role of freshwater eutrophication in greenhouse
- gas emissions: A review. Science of The Total Environment, 768: p. 144582., 2021
- Lin, X., Indira, N. K., Ramonet, M., Delmotte, M., Ciais, P., Bhatt, B. C., Reddy, M. V., Angchuk, D., Balakrishnan, S.,
- Jorphail, S., Dorjai, T., Mahey, T. T., Patnaik, S., Begum, M., Brenninkmeijer, C., Durairaj, S., Kirubagaran, R.,
- 3003 Schmidt, M., Swathi, P. S., Vinithkumar, N. V., Yver Kwok, C. and Gaur, V. K.: Long-lived atmospheric trace gases
- measurements in flask samples from three stations in India, Atmospheric Chem. Phys., 15(17), 9819–9849,
- 3005 doi:10.5194/acp-15-9819-2015, 2015.
- Lin, P., Pan, M., Beck, H. E., Yang, Y., Yamazaki, D., Frasson, R., et al.: Global reconstruction of naturalized river
- 3007 flows at 2.94 million reaches. *Water Resources Research*, 55, 6499–6516. https://doi.org/10.1029/2019WR025287,
- 3008 2019
- Liu, Z., Guan, D., Wei, W., Davis, S. J., Ciais, P., Bai, J., Peng, S., Zhang, Q., Hubacek, K., Marland, G., Andres, R. J.,
- Crawford-Brown, D., Lin, J., Zhao, H., Hong, C., Boden, T. A., Feng, K., Peters, G. P., Xi, F., Liu, J., Li, Y., Zhao,
- 3011 Y., Zeng, N. and He, K.: Reduced carbon emission estimates from fossil fuel combustion and cement production in
- 3012 China, Nature, 524(7565), 335–338, doi:10.1038/nature14677, 2015.
- 3013 Liu, G., Peng, S., Lin, X., Ciais, P., Li, X., Xi, Y., Lu, Z., Chang, J., Saunois, M., Wu, Y., Patra, P., Chandra, N., Zeng,
- 3014 H., and Piao, S.: Recent Slowdown of Anthropogenic Methane Emissions in China Driven by Stabilized Coal
- 3015 Production, Environ. Sci. Technol. Lett., 8, 739–746, https://doi.org/10.1021/acs.estlett.1c00463, 2021a.
- Liu, S., Fang, S., Liu, P., Liang, M., Guo, M., and Feng, Z.: Measurement report: Changing characteristics of atmospheric
- 3017 CH4 in the Tibetan Plateau: records from 1994 to 2019 at the Mount Waliguan station, Atmos. Chem. Phys., 21, 393–
- 3018 413, https://doi.org/10.5194/acp-21-393-2021, 2021b
- 3019 Liu, S., C. Kuhn, G. Amatulli, K. Aho, D.E. Butman, G.H. Allen, P. Lin, M. Pan, D. Yamazaki, C. Brinkerhoff, C. Gleason,
- 3020 X. Xia, and P.A. Raymond: The importance of hydrology in routing terrestrial carbon to the atmosphere via global
- streams and rivers. Proceedings of the National Academy of Sciences, 119(11): p. e2106322119, 2022.
- Lloret, Z., Chevallier, F., Cozic, A., Remaud, M., and Meurdesoif, Y.: Simulating the variations of carbon dioxide in the
- 3023 global atmosphere on the hexagonal grid of DYNAMICO coupled with the LMDZ6 model, Geosci. Model Dev.
- 3024 Discuss. [preprint], https://doi.org/10.5194/gmd-2023-140, in review, 2023.
- Locatelli, R., Bousquet, P., Saunois, M., Chevallier, F. and Cressot, C.: Sensitivity of the recent methane budget to LMDz





- 3026 sub-grid-scale physical parameterizations, Atmospheric Chem. Phys., 15(17), 9765–9780, doi:10.5194/acp-15-9765-3027 2015, 2015.
- Lohila, A., Aalto, T., Aurela, M., Hatakka, J., Tuovinen, J.-P., Kilkki, J., Penttilä, T., Vuorenmaa, J., Hänninen, P., Sutinen,
- R., Viisanen, Y. and Laurila, T.: Large contribution of boreal upland forest soils to a catchment-scale CH₄ balance in
- 3030 a wet year, Geophys. Res. Lett., 43(6), 2946–2953, doi:10.1002/2016gl067718, 2016.
- Lorente, A., Borsdorff, T., Martinez-Velarte, M. C., and Landgraf, J.: Accounting for surface reflectance spectral features
- in TROPOMI methane retrievals, Atmos. Meas. Tech., 16, 1597–1608, https://doi.org/10.5194/amt-16-1597-2023,
- 3033 2023.
- Lu, X., Jacob, D. J., Zhang, Y., Maasakkers, J. D., Sulprizio, M. P., Shen, L., Qu, Z., Scarpelli, T. R., Nesser, H., Yantosca,
- R. M., Sheng, J., Andrews, A., Parker, R. J., Boesch, H., Bloom, A. A., and Ma, S.: Global methane budget and trend,
- 3036 2010-2017: complementarity of inverse analyses using in situ (GLOBALVIEWplus CH4 ObsPack) and satellite
- 3037 (GOSAT) observations, Atmos. Chem. Phys., 21, 4637–4657, https://doi.org/10.5194/acp-21-4637-2021, 2021
- Lu, X., Jacob, D. J., Zhang, Y., Maasakkers, J. D., Zhang, Y., Qu, Z., Chen, Z., Sulprizio, M. P., Varon, D., Hmiel, H.,
- Park, R. J., Boesch, H., and Fan, S.: Observation-derived 2010–2019 trends in methane emissions and intensities from
- 3040 US oil and gas fields tied to activity metrics, P. Natl. Acad. Sci. USA, 120, e2217900120,
- 3041 https://doi.org/10.1073/pnas.2217900120, 2023.
- Maasakkers, J. D., Jacob, D. J., Sulprizio, M. P., Scarpelli, T. R., Nesser, H., Sheng, J.-X., Zhang, Y., Hersher, M., Bloom,
- A. A., Bowman, K. W., Worden, J. R., Janssens-Maenhout, G., and Parker, R. J.: Global distribution of methane
- 3044 emissions, emission trends, and OH concentrations and trends inferred from an inversion of GOSAT satellite data for
- 3045 2010–2015, Atmos. Chem. Phys., 19, 7859–7881, https://doi.org/10.5194/acp-19-7859-2019, 2019.
- Massakkers, J. D., Jacob, D. J., Sulprizio, M. P., Scarpelli, T. R., Nesser, H., Sheng, J., Zhang, Y., Lu, X., Bloom, A. A.,
- Bowman, K. W., Worden, J. R., and Parker, R. J.: 2010–2015 North American methane emissions, sectoral
- 3048 contributions, and trends: a high-resolution inversion of GOSAT observations of atmospheric methane, Atmos. Chem.
- 3049 Phys., 21, 4339–4356, https://doi.org/10.5194/acp-21-4339-2021, 2021.
- Maavara, T., Lauerwald, R., Regnier, P. and Van Capellen P.: Global perturbation of organic carbon cycling by river
- damming, Nat Commun 8, 153, https://doi.org/10.1038/ncomms15347, 2017.
- Machida, T., H. Matsueda, Y. Sawa, Y. Nakagawa, K. Hirotani, N. Kondo, K. Goto, N. Nakazawa, K. Ishikawa and T.
- 3053 Ogawa: Worldwide measurements of atmospheric CO2 and other trace gas species using commercial airlines, J. Atmos.
- 3054 Oceanic Technol., 25(10), 1744-1754, doi:10.1175/2008JTECHA1082.1, 2008
- Maksyutov, S., Oda, T., Saito, M., Janardanan, R., Belikov, D., Kaiser, J. W., Zhuravlev, R., Ganshin, A., Valsala, V. K.,
- 3056 Andrews, A., Chmura, L., Dlugokencky, E., Haszpra, L., Langenfelds, R. L., Machida, T., Nakazawa, T., Ramonet,
- 3057 M., Sweeney, C. and Worthy, D.: Technical note: A high-resolution inverse modelling technique for estimating surface
- 3058 CO₂ fluxes based on the NIES-TM – FLEXPART coupled transport model and its adjoint, Atmospheric Chem.





- 3059 Phys. Discuss., 1–33, doi:10.5194/acp-2020-251, 2020.
- Malerba, M.E., T. de Kluyver, N. Wright, L. Schuster, and P.I. Macreadie: Methane emissions from agricultural ponds are underestimated in national greenhouse gas inventories. Communications Earth & Environment, 3(1): p. 306, 2022
- Maltby, J., L. Steinle, C. R. Löscher, H. W. Bange, M. A. Fischer, M. Schmidt, and T. Treude: Microbial methanogenesis in the sulfate-reducing zone of sediments in the Eckernförde Bay, SW Baltic Sea. Biogeosciences **15**: 137–157.
- 3064 doi:10.5194/bg-15-137-2018, 2018
- Manning, F. C., Kho, L. K., Hill, T. C., Cornulier, T., and Teh, Y A: Carbon Emissions From Oil Palm Plantations on Peat Soil, Front. For. Glob. Change, Sec. Tropical Forests, Volume 2, https://doi.org/10.3389/ffgc.2019.0003, 2019
- Mannisenaho V, Tsuruta A, Backman L, Houweling S, Segers A, Krol M, Saunois M, Poulter B, Zhang Z, Lan X, et al.
- Global Atmospheric δ^{13} CH₄ and CH₄ Trends for 2000–2020 from the Atmospheric Transport Model TM5 Using CH₄
- from Carbon Tracker Europe–CH₄ Inversions. *Atmosphere*, 14(7):1121. https://doi.org/10.3390/atmos14071121, 2023
- van Marle, M. J. E., Kloster, S., Magi, B. I., Marlon, J. R., Daniau, A.-L., Field, R. D., Arneth, A., Forrest, M., Hantson,
- 3071 S., Kehrwald, N. M., Knorr, W., Lasslop, G., Li, F., Mangeon, S., Yue, C., Kaiser, J. W. and Werf, G. R. van der:
- Historic global biomass burning emissions for CMIP6 (BB4CMIP) based on merging satellite observations with
- proxies and fire models (1750–2015), Geosci. Model Dev., 10(9), 3329–3357, doi:10.5194/gmd-10-3329-2017, 2017.
- Martinez, A., Saunois, M., Poulter B., Zhen, Z., Raymond, P., Regnier, P. Canadell, J. G., Jackson, R. B., Patra, P. K.,
- Bousquet, P., Ciais, P., Dlugokencky, E.J., Lan, X., Allen, G., Bastviken, D., Beerling, D. J., Belikov, D., Blake, D.,
- Castaldi, S., Crippa, M., Deemer, B.R., Dennison, F., Etiope, G., Gedney, N., Höglund-Isaksson, L., Holgerson, M.A.,
- Hopcroft, P. O., Hugelius, G., Ito, A., Jain, A. K., Janardanan, R., Johnson, M. S., Kleinen, T., Krummel, P. B.,
- Lauerwald, R., Li, T., Liu, X., McDonald, K. C., Melton, J. R., Mühle, J., Müller, J., Murguia-Flores, F., Niwa, Y.,
- Noce, S., Pan, S., Parker, R. J., Peng, C., Ramonet, M., Riley, W. J., Rocher-Ros, G., Rosentreter, J. A., Sasakawa,
- 3080 M., Segers A., Smith, S. J., Stanley, E. H., Thanwerdas, J., Tian, H., Tsuruta, A., Tubiello, F. N., Weber, T. S., van
- der Werf, G. R., Worthy, D. E. J., Xi, Y., Yoshida Y., Zhang, W., Zheng, B., Zhu, Qing, Zhu, Qiuan, and Zhuang,
- 3082 Q.: Supplemental data of the Global Carbon Project Methane Budget 2024 v1. [Data set],
- 3083 https://doi.org/10.18160/GKQ9-2RHT, 2024
- Matthews, E. and Fung, I.: Methane emission from natural wetlands: Global distribution, area, and environmental characteristics of sources, Glob. Biogeochem. Cycles, 1(1), 61–86, doi:d10.1029/GB001i001p00061, 1987.
- 3086 Mazzini A., Etiope G. (2017). Mud volcanism: an updated review. Earth Sci. Rev., 168, 81-112. 3087 http://dx.doi.org/10.1016/j.earscirev.2017.03.001., 2017
- McCalley, C. K., Woodcroft, B. J., Hodgkins, S. B., Wehr, R. A., Kim, E.-H., Monday, R., Crill, P. M., Chanton, J. P.,
- Rich, V. I., Tyson, G. W. and Saleska, S. R.: Methane dynamics regulated by microbial community response to
- permafrost thaw, Nature, 514(7523), 478–481, doi:10.1038/nature13798, 2014.
- 3091 McCarthy, M. C., Boering, K. A., Rice, A. L., Tyler, S. C., Connell, P. and Atlas, E.: Carbon and hydrogen isotopic





- compositions of stratospheric methane: 2. Two-dimensional model results and implications for kinetic isotope effects,
- J. Geophys. Res. Atmospheres, 108(D15), doi:10.1029/2002JD003183, 2003.
- McGinnis, D. F., J. Greinert, Y. Artemov, S. E. Beaubien, and A. Wüest: Fate of rising methane bubbles in stratified
- waters: How much methane reaches the atmosphere?, J. Geophys. Res., 111, C09007, doi:10.1029/2005JC003183,
- 3096 2006
- McGuire, A. D., Christensen, T. R., Heroult, A., Miller, P. A., Hayes, D., Euskirchen, E., Kimball, J. S., Yi, Y., Koven,
- 3098 C., Lafleur, P., Oechel, W., Peylin, P. and Williams, M.: An assessment of the carbon balance of Arctic tundra, Comp.
- 3099 Obs. Process Models Atmospheric Inversions, 9(Article), 3185–3204, doi:10.5194/bg-9-3185-2012, 2012.
- McKain, K., Down, A., Raciti, S. M., Budney, J., Hutyra, L. R., Floerchinger, C., Herndon, S. C., Nehrkorn, T., Zahniser,
- 3101 M. S., Jackson, R. B., Phillips, N. and Wofsy, S. C.: Methane emissions from natural gas infrastructure and use in the
- 3102 urban region of Boston, Massachusetts, Proc. Natl. Acad. Sci., 112(7), 1941–1946, doi:10.1073/pnas.1416261112,
- 3103 2015.
- McNicol, G., Fluet-Chouinard, E., Ouyang, Z., Knox, S., Zhang, Z., Aalto, T., et al.: Upscaling wetland methane
- emissions from the FLUXNET-CH4 eddy covariance network (UpCH4 v1.0): Model development, network
- assessment, and budget comparison. AGU Advances, 4, e2023AV000956. https://doi.org/10.1029/2023AV000956,
- 3107 2023
- Meinshausen, M., Smith, S., Calvin, K., Daniel, J., Kainuma, M., Lamarque, J. F., Matsumoto, K., Montzka, S., Raper,
- 3109 S., Riahi, K., Thomson, A., Velders, G. and van Vuuren, D. P.: The RCP greenhouse gas concentrations and their
- extensions from 1765 to 2300, Clim. Change, 109(1), 213–241, doi:10.1007/s10584-011-0156-z, 2011.
- Meinshausen, M., Vogel, E., Nauels, A., Lorbacher, K., Meinshausen, N., Etheridge, D. M., Fraser, P. J., Montzka, S. A.,
- Rayner, P. J., Trudinger, C. M., Krummel, P. B., Beyerle, U., Canadell, J. G., Daniel, J. S., Enting, I. G., Law, R. M.,
- Lunder, C. R., O'Doherty, S., Prinn, R. G., Reimann, S., Rubino, M., Velders, G. J. M., Vollmer, M. K., Wang, R. H.
- J., and Weiss, R.: Historical greenhouse gas concentrations for climate modelling (CMIP6), Geosci. Model Dev., 10,
- 3115 2057–2116, https://doi.org/10.5194/gmd-10-2057-2017, 2017.
- Meinshausen, M., Nicholls, Z. R. J., Lewis, J., Gidden, M. J., Vogel, E., Freund, M., Beyerle, U., Gessner, C., Nauels, A.,
- Bauer, N., Canadell, J. G., Daniel, J. S., John, A., Krummel, P. B., Luderer, G., Meinshausen, N., Montzka, S. A.,
- Rayner, P. J., Reimann, S., Smith, S. J., van den Berg, M., Velders, G. J. M., Vollmer, M. K., and Wang, R. H. J.: The
- shared socio-economic pathway (SSP) greenhouse gas concentrations and their extensions to 2500, Geosci. Model
- 3120 Dev., 13, 3571–3605, https://doi.org/10.5194/gmd-13-3571-2020, 2020.
- Melton, J. R. and Arora, V. K.: Competition between plant functional types in the Canadian Terrestrial Ecosystem Model
- 3122 (CTEM) v. 2.0, Geosci. Model Dev., 9(1), 323–361, doi:10.5194/gmd-9-323-2016, 2016.
- Melton, J. R., Wania, R., Hodson, E. L., Poulter, B., Ringeval, B., Spahni, R., Bohn, T., Avis, C. A., Beerling, D. J., Chen,
- G., Eliseev, A. V., Denisov, S. N., Hopcroft, P. O., Lettenmaier, D. P., Riley, W. J., Singarayer, J. S., Subin, Z. M.,





- Tian, H., Zürcher, S., Brovkin, V., van Bodegom, P. M., Kleinen, T., Yu, Z. C. and Kaplan, J. O.: Present state of
- 3126 global wetland extent and wetland methane modelling: conclusions from a model intercomparison project
- 3127 (WETCHIMP), Biogeosciences, 10(2), 753–788, doi:10.5194/bg-10-753-2013, 2013.
- Membrive, O., Crevoisier, C., Sweeney, C., Danis, F., Hertzog, A., Engel, A., Bönisch, H. and Picon, L.: AirCore-HR: a
- high-resolution column sampling to enhance the vertical description of CH₄ and CO₂, Atmospheric Meas. Tech., 10(6),
- 3130 2163–2181, doi:10.5194/amt-10-2163-2017, 2017.
- Messager, M. L., Lehner, B., Grill, G., Nedeva, I. and Schmitt, O.: Estimating the volume and age of water stored in global
- lakes using a geo-statistical approach, Nat. Commun., 7(1), 1–11, doi:10.1038/ncomms13603, 2016.
- Mijling, B., van der A, R. J. and Zhang, Q.: Regional nitrogen oxides emission trends in East Asia observed from space,
- 3134 Atmospheric Chem. Phys., 13(23), 12003–12012, doi:doi:10.5194/acp-13-12003-2013, 2013.
- Milkov, A. V.: Molecular and stable isotope compositions of natural gas hydrates: A revised global dataset and basic
- interpretations in the context of geological settings, Org. Geochem., 36(5), 681–702, 2005.
- Minkkinen, K. and Laine, J.: Vegetation heterogeneity and ditches create spatial variability in methane fluxes from
- peatlands drained for forestry, Plant Soil, 285(1), 289–304, doi:10.1007/s11104-006-9016-4, 2006.
- Monforti Ferrario, Fabio; Crippa, Monica; Guizzardi, Diego; Muntean, Marilena; Schaaf, Edwin; Lo Vullo, Eleonora;
- 3140 Solazzo, Efisio; Olivier, Jos; Vignati, Elisabetta: EDGAR v6.0 Greenhouse Gas Emissions. European Commission,
- Joint Research Centre (JRC) [Dataset] PID: http://data.europa.eu/89h/97a67d67-c62e-4826-b873-9d972c4f670b, 2021
- Montzka, S. A., Krol, M., Dlugokencky, E., Hall, B., Jockel, P. and Lelieveld, J.: Small Interannual Variability of Global
- 3143 Atmospheric Hydroxyl, Science, 331(6013), 67–69, 2011.
- Moore, C. W., Zielinska, B., Pétron, G. and Jackson, R. B.: Air impacts of increased natural gas acquisition, processing,
- and use: a critical review, Environ. Sci. Technol., 48, 8349–8359, doi:10.1021/es4053472, 2014.
- Morgenstern, O., Hegglin, M. I., Rozanov, E., O'Connor, F. M., Abraham, N. L., Akiyoshi, H., Archibald, A. T., Bekki,
- 3147 S., Butchart, N., Chipperfield, M. P., Deushi, M., Dhomse, S. S., Garcia, R. R., Hardiman, S. C., Horowitz, L. W.,
- Jöckel, P., Josse, B., Kinnison, D., Lin, M., Mancini, E., Manyin, M. E., Marchand, M., Marécal, V., Michou, M.,
- Oman, L. D., Pitari, G., Plummer, D. A., Revell, L. E., Saint-Martin, D., Schofield, R., Stenke, A., Stone, K., Sudo,
- K., Tanaka, T. Y., Tilmes, S., Yamashita, Y., Yoshida, K., and Zeng, G.: Review of the global models used within
- phase 1 of the Chemistry-Climate Model Initiative (CCMI), Geosci. Model Dev., 10, 639-671,
- 3152 https://doi.org/10.5194/gmd-10-639-2017, 2017.
- Morino, I., Uchino, O., Inoue, M., Yoshida, Y., Yokota, T., Wennberg, P. O., Toon, G. C., Wunch, D., Roehl, C. M.,
- Notholt, J., Warneke, T., Messerschmidt, J., Griffith, D. W. T., Deutscher, N. M., Sherlock, V., Connor, B., Robinson,
- 3155 J., Sussmann, R. and Rettinger, M.: Preliminary validation of column-averaged volume mixing ratios of carbon dioxide
- and methane retrieved from GOSAT short-wavelength infrared spectra, Atmospheric Meas. Tech., 4(6), 1061–1076,
- 3157 2011.





- Murguia-Flores, F., Arndt, S., Ganesan, A. L., Murray-Tortarolo, G. and Hornibrook, E. R. C.: Soil Methanotrophy Model
- (MeMo v1.0): a process-based model to quantify global uptake of atmospheric methane by soil, Geosci. Model Dev.,
- 3160 11(6), 2009–2032, doi:10.5194/gmd-11-2009-2018, 2018.
- Myer, A., Myer, M.H., Trettin, C.C. and Forschler, B.T.: The fate of carbon utilized by the subterranean termite
- 3162 Reticulitermes flavipes. Ecosphere 12 (12):e03872,doi:10.1002/ecs2.3872, 2021
- Myhre, G., Shindell, D., Bréon, F.-M., Collins, W., Fuglestvedt, J., Huang, J., Koch, D., Lamarque, J.-F., Lee, D.,
- Mendoza, B., Nakajima, T., Robock, A., Stephens, G., Takemura, T. and Zhang, H.: Anthropogenic and Natural
- Radiative Forcing., in In Climate Change 2013: The Physical Science Basis. Contribution of Working Group I to the
- Fifth Assessment Report of the Intergovernmental Panel on Climate Change, edited by T. F. Stocker, D. D. Qin, G.-
- 3167 K. Plattner, M. Tignor, S. K. Allen, J. Boschung, A. Nauels, Y. Xia, V. Bex, and P. M. Midgley, Cambridge University
- Press, Cambridge, United Kingdom and New York, NY, USA., 2013.
- Naik, V., Voulgarakis, A., Fiore, A. M., Horowitz, L. W., Lamarque, J. F., Lin, M., Prather, M. J., Young, P. J., Bergmann,
- D., Cameron-Smith, P. J., Cionni, I., Collins, W. J., Dalsoren, S. B., Doherty, R., Eyring, V., Faluvegi, G., Folberth,
- 3171 G. A., Josse, B., Lee, Y. H., MacKenzie, I. A., Nagashima, T., van Noije, T. P. C., Plummer, D. A., Righi, M., Rumbold,
- S. T., Skeie, R., Shindell, D. T., Stevenson, D. S., Strode, S., Sudo, K., Szopa, S. and Zeng, G.: Preindustrial to present
- day changes in tropospheric hydroxyl radical and methane lifetime from the Atmospheric Chemistry and Climate
- 3174 Model Intercomparison Project (ACCMIP), Atmospheric Chem. Phys., 13(10), 5277–5298, doi:10.5194/acp-13-5277-
- 3175 2013, 2013.
- Nakazawa, T., Machida, T., Tanaka, M., Fujii, Y., Aoki, S. and Watanabe, O.: Differences of the atmospheric CH4
- 3177 concentration between the Arctic and Antarctic regions in pre-industrial/pre-agricultural era, Geophys. Res. Lett.,
- 3178 20(10), 943–946, doi:10.1029/93GL00776, 1993.
- Natchimuthu, S., I. Sundgren, M. Gålfalk, L. Klemedtsson, P. Crill, Å. Danielsson, and D. Bastviken, Spatio-temporal
- variability of lake CH₄ fluxes and its influence on annual whole lake emission estimates. Limnology and
- 3181 Oceanography, 61(S1): p. S13-S26, 2016.
- Nauer, P. A., Hutley, L. B., and Arndt, S. K.: Termite mounds mitigate half of termite methane emissions, P. Natl. Acad.
- 3183 Sci. USA, 115, 13306–13311, 2018.
- Nicely, J. M., Salawitch, R. J., Canty, T., Anderson, D. C., Arnold, S. R., Chipperfield, M. P., Emmons, L. K., Flemming,
- J., Huijnen, V., Kinnison, D. E., Lamarque, J.-F., Mao, J., Monks, S. A., Steenrod, S. D., Tilmes, S. and Turquety, S.:
- Quantifying the causes of differences in tropospheric OH within global models, J. Geophys. Res. Atmospheres, 122(3),
- 3187 1983–2007, doi:10.1002/2016JD026239, 2017.
- Nirmal Rajkumar, A., J. Barnes, R. Ramesh, R. Purvaja, and R.C. Upstill-Goddard, Methane and nitrous oxide fluxes in
- the polluted Adyar River and estuary, SE India. Marine Pollution Bulletin, 56(12): p. 2043-2051, 2008
- Nisbet, E. G., Manning, M. R., Dlugokencky, E. J., Fisher, R. E., Lowry, D., Michel, S. E., Myhre, C. L., Platt, S. M.,





- Allen, G., Bousquet, P., Brownlow, R., Cain, M., France, J. L., Hermansen, O., Hossaini, R., Jones, A. E., Levin, I.,
- Manning, A. C., Myhre, G., Pyle, J. A., Vaughn, B., Warwick, N. J. and White, J. W. C.: Very strong atmospheric
- methane growth in the four years 2014-2017: Implications for the Paris Agreement, Glob. Biogeochem. Cycles, 0(ja),
- 3194 doi:10.1029/2018GB006009, 2019.
- Nisbet, E. G., Manning, M. R., Dlugokencky, E. J., Michel, S. E., Lan, X., Röckmann, T., van der Denier Gon, H. A.,
- 3196 Schmitt, J., Palmer, P. I., Dyonisius, M. N., Oh, Y., Fisher, R. E., Lowry, D., France, J. L., White, J. W. C., Brailsford,
- 3197 G., and Bromley, T.: Atmospheric methane: Comparison between methane's record in 2006–2022 and during glacial
- terminations, Global Biogeochem. Cy., 37, e2023GB007875, https://doi.org/10.1029/2023GB007875, 2023.
- Nisbet, R. E. R., Fisher, R., Nimmo, R. H., Bendall, D. S., Crill, P. M., Gallego-Sala, A. V., Hornibrook, E. R. C., Lopez-
- Juez, E., Lowry, D., Nisbet, P. B. R., Shuckburgh, E. F., Sriskantharajah, S., Howe, C. J. and Nisbet, E. G.: Emission
- 3201 of methane from plants, Proc. R. Soc. B-Biol. Sci., 276(1660), 1347–1354, 2009.
- Niwa, Y., Fujii, Y., Sawa, Y., Iida, Y., Ito, A., Satoh, M., Imasu, R., Tsuboi, K., Matsueda, H. and Saigusa, N.: A 4D-Var
- 3203 inversion system based on the icosahedral grid model (NICAM-TM 4D-Var v1.0) Part 2: Optimization scheme and
- identical twin experiment of atmospheric CO₂ inversion, Geosci. Model Dev., 10(6), 2201–2219, doi:10.5194/gmd-
- 3205 10-2201-2017, 2017.
- Niwa, Y., Ishijima, K., Ito, A. and Iida, Y.: Toward a long-term atmospheric CO₂ inversion for elucidating natural carbon
- 3207 fluxes: technical notes of NISMON-CO₂ v2021.1. Prog. Earth Planet Sci. 9, 42, doi:10.1186/s40645-022-00502-6,
- 3208 2022
- Noël, S., Reuter, M., Buchwitz, M., Borchardt, J., Hilker, M., Schneising, O., Bovensmann, H., Burrows, J. P., Di Noia,
- A., Parker, R. J., Suto, H., Yoshida, Y., Buschmann, M., Deutscher, N. M., Feist, D. G., Griffith, D. W. T., Hase, F.,
- 3211 Kivi, R., Liu, C., Morino, I., Notholt, J., Oh, Y.-S., Ohyama, H., Petri, C., Pollard, D. F., Rettinger, M., Roehl, C.,
- Rousogenous, C., Sha, M. K., Shiomi, K., Strong, K., Sussmann, R., Té, Y., Velazco, V. A., Vrekoussis, M., and
- Warneke, T.: Retrieval of greenhouse gases from GOSAT and GOSAT-2 using the FOCAL algorithm, Atmos. Meas.
- 3214 Tech., 15, 3401–3437, https://doi.org/10.5194/amt-15-3401-2022, 2022.
- Nomura, S., Naja, M., Ahmed, M. K., Mukai, H., Terao, Y., Machida, T., Sasakawa, M., and Patra, P. K.: Measurement
- 3216 report: Regional characteristics of seasonal and long-term variations in greenhouse gases at Nainital, India, and
- 3217 Comilla, Bangladesh, Atmos. Chem. Phys., 21, 16427–16452, https://doi.org/10.5194/acp-21-16427-2021, 2021
- 3218 Obu, J., Westermann, S., Bartsch, A., Berdnikov, N., Christiansen, H. H., Dashtseren, A., Delaloye, R., Elberling, B.,
- Etzelmüller, B., Kholodov, A., Khomutov, A., Kääb, A., Leibman, M. O., Lewkowicz, A. G., Panda, S. K.,
- Romanovsky, V., Way, R. G., Westergaard-Nielsen, A., Wu, T., Yamkhin, J. and Zou, D.: Northern Hemisphere
- permafrost map based on TTOP modelling for 2000–2016 at 1 km2 scale, Earth-Sci. Rev., 193, 299–316,
- 3222 doi:10.1016/j.earscirev.2019.04.023, 2019.





- Ocko, I. B, Sun, T., Shindell, D., Oppenheimer, M., Hristov, A. N, Pacala, S. W, Mauzerall, D. L, Xu, Y. and Hamburg,
- 3224 S. P. Acting rapidly to deploy readily available methane mitigation measures by sector can immediately slow global
- 3225 warming, Environ. Res. Lett., 16, 054042, doi:10.1088/1748-9326/abf9c8, 2021
- Odelson, D.A. and Breznak, J. A. Volatile fatty acid production by the hindgut microbiota of xilophagus termites. Applied
- and Environmental Microbiology, 45, 1602-1613, 1983. doi: 10.1128/aem.45.5.1602-1613.1983.
- Olivier, J. G. J. and Janssens-Maenhout, G.: Part III: Total Greenhouse Gas Emissions, of CO₂ Emissions from Fuel
- Combustion (2014 ed.), International Energy Agency, Paris, ISBN-978-92-64-21709-6., 2014.
- Ollivier, Q. R., Maher, D. T., Pitfield, C. and Macreadie, P. I.: Punching above their weight: Large release of greenhouse
- 3231 gases from small agricultural dams, Glob. Change Biol., 25(2), 721–732, doi:10.1111/gcb.14477, 2019.
- O'Neill, B. C., Tebaldi, C., Vuuren, D. P. van, Eyring, V., Friedlingstein, P., Hurtt, G., Knutti, R., Kriegler, E., Lamarque,
- J.-F., Lowe, J., Meehl, G. A., Moss, R., Riahi, K. and Sanderson, B. M.: The Scenario Model Intercomparison Project
- 3234 (ScenarioMIP) for CMIP6, Geosci. Model Dev., 9(9), 3461–3482, doi:https://doi.org/10.5194/gmd-9-3461-2016,
- 3235 2016.
- Oreggioni, G. D., F. Monforti Ferrario, M. Crippa, M. Muntean, E. Schaaf, D. Guizzardi, E. Solazzo, M. Duerr, M. Perry
- and E. Vignati: Climate change in a changing world: Socio-economic and technological transitions, regulatory
- frameworks and trends on global greenhouse gas emissions from EDGAR v.5.0, Global Environmental Change,
- 3239 doi:10.1016/j.gloenvcha.2021.10235, 2021
- 3240 Oremland, R. S. Methanogenic activity in plankton samples and fish intestines: a mechanism for *in situ* methanogenesis
- in oceanic surface waters. *Limnol. Oceanogr.* **24,** 1136–1141, 1979.
- O'Rourke, P. R, Smith, S. J., Mott, A., Ahsan, H., McDuffie, E. E., Crippa, M., Klimont, S., McDonald, B., Z., Wang,
- 3243 Nicholson, M. B, Feng, L., and Hoesly, R. M., CEDS v-2021-02-05 Emission Data 1975-2019 (Version Feb-05-2021).
- 3244 Zenodo. http://doi.org/10.5281/zenodo.4509372, 2021
- Ovalle, A. R. C., C. E. Rezende, L. D. Lacerda, and C. A. R. Silva: Factors affecting the hydrochemistry of a mangrove
- 3246 tidal creek, Sepetiba Bay, Brazil. Estuar. Coast. Shelf Sci. 31: 639–650. doi:10.1016/0272-7714(90)90017-L, 1990
- Pacala, S. W.: Verifying greenhouse gas emissions: Methods to support international climate agreements, National
- 3248 Academies Press., 2010
- Pandey, S., Gautam, R., Houweling, S., Gon, H. D. van der, Sadavarte, P., Borsdorff, T., Hasekamp, O., Landgraf, J., Tol,
- 3250 P., Kempen, T. van, Hoogeveen, R., Hees, R. van, Hamburg, S. P., Maasakkers, J. D. and Aben, I.: Satellite
- 3251 observations reveal extreme methane leakage from a natural gas well blowout, Proc. Natl. Acad. Sci., 116(52), 26376–
- 3252 26381, doi:10.1073/pnas.1908712116, 2019.
- Pangala, S. R., Moore, S., Hornibrook, E. R. C. and Gauci, V.: Trees are major conduits for methane egress from tropical
- 3254 forested wetlands, New Phytol., 197(2), 524–531, doi:10.1111/nph.12031, 2013.
- Pangala, S. R., Hornibrook, E. R. C., Gowing, D. J. and Gauci, V.: The contribution of trees to ecosystem methane





- emissions in a temperate forested wetland, Glob. Change Biol., 21(7), 2642–2654, doi:10.1111/gcb.12891, 2015.
- Pangala, S. R., Enrich-Prast, A., Basso, L. S., Peixoto, R. B., Bastviken, D., Hornibrook, E. R. C., Gatti, L. V., Marotta,
- H., Calazans, L. S. B., Sakuragui, C. M., Bastos, W. R., Malm, O., Gloor, E., Miller, J. B. and Gauci, V.: Large
- emissions from floodplain trees close the Amazon methane budget, Nature, 552(7684), 230-234,
- 3260 doi:10.1038/nature24639, 2017.
- Paris, J.-D., Ciais, P., Nedelec, P., Stohl, A., Belan, B. D., Arshinov, M. Y., Carouge, C., Golitsyn, G. S. and Granberg, I.
- 3262 G.: New insights on the chemical composition of the Siberian air shed from the YAK AEROSIB aircraft campaigns,
- 3263 Bull. Am. Meteorol. Soc., 91(5), 625–641, doi:10.1175/2009BAMS2663.1., 2010.
- Parker, R. J., Webb, A., Boesch, H., Somkuti, P., Barrio Guillo, R., Di Noia, A., Kalaitzi, N., Anand, J. S., Bergamaschi,
- P., Chevallier, F., Palmer, P. I., Feng, L., Deutscher, N. M., Feist, D. G., Griffith, D. W. T., Hase, F., Kivi, R., Morino,
- 3266 I., Notholt, J., Oh, Y.-S., Ohyama, H., Petri, C., Pollard, D. F., Roehl, C., Sha, M. K., Shiomi, K., Strong, K., Sussmann,
- R., Té, Y., Velazco, V. A., Warneke, T., Wennberg, P. O., and Wunch, D.: A decade of GOSAT Proxy satellite CH4
- 3268 observations, Earth Syst. Sci. Data, 12, 3383–3412, https://doi.org/10.5194/essd-12-3383-2020, 2020.
- Parker, R. and Boesch, H. (2020): University of Leicester GOSAT Proxy XCH4 v9.0. Centre for Environmental Data
- 3270 Analysis, 07 May 2020. https://dx.doi.org/10.5285/18ef8247f52a4cb6a14013f8235cc1eb, 2020
- Parker, R. J., Wilson, C., Comyn-Platt, E., Hayman, G., Marthews, T. R., Bloom, A. A., Lunt, M. F., Gedney, N., Dadson,
- 3272 S. J., McNorton, J., Humpage, N., Boesch, H., Chipperfield, M. P., Palmer, P. I., and Yamazaki, D.: Evaluation of
- wetland CH4 in the Joint UK Land Environment Simulator (JULES) land surface model using satellite observations,
- 3274 Biogeosciences, 19, 5779–5805, https://doi.org/10.5194/bg-19-5779-2022, 2022.
- Pathak, H., Li, C. and Wassmann, R.: Greenhouse gas emissions from Indian rice fields: calibration and upscaling using
- 3276 the DNDC model, Biogeosciences, 1(1), 1–11, 2005.
- Patra, P. K., Houweling, S., Krol, M., Bousquet, P., Belikov, D., Bergmann, D., Bian, H., Cameron-Smith, P., Chipperfield,
- M. P., Corbin, K., Fortems-Cheiney, A., Fraser, A., Gloor, E., Hess, P., Ito, A., Kawa, S. R., Law, R. M., Loh, Z.,
- Maksyutov, S., Meng, L., Palmer, P. I., Prinn, R. G., Rigby, M., Saito, R. and Wilson, C.: TransCom model simulations
- 3280 of CH₄ and related species: linking transport, surface flux and chemical loss with CH₄ variability in the troposphere
- and lower stratosphere, Atmospheric Chem. Phys., 11(24), 12,813-12,837, doi:10.5194/acp-11-12813-2011, 2011.
- Patra, P. K., Krol, M. C., Montzka, S. A., Arnold, T., Atlas, E. L., Lintner, B. R., Stephens, B. B., Xiang, B., Elkins, J. W.,
- Fraser, P. J., Ghosh, A., Hintsa, E. J., Hurst, D. F., Ishijima, K., Krummel, P. B., Miller, B. R., Miyazaki, K., Moore,
- F. L., Mühle, J., O'Doherty, S., Prinn, R. G., Steele, L. P., Takigawa, M., Wang, H. J., Weiss, R. F., Wofsy, S. C. and
- Young, D.: Observational evidence for interhemispheric hydroxyl-radical parity, Nature, 513(7517), 219–223,
- 3286 doi:10.1038/nature13721, 2014.
- Patra, P. K., Takigawa, M., Watanabe, S., Chandra, N., Ishijima, K. and Yamashita, Y.: Improved Chemical Tracer
- 3288 Simulation by MIROC4.0-based Atmospheric Chemistry-Transport Model (MIROC4-ACTM), SOLA, 14(0), 91–96,





- 3289 doi:10.2151/sola.2018-016, 2018.
- Patra, P. K., Krol, M. C., Prinn, R. G., Takigawa, M., Mühle, J., Montzka, S. A., Lal, S., Yamashita, Y., Naus, S., Chandra,
- N., Weiss, R. F., Krummel, P. B., Fraser, P. J., O'Doherty, S., and Elkins, J. W.: Methyl Chloroform Continues to
- Constrain the Hydroxyl (OH) Variability in the Troposphere, J. Geophys. Res.-Atmos., 126, e2020JD033862,
- 3293 https://doi.org/10.1029/2020JD033862, 2021.
- Paull, C. K., Brewer, P. G., Ussler, W., Peltzer, E. T., Rehder, G. and Clague, D.: An experiment demonstrating that marine
- 3295 slumping is a mechanism to transfer methane from seafloor gas-hydrate deposits into the upper ocean and atmosphere,
- 3296 Geo-Mar. Lett., 22(4), 198–203, doi:10.1007/s00367-002-0113-y, 2002.
- Peacock, M., J. Audet, D. Bastviken, M.N. Futter, V. Gauci, A. Grinham, J.A. Harrison, M.S. Kent, S. Kosten, C.E.
- Lovelock, A.J. Veraart, and C.D. Evans, Global importance of methane emissions from drainage ditches and canals.
- 3299 Environmental Research Letters, 16(4): p. 044010., 2021
- Peischl, J., Ryerson, T. B., Aikin, K. C., de Gouw, J. A., Gilman, J. B., Holloway, J. S., Lerner, B. M., Nadkarni, R.,
- Neuman, J. A., Nowak, J. B., Trainer, M., Warneke, C. and Parrish, D. D.: Quantifying atmospheric methane emissions
- from the Haynesville, Fayetteville, and northeastern Marcellus shale gas production regions, J. Geophys. Res.
- 3303 Atmospheres, 120(5), 2119–2139, doi:10.1002/2014jd022697, 2015.
- Pekel, J.-F., Cottam, A., Gorelick, N. and Belward, A. S.: High-resolution mapping of global surface water and its long-
- 3305 term changes, Nature, 540(7633), 418–422, doi:10.1038/nature20584, 2016.
- Peltola, O., Vesala, T., Gao, Y., Räty, O., Alekseychik, P., Aurela, M., Chojnicki, B., Desai, A. R., Dolman, A. J.,
- Euskirchen, E. S., Friborg, T., Göckede, M., Helbig, M., Humphreys, E., Jackson, R. B., Jocher, G., Joos, F., Klatt, J.,
- Knox, S. H., Kowalska, N., Kutzbach, L., Lienert, S., Lohila, A., Mammarella, I., Nadeau, D. F., Nilsson, M. B.,
- Oechel, W. C., Peichl, M., Pypker, T., Quinton, W., Rinne, J., Sachs, T., Samson, M., Schmid, H. P., Sonnentag, O.,
- Wille, C., Zona, D. and Aalto, T.: Monthly gridded data product of northern wetland methane emissions based on
- 3311 upscaling eddy covariance observations, Earth Syst. Sci. Data, 11(3), 1263–1289, doi:10.5194/essd-11-1263-2019,
- 3312 2019.
- Peng, S. S., Piao, S. L., Bousquet, P., Ciais, P., Li, B. G., Lin, X., Tao, S., Wang, Z. P., Zhang, Y. and Zhou, F.: Inventory
- of anthropogenic methane emissions in Mainland China from 1980 to 2010, Atmospheric Chem. Phys. Discuss., 2016,
- 3315 1–29, doi:10.5194/acp-2016-139, 2016.
- Peng, S., Lin, X., Thompson, R. L., Xi, Y., Liu, G., Hauglustaine, D., Lan, X., Poulter, B., Ramonet, M., Saunois, M.,
- 3317 Yin, Y., Zhang, Z., Zheng, B., and Ciais, P.: Wetland emission and atmospheric sink changes explain methane growth
- 3318 in 2020, Nature, 612, 477–482, https://doi.org/10.1038/s41586-022-05447-w, 2022.
- 3319 Pérez-Barbería, F. J.: Scaling methane emissions in ruminants and global estimates in wild populations, Sci. Total
- Environ., 579, 1572–1580, doi:10.1016/j.scitotenv.2016.11.175, 2017.
- Petersen, H. and Luxton, M. A comparative analysis of soil fauna populations and their role in decomposition processes.





- 3322 Oikos 39: 287–388,<u>doi.org/10.2307/3544689.</u>, 1982
- Petrenko, V. V., Smith, A. M., Schaefer, H., Riedel, K., Brook, E., Baggenstos, D., Harth, C., Hua, Q., Buizert, C., Schilt,
- A., Fain, X., Mitchell, L., Bauska, T., Orsi, A., Weiss, R. F. and Severinghaus, J. P.: Minimal geological methane
- emissions during the Younger Dryas–Preboreal abrupt warming event, Nature, 548, 443, doi:10.1038/nature23316
- https://www.nature.com/articles/nature23316#supplementary-information, 2017.
- Petrescu, A. M. R., Qiu, C., Ciais, P., Thompson, R. L., Peylin, P., McGrath, M. M., Solazzo, E., Janssens-Maenhout, G.,
- Tubiello, F. N., Bergamaschi, P., Brunner, D., Peters, G. P., Höglund- Isaksson, L., Regnier, P., Lauerwald, R.,
- Bastviken, D., Tsuruta, A., Winiwarter, W., Patra, P. P., Kuhnert, M., Oreggioni, G. D., Crippa, M., Saunois, M.,
- Perugini, L., Markkanen, T., Aalto, T., Groot Zwaaftink, C. C., Yao, Y., Wilson, C. C., Conchedda, G., Günther, D.,
- Leip, A., Smith, P., Haussaire, J. M., Leppänen, A., Manning, A. J., McNorton, J., Brockmann, P., & Dolman, A. J. H.
- A. The consolidated European synthesis of CH4 and N2O emissions for the European Union and United Kingdom:
- 3333 1990-2017. Earth System Science Data, 13(5), 2307-2362. doi:10.5194/essd-13-2307-2021, 2021.
- Petrescu, A. M. R., Qiu, C., McGrath, M. J., Peylin, P., Peters, G. P., Ciais, P., Thompson, R. L., Tsuruta, A., Brunner,
- D., Kuhnert, M., Matthews, B., Palmer, P. I., Tarasova, O., Regnier, P., Lauerwald, R., Bastviken, D., Höglund-
- Isaksson, L., Winiwarter, W., Etiope, G., Aalto, T., Balsamo, G., Bastrikov, V., Berchet, A., Brockmann, P., Ciotoli,
- 3337 G., Conchedda, G., Crippa, M., Dentener, F., Groot Zwaaftink, C. D., Guizzardi, D., Günther, D., Haussaire, J.-M.,
- Houweling, S., Janssens-Maenhout, G., Kouyate, M., Leip, A., Leppänen, A., Lugato, E., Maisonnier, M., Manning,
- A. J., Markkanen, T., McNorton, J., Muntean, M., Oreggioni, G. D., Patra, P. K., Perugini, L., Pison, I., Raivonen, M.
- T., Saunois, M., Segers, A. J., Smith, P., Solazzo, E., Tian, H., Tubiello, F. N., Vesala, T., van der Werf, G. R., Wilson,
- C., and Zaehle, S.: The consolidated European synthesis of CH₄ and N₂O emissions for the European Union and United
- 3342 Kingdom: 1990–2019, Earth Syst. Sci. Data, 15, 1197–1268, https://doi.org/10.5194/essd-15-1197-2023, 2023.
- Pétron, G., Karion, A., Sweeney, C., Miller, B. R., Montzka, S. A., Frost, G. J., Trainer, M., Tans, P., Andrews, A., Kofler,
- J., Helmig, D., Guenther, D., Dlugokencky, E., Lang, P., Newberger, T., Wolter, S., Hall, B., Novelli, P., Brewer, A.,
- 3345 Conley, S., Hardesty, M., Banta, R., White, A., Noone, D., Wolfe, D. and Schnell, R.: A new look at methane and
- nonmethane hydrocarbon emissions from oil and natural gas operations in the Colorado Denver-Julesburg Basin, J.
- 3347 Geophys. Res. Atmospheres, 119(11), 6836–6852, doi:10.1002/2013jd021272, 2014.
- Phillips, N. G., Ackley, R., Crosson, E. R., Down, A., Hutyra, L. R., Brondfield, M., Karr, J. D., Zhao, K. and Jackson, R.
- B.: Mapping urban pipeline leaks: Methane leaks across Boston, Environ. Pollut., 173, 1-4,
- 3350 doi:10.1016/j.envpol.2012.11.003, 2013.
- Pison, I., Ringeval, B., Bousquet, P., Prigent, C. and Papa, F.: Stable atmospheric methane in the 2000s: key-role of
- emissions from natural wetlands, Atmospheric Chem. Phys. Discuss., 13(4), 9017–9049, doi:10.5194/acpd-13-9017-
- 3353 2013, 2013.
- Pitz, S. and Megonigal, J. P.: Temperate forest methane sink diminished by tree emissions, New Phytol., 214(4), 1432–





- 3355 1439, doi:10.1111/nph.14559, 2017.
- Platt, U., Allan, W. and Lowe, D.: Hemispheric average Cl atom concentration from ¹³C/¹²C ratios in atmospheric methane, Atmos Chem Phys, 4, 2393–2399, 2004.
- Plummer, D., Nagashima, T., Tilmes, S., Archibald, A., Chiodo, G., Fadnavis, S., Garny, H., Josse, B., Kim, J., Lamarque,
- J.-F., Morgenstern, O., Murray, L., Orbe, C., Tai, A., Chipperfield, M., Funke, B., Juckes, M., Kinnison, D., Kunze,
- 3360 M., Luo, B., Matthes, K., Newman, P. A., Pascoe, C. and Peter, T.: CCMI- 2022: a new set of Chemistry-Climate
- Model Initiative (CCMI) community simulations to update the assessment of models and support upcoming ozone
- assessment activities. SPARC Newsletter 57, 22–30, 2021.
- Pollard, D. F., Sherlock, V., Robinson, J., Deutscher, N. M., Connor, B. and Shiona, H.: The Total Carbon Column
- Observing Network site description for Lauder, New Zealand, Earth Syst. Sci. Data, 9(2), 977–992, doi:10.5194/essd-
- 3365 9-977-2017, 2017.
- Portmann, F. T., Siebert, S. & Döll, P.: MIRCA2000 Global monthly irrigated and rainfed crop areas around the year
- 2000: A new high-resolution data set for agricultural and hydrological modeling, Global Biogeochemical Cycles, 24,
- 3368 GB 1011, doi:10.1029/2008GB003435, 2010
- Portmann, R. W., Daniel, J. S. and Ravishankara, A. R.: Stratospheric ozone depletion due to nitrous oxide: influences of
- other gases, Philos. Trans. R. Soc. Lond. B Biol. Sci., 367(1593), 1256–1264, doi:10.1098/rstb.2011.0377, 2012.
- Poulter, B., Bousquet, P., Canadell, J. G., Ciais, P., Peregon, A., Saunois, M., Arora, V. K., Beerling, D. J., Brovkin, V.,
- Jones, C. D., Joos, F., Gedney, N., Ito, A., Kleinen, T., Koven, C. D., McDonald, K., Melton, J. R., Peng, C. H., Peng,
- S. S., Prigent, C., Schroeder, R., Riley, W. J., Saito, M., Spahni, R., Tian, H. Q., Taylor, L., Viovy, N., Wilton, D.,
- Wiltshire, A., Xu, X. Y., Zhang, B. W., Zhang, Z. and Zhu, Q. A.: Global wetland contribution to 2000-2012
- 3375 atmospheric methane growth rate dynamics, Environ. Res. Lett., 12(9), doi:10.1088/1748-9326/aa8391, 2017.
- Prairie, Y.T., J. Alm, J. Beaulieu, N. Barros, T. Battin, J. Cole, P. del Giorgio, T. DelSontro, F. Guérin, A. Harby, J.
- Harrison, S. Mercier-Blais, D. Serça, S. Sobek, and D. Vachon, Greenhouse Gas Emissions from Freshwater
- Reservoirs: What Does the Atmosphere See? Ecosystems, 21(5): p. 1058-1071, 2018
- Prather, M. J., Holmes, C. D. and Hsu, J.: Reactive greenhouse gas scenarios: Systematic exploration of uncertainties and
- the role of atmospheric chemistry, Geophys. Res. Lett., 39(9), L09803, doi:10.1029/2012gl051440, 2012.
- Prinn, R. G., Weiss, R. F., Arduini, J., Arnold, T., DeWitt, H. L., Fraser, P. J., Ganesan, A. L., Gasore, J., Harth, C. M.,
- Hermansen, O., Kim, J., Krummel, P. B., Li, S., Loh, Z. M., Lunder, C. R., Maione, M., Manning, A. J., Miller, B. R.,
- Mitrevski, B., Mühle, J., O'Doherty, S., Park, S., Reimann, S., Rigby, M., Saito, T., Salameh, P. K., Schmidt, R.,
- 3384 Simmonds, P. G., Steele, L. P., Vollmer, M. K., Wang, R. H., Yao, B., Yokouchi, Y., Young, D., and Zhou, L.: History
- of chemically and radiatively important atmospheric gases from the Advanced Global Atmospheric Gases Experiment
- 3386 (AGAGE), Earth Syst. Sci. Data, 10, 985–1018, https://doi.org/10.5194/essd-10-985-2018, 2018.
- Prosperi, P., Bloise, M., Tubiello, F.N. et al. New estimates of greenhouse gas emissions from biomass burning and peat





- fires using MODIS Collection 6 burned areas. Climatic Change 161, 415–432, https://doi.org/10.1007/s10584-020-
- 3389 02654-0, 2020
- Purvaja, R., Ramesh, R., & Frenzel, P.: Plant-mediated methane emission from an Indian mangrove, Global Change
- 3391 *Biology*, 10, 1825–1834, 2004
- Qin, B., Zhou, J., Elser, J.J., Gardner, W.S., Deng, J., and J.D. Brookes: Water depth underpins the relative roles and fates
- of nitrogen and phosphorus in lakes, Environmental Science & Technology 2020 54 (6), 3191-3198, DOI:
- 3394 10.1021/acs.est.9b05858, 2020.
- Qu, Z., Jacob, D. J., Shen, L., Lu, X., Zhang, Y., Scarpelli, T. R., Nesser, H., Sulprizio, M. P., Maasakkers, J. D., Bloom,
- A. A., Worden, J. R., Parker, R. J., and Delgado, A. L.: Global distribution of methane emissions: a comparative inverse
- analysis of observations from the TROPOMI and GOSAT satellite instruments, Atmos. Chem. Phys., 21, 14159–
- 3398 14175, https://doi.org/10.5194/acp-21-14159-2021, 2021.
- Qu, Z., Jacob, D. J., Zhang, Y., Shen, L., Varon, D. J., Lu, X., Scarpelli, T., Bloom, A., Worden, J., and Parker, R. J.:
- Attribution of the 2020 surge in atmospheric methane by inverse analysis of GOSAT observations, Environ. Res. Lett.,
- 3401 17, 094003, https://doi.org/10.1088/1748-9326/ac8754, 2022.
- Randerson, J. T., Chen, Y., van der Werf, G. R., Rogers, B. M. and Morton, D. C.: Global burned area and biomass burning
- emissions from small fires, J. Geophys. Res. Biogeosciences, 117, G4, doi:10.1029/2012jg002128, 2012.
- Ramage, J.L., Kuhn, M., Virkkala, A.M., Voigt, C., Marushchak, M.E., Bastos, A., Biasi, C., Canadell, J.G., Ciais, P.,
- Lopez-Blanco, E. Natali, S.M., et al.: The net GHG balance and budget of the permafrost region (2000-2020) from
- 3406 ecosystem flux upscaling. Preprint in ESS Open Archive. September 11, 2023. DOI:
- 3407 10.22541/essoar.169447408.86275712/v1, 2023
- Ramsden, A. E., Ganesan, A. L., Western, L. M., Rigby, M., Manning, A. J., Foulds, A., France, J. L., Barker, P., Levy,
- P., Say, D., Wisher, A., Arnold, T., Rennick, C., Stanley, K. M., Young, D., and O'Doherty, S.: Quantifying fossil fuel
- methane emissions using observations of atmospheric ethane and an uncertain emission ratio, Atmos. Chem. Phys.,
- 3411 22, 3911–3929, https://doi.org/10.5194/acp-22-3911-2022, 2022.
- Ray, N.E., Holgerson, M.A., Andersen, M.R., Bikše, J., Bortolotti, L.E., Futter, M., Kokorīte, I., Law, A., McDonald, C.,
- Mesman, J.P., Peacock, M., Richardson, D.C., Arsenault, J., Bansal, S., Cawley, K., Kuhn, M., Shahabinia, A.R. and
- 3414 Smufer, F.: Spatial and temporal variability in summertime dissolved carbon dioxide and methane in temperate ponds
- 3415 and shallow lakes. Limnol Oceanogr, 68: 1530-1545. https://doi.org/10.1002/lno.12362, 2023
- Regnier P., Arndt, S., Dale, A.W., LaRowe, D.E., Mogollon, J. and Van Cappellen, P. Advances in the biogeochemical
- 3417 modeling of anaerobic oxidation of methane (AOM). Earth Science Reviews. 106, 105-130, 2011;
- Ren, W. E. I., Tian, H., Xu, X., Liu, M., Lu, C., Chen, G., Melillo, J., Reilly, J. and Liu, J.: Spatial and temporal patterns
- of CO₂ and CH₄ fluxes in China's croplands in response to multifactor environmental changes, Tellus B, 63(2), 222–
- 3420 240, doi:10.1111/j.1600-0889.2010.00522.x, 2011.





- Repeta, D. J., Ferrón, S., Sosa, O. A., Johnson, C. G., Repeta, L. D., Acker, M., DeLong, E. F. and Karl, D. M.: Marine
- methane paradox explained by bacterial degradation of dissolved organic matter, Nat. Geosci., 9(12), 884-887,
- 3423 doi:10.1038/ngeo2837, 2016.
- Riahi, K., van Vuuren, D. P., Kriegler, E., Edmonds, J., O'Neill, B. C., Fujimori, S., Bauer, N., Calvin, K., Dellink, R.,
- Fricko, O., Lutz, W., Popp, A., Cuaresma, J. C., Kc, S., Leimbach, M., Jiang, L., Kram, T., Rao, S., Emmerling, J.,
- Ebi, K., Hasegawa, T., Havlik, P., Humpenöder, F., Da Silva, L. A., Smith, S., Stehfest, E., Bosetti, V., Eom, J.,
- Gernaat, D., Masui, T., Rogelj, J., Strefler, J., Drouet, L., Krey, V., Luderer, G., Harmsen, M., Takahashi, K.,
- Baumstark, L., Doelman, J. C., Kainuma, M., Klimont, Z., Marangoni, G., Lotze-Campen, H., Obersteiner, M., Tabeau,
- A. and Tavoni, M.: The Shared Socioeconomic Pathways and their energy, land use, and greenhouse gas emissions
- 3430 implications: An overview, Glob. Environ. Change, 42, 153–168, doi:10.1016/j.gloenvcha.2016.05.009, 2017.
- Rice, A. L., Butenhoff, C. L., Shearer, M. J., Teama, D., Rosenstiel, T. N. and Khalil, M. A. K.: Emissions of anaerobically
- produced methane by trees, Geophys. Res. Lett., 37, L03807, doi:10.1029/2009GL041565, 2010.
- Ridgwell, A. J., Marshall, S. J. and Gregson, K.: Consumption of atmospheric methane by soils: A process-based model,
- 3434 Glob. Biogeochem. Cycles, 13(1), 59–70, doi:10.1029/1998gb900004, 1999.
- Riedel, T. P., Wolfe, G. M., Danas, K. T., Gilman, J. B., Kuster, W. C., Bon, D. M., Vlasenko, A., Li, S. M., Williams, E.
- J., Lerner, B. M., Veres, P. R., Roberts, J. M., Holloway, J. S., Lefer, B., Brown, S. S. and Thornton, J. A.: An MCM
- modeling study of nitryl chloride (ClNO₂) impacts on oxidation, ozone production and nitrogen oxide partitioning in
- 3438 polluted continental outflow, Atmospheric Chem. Phys., 14(8), 3789–3800, doi:10.5194/acp-14-3789-2014, 2014.
- Rigby, M., Montzka, S. A., Prinn, R. G., White, J. W. C., Young, D., O'Doherty, S., Lunt, M. F., Ganesan, A. L., Manning,
- A. J., Simmonds, P. G., Salameh, P. K., Harth, C. M., Mühle, J., Weiss, R. F., Fraser, P. J., Steele, L. P., Krummel, P.
- B., McCulloch, A. and Park, S.: Role of atmospheric oxidation in recent methane growth, Proc. Natl. Acad. Sci.,
- 3442 114(21), 5373, 2017.
- Riley, W. J., Subin, Z. M., Lawrence, D. M., Swenson, S. C., Torn, M. S., Meng, L., Mahowald, N. M. and Hess, P.:
- Barriers to predicting changes in global terrestrial methane fluxes: analyses using CLM4Me, a methane
- 3445 biogeochemistry model integrated in CESM, Biogeosciences, 8(7), 1925–1953, doi:10.5194/bg-8-1925-2011, 2011.
- Ringeval, B., Friedlingstein, P., Koven, C., Ciais, P., de Noblet-Ducoudre, N., Decharme, B. and Cadule, P.: Climate-CH₄
- feedback from wetlands and its interaction with the climate-CO₂ feedback, Biogeosciences, 8(8), 2137–2157,
- 3448 doi:10.5194/bg-8-2137-2011, 2011.
- Robison, A.L., W.M. Wollheim, B. Turek, C. Bova, C. Snay, and R.K. Varner, Spatial and temporal heterogeneity of
- methane ebullition in lowland headwater streams and the impact on sampling design, Limnology and Oceanography,
- 3451 66(12): p. 4063-4076, 2021
- Rocher-Ros, G., Stanley, E.H., Loken, L.C., Casson, N.J., Raymond, P.A., Liu, S., Amatulli, G. and Sponseller, R.A.,
- 3453 Global methane emissions from rivers and streams. *Nature*, pp.1-6.,621,530–535, https://doi.org/10.1038/s41586-023-





- 3454 06344-6, 2023
- Rosentreter, J. A., Maher, D. T., Erler, D. V., Murray, R. H. and Eyre, B. D.: Methane emissions partially offset "blue
- 3456 carbon" burial in mangroves, Sci. Adv., 4(6), eaao4985, doi:10.1126/sciadv.aao4985, 2018.
- Rosentreter, J. A., A. V Borges, B. R. Deemer, and others: Half of global methane emissions come from highly variable aquatic ecosystem sources. Nat. Geosci. **14**: 225–230. doi:10.1038/s41561-021-00715-2, 2021
- Rosentreter, J.A., Laruelle, G.G., Bange, H.W., Bianchi, T.S., Busecke, J.J.M., Cai, W-J, Eyre, B.D., Forbrich, I., Kwon,
- E.Y., Mavara, T., Moosdorf, N., Van Dam, B. and Regnier, P. Coastal vegetation and estuaries are collectively a
- greenhouse gas sink. Nature Climate Change, 13, 579–587, doi: 10.1038/s41558-023-01682-9, 2023.
- Rosentreter, J.A., Alcott, L., Maavara, T., Sun, X., Zhou, Y., Planavsky, N., & Raymond, P. Revisiting the Global Methane

 Cycle Through Expert Opinion (submitted to Earth Future).
- Ruppel, C. D., and J. D. Kessler (2017), The interaction of climate change and methane hydrates, Rev. Geophys., 55, 126-168, doi:10.1002/2016RG000534, 2017
- Saad, K. M., Wunch, D., Toon, G. C., Bernath, P., Boone, C., Connor, B., Deutscher, N. M., Griffith, D. W. T., Kivi, R.,
- Notholt, J., Roehl, C., Schneider, M., Sherlock, V. and Wennberg, P. O.: Derivation of tropospheric methane from
- TCCON CH₄ and HF total column observations, Atmospheric Meas. Technol., 7(9), 2907–2918, doi:10.5194/amt-7-
- 3469 2907-2014, 2014.
- Sanderson, M. G.: Biomass of termites and their emissions of methane and carbon dioxide: A global database, Glob.
- 3471 Biogeochem. Cycles, 10(4), 543–557, doi:10.1029/96gb01893, 1996.
- Sasakawa, M., Shimoyama, K., Machida, T., Tsuda, N., Suto, H., Arshinov, M., Davydov, D., Fofonov, A., Krasnov, O.,
- Saeki, T., Koyama, Y. and Maksyutov, S.: Continuous measurements of methane from a tower network over Siberia,
- 3474 Tellus B, 62(5), 403–416, doi:10.1111/j.1600-0889.2010.00494.x, 2010.
- Sasakawa, M., Machida, T., Ishijima, K., Arshinov, M., Patra, P. K., Ito, A., Aoki, S., and Petrov, V.: Temporal
- 3476 characteristics of CH4 vertical profiles observed in the West Siberian Lowland over Surgut from 1993 to 2015 and
- Novosibirsk from 1997 to 2015. Journal of Geophysical Research: Atmospheres, 122, 11,261–11,273.
- 3478 https://doi.org/10.1002/2017JD026836, 2017.
- Saunois, M., Bousquet, P., Poulter, B., Peregon, A., Ciais, P., Canadell, J. G., Dlugokencky, E. J., Etiope, G., Bastviken,
- D., Houweling, S., Janssens-Maenhout, G., Tubiello, F. N., Castaldi, S., Jackson, R. B., Alexe, M., Arora, V. K.,
- Beerling, D. J., Bergamaschi, P., Blake, D. R., Brailsford, G., Brovkin, V., Bruhwiler, L., Crevoisier, C., Crill, P.,
- Covey, K., Curry, C., Frankenberg, C., Gedney, N., Höglund-Isaksson, L., Ishizawa, M., Ito, A., Joos, F., Kim, H. S.,
- Kleinen, T., Krummel, P., Lamarque, J. F., Langenfelds, R., Locatelli, R., Machida, T., Maksyutov, S., McDonald, K.
- 3484 C., Marshall, J., Melton, J. R., Morino, I., Naik, V., O'Doherty, S., Parmentier, F. J. W., Patra, P. K., Peng, C., Peng,
- 3485 S., Peters, G. P., Pison, I., Prigent, C., Prinn, R., Ramonet, M., Riley, W. J., Saito, M., Santini, M., Schroeder, R.,
- 3486 Simpson, I. J., Spahni, R., Steele, P., Takizawa, A., Thornton, B. F., Tian, H., Tohjima, Y., Viovy, N., Voulgarakis,





- A., van Weele, M., van der Werf, G. R., Weiss, R., Wiedinmyer, C., Wilton, D. J., Wiltshire, A., Worthy, D., Wunch, D., Xu, X., Yoshida, Y., Zhang, B., Zhang, Z. and Zhu, Q.: The global methane budget 2000–2012, Earth Syst Sci
- 3489 Data, 8(2), 697–751, doi:10.5194/essd-8-697-2016, 2016.
- Saunois, M., Bousquet, P., Poulter, B., Peregon, A., Ciais, P., Canadell, J. G., Dlugokencky, E. J., Etiope, G., Bastviken,
- D., Houweling, S., Janssens-Maenhout, G., Tubiello, F. N., Castaldi, S., Jackson, R. B., Alexe, M., Arora, V. K.,
- Beerling, D. J., Bergamaschi, P., Blake, D. R., Brailsford, G., Bruhwiler, L., Crevoisier, C., Crill, P., Covey, K.,
- Frankenberg, C., Gedney, N., Höglund-Isaksson, L., Ishizawa, M., Ito, A., Joos, F., Kim, H. S., Kleinen, T., Krummel,
- P., Lamarque, J. F., Langenfelds, R., Locatelli, R., Machida, T., Maksyutov, S., Melton, J. R., Morino, I., Naik, V.,
- O'Doherty, S., Parmentier, F. J. W., Patra, P. K., Peng, C., Peng, S., Peters, G. P., Pison, I., Prinn, R., Ramonet, M.,
- Riley, W. J., Saito, M., Santini, M., Schroeder, R., Simpson, I. J., Spahni, R., Takizawa, A., Thornton, B. F., Tian, H.,
- Tohjima, Y., Viovy, N., Voulgarakis, A., Weiss, R., Wilton, D. J., Wiltshire, A., Worthy, D., Wunch, D., Xu, X.,
- Yoshida, Y., Zhang, B., Zhang, Z. and Zhu, Q.: Variability and quasi-decadal changes in the methane budget over the
- period 2000-2012, Atmospheric Chem. Phys., 17(18), 11135–11161, doi:10.5194/acp-17-11135-2017, 2017.
- 3500 Saunois, M., Stavert, A. R., Poulter, B., Bousquet, P., Canadell, J. G., Jackson, R. B., Raymond, P. A., Dlugokencky, E.
- J., Houweling, S., Patra, P. K., Ciais, P., Arora, V. K., Bastviken, D., Bergamaschi, P., Blake, D. R., Brailsford, G.,
- Bruhwiler, L., Carlson, K. M., Carrol, M., Castaldi, S., Chandra, N., Crevoisier, C., Crill, P. M., Covey, K., Curry, C.
- L., Etiope, G., Frankenberg, C., Gedney, N., Hegglin, M. I., Höglund-Isaksson, L., Hugelius, G., Ishizawa, M., Ito, A.,
- Janssens-Maenhout, G., Jensen, K. M., Joos, F., Kleinen, T., Krummel, P. B., Langenfelds, R. L., Laruelle, G. G., Liu,
- L., Machida, T., Maksyutov, S., McDonald, K. C., McNorton, J., Miller, P. A., Melton, J. R., Morino, I., Müller, J.,
- Murguia-Flores, F., Naik, V., Niwa, Y., Noce, S., O'Doherty, S., Parker, R. J., Peng, C., Peng, S., Peters, G. P., Prigent,
- 3507 C., Prinn, R., Ramonet, M., Regnier, P., Riley, W. J., Rosentreter, J. A., Segers, A., Simpson, I. J., Shi, H., Smith, S.
- J., Steele, L. P., Thornton, B. F., Tian, H., Tohjima, Y., Tubiello, F. N., Tsuruta, A., Viovy, N., Voulgarakis, A., Weber,
- T. S., van Weele, M., van der Werf, G. R., Weiss, R. F., Worthy, D., Wunch, D., Yin, Y., Yoshida, Y., Zhang, W.,
- 3510 Zhang, Z., Zhao, Y., Zheng, B., Zhu, Q., Zhu, Q., and Zhuang, Q.: The Global Methane Budget 2000–2017, Earth
- 3511 Syst. Sci. Data, 12, 1561–1623, https://doi.org/10.5194/essd-12-1561-2020, 2020.
- Sayers, M.J., Grimm, A.G., Shuchman, R.A., Deines, A.M., Bunnel, D.B., Raymer, Z.B., Rogers, M.W., Woelmer, W.,
- Bennion, D.H., Brooks, C.N., Whitley, MA.A., Warner, D.M, and J. Mychek-Londer: A new method to generate a
- high-resolution global distribution map of lake chlorophyll, International Journal of Remote Sensing, 36:7, 1942-1964,
- 3515 DOI: <u>10.1080/01431161.2015.1029099</u>, 2015
- 3516 Schepers, D., Guerlet, S., Butz, A., Landgraf, J., Frankenberg, C., Hasekamp, O., Blavier, J. F., Deutscher, N. M., Griffith,
- D. W. T., Hase, F., Kyro, E., Morino, I., Sherlock, V., Sussmann, R. and Aben, I.: Methane retrievals from Greenhouse
- Gases Observing Satellite (GOSAT) shortwave infrared measurements: Performance comparison of proxy and physics
- 3519 retrieval algorithms, J. Geophys. Res. Atmospheres, 117, D10, doi:10.1029/2012jd017549, 2012.





- Schmale O, Greinert J, Rehder G (2005) Methane emission from high-intensity marine gas seeps in the Black Sea into the atmosphere. Geophys Res Lett 32:L07609. doi:10.1029/2004GL021138, 2005
- Schmid, M., Batist, M.D., Granin, N.G., Kapitanov, V.A., McGinnis, D.F., Mizandrontsev, I.B., Obzhirov, A.I., and
- Wüest, A.. Sources and sinks of methane in Lake Baikal: A synthesis of measurements and modelling. Limnol.
- 3524 Oceanogr., 52(5), 1824–1837. doi: 10.4319/lo.2007.52.5.1824, 2007
- Schneising, O., Burrows, J. P., Dickerson, R. R., Buchwitz, M., Reuter, M. and Bovensmann, H.: Remote sensing of
- fugitive methane emissions from oil and gas production in North American tight geologic formations, Earths Future,
- 3527 2, 548–558, doi:10.1002/2014EF000265, 2014.
- Schorn, S., S. Ahmerkamp, E. Bullock, and others. : Diverse methylotrophic methanogenic archaea cause high methane
- 3529 emissions from seagrass meadows. Proc. Natl. Acad. Sci. 119: 1–12. doi:10.1073/pnas.2106628119, 2022
- Schuldt, K. N., Mund, J., Aalto, T., Arlyn Andrews, Apadula, F., Jgor Arduini, Arnold, S., Baier, B., Bäni, L., Bartyzel,
- J., Bergamaschi, P., Biermann, T., Biraud, S. C., Pierre-Eric Blanc, Boenisch, H., Brailsford, G., Brand, W. A.,
- Brunner, D., Bui, T. P. V., ... Miroslaw Zimnoch. : Multi-laboratory compilation of atmospheric carbon dioxide data
- for the period 1983-2022; obspack ch4 1 GLOBALVIEWplus v6.0 2023-12-01 [Data set]. NOAA Global
- 3534 Monitoring Laboratory. https://doi.org/10.25925/20231001, 2023
- Schuur, E.A., Abbott, B.W., Commane, R., Ernakovich, J., Euskirchen, E., Hugelius, G., Grosse, G., Jones, M., Koven,
- 3536 C., Leshyk, V. and Lawrence, D. (2022) Permafrost and climate change: carbon cycle feedbacks from the warming
- Arctic. Annual Review of Environment and Resources, 47, pp.343-371. https://doi.org/10.1146/annurev-environ-
- 3538 012220-011847, 2022
- Schwietzke, S., Sherwood, O. A., Bruhwiler, L. M. P., Miller, J. B., Etiope, G., Dlugokencky, E. J., Michel, S. E., Arling,
- V. A., Vaughn, B. H., White, J. W. C. and Tans, P. P.: Upward revision of global fossil fuel methane emissions based
- on isotope database, Nature, 538(7623), 88–91, doi:10.1038/nature19797, 2016.
- 3542 Segers, A., Steinke, T., and Houweling, S.: Description of the CH4 Inversion Production Chain, CAMS (Copernicus
- 3543 Atmospheric Monitoring Service) Report.. [online] Available from:
- https://atmosphere.copernicus.eu/sites/default/files/2022-10/CAMS255 2021SC1 D55.5.2.1-
- 3545 2021CH4 202206 production chain CH4 v1.pdf (Accessed 1 février 2024), 2022.
- 3546 Shen, L., Gautam, R., Omara, M., Zavala-Araiza, D., Maasakkers, J. D., Scarpelli, T. R., Lorente, A., Lyon, D., Sheng, J.,
- Varon, D. J., Nesser, H., Qu, Z., Lu, X., Sulprizio, M. P., Hamburg, S. P., and Jacob, D. J.: Satellite quantification of
- oil and natural gas methane emissions in the US and Canada including contributions from individual basins, Atmos.
- 3549 Chem. Phys., 22, 11203–11215, https://doi.org/10.5194/acp-22-11203-2022, 2022.
- 3550 Shen, L., Jacob, D.J., Gautam, R. et al. National quantifications of methane emissions from fuel exploitation using high
- resolution inversions of satellite observations. Nat Commun 14, 4948, https://doi.org/10.1038/s41467-023-40671-6,
- 3552 2023





- Sherwen, T., Schmidt, J. A., Evans, M. J., Carpenter, L. J., Großmann, K., Eastham, S. D., Jacob, D. J., Dix, B., Koenig,
- T. K., Sinreich, R., Ortega, I., Volkamer, R., Saiz-Lopez, A., Prados-Roman, C., Mahajan, A. S., and Ordóñez, C.:
- Global impacts of tropospheric halogens (Cl, Br, I) on oxidants and composition in GEOS-Chem, Atmos. Chem. Phys.,
- 3556 16, 12239–12271, https://doi.org/10.5194/acp-16-12239-2016, 2016.
- Shindell, D., Kuylenstierna, J. C. I., Vignati, E., van Dingenen, R., Amann, M., Klimont, Z., Anenberg, S. C., Muller, N.,
- Janssens-Maenhout, G., Raes, F., Schwartz, J., Faluvegi, G., Pozzoli, L., Kupiainen, K., Höglund-Isaksson, L.,
- Emberson, L., Streets, D., Ramanathan, V., Hicks, K., Oanh, N. T. K., Milly, G., Williams, M., Demkine, V. and
- Fowler, D.: Simultaneously Mitigating Near-Term Climate Change and Improving Human Health and Food Security,
- 3561 Science, 335(6065), 183–189, doi:10.1126/science.1210026, 2012.
- Shorter, J. H., Mcmanus, J. B., Kolb, C. E., Allwine, E. J., Lamb, B. K., Mosher, B. W., Harriss, R. C., Partchatka, U.,
- Fischer, H., Harris, G. W., Crutzen, P. J. and Karbach, H.-J.: Methane emission measurements in urban areas in Eastern
- 3564 Germany, J. Atmospheric Chem., 124(2), 121–140, 1996.
- Shu, S., Jain, A.K. and Kheshgi, H.S.: Investigating Wetland and Nonwetland Soil Methane Emissions and Sinks Across
- the Contiguous United States Using a Land Surface Model. Global Biogeochem. Cycles, 34: e2019GB006251.
- 3567 https://doi-org.insu.bib.cnrs.fr/10.1029/2019GB006251, 2020
- 3568 Simpson, I. J., Thurtell, G. W., Kidd, G. E., Lin, M., Demetriades-Shah, T. H., Flitcroft, I. D., Kanemasu, E. T., Nie, D.,
- Bronson, K. F. and Neue, H. U.: Tunable diode laser measurements of methane fluxes from an irrigated rice paddy
- 3570 field in the Philippines, J. Geophys. Res. Atmospheres, 100(D4), 7283–7290, doi:10.1029/94jd03326, 1995.
- Simpson, I. J., Sulbaek Andersen, M. P., Meinardi, S., Bruhwiler, L., Blake, N. J., Helmig, D., Rowland, F. S. and Blake,
- D. R.: Long-term decline of global atmospheric ethane concentrations and implications for methane, Nature,
- 3573 488(7412), 490–494, doi:10.1038/nature11342, 2012.
- 3574 Smith I.R., Grasby S.E., Lane L.S.: An investigation of gas seeps and aquatic chemistry in Fisherman Lake, southwest
- Northwest Territories. Geological Survey of Canada, Current Research 2005-A3, 8 p., 2005

3576 Solomon EA, Kastner M, MacDonald IR, Leifer I: Considerable methane fluxes to the atmosphere from hydrocarbon

- seeps in the Gulf of Mexico. Nat Geosci 2:561–565, 2009
- 3578 Spahni, R., Wania, R., Neef, L., van Weele, M., Pison, I., Bousquet, P., Frankenberg, C., Foster, P. N., Joos, F., Prentice,
- I. C. and van Velthoven, P.: Constraining global methane emissions and uptake by ecosystems, Biogeosciences, 8(6),
- 3580 1643–1665, doi:10.5194/bg-8-1643-2011, 2011.
- Stanley, E. H., Casson, N. J., Christel, S. T., Crawford, J. T., Loken, L. C. and Oliver, S. K.: The ecology of methane in
- streams and rivers: patterns, controls, and global significance, Ecol. Monogr., doi:10.1890/15-1027, 2016.
- Stanley, K. M., Grant, A., O'Doherty, S., Young, D., Manning, A. J., Stavert, A. R., Spain, T. G., Salameh, P. K., Harth,
- 3584 C. M., Simmonds, P. G., Sturges, W. T., Oram, D. E. and Derwent, R. G.: Greenhouse gas measurements from a UK
- network of tall towers: technical description and first results, Atmospheric Meas. Tech., 11(3), 1437–1458,





- 3586 doi:10.5194/amt-11-1437-2018, 2018.
- Stanley, E. H., Loken, L. C., Casson, N. J., Oliver, S. K., Sponseller, R. A., Wallin, M. B., Zhang, L., and Rocher-Ros,
- 3588 G.: GRiMeDB: the Global River Methane Database of concentrations and fluxes, Earth Syst. Sci. Data, 15, 2879–
- 3589 2926, https://doi.org/10.5194/essd-15-2879-2023, 2023.
- Stavert, A. R., Saunois, M., Canadell, J. G., Poulter, B., Jackson, R. B., Regnier, P., Lauerwald, R., Raymond, P. A.,
- Allen, G. H., Patra, P. K., Bergamaschi, P., Bousquet, P., Chandra, N., Ciais, P., Gustafson, A., Ishizawa, M., Ito,
- A., Kleinen, T., Maksyutov, S., Joe McNorton, Joe R. Melton, Jurek Müller, Yosuke Niwa, Shushi Peng, William
- J. Riley, Arjo Segers, Hanqin Tian, Aki Tsuruta, Yi Yin, Zhen Zhang, Bo Zheng, Zhuang, Q. Regional trends
- and drivers of the global methane budget. Global Change Biology, 28, 182–200. https://doi.org/10.1111/gcb.15901,
- 3595 2021
- Steele, L. P., Fraser, P. J., Rasmussen, R. A., Khalil, M. A. K., Conway, T. J., Crawford, A. J., Gammon, R. H., Masarie,
- K. A. and Thoning, K. W.: The global distribution of methane in the troposphere, J. Atmospheric Chem., 5, 125–171,
- 3598 1987.
- 3599 Stevenson, D. S., Derwent, R. G., Wild, O., and Collins, W. J.: COVID-19 lockdown emission reductions have the
- potential to explain over half of the coincident increase in global atmospheric methane, Atmos. Chem. Phys., 22,
- 3601 14243–14252, https://doi.org/10.5194/acp-22-14243-2022, 2022.
- 3602 Stocker, B. D., Spahni, R. and Joos, F.: DYPTOP: a cost-efficient TOPMODEL implementation to simulate sub-grid
- spatio-temporal dynamics of global wetlands and peatlands, Geosci. Model Dev., 7(6), 3089–3110, doi:10.5194/gmd-
- 3604 7-3089-2014, 2014.
- Strauss, J., Abbott, B.W., Hugelius, G., Schuur, E., Treat, C., Fuchs, M., Schädel, C., Ulrich, M., Turetsky, M., Keuschnig,
- 3606 M. and Biasi, C. (2021) Chapter 9. Permafrost. In FAO Recarbonizing global soils-A technical manual of
- recommended management practices: Volume 2–Hot spots and bright spots of soil organic carbon, p.130, 2021
- 3608 Strode, S. A., Wang, J. S., Manyin, M., Duncan, B., Hossaini, R., Keller, C. A., Michel, S. E., and White, J. W. C.: Strong
- sensitivity of the isotopic composition of methane to the plausible range of tropospheric chlorine, Atmos. Chem. Phys.,
- 3610 20, 8405–8419, https://doi.org/10.5194/acp-20-8405-2020, 2020.
- 3611 Sugimoto, A., Inoue, T., Kitibutr, N., Abe, T. Methane oxidation by termite mounds estimate by the carbon isotope
- 3612 composition of methane. Glob. Biogeochem. Cy. 12, 595-605. 1998.
- 3613 Sweeney, C., Karion, A., Wolter, S., Newberger, T., Guenther, D., Higgs, J. A., Andrews, A. E., Lang, P. M., Neff, D.,
- Dlugokencky, E., Miller, J. B., Montzka, S. A., Miller, B. R., Masarie, K. A., Biraud, S. C., Novelli, P. C., Crotwell,
- 3615 M., Crotwell, A. M., Thoning, K. and Tans, P. P.: Seasonal climatology of CO₂ across North America from aircraft
- 3616 measurements in the NOAA/ESRL Global Greenhouse Gas Reference Network, J. Geophys. Res. Atmospheres,
- 3617 120(10), 5155–5190, doi:10.1002/2014jd022591, 2015.
- Tan, Z. and Zhuang, Q.: Methane emissions from pan-Arctic lakes during the 21st century: An analysis with process-





- based models of lake evolution and biogeochemistry, J. Geophys. Res. Biogeosciences, 120(12), 2641–2653, doi:10.1002/2015JG003184, 2015.
- Tans, P. and Zwellberg, C.: 17th WMO/IAEA Meeting on Carbon Dioxide, Other Greenhouse Gases and Related Tracers
 Measurement Techniques (GGMT-2013), GAW Report, WMO, Geneva. [online] Available from:
 https://library.wmo.int/index.php?lvl=notice_display&id=16373#.XnpBPW7jIq8, 2014.
- Taranu, Z.E., I. Gregory-Eaves, P.R. Leavitt, L. Bunting, T. Buchaca, J. Catalan, I. Domaizon, P. Guilizzoni, A. Lami, S.
 McGowan, H. Moorhouse, G. Morabito, F.R. Pick, M.A. Stevenson, P.L. Thompson, and R.D. Vinebrooke:
 Acceleration of cyanobacterial dominance in north temperate-subarctic lakes during the Anthropocene. Ecology
 Letters, 18(4): p. 375-384., 2015
- Taylor, P. G., Bilinski, T. M., Fancher, H. R. F., Cleveland, C. C., Nemergut, D. R., Weintraub, S. R., Wieder, W. R. and Townsend, A. R.: Palm oil wastewater methane emissions and bioenergy potential, Nat. Clim. Change, 4(3), 151–152, doi:10.1038/nclimate2154, 2014.
- le Texier, H., Solomon, S. and Garcia, R. R.: The role of molecular hydrogen and methane oxidation in the water vapour budget of the stratosphere, Q. J. R. Meteorol. Soc., 114(480), 281–295, doi:10.1002/qi.49711448002, 1988.
- Thanwerdas, J., Saunois, M., Berchet, A., Pison, I., Vaughn, B. H., Michel, S. E., and Bousquet, P.: Variational inverse modeling within the Community Inversion Framework v1.1 to assimilate δ13C(CH4) and CH4: a case study with model LMDz-SACS, Geosci. Model Dev., 15, 4831–4851, https://doi.org/10.5194/gmd-15-4831-2022, 2022a.
- Thanwerdas, J., Saunois, M., Pison, I., Hauglustaine, D., Berchet, A., Baier, B., Sweeney, C., and Bousquet, P.: How do
 Cl concentrations matter for the simulation of CH4 and δ13C(CH4) and estimation of the CH4 budget through
 atmospheric inversions?, Atmos. Chem. Phys., 22, 15489–15508, https://doi.org/10.5194/acp-22-15489-2022, 2022b.
- Thanwerdas, J., Saunois, M., Berchet, A., Pison, I., and Bousquet, P.: Investigation of the renewed methane growth post-2007 with high-resolution 3-D variational inverse modeling and isotopic constraints, Atmos. Chem. Phys., 24, 2129– 2167, https://doi.org/10.5194/acp-24-2129-2024, 2024.
- Thompson, R. L., Montzka, S. A., Vollmer, M. K., Arduini, J., Crotwell, M., Krummel, P. B., Lunder, C., Mühle, J., O'Doherty, S., Prinn, R. G., Reimann, S., Vimont, I., Wang, H., Weiss, R. F., and Young, D.: Estimation of the atmospheric hydroxyl radical oxidative capacity using multiple hydrofluorocarbons (HFCs), Atmos. Chem. Phys., 24, 1415–1427, https://doi.org/10.5194/acp-24-1415-2024, 2024.
- Thoning, K. W., Tans, P. P. and Komhyr, W. D.: Atmospheric carbon dioxide at Mauna Loa Observatory. 2. Analysis of the NOAA GMCC data, 1974,1985, J. Geophys. Res., 94(D6), 8549–8565, 1989.
- Thorneloe, S. A., Barlaz, M. A., Peer, R., Huff, L. C., Davis, L. and Mangino, J.: Waste management, in Atmospheric Methane: Its Role in the Global Environment, edited by M. Khalil, pp. 234–262, Springer-Verlag, New York., 2000.
- Thornton, B. F., Prytherch, J., Andersson, K., Brooks, I. M., Salisbury, D., Tjernström, M. and Crill, P. M.: Shipborne eddy covariance observations of methane fluxes constrain Arctic sea emissions, Sci. Adv., 6(5), eaay7934,





- 3652 doi:10.1126/sciadv.aay7934, 2020.
- Thornton B.F., Etiope G., Schwietzke S., Milkov A.V., Klusman R.W., Judd A., Oehler D.Z.: Conflicting estimates of natural geologic methane emissions. Elem. Sci. Anth., 9, 1, doi:https://doi.org/10.1525/elementa.2021.00031, 2021
- Thornton, J. A., Kercher, J. P., Riedel, T. P., Wagner, N. L., Cozic, J., Holloway, J. S., Dubé, W. P., Wolfe, G. M., Quinn, P. K., Middlebrook, A. M., Alexander, B. and Brown, S. S.: A large atomic chlorine source inferred from mid-
- 3657 continental reactive nitrogen chemistry, Nature, 464(7286), 271–274, doi:10.1038/nature08905, 2010.
- Thorpe, A. K., Kort, E. A., Cusworth, D. H., Ayasse, A. K., Bue, B. D., Yadav, V., Thompson, D. R., Frankenberg, C. Herner, J., Falk, M., Green, R. O., Miller, C. E., and Duren, R. M.: Methane emissions decline from reduced oil,
- natural gas, and refinery production during COVID-19, Environmental Research Communications, 5, 021006, 2023
- Tian, H., Xu, X., Liu, M., Ren, W., Zhang, C., Chen, G. and Lu, C.: Spatial and temporal patterns of CH₄ and N₂O fluxes
- in terrestrial ecosystems of North America during 1979–2008: application of a global biogeochemistry model,
- 3663 Biogeosciences, 7(9), 2673–2694, doi:10.5194/bg-7-2673-2010, 2010.
- Tian, H., Xu, X., Lu, C., Liu, M., Ren, W., Chen, G., Melillo, J. and Liu, J.: Net exchanges of CO₂, CH₄, and N₂O between
- China's terrestrial ecosystems and the atmosphere and their contributions to global climate warming, J. Geophys. Res.
- Biogeosciences, 116, G2, doi:10.1029/2010jg001393, 2011.
- Tian, H., Chen, G., Lu, C., Xu, X., Ren, W., Zhang, B., Banger, K., Tao, B., Pan, S., Liu, M., Zhang, C., Bruhwiler, L.
- and Wofsy, S.: Global methane and nitrous oxide emissions from terrestrial ecosystems due to multiple environmental
- 3669 changes, Ecosyst. Health Sustain., 1(1), 1–20, doi:doi:10.1890/ehs14-0015.1, 2015.
- Tian, H., Lu, C., Ciais, P., Michalak, A. M., Canadell, J. G., Saikawa, E., Huntzinger, D. N., Gurney, K. R., Sitch, S.,
- Zhang, B., Yang, J., Bousquet, P., Bruhwiler, L., Chen, G., Dlugokencky, E., Friedlingstein, P., Melillo, J., Pan, S.,
- Poulter, B., Prinn, R., Saunois, M., Schwalm, C. R. and Wofsy, S. C.: The terrestrial biosphere as a net source of
- greenhouse gases to the atmosphere, Nature, 531(7593), 225–228, doi:10.1038/nature16946, 2016.
- Tian, H., Xu, R., Canadell, J. G., Thompson, R. L., Winiwarter, W., Suntharalingam, P., Davidson, E. A., Ciais, P.,
- Jackson, R. B., Janssens-Maenhout, G., Prather, M. J., Regnier, P., Pan, N., Pan, S., Peters, G. P., Shi, H., Tubiello, F.
- 3676 N., Zaehle, S., Zhou, F., Arneth, A., Battaglia, G., Berthet, S., Bopp, L., Bouwman, A. F., Buitenhuis, E. T., Chang,
- J., Chipperfield, M. P., Dangal, S. R. S., Dlugokencky, E., Elkins, J. W., Eyre, B. D., Fu, B., Hall, B., Ito, A., Joos, F.,
- Krummel, P. B., Landolfi, A., Laruelle, G. G., Lauerwald, R., Li, W., Lienert, S., Maavara, T., MacLeod, M., Millet,
- D. B., Olin, S., Patra, P. K., Prinn, R. G., Raymond, P. A., Ruiz, D. J., van der Werf, G. R., Vuichard, N., Wang, J.,
- Weiss, R. F., Wells, K. C., Wilson, C., Yang, J., and Yao, Y.: A comprehensive quantification of global nitrous oxide
- 3681 sources and sinks, Nature, 586, 248–256, https://doi.org/10.1038/s41586-020-2780-0, 2020.
- Tian, H., Yao, Y., Li, Y., Shi, H., Pan, S., Najjar, R. G., et al. (2023). Increased terrestrial carbon export and CO2 evasion
- from global inland waters since the preindustrial era. Global Biogeochemical Cycles, 37, e2023GB007776.
- 3684 https://doi.org/10.1029/2023GB007776, 2023





- Tibrewal, K., Ciais, P., Saunois, M. Martinez, A., Lin, X., Thanwerdas, J., Deng, Z., Chevallier, F., Giron, C., Albergel,
- 3686 C., Tanaka, K., Patra, P., Tsuruta, A., Zheng, B., Belikov, D., Niwa, Y., Janardanan, R., Maksyutov, S., Segers, A.,
- Tzompa-Sosa, Z. A., Bousquet, P., and Sciare, J.: Assessment of methane emissions from oil, gas and coal sectors
- across inventories and atmospheric inversions, Commun Earth Environ 5, 26, https://doi.org/10.1038/s43247-023-
- 3689 01190-w, 2024
- Tiwari, Y. K. and Kumar, K. R.: GHG observation programs in India, Asian GAWgreenhouse Gases 3 Korea Meteorol.
- 3691 Adm. Chungnam South Korea, 2012.
- Tsuruta, A., Aalto, T., Backman, L., Hakkarainen, J., Laan-Luijkx, I. T. van der, Krol, M. C., Spahni, R., Houweling, S.,
- Laine, M., Dlugokencky, E., Gomez-Pelaez, A. J., Schoot, M. van der, Langenfelds, R., Ellul, R., Arduini, J., Apadula,
- F., Gerbig, C., Feist, D. G., Kivi, R., Yoshida, Y. and Peters, W.: Global methane emission estimates for 2000–2012
- 3695 from CarbonTracker Europe-CH₄ v1.0, Geosci. Model Dev., 10(3), 1261–1289, doi:10.5194/gmd-10-1261-2017,
- 3696 2017.
- Tsuruta, A.; Kivimäki, E.; Lindqvist, H.; Karppinen, T.; Backman, L.; Hakkarainen, J.; Schneising, O.; Buchwitz, M.;
- Lan, X.; Kivi, R.; et al. CH4 Fluxes Derived from Assimilation of TROPOMI XCH4 in CarbonTracker Europe-CH4:
- Evaluation of Seasonality and Spatial Distribution in the Northern High Latitudes. Remote Sens. 2023, 15, 1620.
- 3700 <u>https://doi.org/10.3390/rs15061620</u>, 2023
- Tubiello, F. N.: Greenhouse Gas Emissions Due to Agriculture, in Elsevier Encyclopedia of Food Systems., 2019.
- Tubiello, F. N., Salvatore, M., Rossi, S., Ferrara, A., Fitton, N. and Smith, P.: The FAOSTAT database of greenhouse gas
- 3703 emissions from agriculture, Environ. Res. Lett., 8(1), 015009, doi:10.1088/1748-9326/8/1/015009, 2013.
- Tubiello, F. N., Karl, K., Flammini, A., Gütschow, J., Obli-Laryea, G., Conchedda, G., Pan, X., Qi, S. Y., Halldórudóttir
- Heiðarsdóttir, H., Wanner, N., Quadrelli, R., Rocha Souza, L., Benoit, P., Hayek, M., Sandalow, D., Mencos Contreras,
- E., Rosenzweig, C., Rosero Moncayo, J., Conforti, P., and Torero, M.: Pre- and post-production processes increasingly
- dominate greenhouse gas emissions from agri-food systems, Earth Syst. Sci. Data, 14, 1795–1809,
- 3708 https://doi.org/10.5194/essd-14-1795-2022, 2022.
- Turetsky, M. R., Kotowska, A., Bubier, J., Dise, N. B., Crill, P., Hornibrook, E. R. C., Minkkinen, K., Moore, T. R.,
- Myers-Smith, I. H., Nykänen, H., Olefeldt, D., Rinne, J., Saarnio, S., Shurpali, N., Tuittila, E.-S., Waddington, J. M.,
- White, J. R., Wickland, K. P. and Wilmking, M.: A synthesis of methane emissions from 71 northern, temperate, and
- 3712 subtropical wetlands, Glob. Change Biol., 20(7), 2183–2197, doi:10.1111/gcb.12580, 2014.
- Turetsky, M. R., Abbott, B. W., Jones, M. C., Anthony, K. W., Olefeldt, D., Schuur, E. A. G., et al.: Carbon release
- 3714 through abrupt permafrost thaw. *Nature Geoscience*, 13(2), 138–143. https://doi.org/10.1038/s41561-019-0526-0,
- 3715 2020
- Turner, A. J., Fung, I., Naik, V., Horowitz, L. W. and Cohen, R. C.: Modulation of hydroxyl variability by ENSO in the
- 3717 absence of external forcing, Proc. Natl. Acad. Sci., 115(36), 8931–8936, doi:10.1073/pnas.1807532115, 2018.





- Turner, A. J., Frankenberg, C. and Kort, E. A.: Interpreting contemporary trends in atmospheric methane, Proc. Natl. Acad.
- 3719 Sci., 116(8), 2805, doi:10.1073/pnas.1814297116, 2019.
- 3720 UNEP, United Nations Environment Programme and Climate and Clean Air Coalition. Global Methane Assessment:
- Benefits and Costs of Mitigating Methane Emissions. Nairobi: United Nations Environment Programme., 2021
- 3722 UNEP, United Nations Environment Programme/Climate and Clean Air Coalition. Global Methane Assessment: 2030
- 3723 Baseline Report. Nairobi, 2022

3724

- 3725 USEPA: Greenhouse Gas Emissions Estimation Methodologies for Biogenic Emissions from Selected Source Categories:
- 3726 Solid Waste Disposal Wastewater Treatment Ethanol Fermentation, Measurement Policy Group, US EPA. [online]
- 3727 Available from: https://www3.epa.gov/ttnchie1/efpac/ghg/GHG Biogenic Report draft Dec1410.pdf (Accessed 11
- 3728 March 2020a), 2010a.
- USEPA: Office of Atmospheric Programs (6207J), Methane and Nitrous Oxide Emissions From Natural Sources, U.S.
- Environmental Protection Agency, EPA 430-R-10-001. Available online at http://nepis.epa.gov/, Washington, DC
- 3731 20460., 2010b.

USEPA: Draft: Global Anthropogenic Non-CO₂ Greenhouse Gas Emissions: 1990-2030. EPA 430-R-03-002, United

3733 States Environmental Protection Agency, Washington D.C., 2011.

USEPA: Global Anthropogenic Non-CO₂ Greenhouse Gas Emissions 1990-2030, EPA 430-R-12-006, US Environmental

- 3735 Protection Agency, Washington DC., 2012.
- USEPA: Draft Inventory of U.S. Greenhouse gas Emissions and Sinks: 1990-2014. EPA 430-R-16-002. February 2016.
- U.S. Environmental protection Agency, Washington, DC, USA., 2016.

USEPA: Global Non-CO2 Greenhouse Gas Emission Projections & Mitigation Potential: 2015-2050, EPA-430-R-19-010,

U.S. Environmental protection Agency, Washington, DC, USA., 2019

Valentine, D. W., Holland, E. A. and Schimel, D. S.: Ecosystem and physiological controls over methane production in

- 3741 northern wetlands, J. Geophys. Res., 99(D1), 1563–1571, 1994.
- Vardag, S. N., Hammer, S., O'Doherty, S., Spain, T. G., Wastine, B., Jordan, A. and Levin, I.: Comparisons of continuous
- atmospheric CH₄, CO₂ and N₂O measurements – results from a travelling instrument campaign at Mace Head,
- 3744 Atmospheric Chem. Phys., 14(16), 8403–8418, doi:10.5194/acp-14-8403-2014, 2014.

VODCA2GPP – a new, global, long-term (1988–2020) gross primary production dataset from microwave remote sensing,

- 3746 Earth Syst. Sci. Data, 14, 1063–1085, https://doi.org/10.5194/essd-14-1063-2022, 2022.
- Voulgarakis, A., Naik, V., Lamarque, J. F., Shindell, D. T., Young, P. J., Prather, M. J., Wild, O., Field, R. D., Bergmann,
- D., Cameron-Smith, P., Cionni, I., Collins, W. J., Dals√∏ren, S. B., Doherty, R. M., Eyring, V., Faluvegi, G., Folberth,
- G. A., Horowitz, L. W., Josse, B., MacKenzie, I. A., Nagashima, T., Plummer, D. A., Righi, M., Rumbold, S. T.,
- 3750 Stevenson, D. S., Strode, S. A., Sudo, K., Szopa, S. and Zeng, G.: Analysis of present day and future OH and methane





- lifetime in the ACCMIP simulations, Atmospheric Chem. Phys., 13(5), 2563–2587, doi:10.5194/acp-13-2563-2013,
- 3752 2013.
- Voulgarakis, A., Marlier, M. E., Faluvegi, G., Shindell, D. T., Tsigaridis, K. and Mangeon, S.: Interannual variability of
- tropospheric trace gases and aerosols: The role of biomass burning emissions, J. Geophys. Res. Atmospheres, 120(14),
- 3755 7157–7173, doi:10.1002/2014jd022926, 2015.
- Wallmann, K., Pinero, E., Burwicz, E., Haeckel, M., Hensen, C., Dale, A. and Ruepke, L.: The Global Inventory of
- Methane Hydrate in Marine Sediments: A Theoretical Approach, Energies, 5(7), 2449, 2012.
- Walter Anthony, K.M., Anthony, P., Grosse, G. and Chanton, J.: Geologic methane seeps along boundaries of Arctic
- permafrost thaw and melting glaciers. Nature Geoscience, 5(6), pp.419-426., DOI: 10.1038/ngeo1480, 2012
- Wang, F., Maksyutov, S., Tsuruta, A., Janardanan, R., Ito, A., Sasakawa, M., Machida, T., Morino, I., Yoshida, Y., Kaiser,
- J. W., Janssens-Maenhout, G., Dlugokencky, E. J., Mammarella, I., Lavric, J. V. and Matsunaga, T.: Methane Emission
- Estimates by the Global High-Resolution Inverse Model Using National Inventories, Remote Sens., 11(21), 2489,
- 3763 doi:10.3390/rs11212489, 2019a.
- Wang, G., X. Xia, S. Liu, L. Zhang, S. Zhang, J. Wang, N. Xi, and Q. Zhang, Intense methane ebullition from urban inland
- waters and its significant contribution to greenhouse gas emissions. Water Research, 189: p. 116654, 2021a
- Wang, X., Jacob, D. J., Eastham, S. D., Sulprizio, M. P., Zhu, L., Chen, Q., Alexander, B., Sherwen, T., Evans, M. J., Lee,
- B. H., Haskins, J. D., Lopez-Hilfiker, F. D., Thornton, J. A., Huey, G. L. and Liao, H.: The role of chlorine in global
- 3768 tropospheric chemistry, Atmospheric Chem. Phys., 19(6), 3981–4003, doi:10.5194/acp-19-3981-2019, 2019b.
- Wang, X., Jacob, D. J., Downs, W., Zhai, S., Zhu, L., Shah, V., Holmes, C. D., Sherwen, T., Alexander, B., Evans, M. J.,
- Eastham, S. D., Neuman, J. A., Veres, P. R., Koenig, T. K., Volkamer, R., Huey, L. G., Bannan, T. J., Percival, C. J.,
- Lee, B. H., and Thornton, J. A.: Global tropospheric halogen (Cl, Br, I) chemistry and its impact on oxidants, Atmos.
- 3772 Chem. Phys., 21, 13973–13996, https://doi.org/10.5194/acp-21-13973-2021, 2021b.
- Wang, Z., Deutscher, N. M., Warneke, T., Notholt, J., Dils, B., Griffith, D. W. T., Schmidt, M., Ramonet, M. and Gerbig,
- 3774 C.: Retrieval of tropospheric column-averaged CH₄ mole fraction by solar absorption FTIR-spectrometry using N₂O
- 3775 as a proxy, Atmospheric Meas. Tech., 7(10), 3295–3305, doi:10.5194/amt-7-3295-2014, 2014.
- 3776 Wang, Z.-P., Gu, Q., Deng, F.-D., Huang, J.-H., Megonigal, J. P., Yu, Q., Lü, X.-T., Li, L.-H., Chang, S., Zhang, Y.-H.,
- Feng, J.-C. and Han, X.-G.: Methane emissions from the trunks of living trees on upland soils, New Phytol., 211(2),
- 3778 429–439, doi:10.1111/nph.13909, 2016.
- Wania, R., I. Ross and I. C. Prentice: Implementation and evaluation of a new methane model within a dynamic global
- vegetation model: LPJ-WHyMe v1.3, Geosci. Model Dev. Discuss., 3, 1–59, 2010.
- Wania, R., Melton, J. R., Hodson, E. L., Poulter, B., Ringeval, B., Spahni, R., Bohn, T., Avis, C. A., Chen, G., Eliseev, A.
- V., Hopcroft, P. O., Riley, W. J., Subin, Z. M., Tian, H., van Bodegom, P. M., Kleinen, T., Yu, Z. C., Singarayer, J.
- 3783 S., Zurcher, S., Lettenmaier, D. P., Beerling, D. J., Denisov, S. N., Prigent, C., Papa, F. and Kaplan, J. O.: Present state





- of global wetland extent and wetland methane modelling: Methodology of a model inter-comparison project (WETCHIMP), Geosci. Model Dev., 6(3), 617–641, 2013.
- Wassmann, R., Lantin, R. S., Neue, H. U., Buendia, L. V., Corton, T. M. and Lu, Y.: Characterization of methane emissions in Asia III: Mitigation options and future research needs, Nutr. Cycl. Agroecosystems, 58, 23–36, 2000.
- Weber, T., Wiseman, N. A. and Kock, A.: Global ocean methane emissions dominated by shallow coastal waters, Nat. Commun., 10(1), 1–10, doi:10.1038/s41467-019-12541-7, 2019.
- Wells, N. S., J. J. Chen, D. T. Maher, P. Huang, D. V. Erler, M. Hipsey, and B. D. Eyre: Changing sediment and surface water processes increase CH4 emissions from human-impacted estuaries. Geochim. Cosmochim. Acta **280**: 130–147. doi:10.1016/j.gca.2020.04.020, 2020
- van der Werf, G. R., Randerson, J. T., Giglio, L., Collatz, G. J., Mu, M., Kasibhatla, P. S., Morton, D. C., DeFries, R. S., Jin, Y. and van Leeuwen, T. T.: Global fire emissions and the contribution of deforestation, savanna, forest, agricultural, and peat fires (1997-2009), Atmospheric Chem. Phys., 10(23), 11,707-11,735, 2010.
- van der Werf, G. R., Randerson, J. T., Giglio, L., Leeuwen, T. T. van, Chen, Y., Rogers, B. M., Mu, M., Marle, M. J. E. van, Morton, D. C., Collatz, G. J., Yokelson, R. J. and Kasibhatla, P. S.: Global fire emissions estimates during 1997–2016, Earth Syst. Sci. Data, 9(2), 697–720, doi:10.5194/essd-9-697-2017, 2017.
- Whalen, S. C.: Biogeochemistry of Methane Exchange between Natural Wetlands and the Atmosphere, Environ. Eng. Sci., 22(1), 73–94, doi:10.1089/ees.2005.22.73, 2005.
- Wiedinmyer, C., Kimura, Y., McDonald-Buller, E. C., Emmons, L. K., Buchholz, R. R., Tang, W., Seto, K., Joseph, M. B., Barsanti, K. C., Carlton, A. G., and Yokelson, R.: The Fire Inventory from NCAR version 2.5: an updated global fire emissions model for climate and chemistry applications, EGUsphere [preprint], https://doi.org/10.5194/egusphere-2023-124, 2023.
- Wik, M., Thornton, B. F., Bastviken, D., Uhlbäck, J. and Crill, P. M.: Biased sampling of methane release from northern lakes: A problem for extrapolation, Geophys. Res. Lett., 43(3), 1256–1262, doi:10.1002/2015gl066501, 2016a.
- Wik, M., Varner, R. K., Anthony, K. W., MacIntyre, S. and Bastviken, D.: Climate-sensitive northern lakes and ponds are critical components of methane release, Nat. Geosci., 9(2), 99–105, doi:10.1038/ngeo2578, 2016b.
- Wild, B., Teubner, I., Moesinger, L., Zotta, R.-M., Forkel, M., van der Schalie, R., Sitch, S., and Dorigo, W.: VODCA2GPP a new, global, long-term (1988–2020) gross primary production dataset from microwave remote sensing, Earth Syst. Sci. Data, 14, 1063–1085, https://doi.org/10.5194/essd-14-1063-2022, 2022.
- Winderlich, J., Chen, H., Gerbig, C., Seifert, T., Kolle, O., Lavrič, J. V., Kaiser, C., Höfer, A. and Heimann, M.:
 Continuous low-maintenance CO₂/CH₄/H₂O measurements at the Zotino Tall Tower Observatory (ZOTTO) in Central
 Siberia, Atmospheric Meas. Tech., 3(4), 1113–1128, doi:10.5194/amt-3-1113-2010, 2010.
- Wilson, C., Chipperfield, M. P., Gloor, M., Parker, R. J., Boesch, H., McNorton, J., Gatti, L. V., Miller, J. B., Basso, L. S., and Monks, S. A.: Large and increasing methane emissions from eastern Amazonia derived from satellite data,





- 3817 2010–2018, Atmos. Chem. Phys., 21, 10643–10669, https://doi.org/10.5194/acp-21-10643-2021, 2021.
- Wood, T.G. and Sands, W.A. The role of termites in ecosystems. In: Brian, M.V. (Ed.), Production Ecology of Ants and Termites. Cambridge University Press, Cambridge, UK, 245–292, 1978.
- Woodward G, Perkins D.M., and Brown L. E.: Climate change and freshwater ecosystems: impacts across multiple levels of organization, Philos Trans R Soc Lond B Biol Sci. 365(1549), 2093-106, doi: 10.1098/rstb.2010.0055, 2010
- Woodward, G., Gessner, M. O., Giller, P. S., Gulis, V., Hladyz, S., Lecerf, A., Malmqvist, B., McKie, B. G., Tiegs, S. D.,
- Cariss, H., Dobson, M., Elosegi, A., Ferreira, V., Graça, M. A. S., Fleituch, T., Lacoursière, J. O., Nistorescu, M.,
- Pozo, J., Risnoveanu, G., Schindler, M., Vadineanu, A., Vought, L. B.-M. and Chauvet, E.: Continental-Scale Effects
- of Nutrient Pollution on Stream Ecosystem Functioning, Science, 336(6087), 1438–1440,
- 3826 doi:10.1126/science.1219534, 2012.
- Woolway RI, Jones ID, Maberly SC, French JR, Livingstone DM, Monteith DT, et al.: Diel Surface Temperature Range Scales with Lake Size, PLoS ONE 11(3): e0152466, doi:10.1371/journal.pone.0152466, 2016
- Worden, J. R., Bloom, A. A., Pandey, S., Jiang, Z., Worden, H. M., Walker, T. W., Houweling, S. and Röckmann, T.:
- Reduced biomass burning emissions reconcile conflicting estimates of the post-2006 atmospheric methane budget,
- 3831 Nat. Commun., 8(1), 2227, doi:10.1038/s41467-017-02246-0, 2017.
- Wu, Z., Li, J., Sun, Y. et al.: Imbalance of global nutrient cycles exacerbated by the greater retention of phosphorus over
- nitrogen in lakes. *Nat. Geosci.* 15, 464–468, https://doi.org/10.1038/s41561-022-00958-7, 2022
- Wuebbles, D. J. and Hayhoe, K.: Atmospheric methane and global change, Earth-Sci. Rev., 57(3–4), 177–210, 2002.
- Wunch, D., Toon, G. C., Blavier, J.-F. L., Washenfelder, R. A., Notholt, J., Connor, B. J., Griffith, D. W. T., Sherlock, V.
- and Wennberg, P. O.: The Total Carbon Column Observing Network, Philos. Trans. R. Soc. A, 369(1943),
- 3837 doi:10.1098/rsta.2010.0240, 2011.
- Wunch, D., Toon, G. C., Hedelius, J. K., Vizenor, N., Roehl, C. M., Saad, K. M., Blavier, J.-F. L., Blake, D. R. and
- Wennberg, P. O.: Quantifying the loss of processed natural gas within California's South Coast Air Basin using long-
- term measurements of ethane and methane, Atmospheric Chem. Phys., 16(22), 14091–14105, doi:10.5194/acp-16-
- 3841 14091-2016, 2016.
- Wunch, D., Jones, D. B. A., Toon, G. C., Deutscher, N. M., Hase, F., Notholt, J., Sussmann, R., Warneke, T., Kuenen, J.,
- Denier van der Gon, H., Fisher, J. A. and Maasakkers, J. D.: Emissions of methane in Europe inferred by total column
- 3844 measurements, Atmos Chem Phys, 19(6), 3963–3980, doi:10.5194/acp-19-3963-2019, 2019.
- Xiao, K., F. Beulig, H. Røy, B. B. Jørgensen, and N. Risgaard-Petersen: Methylotrophic methanogenesis fuels cryptic
- methane cycling in marine surface sediment. Limnol. Oceanogr. 63: 1519–1527. doi:10.1002/lno.10788, 2018
- 3847 Xu, X. F., Tian, H. Q., Zhang, C., Liu, M. L., Ren, W., Chen, G. S., Lu, C. Q. and Bruhwiler, L.: Attribution of spatial and
- temporal variations in terrestrial methane flux over North America, Biogeosciences, 7(11), 3637–3655,
- 3849 doi:10.5194/bg-7-3637-2010, 2010.





- Xu, X., P Sharma, S Shu, TZ Lin, P Ciais, F Tubiello, P Smith, N Campbell and AK Jain (2021), Global Greenhouse Gas
 Emissions from Plant- and Animal-Based Food, Nature Food, https://doi.org/10.1038/s43016-021-00358-x, 2021
- Yacovitch, T. I., C. Daube, S. C. Herndon, and J. B. McManus: Isotopes on a Boat: Real-Time Spectroscopic Measurement
- of Methane Isotopologues from Offshore Oil and Gas Emissions, OSA Optical Sensors and Sensing Congress 2021
- 3854 (AIS, FTS, HISE, SENSORS, ES), S. Buckley, F. Vanier, S. Shi, K. Walker, I. Coddington, S. Paine, K. Lok Chan,
- W. Moses, S. Qian, P. Pellegrino, F. Vollmer, G., J. Jágerská, R. Menzies, L. Emmenegger, and J. Westberg, eds.,
- 3856 OSA Technical Digest (Optica Publishing Group, 2021), paper EW5D.3, 2021
- Yan, X., Akiyama, H., Yagi, K. and Akimoto, H.: Global estimations of the inventory and mitigation potential of methane
- emissions from rice cultivation conducted using the 2006 Intergovernmental Panel on Climate Change Guidelines,
- 3859 Glob. Biogeochem. Cycles, 23(2), doi:10.1029/2008gb003299, 2009.
- Yang, P., D. Y. F. Lai, H. Yang, and others: Large increase in CH4 emission following conversion of coastal marsh to
- aquaculture ponds caused by changing gas transport pathways. Water Res. 222: 118882.
- 3862 doi:10.1016/j.watres.2022.118882, 2022
- Yin, Y., Chevallier, F., Ciais, P., Broquet, G., Fortems-Cheiney, A., Pison, I. and Saunois, M.: Decadal trends in global
- 3864 CO emissions as seen by MOPITT, Atmospheric Chem. Phys., 15(23), 13433–13451, doi:10.5194/acp-15-13433-
- 3865 2015, 2015.
- Yoshida, Y., Kikuchi, N., Morino, I., Uchino, O., Oshchepkov, S., Bril, A., Saeki, T., Schutgens, N., Toon, G. C., Wunch,
- D., Roehl, C. M., Wennberg, P. O., Griffith, D. W. T., Deutscher, N. M., Warneke, T., Notholt, J., Robinson, J.,
- 3868 Sherlock, V., Connor, B., Rettinger, M., Sussmann, R., Ahonen, P., Heikkinen, P., Kyrö, E., Mendonca, J., Strong, K.,
- Hase, F., Dohe, S. and Yokota, T.: Improvement of the retrieval algorithm for GOSAT SWIR XCO₂ and XCH₄ and
- their validation using TCCON data, Atmospheric Meas. Tech., 6(6), 1533–1547, doi:10.5194/amt-6-1533-2013, 2013.
- Yuan, J., J. Xiang, D. Liu, and others: Rapid growth in greenhouse gas emissions from the adoption of industrial-scale
- 3872 aquaculture. Nat. Clim. Chang. 9: 318–322. doi:10.1038/s41558-019-0425-9, 2019
- 3873 Yver Kwok, C. E., Müller, D., Caldow, C., Lebègue, B., Mønster, J. G., Rella, C. W., Scheutz, C., Schmidt, M., Ramonet,
- 3874 M., Warneke, T., Broquet, G. and Ciais, P.: Methane emission estimates using chamber and tracer release experiments
- for a municipal waste water treatment plant, Atmospheric Meas. Tech., 8(7), 2853–2867, doi:10.5194/amt-8-2853-
- 3876 2015, 2015.
- Zavala-Araiza, D., Lyon, D. R., Alvarez, R. A., Davis, K. J., Harriss, R., Herndon, S. C., Karion, A., Kort, E. A., Lamb,
- 3878 B. K., Lan, X., Marchese, A. J., Pacala, S. W., Robinson, A. L., Shepson, P. B., Sweeney, C., Talbot, R., Townsend-
- Small, A., Yacovitch, T. I., Zimmerle, D. J. and Hamburg, S. P.: Reconciling divergent estimates of oil and gas methane
- 3880 emissions, Proc. Natl. Acad. Sci. USA, 112, 15597–15602, doi:10.1073/pnas.1522126112, 2015.
- 3881 Zhang: Magnitude, spatio-temporal variability and environmental controls of methane emissions from global rice fields:
- 3882 Implications for water management and climate mitigation, Glob. Change Biol., 2016.



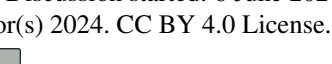


- Zhang, B. and Chen, G. Q.: China's CH₄ and CO₂ Emissions: Bottom-Up Estimation and Comparative Analysis, Ecol.
- 3884 Indic., 47, 112–122, doi:10.1016/j.ecolind.2014.01.022, 2014.
- Zhang, L., X. Xia, S. Liu, S. Zhang, S. Li, J. Wang, G. Wang, H. Gao, Z. Zhang, Q. Wang, W. Wen, R. Liu, Z. Yang, E.H.
- Stanley, and P.A. Raymond: Significant methane ebullition from alpine permafrost rivers on the East Qinghai–Tibet
- 3887 Plateau. Nature Geoscience, 13(5): p. 349-354, 2020
- Zhang, L., H. Tian, H. Shi, S. Pan, J. Chang, S. R. S. Dangal, X. Qin, S. Wang, F. N. Tubiello, J. G. Canadell, R. B.
- Jackson: A 130-year global inventory of methane emissions from livestock: Trends, patterns, and drivers, Global
- 3890 Change Biology, 28 (17), 5142-5158. https://doi.org/10.1111/gcb.16280, 2022
- Zhang, Y., Xiao, X., Wu, X., Zhou, S., Zhang, G., Qin, Y., and Dong, J.: A global moderate resolution dataset of gross
- primary production of vegetation for 2000–2016, Sci. Data, 4, 1–13, https://doi.org/10.1038/sdata.2017.165, 2017.
- Zhang, Y., Jacob, D. J., Maasakkers, J. D., Sulprizio, M. P., Sheng, J.-X., Gautam, R., and Worden, J.: Monitoring global
- tropospheric OH concentrations using satellite observations of atmospheric methane, Atmos. Chem. Phys., 18, 15959–
- 3895 15973, https://doi.org/10.5194/acp-18-15959-2018, 2018.
- Zhang, Z., Zimmermann, N. E., Kaplan, J. O. and Poulter, B.: Modeling spatiotemporal dynamics of global wetlands:
- comprehensive evaluation of a new sub-grid TOPMODEL parameterization and uncertainties, Biogeosciences, 13(5),
- 3898 1387–1408, doi:10.5194/bg-13-1387-2016, 2016.
- Zhang, Z., Fluet-Chouinard, E., Jensen, K., McDonald, K., Hugelius, G., Gumbricht, T., et al. Development of the global
- dataset of Wetland Area and Dynamics for Methane Modeling (WAD2M). Earth System Science Data, 13(5), 2001–
- 3901 2023. https://doi.org/10.5194/essd-13-2001-2021, 2021.
- Zhang, Z., Poulter, B., Feldman, A.F., Ying, Q, Ciais, P., Peng, S. and Li, X.: Recent intensification of wetland methane
- 3903 feedback, Nat. Clim. Chang, 13, 430–433, https://doi.org/10.1038/s41558-023-01629-0, 2023
- Zhang, Z., Poulter, B., Melton, J., Riley, W., Allen, G., Beerling D., Bousquet P., Canadell, J., Fluet-Chouinard E., Ciais,
- P., Gedney, N., Hopcroft, P., Ito, A., Jackson, R., Jain, A., Jensen, K., Joos, F., Kleinen, T., Knox, S., Li., T., Li, X.,
- Liu, X., McDonald, K., McNicol, G., Miller, P., Müller, J., Patra, P., Prigent, C., Peng, C., Peng, S., Qin, Z., Riggs,
- 3907 R., Saunois, M., Sun Q., Tian, H., Xu, X., Yao Y., Yi, X., Zhang, W., Zhu, Q., Zhu, Q., and Zhuang, Q.: Ensemble
- 3908 estimates of global wetland methane emissions over 2000-2020. Global Change Biology, in review.
- Zhao, J., M. Zhang, W. Xiao, L. Jia, X. Zhang, J. Wang, Z. Zhang, Y. Xie, Y. Pu, S. Liu, Z. Feng, and X. Lee: Large
- 3910 methane emission from freshwater aquaculture ponds revealed by long-term eddy covariance observation. Agricultural
- 3911 and Forest Meteorology, 308-309: p. 108600, 2021
- Zhao, Y., Saunois, M., Bousquet, P., Lin, X., Berchet, A., Hegglin, M. I., Canadell, J. G., Jackson, R. B., Hauglustaine,
- D. A., Szopa, S., Stavert, A. R., Abraham, N. L., Archibald, A. T., Bekki, S., Deushi, M., Jöckel, P., Josse, B., Kinnison,
- D., Kirner, O., Marécal, V., O'Connor, F. M., Plummer, D. A., Revell, L. E., Rozanov, E., Stenke, A., Strode, S.,
- 3915 Tilmes, S., Dlugokencky, E. J. and Zheng, B.: Inter-model comparison of global hydroxyl radical (OH) distributions





- and their impact on atmospheric methane over the 2000–2016 period, Atmospheric Chem. Phys., 19(21), 13701–13723, doi:10.5194/acp-19-13701-2019, 2019.
- Zhao, Y., Saunois, M., Bousquet, P., Lin, X., Berchet, A., Hegglin, M. I., Canadell, J. G., Jackson, R. B., Dlugokencky,
- E. J., Langenfelds, R. L., Ramonet, M., Worthy, D. and Zheng, B.: Influences of hydroxyl radicals (OH) on top-down
- estimates of the global and regional methane budgets, Atmospheric Chem. Phys. Discuss., 1-45, doi:10.5194/acp-
- 3921 2019-1208, 2020.
- Zhao, Y., Saunois, M., Bousquet, P., Lin, X., Hegglin, M. I., Canadell, J. G., Jackson, R. B., and Zheng, B.: Reconciling
- the bottom-up and top-down estimates of the methane chemical sink using multiple observations, Atmos. Chem. Phys.,
- 3924 23, 789–807, https://doi.org/10.5194/acp-23-789-2023, 2023.
- Zheng, B., Chevallier, F., Ciais, P., Yin, Y. and Wang, Y.: On the Role of the Flaming to Smoldering Transition in the
- 3926 Seasonal Cycle of African Fire Emissions, Geophys. Res. Lett., 45(21), 11,998-12,007, doi:10.1029/2018GL079092,
- 3927 2018a.
- Zheng, B., Chevallier, F., Ciais, P., Yin, Y., Deeter, M. N., Worden, H. M., Wang, Y., Zhang, Q. and He, K.: Rapid decline
- in carbon monoxide emissions and export from East Asia between years 2005 and 2016, Environ. Res. Lett., 13(4),
- 3930 044007, doi:10.1088/1748-9326/aab2b3, 2018b.
- Zheng, B., Chevallier, F., Yin, Y., Ciais, P., Fortems-Cheiney, A., Deeter, M. N., Parker, R. J., Wang, Y., Worden, H. M.,
- and Zhao, Y.: Global atmospheric carbon monoxide budget 2000–2017 inferred from multi-species atmospheric
- inversions, Earth Syst. Sci. Data, 11, 1411–1436, doi: 10.5194/essd-11-1411-2019, 2019.
- Zheng, B., Ciais, P., Chevallier, F., Yang, H., Canadell, J. G., Chen, Y., van der Velde, I. R., Aben, I., Chuvieco, E., Davis,
- S. J., Deeter, M., Hong, C., Kong, Y., Li, H., Li, H., Lin, X., He, K., and Zhang, Q.: Record-high CO2 emissions from
- 3936 boreal fires in 2021, Science, 379, 912-917, doi: 10.1126/science.ade0805, 2023.
- Zhu, Q., Liu, J., Peng, C., Chen, H., Fang, X., Jiang, H., Yang, G., Zhu, D., Wang, W. and Zhou, X.: Modelling methane
- emissions from natural wetlands by development and application of the TRIPLEX-GHG model, Geosci. Model Dev.,
- 3939 7(3), 981–999, doi:10.5194/gmd-7-981-2014, 2014.
- Zhu, Q., Peng, C., Chen, H., Fang, X., Liu, J., Jiang, H., Yang, Y. and Yang, G.: Estimating global natural wetland methane
- 3941 emissions using process modelling: spatio-temporal patterns and contributions to atmospheric methane fluctuations,
- 3942 Glob. Ecol. Biogeogr., 24, 959–972, 2015.
- Zhu, Y., K.J. Purdy, Ö. Eyice, L. Shen, S.F. Harpenslager, G. Yvon-Durocher, A.J. Dumbrell, and M. Trimmer:
- Disproportionate increase in freshwater methane emissions induced by experimental warming. Nature Climate Change,
- 3945 10(7): p. 685-690., 2020
- Zhuang, Q., Melillo, J. M., Kicklighter, D. W., Prinn, R. G., McGuire, A. D., Steudler, P. A., Felzer, B. S. and Hu, S.:
- Methane fluxes between terrestrial ecosystems and the atmosphere at northern high latitudes during the past century:
- A retrospective analysis with a process-based biogeochemistry model, Glob. Biogeochem Cycles, 18(3), GB3010,



doi:10.1029/2004gb002239, 2004.



(0)	•
	BY

3949

3950 Zhuang, Q., Chen, M., Xu, K., Tang, J., Saikawa, E., Lu, Y., Melillo, J. M., Prinn, R. G. and McGuire, A. D.: Response 3951 of global soil consumption of atmospheric methane to changes in atmospheric climate and nitrogen deposition, Glob. 3952 Biogeochem. Cycles, 27(3), 650-663, doi:10.1002/gbc.20057, 2013. 3953 Zhuang, Q., M. Guo, J.M. Melack, X. Lan, Z. Tan, Y. Oh, and L.R. Leung: Current and Future Global Lake Methane Emissions: A Process-Based Modeling Analysis. Journal of Geophysical Research: Biogeosciences, 128(3): p. 3954 3955 e2022JG007137, 2023





Table 1: Bottom-up (BU) models and inventories for anthropogenic and biomass burning used in this study. *Due to its limited sectoral breakdown this dataset was not used in Table 3.

B-U models and inventories	Contribution	Time period (resolution)	Gridded	References
CEDS (country based)	Fossil fuels, Agriculture and waste, Biofuel	ture and		Hoesly et al. (2018)
CEDS (gridded)*	Fossil fuels, Agriculture and waste, Biofuel	1970-2020 (monthly)	0.5x0.5°	Hoesly et al. (2018) O'Rourke et al (2021)
EDGARv6	Fossil fuels, Agriculture and waste, Biofuel	1990-2018^ (yearly, monthly for some sectors)	0.1x0.1°	Oreggioni et al. (2021), Crippa et al. (2021)
EDGARv7	Fossil fuels, GARv7 Agriculture and waste, Biofuel		0.1x0.1°	Crippa et al. (2023)
IIASA GAINS v4.0	Fossil fuels, Agriculture and waste, Biofuel	1990-2020 (yearly)	0.5x0.5°	Höglund-Isaksson et al., (2020)
USEPA	Fossil fuels, Agriculture and waste, Biofuel, Biomass Burning	1990-2030 (10-yr interval, interpolated to yearly)	no	USEPA (2019)
FAO-CH4	Agriculture, Biomass Burning	1961-2020 1990-2020 (Yearly)	no	Federici et al. (2015); Tubiello et al. (2013); Tubiello (2019)
FINNv2.5	Biomass burning	2002-2020 (daily)	1km resolution	Wiedinmyer et al. (2023)
GFASv1.3	Biomass burning	2003-2020 (daily)	0.1x0.1°	Kaiser et al. (2012)
GFEDv4.1s	Biomass burning	1997-2020 (monthly)	0.25x0.25°	Giglio et al. (2013); van der Werf et al (2017)
QFEDv2.5	Biomass burning	2000-2020 (daily)	0.1x0.1°	Darmenov and da Silva (2015)





Table 2: Biogeochemical models that computed wetland emissions used in this study. Model runs were performed with two climate inputs, CRU and GSWP3-W5E5. Models were run with prognostic (using their own calculation of wetland areas) and/or diagnostic (using WAD2M (Zhang et al., 2021b)) wetland surface areas (see Sect 3.2.1).

Model	Institution	Pi	rognostic	Γ	Diagnostic	References
		CRU	GSWP3-W5E5	CRU	GSWP3-W5E5	
CH4MOD _{wetland}	Institute of Atmospheric Physics, CAS	n	n	у	у	Li et al. (2010)
CLASSIC	Environment and Climate Change Canada	у	y*	у	y*	Arora et al. (2018); Melton and Arora (2016)
DLEM	Boston College	у	у	у	у	Tian et al. (2015, 2023)
ELM-ECA	Lawrence Berkeley National Laboratory	у	у	у	у	Riley et al. (2011)
ISAM	University of Illinois, Urbana- Champaign	у	у	у	у	Shu et al. (2020) Xu et al. (2021)
JSBACH	MPI	у	у	у	у	Kleinen et al. (2020, 2021, 2023)
JULES	UKMO	у	у	у	у	Gedney et al. (2019)
LPJ-GUESS	Lund University	n	n	у	у	McGuire et al. (2012)
LPJ-MPI	MPI	у	у	у	у	Kleinen et al. (2012)
LPJ-WSL	NASA GSFC	у	у	у	у	Zhang et al. (2016)
LPX-Bern	University of Bern	у	y	у	у	Spahni et al. (2011), Stocker et al. (2014)
ORCHIDEE	LSCE	у	у	у	у	Ringeval et al. (2011)





SDGVM	University of Birmingham/ University of Sheffield	у	у	у	y	Beerling & Woodward (2001), Hopcroft et al. (2011, 2020)
TEM-MDM	Purdue University	n	n	у	y	Zhuang et al. (2004)
TRIPLEX-GHG	UQAM	n	n	у	y	Zhu et al. (2014, 2015)
VISIT	NIES	у	y	у	y	Ito and Inatomi (2012)

^{*}CLASSIC uses GSWP3-W5E version 2 that covers the time period till 2016. All other models use GSWP-W5E5 version 3.





Table 3: Global methane emissions by source type in $Tg CH_4 \ yr^{-1}$ from Saunois et al. (2020) (left column pair) and from this work using bottom-up and top-down approaches. Because top-down models cannot fully separate individual processes, only five categories of emissions are provided (see text). Uncertainties are reported as [min-max] range of reported studies. The mean, minimum and maximum values are calculated while discarding outliers, for each category of source and sink. As a result, discrepancies may occur when comparing the sum of categories and their corresponding total due to differences in outlier detections. Differences of 1 $Tg CH_4 \ yr^{-1}$ in the totals can also occur due to rounding errors. Compared to Saunois et al. (2020), emissions are split between "direct anthropogenic" emissions and "natural and indirect anthropogenic" sources. We also propose an estimate of the double-counting between bottom-up wetland and inland freshwater ecosystems emissions.

	Saunois e	t al. (2020)			This	work		
Period of time		-2009	2000	-2009		-2019	20	20
Approaches	bottom-up	top-down	bottom-up	top-down	bottom-up	top-down	bottom-up	top-down
	NA	TURAL &	& indirect	anthropo	genic SO	URCES		
Combined	306 [229-	180	242	158 [145-	248	165 [145-	251 [171-	175 [151-
wetlands and	391]	[153-196]	[156-355]	172]	[159-369]	214]	364]	229]
inland								
freshwaters								
Wetlands	147	180	153	158 [145-	159 [119-	165 [145-	161	175 [151-
	[102-179]	[153-196]	[116-189] (***)	172]	203] (***)	214]	[131-198] (***)	229]
Inland freshwaters	159		112 [49-		112		112 [49-	
a	[117-212]		202]		[49-202]		202]	
			_				-	
Double counting b	NA		-23 [-9		-23 [-9		-23 [-9	
			36]		36]		36]	
Other natural	63	35	63	44	63	43	63	44
sources	[26-94]	[21-47]	[24-93]	[40-46]	[24-93]	[40-46]	[24-93]	[40-47]
Land sources	50 [17-72]		51 [18-73]					
Geological	38 [13-53]		38 [13-53]					
(onshore) Wild animals	2 [1-3]		2 [1-3]					
Termites	9 [3-15]		10 [4-16]					
Wildfires	(**)		(**)					
Permafrost soils	1 [0-1]		1 [0-1]					
(direct)	(*)		(*)					
Vegetation	(*)		(*)					
Coastal and Oceanic sources ^c	13 [9-22]		12 [6-20]					
Biogenic	6 [4-10]		5 [3-10]					
Geological	7 [5-12]		7 [5-12]					
(offshore)								
TOTAL								
NATURAL &	369	215	305	204 [189-	311	206 [188-	314	216 [193-
INDIRECT SOURCES	[245-485]	[176-243]	[180-448]	223]	[183-462]	225]	[195-457]	241]
SOURCES		DIRECT	ANTHRO)PACENI	IC SOUR	CEC	ı	
Agriculture and	192	202	194	210	211	228	211	245
waste	[178-206]	[198-219]	[181-208]	[197-223]	[195-231]	[213-242]	[204-216]	[232-259]
Agriculture	132 [NA]	1	134 [125-		143 [132-		147 [143-	
			142]		155]		149]	
Enteric ferm. & manure	104 [93-109]		104		112		117	
manure Rice cultivation	28 [23-34]		[100 -110] 30 [24-34]		[107 -118] 32 [25-37]		[114 -124] 32 [29-37]	
Landfills and waste	60 [55-63]		61 [52-71]		69 [56-80]		71 [60-84]	
Fossil fuels	110	101	105 [97-	105 [88-	120 [117-	115 [100-	128 [120-	122 [101-
	[94-129]	[71-151]	123]	115]	125]	124]	133]	133]
Coal mining	32 [24-42]		(****)		(****)		(****)	





	Saunois et	t al. (2020)			This	work		
Period of time	2000	-2009	2000	-2009	2010	-2019	20	020
Oil & Gas Industry Transport	73 [60-85] 2 [0-6] 4 [1-11]		30 [26-32] 65 [63-71] 4 [1-8] 3 [1-8]		40 [37-44] 67 [57-74] 5 [1-9] 2 [1-3]		41 [38-43] 74 [67-80] 5 [1-8] 2 [1-3]	
Biomass & biof.	31 [26-46]	29 [23-35]	30 [22-44]	26 [22-29]	28 [21-39]	27 [26-27]	27 [20-41]	26 [22-27]
burn.				,		,		,
Biomass burning Biofuel burning	19 [15-32] 12 [9-14]		19 [14-29] 11 [8-14]		17 [12-24] 11 [8-14]		17 [13-27] 10 [7-14]	
TOTAL DIRECT ANTHROPOGENI C SOURCES	334 ^d [321-358]	332 [312-347]	333 ^d [305-365]	341 [319-355]	358 ^d [329-387]	369 [350-391]	372 ^d [345-409]	392 [368-409]
			S	INKS				
Total chemical loss	595 [489-749]	505 [459-516]	585 [481-716]	504 ^e [496-511]	602 [496-747]	521 ^e [485-532]	602 [496- 747]	538 ^e [503-554]
Tropospheric OH	553 [476-677]	[,]	546 [446-663]	[]	563 [462- 663]	[563 [462- 663]	[200 20 1]
Stratospheric loss Tropospheric Cl	31 [12-37] 11 [1-35]		34 [10-51] 6 [1-13]		35 [10-51] 6 [1-13]		35 [10-51] 6 [1-13]	
Soil uptake	30 [11-49]	34 [27-41]	30 [11-49]	34 [34-34]	31 [11-49]	35 [35-35]	31 [11-49]	36 [35-36]
TOTAL SINKS	625 [500-798]	540 [486-556]	615 [492-765]	538 [530- 545] ^e	633 [507-796]	554 [520- 567]°	633 [507-796]	575 [566- 589]°
		SOUR	CES – SI	NKS IMB	BALANCE			
TOTAL	703	547	638 [485-	543 [526-	669 [512-	575 [553-	685 [540-	608 [581-
SOURCES	[566-842]	[524-560]	813]	558]	849]	586]	865]	627]
TOTAL SINKS	625 [500-798]	540 [486-556]	615 [492-765]	538 [530-545] ^e	633 [507-796]	554 [550-567] ^e	633 [507-796]	575 [566- 589]°
IMBALANCE	78	3 [-10-38]	23	5 [-4-13] ^e	36	21 [19-33] ^e	52	32 [15-38] ^e
ATMOSPHERIC GROWTH ^f		5.8 [4.9-6.6] ^f		6.1 [5.2-6.9] ^f		20.9 [20.1-21.7] ^f		41.8 [40.7-42.9] ^f

^(*) uncertain but likely small for upland forest and aerobic emissions, potentially large for forested wetland, but likely included elsewhere

^(**) We stop reporting this value to avoid potential double counting with satellite-based products of biomass burning (see Sect. 3.1.5)

^(***) Here the numbers are from prognostic runs. To ensure a fair comparison with previous budgets (Saunois et al., 2020), the numbers are 163[117-195] for 2000-2009 from diagnostic runs with CRU/CRU-JRA-55 climate inputs (see Sect. 3.2.1).

^(****) Up to 8 Tg of additional emissions could account for ultra emitters (Lauvaux et al., 2022), as in Tibrewal et al. (2024), that are fully or partly missed in regular anthropogenic inventories

a: Freshwater includes lakes, ponds, reservoirs, streams and rivers, part of it is due to anthropogenic disturbances estimated in Sect.3.2.2

b: The double counting estimate is discussed in Sect. 3.2.2

c: includes flux from hydrates considered at 0 for this study, includes estuaries

d: Total anthropogenic emissions are based on estimates of full anthropogenic inventory and not on the sum of "Agriculture and Waste", "Fossil fuels" and "Biofuel and biomass burning" categories (see Sect. 3.1.2)

e: Some inversions did not provide the chemical sink. These values are derived from a subset of the inversion ensemble.

f: Atmospheric growth rates are given in the same unit Tg CH₄ yr⁻¹, based on the conversion factor of 2.75 Tg CH₄ ppb⁻¹ given by Prather et al. (2012) and the atmospheric growth rates provided in the text in ppb yr⁻¹.





Table 4: Top-down studies used here with their contribution to the decadal and yearly estimates noted. For decadal means, top down studies must provide at least 8 years of data over the decade to contribute to the estimate. Details on each inverse system and inversions are provided in Table S8 to S11 in the Supplementary Material.

Model	Institution	Observation used	Time period	Number of inversions	2000- 2009	2010- 2019	2020	References
Carbon Tracker- Europe CH ₄	FMI	Surface stations	2000-2020	4	у	у	у	Tsuruta et al. (2017)
LMDz-CIF	LSCE/CE A	Surface stations	2000-2020	4	у	у	у	Thanwerdas et al. (2022a)
LMDz-PYVAR	LSCE/CE A/THU	GOSAT Leicester v9.0	2010-2020	4	n	у	у	Zheng et al. (2018a, 2018b, 2019)
MIROC4-ACTM	JAMSTEC	Surface stations	2000-2020	5	у	у	у	Patra et al. (2018); Chandra et al. (2021)
NISMON-CH4	NIES/MRI	Surface stations	2000-2020	2	у	у	у	Niwa et al. (2022)
NIES-TM- FLEXPART (NTFVAR)	NIES	Surface stations	2000-2020	2	у	у	у	Maksyutov et al. (2020); Wang et al. (2019a)
NIES-TM- FLEXPART (NTFVAR)	NIES	GOSAT NIES L2 v02.95	2010-2020	1	n	у	у	Maksyutov et al. (2020); Wang et al. (2019a)
TM5-CAMS	TNO/VU	Surface stations	2000-2020	1	у	у	у	Segers et al. (2022)
TM5-CAMS	TNO/VU	GOSAT ESA/CCI v2.3.8 (combined with surface observations)	2010-2020	1	n	у	y	Segers et al. (2022)
	Total number of runs			24	18	24	24	





Table 5: Global and latitudinal total methane emissions in Tg CH₄ yr⁻¹, as decadal means (2000-2009 and 2010-2019) and for the year 2020 from this work using bottom-up and top-down approaches. Global and latitudinal emissions for 2000-2009 are also compared with Saunois et al. (2016, 2020) for top-down and bottom-up approaches when available. Uncertainties are reported as [min-max] range. The mean, minimum and maximum values are calculated while discarding outliers, for each category of source and sink. As a result, discrepancies may occur when comparing the sum of categories and their corresponding total due to differences in outlier detections. Differences of 1 Tg CH₄ yr⁻¹ in the totals can also occur due to rounding errors. For the latitudinal breakdown, bottom-up anthropogenic estimates are based only on the gridded products (see Table 1). As a result, the total from the latitudinal breakdown (line called "This work (gridded BU products only") is slightly different from the values provided in Table 3 and recalled in the line "This work (all BU products)".

Period	2000-	0-2009 2010-2019		20)20					
Approach	Bottom-up	Top-down	Bottom-up	Top-down	Bottom-up	Top-down				
	Global									
This work (all BU products)	638 [485-813]	543 [526-558]	669 [512-849]	575 [553-586]	685 [540-865]	608 [581-627]				
This work (gridded BU products only)	642 [501-809]		676 [526-845]		691 [565-862]					
S2020	703 [566-842]	547 [524-560]	-	-	-	-				
S2016	719[583-861]	552[535-566]	-	-	-	-				
			90°S-30°N							
This work	367 [254-487]	337 [311-361]	388 [275-503]	364 [337-390]	395 [292-521]	386 [353-425]				
S2020	408 [322-532]	346 [320-379]	-	-	-	-				
S2016	-	356 [334-381]	-	-	-	-				
			30°N-60°N							
This work	234 [169-335]	182 [162-197]	250 [184-345]	187 [160-204]	256 [186-356]	197 [170-215]				
S2020	252 [202-342]	178 [159-199]	-	-	-	-				
S2016	-	176[159-195]	-	-	-	-				
60°N-90°N										
This work	42 [22-79]	26 [22-33]	38[17-73]	24 [18-29]	39 [17-74]	25 [20-32]				
S2020	42 [28-70]	23 [17- 32]	-	-	-	-				
S2016	-	20 [15-25]	-	-	-	-				





Table 6: Latitudinal methane emissions in Tg CH₄ yr⁻¹ for the last decade 2010-2019, based on top-down and bottom-up approaches. Uncertainties are reported as [min-max] range of reported studies. The mean, minimum, and maximum values are calculated while discarding outliers, for each category of source and sink. As a result, discrepancies may occur when comparing the sum of categories and their corresponding total due to differences in outlier detections. Differences of 1 Tg CH₄ yr⁻¹ in the totals can also occur due to rounding errors. For bottom-up approaches, natural and indirect anthropogenic sources are estimated based on available gridded data sets (see text Sect 5.2). As some emissions are missing gridded products (wild animals, permafrost, and hydrates), discrepancies may occur in terms of totals proposed in Table 3. Bottom-up direct anthropogenic estimates are based only on the gridded products (see Table 1).

Latitudinal band	eatitudinal band 90°S- 30°N		30°N	-60°N	60°-90°N	
Approach	Bottom-up	Top-Down	Bottom-up	Top-Down	Bottom-up	Top-Down
Natural and indirect anthropogenic Sources	178 [95-276]	148 [133-164]	100 [43-188]	42 [36-50]	28 [9-53]	14 [10-21]
Combined wetland and Inland freshwaters	151 [85-234]	128 [112-155]	73 [32-147]	27 [20-42]	24 [9-53]	9 [7-17]
Other natural	27 [11-42]	22 [20-29]	27 [10-41]	19 [16-22]	4 [2-6]	3 [1-5]
Anthropogenic direct sources	210 [180-227]	215 [191-238]	151 [142-157]	144 [121-162]	10 [6-14]	10 [6-16]
Agriculture & Waste	140 [121-150]	150 [135-168]	81 [77-84]	77 [56-88]	1 [1-2]	2 [2-2]
Fossil Fuels	52 [44-65]	46 [36-62]	65 [61-71]	61 [50-69]	7 [4-10]	7 [3-13]
Biomass & biofuel burning	22 [18-30]	19 [16-21]	7 [4-10]	6 [2-7]	1 [0-1]	1 [1-2]
Sum of sources	388 [275-503]	364 [337-390]	250 [184-345]	187 [160-204]	38 [7-73]	24 [18- 29]





Table 7: Regional methane emissions (regions ranked by continent) in Tg CH_4 yr $^{-1}$ for the last decade 2010-2019, based on top-down and bottom-up approaches. Uncertainties are reported as [min-max] range of reported studies. Differences of 1 Tg CH_4 yr $^{-1}$ in the totals can occur due to rounding errors. For bottom-up approaches, natural and indirect anthropogenic sources are estimated based on available gridded data sets (see text Sect 5.2). As some emissions are missing gridded products (wild animals, permafrost, and hydrates), discrepancies may occur in terms of totals proposed in Table 3. Bottom-up direct anthropogenic estimates are based on all products (gridded and per country).

Region	Total e	emissions		nd indirect nic emissions	Direct anthrop	ogenic emissions
	Bottom-up	Top-down	Bottom-up	Top-down	Bottom-up	Top-down
USA	49 [27-77]	38 [32-46]	24 [7-43]	12 [7-22]	26 [19-34]	25 [16-31]
Canada	38 [14-71]	20 [17-24]	32 [11-63]	14 [11-22]	6 [3-8]	7[5-9]
Central America	18 [10-28]	17 [14-19]	8 [3-17]	5 [2-6]	10 [8-12]	12 [11-13]
Northern South America	19 [9-35]	16 [13-20]	10 [3-17]	9 [7-11]	9 [6-17]	7 [6-8]
Brazil	51 [26-79]	47 [41-58]	32 [11-57]	26 [22-36]	19 [16-22]	21 [17-26]
Southwest South America	34 [16-51]	38 [30-48]	21 [6-35]	24 [16-34]	13 [10-16]	14 [12-17]
Europe	42 [29-57]	31 [24-36]	17 [6-30]	7 [5-9]	25 [22-27]	24 [20-31]
Northern Africa	24 [18-33]	25 [23-29]	7 [2-13]	6 [6-8]	18 [16-20]	19 [17-21]
Equatorial Africa	47 [28-83]	47 [39-59]	23 [10-49]	24 [20-30]	24 [19-34]	23 [19-29]
Southern Africa	21 [5-43]	19 [16-24]	11 [2-29]	8 [7-10]	10 [3-14]	11 [10-12]
Russia	48 [24-83]	36 [27-45]	25 [9-47]	14 [11-18]	23 [15-36]	21 [14-29]
Central Asia	15 [6-29]	10 [8-13]	8 [2-19]	1 [0-2]	8 [4-10]	9 [7-11]
Middle East	35 [21-47]	31 [24-39]	9 [3-15]	4 [1-6]	26 [18-31]	28 [20-34]
China	71 [55-99]	57 [37-72]	15 [4-33]	4 [3-7]	57 [51-66]	53 [34-66]
Korean-Japan	6 [4-12]	5 [4-6]	3 [1-7]	1 [1-1]	4 [3-5]	4 [3-5]
South Asia	58 [49-72]	52 [43-60]	13 [5-25]	6 [5-6]	45 [44-47]	45[37-49]
Southeast Asia	64 [42-93]	63 [52-71]	32 [19-54]	27 [20-34]	32 [23-39]	35 [31-46]
Australasia	16 [9-26]	13 [10-17]	10 [4-19]	6 [4-7]	7 [6-7]	7 [6-7]



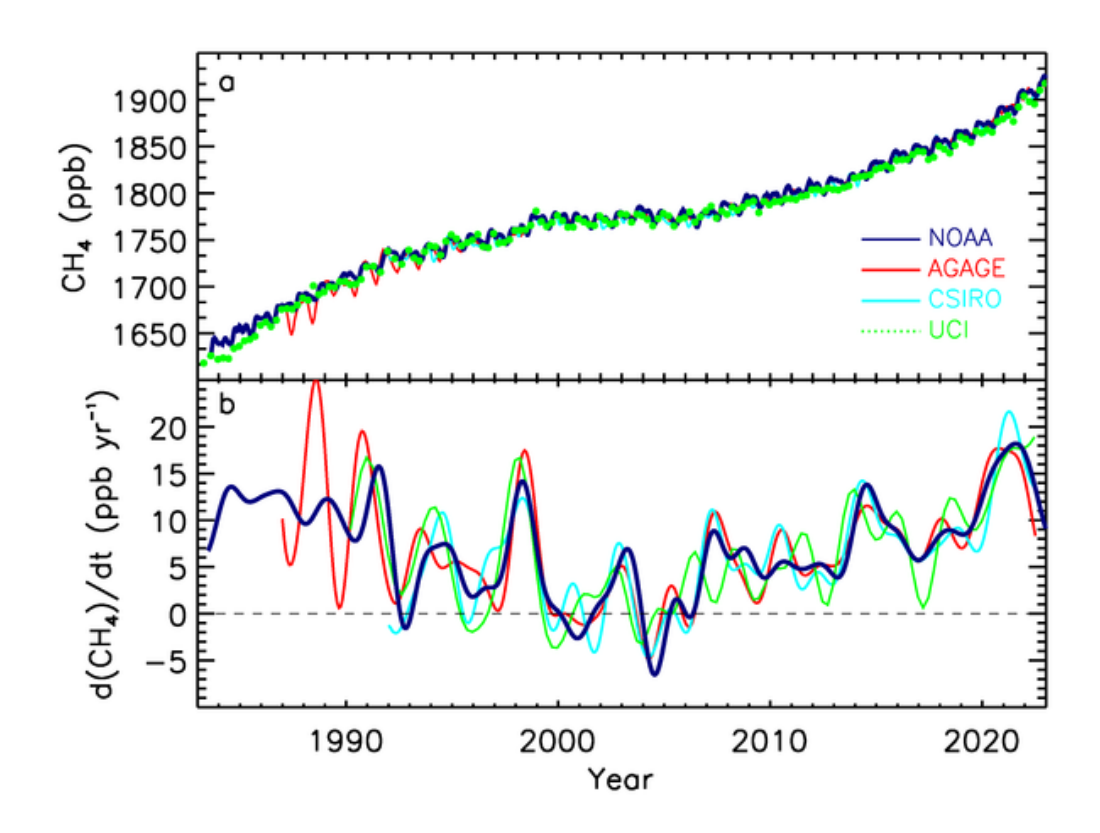


Figure 1: Globally averaged atmospheric CH₄ concentrations (ppb) (a) and annual growth rates G_{ATM} (ppb yr⁻¹) (b) between 1983 and 2022, from four measurement programs, National Oceanic and Atmospheric Administration (NOAA), Advanced Global Atmospheric Gases Experiment (AGAGE), Commonwealth Scientific and Industrial Research Organisation (CSIRO), and University of California, Irvine (UCI). Detailed descriptions of methods are given in the supplementary material of Kirschke et al. (2013).



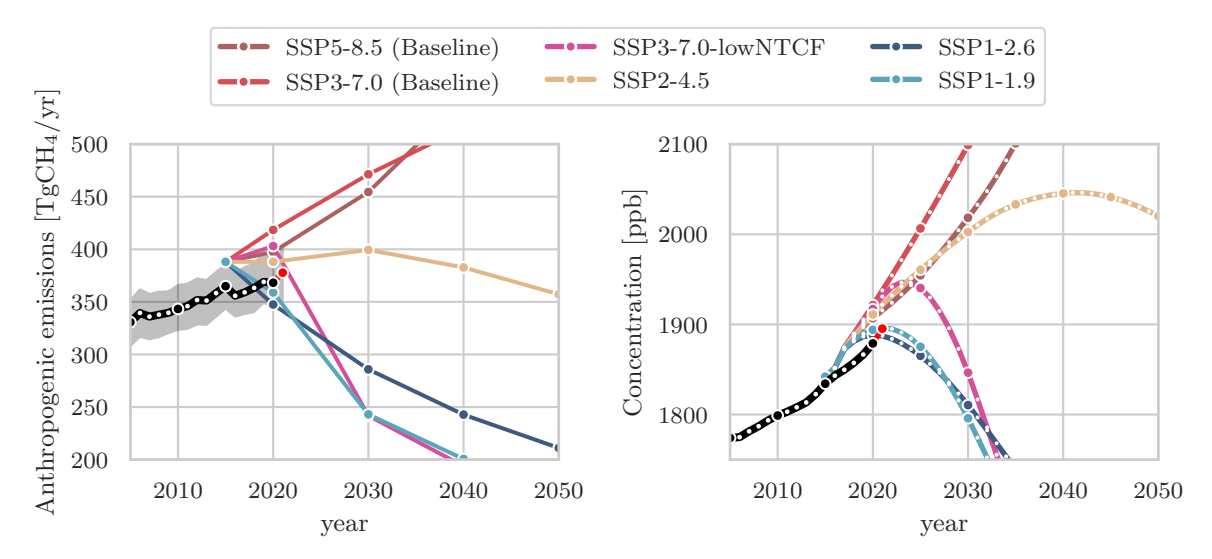


Figure 2: Left: Global anthropogenic methane emissions (including biomass burning) over 2005-2050 from historical inventories (black line and grey shaded area) and future projections (colored lines) (in Tg CH₄ yr⁻¹) from selected scenarios harmonized with historical emissions (CEDS) for CMIP6 activities (Gidden et al., 2019). Historical mean emissions correspond to the average of anthropogenic inventories listed in Table 1 added to the GFEDv4.1s (van der Werf et al., 2017) biomass burning historical emissions. Right: Global atmospheric methane concentrations for NOAA surface site observations (black) and projections based on SSPs (Riahi et al., 2017) with concentrations estimated using MAGICC (Meinshausen et al., 2017, 2020). Red dots show the last year available (2022 for observations).



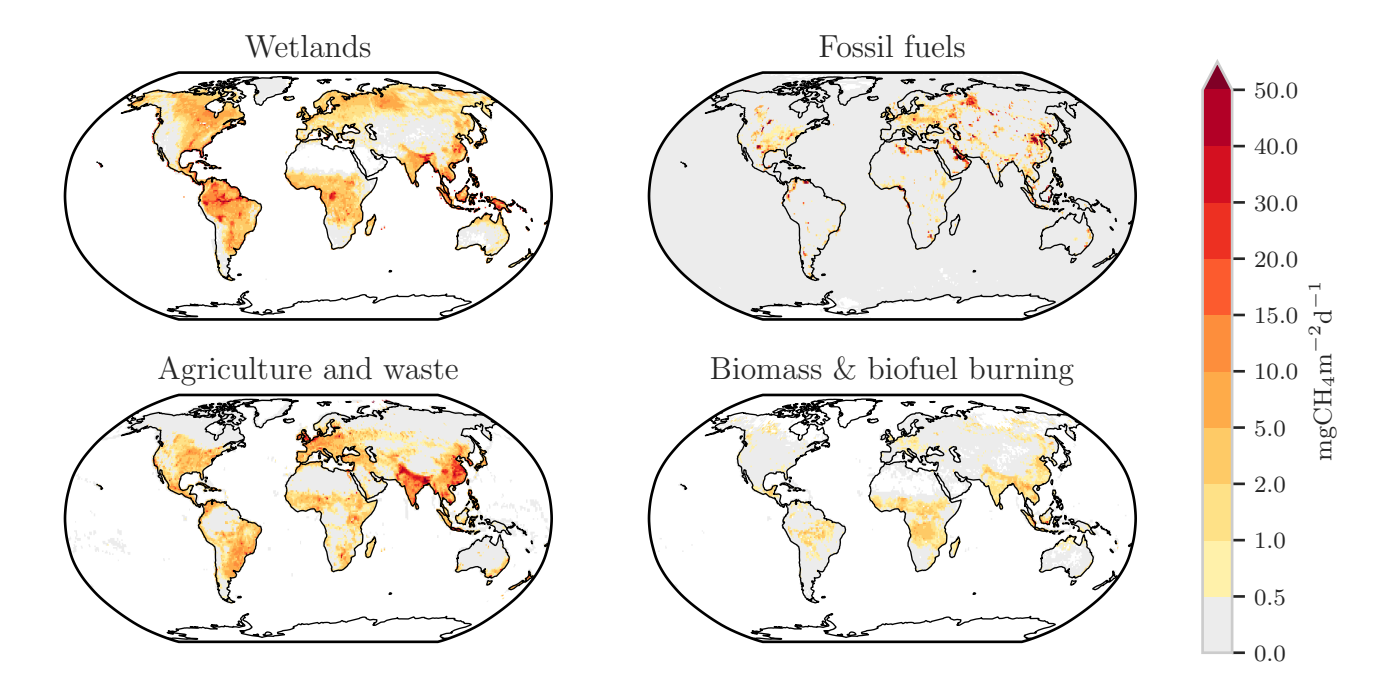


Figure 3: Methane emissions from four source categories: natural wetlands (excluding lakes, ponds, and rivers), biomass and biofuel burning, agriculture and waste, and fossil fuels for the 2010-2019 decade in mg CH_4 m⁻² day⁻¹. The wetland emission map represents the mean daily emission average over the 16 biogeochemical models listed in Table 2 and over the 2010-2019 decade. Fossil fuel and Agriculture and Waste emission maps are derived from the mean estimates of gridded CEDS, EGDARv6, EDGARv7 and GAINS models. The biomass and biofuel burning map results from the mean of the biomass burning inventories listed in Table 1 added to the mean of the biofuel estimate from CEDS (O'Rourke et al., 2021), EDGARv6 (Crippa et al., 2021), EDGARv7 (Crippa et al., 2023) and GAINS (Höglund-Isaksson et al., (2020)) models.





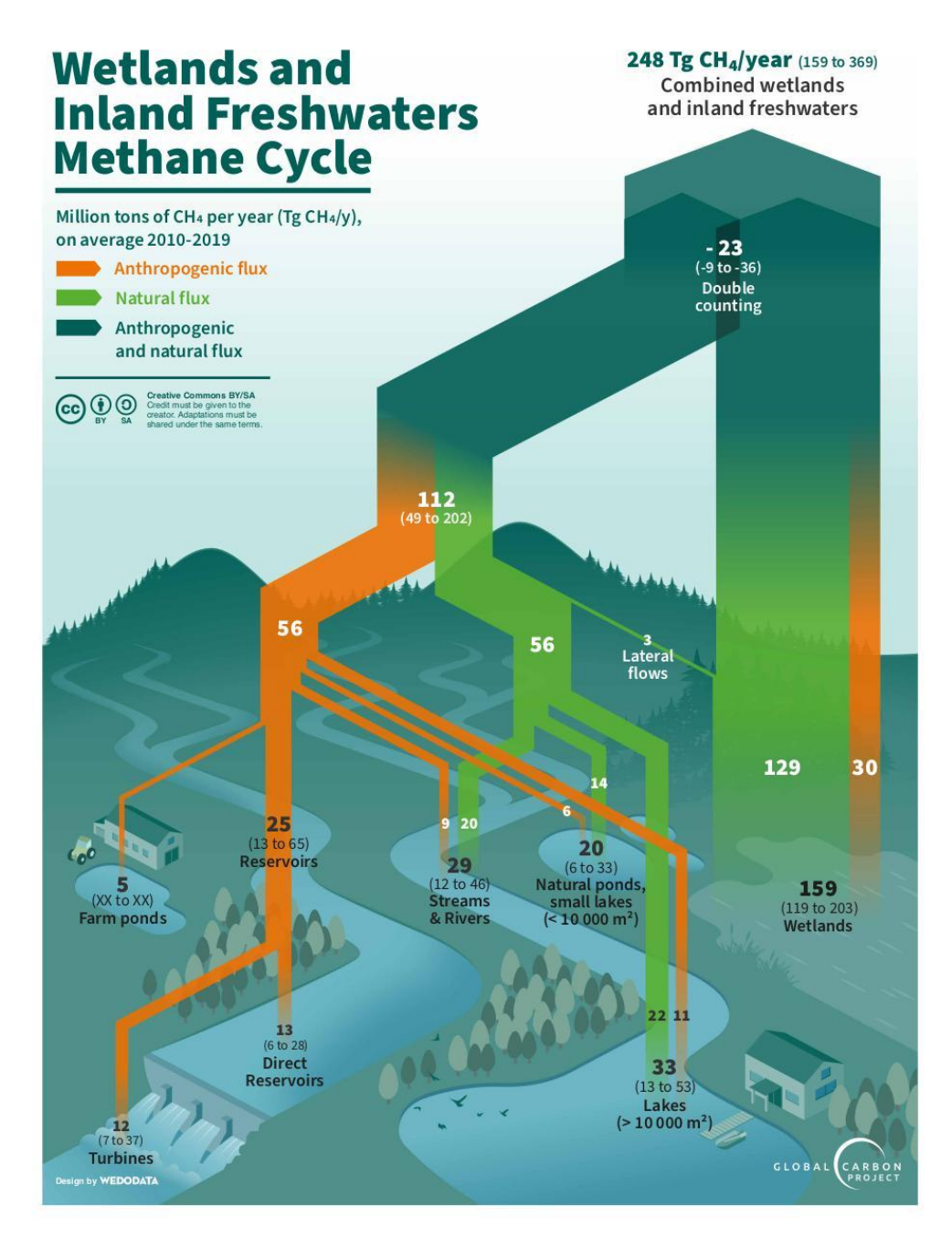


Figure 4: Estimation of wetland and inland freshwater emissions over the 2010-2019 decade in Tg CH₄ yr⁻¹. The fluxes related to voluntary (such as through reservoirs or farm ponds) or involuntary (land use or eutrophication-related) perturbations of the methane cycle are shown here in orange. However, they are accounted for into the "natural and indirect anthropogenic" sources in the Table 3 budget and depicted as natural sources in Fig. 7.





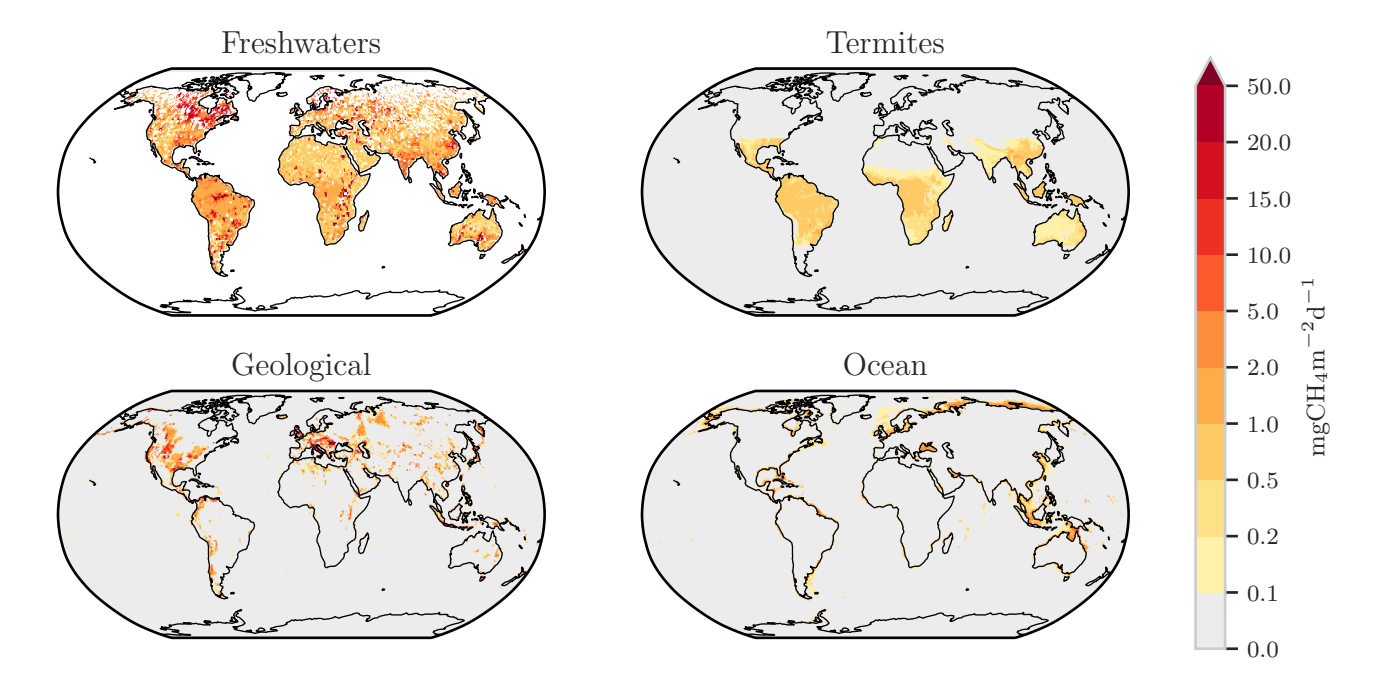


Figure 5: Methane emissions (mg CH₄ m⁻² day⁻¹) from four natural and indirect anthropogenic sources: inland freshwaters (includes lakes, ponds (Johnson et al., 2022), reservoirs (Johnson et al., 2021) and stream and rivers (Rocher-Ros et al., 2023) with a global total scaled to 89 Tg yr⁻¹), geological (Etiope et al., 2019), termites (this study) and oceans (Weber et al., 2019).



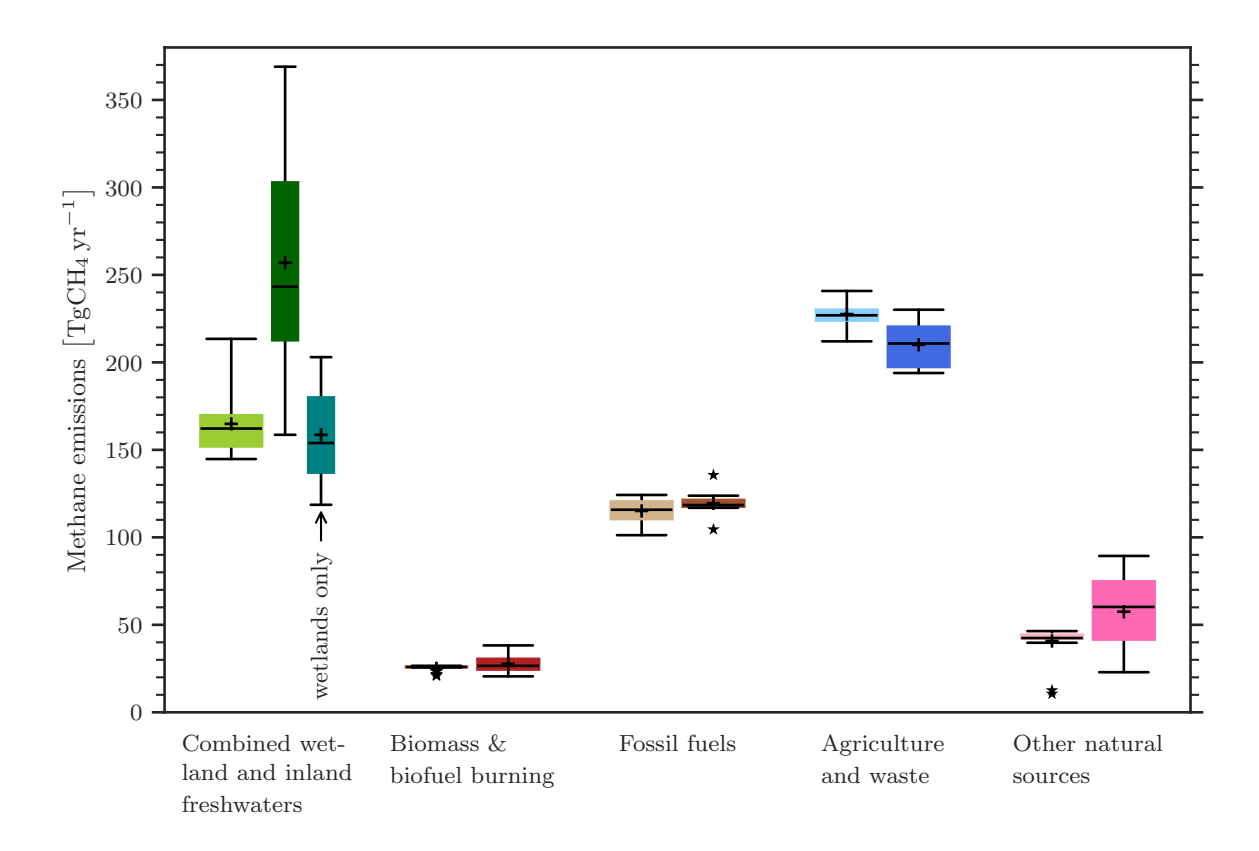


Figure 6: Methane global emissions from five broad categories (see Sect. 2.3) for the 2010-2019 decade for top-down inversion models (left light coloured boxplots) in $Tg CH_4 yr^{-1}$ and for bottom-up models and inventories (right dark coloured boxplots). For combined wetland and inland freshwaters three estimates are given: left = top-down estimates, middle = bottom-up estimates, right = bottom-up estimates for wetlands only. Median value, first and third quartiles are presented in the boxes. The whiskers represent the minimum and maximum values when suspected outliers are removed (see Sect. 2.2). Suspected outliers are marked with stars. Bottom-up quartiles are not available for bottom-up estimates, except for wetland emissions. Mean values are represented with "+" symbols, these are the values reported in Table 3.



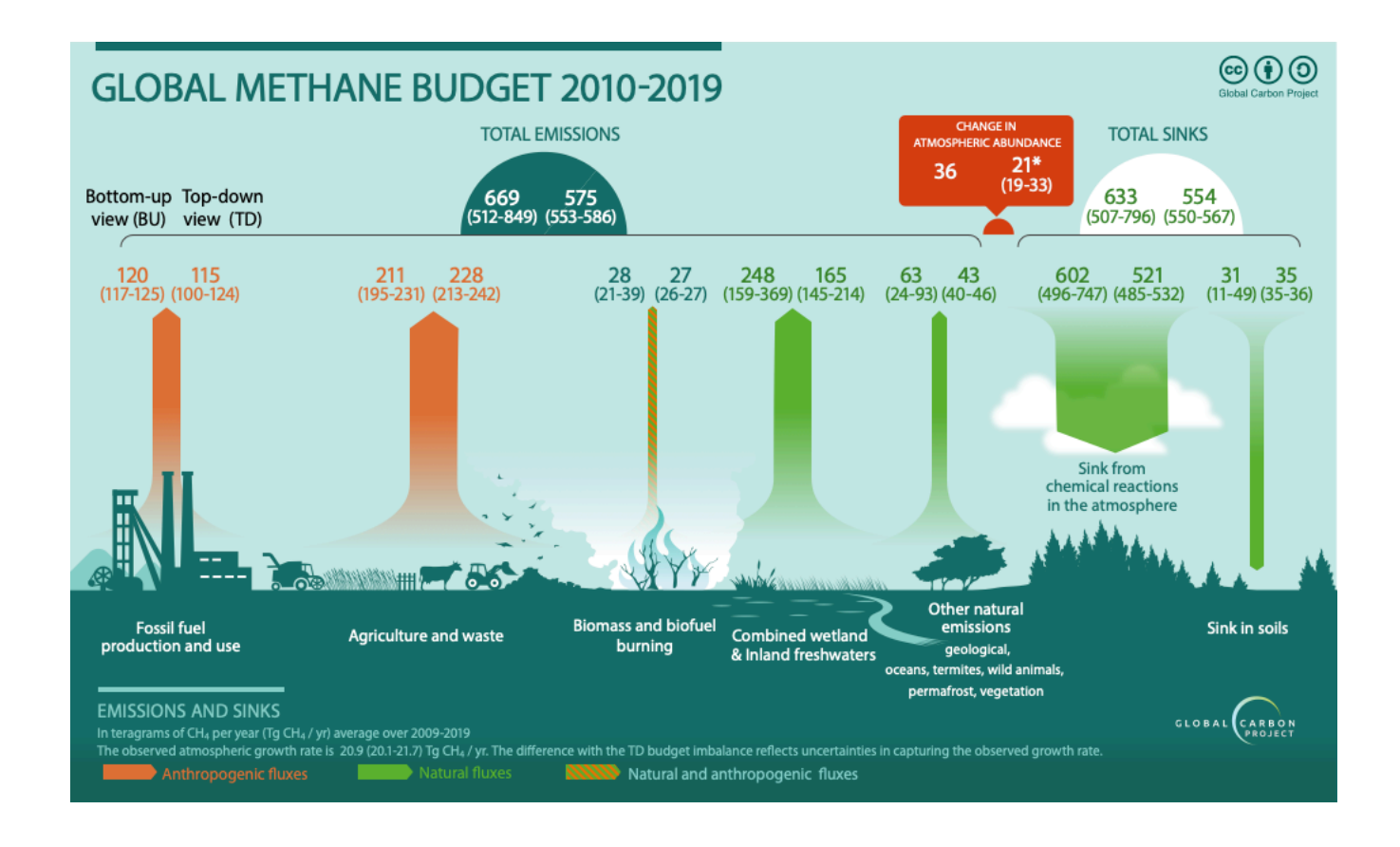


Figure 7: Global Methane Budget for the 2010-2019 decade. Both bottom-up (left) and top-down (right) estimates are provided for each emission and sink category in Tg CH_4 yr⁻¹, as well as for total emissions and total sinks. Biomass and biofuel burning emissions are depicted here as both natural and anthropogenic emissions while they are fully included in anthropogenic emissions in the budget tables and text (Sect. 3.1.5). Combined wetland and inland freshwaters are depicted as fully natural while part has been attributed an indirect anthropogenic component (Sect. 3.2.2 and Figure 4).



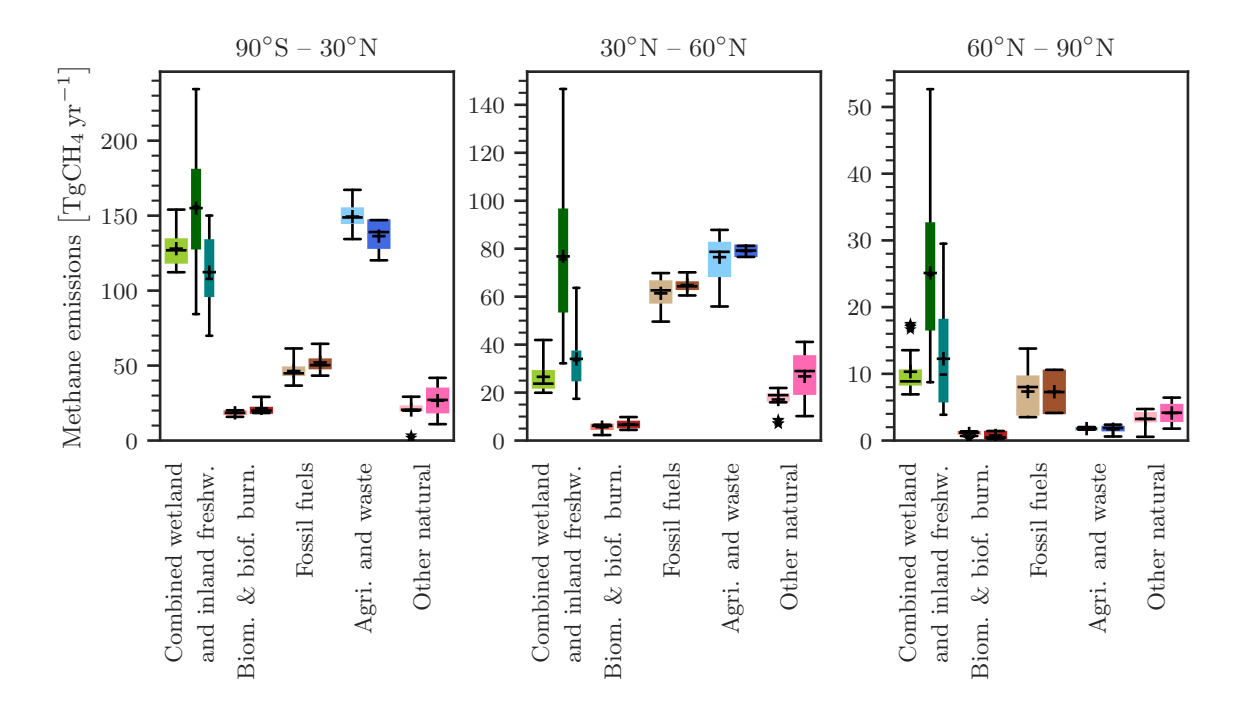


Figure 8: Methane latitudinal emissions from five broad categories (see Sect. 2.3) for the 2010-2019 decade for top-down inversion models (left light coloured boxplots) in Tg CH_4 yr⁻¹ and for bottom-up models and inventories (right dark coloured boxplots). For combined wetland and inland freshwaters three estimates are given: left = top-down estimates, middle = bottom-up estimates, right = bottom-up estimates for wetlands only. Median value, first and third quartiles are presented in the boxes. The whiskers represent the minimum and maximum values when suspected outliers are removed (see Sect. 2.2). Suspected outliers are marked with stars. Bottom-up quartiles are not available for bottom-up estimates, except wetland emissions. Mean values are represented with "+" symbols, these are the values reported in Table 6.





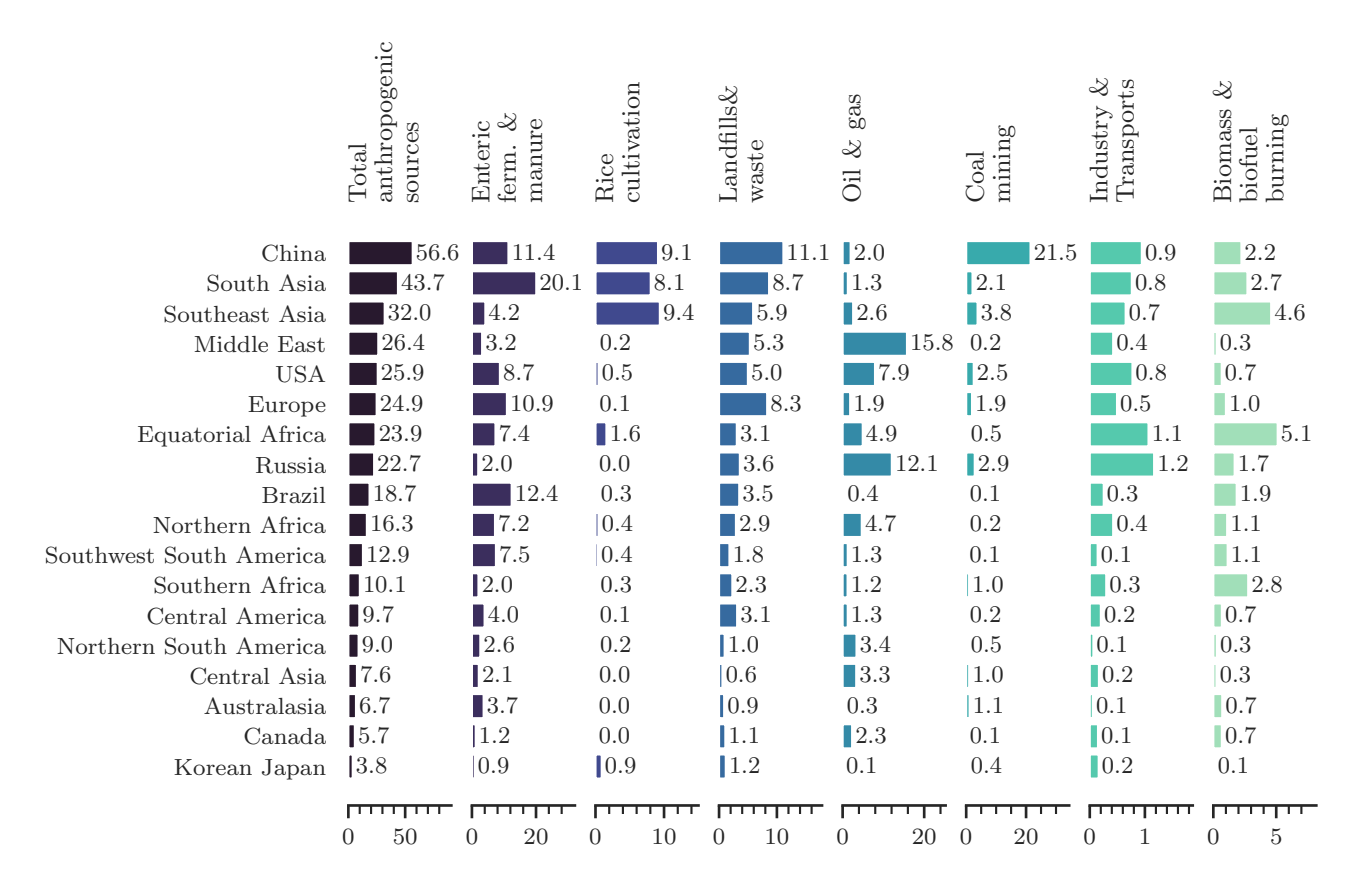


Figure 9: Regional anthropogenic emissions for the 2010-2019 decade from bottom-up estimates in Tg CH₄ yr⁻¹. Regions are ranked by their total anthropogenic emissions. Note that each category has its own emission scale.



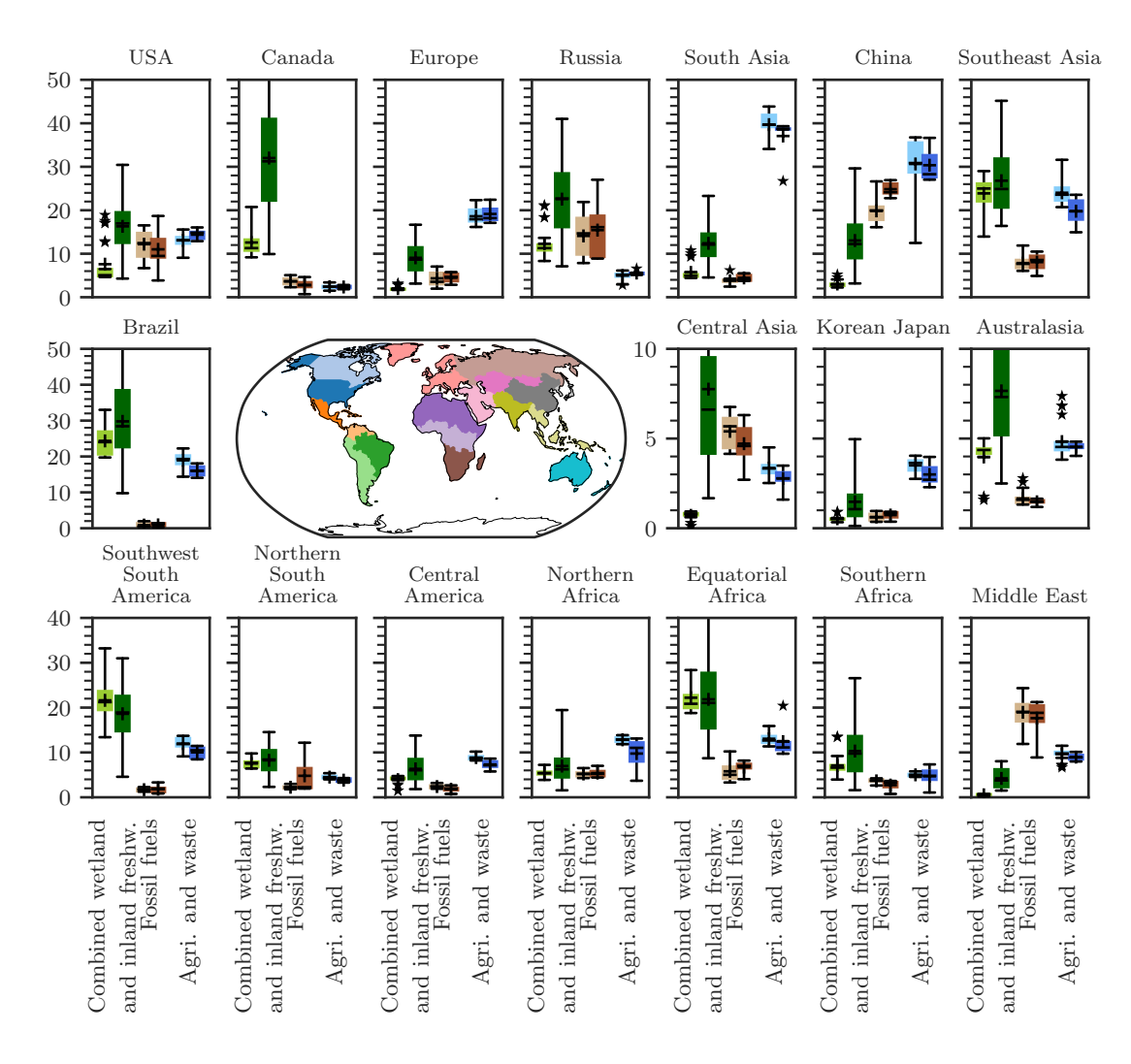


Figure 10: Regional emissions for three broad main emissions categories for the 2010-2019 decade: Combined wetland and inland freshwaters, fossil fuel and agriculture & waste from top-down estimates (left box-plots- and bottom-up estimates (right boxplots). The inner map shows the region's distribution (see also Supplementary material, Table S1 and Fig. S3). More categories are presented in the Supplementary Material in Figure S6.





Table A1. Comparison of terminologies used in this study and previous reports for methane sources.

Table A1. Comparison of	terminologies used in t	his study and previous re	ports for methane sources.	-
GCP terminolo	gy (This study)	IPCC AR6 (Canadell et al., 2021)	National GHG inventories (used by UNFCCC according to IPCC (2006) and IPCC (2019))	IPCC (2006, 2019) Source sector numbering
Anthropogenic Sources				
Fossil fuels	Coal Mining	Coal Mining	Fugitive emissions from Fuels / Solid fuels	1B1
	Oil and gas	Oil and gas	Fugitive emissions from Fuels / Oil and natural gas	1B2
	Transport	Transport	Transport	1A3
	Industry	Industry	Mineral, chemical, metal industry and others	2A, 2B, 2C, 2D, 2E
			Energy/fuel Combustion activities	1A except 1A3 + 1B3
Agriculture	Enteric fermentation and manure management	Enteric fermentation and manure management	Livestock	3A
	Rice cultivation	Rice cultivation	Rice cultivation	3C7
Waste	Landfills and waste	Landfills and waste	Waste	4
Biofuel and biomass burning	Biofuel burning	Biofuel burning	Biofuel burning	1A4b
	Biomass burning	Biomass burning	Biomass burning	3C1
Natural and indirect so	ırces			
Wetlands	Wetlands	Wetlands		
Inland freshwaters	Reservoirs	included in Inland freshwaters	Land (incl Reservoirs)	in 3B
	Lakes, ponds, and rivers	incl in Inland freshwaters	only canal, ditches and ponds for human uses	in 3B
Other natural sources	Oceans	Oceans		
	Termites	Termites		

https://doi.org/10.5194/essd-2024-115 Preprint. Discussion started: 6 June 2024 © Author(s) 2024. CC BY 4.0 License.





Geological sources	Geological sources		
--------------------	--------------------	--	--





Table A2. Summary of methodological changes since the previous budget (Saunois et al., 2020). No significant changes have been applied to the vegetation (Sect. 3.2.8), wild animal (Sect. 3.2.5) and terrestrial permafrost and hydrates (Sect 3.2.7) estimates, though litterature has been expanded and/or updated.

	Saunois et al. (2020)	This study
Regions definition (Table S1, Fig S3)	18 continental regions + ocean	same regions except the last region including only Australia and New- Zealand and called Australasia
Anthropogenic global inventories (See Table 1, Sect 3.1.1)	CEDS, EDGARv4.3.2, USEPA (2012), FAO and GAINS ECLIPSE v6	CEDS, EDGARv6 and v7, USEPA (2019), FAO, IIASA GAINS v4 Add estimate of ultra emitters from Lauvaux et al. (2022)
Biomass burning data sets	FINNv1.5, GFASv1.3, GFEDv4.1s, QFEDv2.5	FINNv2.5, GFASv1.3, GFEDv4.1s, QFEDv2.5
Estimate of wetland emissions (See Tables 2 and S3 and Section 3.2.1)	13 land surface models involved, runs with either prescribed areas or based on Hydrological scheme, single meteorological forcing	16 land surface models involved, runs with either prescribed areas or based on Hydrological scheme, two sets of meteorological forcings
Estimate of reservoirs emissions (Sect.3.2.2)	based on Deemer et al. (2016)	based on Johnson et al. (2021), Rosentreter et al. (2021) and Harrison et al. (2021)
Estimate of lakes and ponds emissions (Sect.3.2.2)	based on Bastviken et al. (2011), Wik et al. (2016b) and Tan and Zhuang (2015)	lakes > .1km2 : based on Rosentreter et al. (2021), Zhuang et al. (2023) and Johnson et al. (2022) lakes and ponds < 0.1 km2 : based on Rosentreter et al. (2021), and Johnson et al. (2022)
Estimates of stream and river emissions (Sect.3.2.2)	From Stanley et al. (2016)	based on Rosentreter et al. (2021) and Rocher-Ros et al. (2023)
Estimates of the anthropogenic perturbation component of inland freshwater emissions (Sect.3.2.2)	-	based on several individual studies on the effect of eutrophication on emissions from lakes, and ponds (See text in Sect. 3.2.2)
Estimate of the double counting in the aquatic systems (Sect.3.2.2)		due to the accounting of small lakes and ponds (<0.1km2) in the vegetated wetlands areas used in land surface models and to lateral transport from vegetated wetland to rivers.





Geological sources (Sect 3.2.3) - onshore and offshore	based on Etiope and Schwiezke et al. (2019)	same as in Saunois et al. (2020)
Termite emissions (Sect. 3.2.4)	GPP: Zhang et al. (2017) termite biomass: Jung et al. (2011) EF: Kirshke et al. (2013) and Fraser et al., 1986)	GPP: Wild et al. (2022) termite biomass: based on different studies depending on regions (see text) EF: Sugimoto et al. (1998) Applied a correction factor for mound from Nauer et al. (2018)
Oceanic sources (Sect 3.2.6)	modern biogenic: based on Wuebbles and Hayhoe (2002), Laruelle et al. (2013) and Rosentreter et al. (2018); geological: based on Etiope (2019)	modern biogenic: based on Rosentreter et al. (2021;2023) and Laruelle et al. (2023) geological: based on Etiope (2019)
Tropospheric OH oxidation (Sect 3.3.2) and stratospheric loss (Sect 3.3.3) (See Supplementary Table S4)	based on results from 11 models contributing to the Chemistry Climate Model Initiative (Morgenstern et al., 2017)	based on results from 11 models contributing to the Chemistry Climate Model Initiative 2022 (Plummer et al., 2021) and the CMIP6 simulations (Collins et al., 2017)
Tropospheric reaction with Cl	based on Hossaini et al. (2016), Wang et al. (2019b) and Gromov (2018)	based on Hossaini et al (2016), Sherwenn et al. (2016), Wang et al (2019b, 2021b) and Gromov (2018)
Soil uptake (See Table S6)	based on Tian et al. (2016)	based on VISIT, JSBACH en MeMo surface models.
Estimates through top-down approaches (See table S7 and S8 to S11)	9 inverse systems contributing, prior fluxes based on EDGARv4.2 or v4.3.2 for most inversions. Most inversion used constant OH.	7 inverse systems contributing, runs with constant and varying OH, prior fluxes based on either EDGARv6 or GAINS





Table A3. Funding supporting the production of the various components of the global methane budget in addition to the authors' supporting institutions (see also acknowledgements).

Funder and grant number (where relevant)	Authors/Simulations/Observation
Director, Office of Science, Office of Biological and Environmental Research of the US Department of Energy under Contract No. DE-AC02-05CH11231 to Lawrence Berkeley National Laboratory as part of the RUBISCO Scientific Focus Area.	WJR, QZ, E3SM/ELM simulations
Funded by NASA's Interdisciplinary Research in Earth Science (IDS) Program and the NASA Terrestrial Ecology and Tropospheric Composition Programs	MSJ; lake and reservoir bottom-up methane emission data sets
Funded by Agence National de la Recherche through the project Advanced Methane Budget through Multi-constraints and Multi-data streams Modelling (AMB-M³) - (ANR-21-CE01-0030)	AM, MS
The Environment Research and Technology Development Fund (JPMEERF21S20800) of the Environmental Restoration and Conservation Agency provided by Ministry of the Environment of Japan	YN, NISMON-CH4
Funded by the German Federal Ministry of Education and Research (BMBF) via the "PalMod" project, grant No. 01LP1921A	TK; CH ₄ emission modelling with JSBACH and LPJ-MPI
Funded by the Swedish Research Council VR (2020-05338) and Swedish National Space Agency (209/19)	WZ; LPJ-GUESS simulations
Funded by BELSPO (project FedTwin ReCAP), EU Horizon 2020 project ESM2025 (nr. 101003536) and FRNS PDR project CH4-lake (T.0191.23)	PR; inland water, coastal and oceanic CH4 emission synthesis
EU H2020 (725546 ERC METLAKE and 101015825 TRIAGE), Swedish Research Councils VR (2022-03841) and Formas (2018-01794)	DB; inland waters - data and bottom up estimation.
Supported by the Newton Fund through the Met Office Climate Science for Service Partnership Brazil (CSSP Brazil)	NG; JULES simulations
Funded by United Nations Environment Programme, Stanford University DTIE21-EN3143	RBJ; inversions and general budget support
the Joint Fund for Regional Innovation and Development of the National Natural Science Foundation (Grant No. U22A20570); the Natural Sciences and Engineering Research Council of Canada (NSERC, #371706)	Changhui Peng/TRIPLEX-GHG
Computing Resources	
LSCE computing resources	Marielle Saunois, Philippe Bousquet, Joël Thanwerdas and Adrien Martinez
NASA High-End Computing (HEC) Program through the NASA Advanced Supercomputing (NAS) Division at NASA Ames Research Center	Matthew S. Johnson (MSJ)
Deutsches Klimarechenzentrum (DKRZ), Hamburg, Germany	Thomas Kleinen (TK)





ALICE High Performance Computing Facility at the University of Leicester FUJITSU PRIMERGY CX2550M5 at MRI and NEC SX-Aurora TSUBASA at NIES

GOSAT retrievals

Yosuke Niwa (YN)

NIES	, ,
Support for atmospheric observations	
Australian Antarctic Division	CSIRO flask network
Australian Institute of Marine Science	CSIRO flask network
Bureau of Meteorology (Australia)	Kennaook/Cape Grim AGAGE, CSIRO flask network
Commonwealth Scientific and Industrial Research Organisation (CSIRO, Australia)	Kennaook/Cape Grim AGAGE, CSIRO flask network
Department of Climate Change, Energy, the Environment and Water (DCCEEW, Australia)	Kennaook/Cape Grim AGAGE
Meteorological Service of Canada	CSIRO flask network
NASA: grants NAG5-12669, NNX07AE89G, NNX11AF17G, NNX16AC98G and 80NSSC21K1369 to MIT with subawards to the University of Bristol (for Barbados and Mace Head) and CSIRO (for Kennaook/Cape Grim); grants NAG5-4023, NNX07AE87G, NNX07AF09G, NNX11AF15G, NNX11AF16G, NNX16AC96G, NNX16AC97G, 80NSSC21K1210 and 80NSSC21K1201 to SIO.	AGAGE calibrations and measurements at SIO, La Jolla and AGAGE station operations at Trinidad Head, Mace Head, Barbados, American Samoa, and Kennaook/Cape Grim
National Oceanic and Atmospheric Administration (NOAA, USA) contract RA133R15CN0008 to the University of Bristol	Barbados
NOAA USA	CSIRO flask network
Refrigerant Reclaim Australia	Kennaook/Cape Grim AGAGE
UK Department for Business, Energy & Industrial Strategy (BEIS) contract TRN1537/06/2018 and TRN 5488/11/2021 to the University of Bristol	Mace Head
National Oceanic and Atmospheric Administration (NOAA, USA)	Cape Matatula
Japanese Ministry of Environment	GOSAT data, Robert Parker
Japanese Aerospace Exploration Agency, National Institute for Environmental Studies	GOSAT data, Robert Parker
NERC UK: grants NE/W004895/1, NE/R016518/1 and NE/X019071/1	GOSAT data, Robert Parker
The Swedish Research Council VR (2022-04839), European Space Agency projects AMPAC-Net and CCI+ permafrost, European Union's Horizon 2020 Research and Innovation Programme to the Nunataryuk project (no. 773421)	Permafrost region, Gustaf Hugelius